

Kurzfassungen der Vorträge

# 14. DEUTSCHES LS-DYNA FORUM

10. - 12. Oktober 2016, Bamberg



Bild mit freundlicher Genehmigung: Dr. Ing. h.c. F. Porsche AG

PLATIN SPONSOREN





Kurzfassungen der Vorträge

# 14. LS-DYNA FORUM 2016

---

10. - 12. Oktober 2016, Bamberg

## Veranstalter

DYNAmore GmbH, Industriestr. 2, D-70565 Stuttgart  
Tel. +49 (0)711 - 459600 – 0, Fax +49 (0)711 - 459600 - 29  
E-Mail: info@dynamore.de, Web: www.dynamore.de

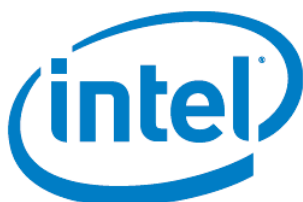
## Copyright

Copyright © 2016 by DYNAmore GmbH.  
Permission to reproduce any papers contained herein is granted provided that credit is given to DYNAmore, the author, and his/her company. Authors retain their respective copyrights.

ISBN 978-3-9816215-3-2

## Sponsoren

Platin



Gold



Silber





Liebe LS-DYNA Anwenderinnen und Anwender,

wir heißen Sie herzlich willkommen auf dem 14. Deutschen LS-DYNA Forum.

In den nächsten zweieinhalb Tagen erwarten Sie über 100 Übersichts- und Fachvorträge von Anwendern aus den unterschiedlichsten Industriezweigen. Weiterhin geben Softwareentwickler von LSTC und DYNAmore Einblick in die Anwendungsmöglichkeiten ihrer neuesten Implementierungen. Abgerundet wird das Forum mit sechs Workshops zu gefragten Themengebieten.

Thematisch fällt auf, dass auch in diesem Jahr die Modellierung faserverstärkter Kunststoffe eine wichtige Rolle spielt. Um hierbei die Lücke zwischen der Prozess- und Gebrauchstauglichkeitssimulation zu schließen, entwickelt DYNAmore derzeit das Mapping-Tool "Envyo", das bereits in etlichen Vorträgen zur Anwendung kommt. Ausführliche Informationen zum Einsatz von "Envyo" erhalten Sie in einem dedizierten Workshop. Weiterhin voll im Trend liegen die klassischen Applikationen aus der Kurzzeitdynamik. Stark vertreten sind auch die Anwendungen aus der Funktions- und Komponentensimulation, die mit den impliziten Methoden von LS-DYNA berechnet werden können.

Wie gewohnt gibt es auch in diesem Jahr eine Ausstellung von ausgewählten Hard- und Softwareherstellern rund um LS-DYNA. Darüber hinaus stehen Ihnen die Mitarbeiter der DYNAmore GmbH für Fragen und mit Tipps und Tricks zur LS-DYNA Produktpalette zur Verfügung.

Wir wünschen Ihnen einen angenehmen Aufenthalt.

Ihre DYNAmore GmbH







### **A success story for almost 40 years**

For almost 40 years Fujitsu provides HPC users the computing resources they need to study scientific and technical problems on the basis of computer simulations. Our cutting-edge technologies enable them to make vital decisions, to promote product innovations, to speed up research and development, and to reduce time to market maintaining competitive advantage.

Today Fujitsu is the most experienced and largest provider of HPC solutions in the Asian market, and has been a leading HPC vendor in Europe almost from the beginning. Fujitsu has established close collaboration with leading ISVs and has jointly developed PRIMEFLEX for HPC cluster solutions optimized to application specific workload requirements. Furthermore, a global HPC competency network supports and further develops the full range of Fujitsu's HPC solutions.

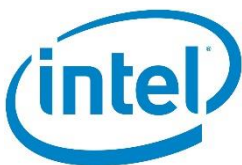
### **High Performance Computing with Fujitsu HPC Cluster Solutions**

High Performance computing tasks are not alike – nor are the requirements of users. Yet as different as they all may be, PRIMEFLEX for HPC cluster solutions from Fujitsu address the requirements at all levels: from workgroup-sized configurations up to divisional-sized HPC cluster environments based on highly reliable hardware components complemented by comprehensive services. Supported by a fully integrated and complete HPC solution stack all HPC Cluster solutions are designed to deliver application results in a shorter time.

Thoroughly designed to customers operational and workflow related requirements, PRIMEFLEX for HPC cluster solutions from Fujitsu provide an optimal price / performance ratio. Ready-to-Go delivery of HPC infrastructures guarantees rapid deployment for production and includes Intel Cluster Ready certification for proven performance and trouble-free operation. The HPC Gateway with application integration makes the use of HPC easier for experts and more broadly accessible to beginners.

HPC Simplicity lowers entry barriers and makes HPC accessible to a much wider set of end-users, including sectors just starting with HPC. Fujitsu's HPC Cluster Suite with its intuitive web based "desktop" guides users through their daily tasks eliminating the complexity of using HPC resources and leading to improved user productivity. PRIMEFLEX for HPC cluster solutions from Fujitsu simplify HPC

[www.fujitsu.com/hpc](http://www.fujitsu.com/hpc)



**Intel Corporation is a world leader in computing innovation.**

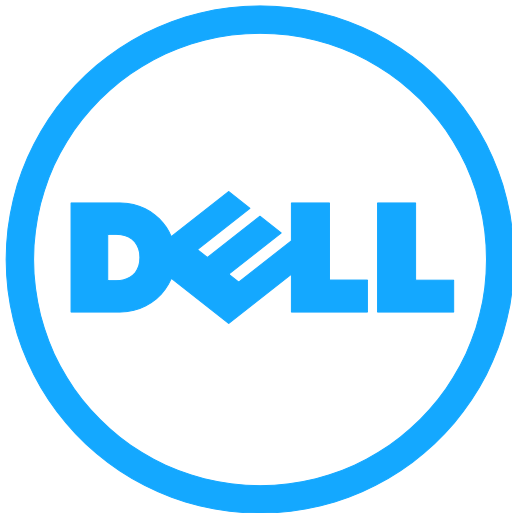
We design and build the essential technologies that serve as the foundation for the world's computing devices. From workstations to the world's most powerful supercomputers, ever-higher performance for technical computing applications is needed to speed time to results, handle today's unprecedented growth in data volumes, and improve the accuracy and precision of modeling and simulation applications. Intel® architecture is designed to address the heavy demands of technical computing at every scale, so users can continue to push the boundaries of discovery.

To learn more about Intel in technical computing, visit

[www.intel.com/hpc](http://www.intel.com/hpc) and [@IntelHPC](https://twitter.com/IntelHPC).





**Listen. Learn. Deliver. That's what we're about.**

Dell empowers countries, communities, customers and people everywhere to use technology to realize their dreams. Customers trust us to deliver technology solutions that help them do and achieve more, whether they're at home, work, school or anywhere in their world. Learn more about our story, purpose and people behind our customer-centric approach.

**Solve HPC challenges at any scale**

Evolving research and technical workloads push the limits of high performance computing (HPC). Our scalable, flexible market-ready solutions — with the latest Intel® processors — readily handle compute and data-intensive workloads to drive breakthroughs faster. Learn how our [HPC Blueprint](#), based on proven reference architectures, can help you:

- Transform data into insights faster with less risk
- Increase bandwidth, throughput and scalability
- Streamline deployment and cluster management

Dell supports industry, research, government and education with market-ready HPC solutions that enable more innovation and discovery.

Our scalable, flexible solutions readily handle compute and data-intensive research workloads, helping drive faster breakthroughs.

Come and visit us in the exhibition and meet one of our Dell HPC specialists who will share with you how Dell is accelerating engineering, analysis, modelling and simulation with HPC.

[www.dell.de/hpc](http://www.dell.de/hpc)





CPU 24/7 GmbH is a leading provider of *CAE as a Service* (CAEaaS) solutions. Headquartered in Potsdam / Germany, CPU 24/7 develops and operates unique on demand services for High Performance Computing (HPC) that are based on the latest globally accepted industry standards for hardware, software, and applications. Since 2006 CPU 24/7 has served in particular the high end CAE markets in e.g. automotive, marine & offshore, transportation, oil & gas, as well as aerospace, where these services are designed to fulfil all requirements of even the most demanding CAE jobs.

CPU 24/7 provides its customers flexible, private and “ready-to-use” CAEaaS infrastructures and gives companies the opportunity to temporarily shift from an in-house HPC cluster or desktop/workstation solution over to scalable HPC resources that can be activated and intensively used as burst capacities for meeting an intermitted demand in trendsetting CAE projects.

Thus, “CAE as a Service” allows customers and engineers to keep their focus 100% on their research, development, and engineering tasks, therefore not wasting any precious time and financial resources with developing, operating, and maintaining a highly specialized HPC infrastructure. The HPC clusters are located at an ISO 27001 certified, verifiable, high-security computing centre in Berlin, Germany. Each CPU 24/7 customer is provided with a non-virtualised, customised simulation environment with access to exclusively dedicated and private bare-metal servers. Customers and their data are isolated by completely separate systems. For communication, secure industry standard and authenticated connections and protocols with basic encryption are used. Data is stored solely in the Berlin high security data centre and is handled in accordance with the Federal Data Protection Act and the Federal Office for Information Security (BSI). Services are provisioned ‘on-demand’ and remotely, eliminate expensive upfront investments and can be used immediately. CAE as a Service solutions are available either as standard and online bookable HPC cluster solutions for smaller projects (CAE Express) or also as enterprise-class highly customised HPC systems (CAE Enterprise). Storage, traffic and comprehensive support is always included. Further information:

[www.cpu-24-7.com](http://www.cpu-24-7.com)



Gompute is a leading HPC Cloud computing company based in Sweden supporting users all around the globe. The solutions offered include HPC on demand, HPC software and Hosting services.

Combined with Gompute On-Demand, a proven solution for remote CAE needs, you have the option to either scale out or completely host your HPC environment, ranging from 1 -> 1000's of cores, in a Gompute owned Super Computing Centre. Using the Gompute service, organizations gets a ready to use environment with a large set of applications and resources pre-integrated and available just as if running on your local Linux desktop (i.e. – native graphical interface of your application), dramatically reducing the learning curve to run your simulations as a service.

Gompute strives to be the natural choice for organizations in need of a secure and reliable partner for their HPC needs. By providing the wide array of building blocks for your HPC environment from one vendor we can help both to consolidate your internal environment, burst to extra capacity when needed, or manage resources for you, coupled with a support organization of HPC professionals and application domain experts.

The Gompute environment is built from ground up to provide stakeholders in the organization with the needed resources for a stable functional HPC resource, including IT, CAE Management and most importantly, high productivity for the engineers performing CAE. Included is Remote Visualization over high latency links, File transfer technology, tools to create application workflows, large scale analytics, dashboards, collaboration features, app-launchers and more.

[www.gompute.com](http://www.gompute.com)



Oasys Ltd is the software house of Arup and distributor of the LS-DYNA software in the UK, India and China. We develop the Oasys Suite of pre- and post-processing software for use with LS-DYNA.

We have been working with Livermore Software Technology Corporation (LSTC), the developers of LS-DYNA, for over twenty years and have an in-depth knowledge of this powerful analysis tool. During this period we have also been involved in developing some of the features within LS-DYNA such as seatbelt system modelling, staged construction, and various material models.

### **Oasys Suite of Software**

The Oasys Suite of software, exclusively written for LS-DYNA, is at the leading edge of the pre- and post-processing markets and is used worldwide by many of the largest LS-DYNA customers.

With the release of version 13, the Oasys Suite provides the user with even more tools and functions to reduce the amount of time needed to build and check an LS-DYNA model, allowing the engineer to concentrate more on the actual problem in hand rather than just the task of getting a model up and running in LS-DYNA.

[www.arup.com/atr](http://www.arup.com/atr)



### **Innovation**

Great organizations and people undoubtedly facilitate innovation, but the best breeding ground for discovery and growth is having the space and tools to explore. This exploration requires scalability. Rescale's simulation platforms allow for infinite scale, customizable tools, and the ability to make on-the-fly adjustments. Rescale's scalability allows engineers to enhance their designs and fully maximize product innovation.

### **Time-to-market**

The ability to fully explore the design space requires access to the latest technology in order to improve product conceptions. A team can generate more comprehensive results faster and yield better designs the first time around, giving an organization a significant competitive edge. Rescale's hardware and software elasticity speeds up product development and optimizes time-to-market.

### **Resource Abundance and Optimization**

Engineers and scientists want the best hardware for the job and need the ideal configuration to optimally scale the simulation. Most importantly, they need instant access to these resources. Rescale's simulation platforms offer this and more by providing a wide range of software and hardware tools in one central location, allowing engineers and scientists immediate and unlimited access to the exact resources they need.

Discover how Rescale can help transform stagnant, on-premise resources into an agile, optimized cloud HPC platform:

[www.rescale.com](http://www.rescale.com)

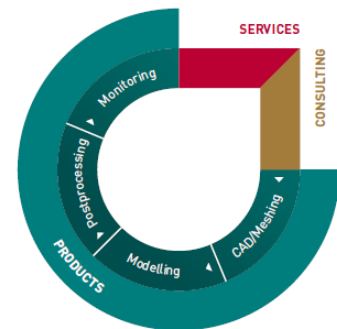
# SCALE

IT-Solutions for CAE

SCALE offers software solutions and IT services for process and data management in the automotive and other industries. As a subsidiary of DYNAmore GmbH, SCALE has a strong background in CAE applications and processes. In particular, our range of services includes software development for process and data management, finite element method development, and numerical optimization for the functional design of vehicle components.

SCALE's lineup includes our standard products CadMe, LoCo, CAViT and Status.E for simulation data, process and requirements management, as well as IT services for individual software solutions on request. Our software products support the entire lifecycle of the typical CAE design workflow: CAD data meshing model -> assembly -> solving -> post processing -> reporting and monitoring

If requested by the customer, the software modules can be individually combined or integrated as desired. In addition to software development and standard products, SCALE offers consulting services for assessing and optimizing your IT environment, requirements analysis, IT architecture design, project planning and management, etc. The name SCALE stands for "Scalable Solutions in Simulation Data and Process Management" and our staff at SCALE are a mix of experienced CAE engineers and professional computer scientists. The majority of our employees are based at the Dresden site and benefit from the excellent scientific environment there.



[www.scale.eu](http://www.scale.eu)



VIRTUAL VEHICLE is an internationally operating research center in Graz, Austria, that develops technologies for affordable, safe and environmentally friendly vehicles for road and rail. The key aspects of the research and development include combining numeric simulation and experimental verification, as well as developing comprehensive, full-vehicle system simulations.

About 200 experts develop new solutions, innovative methods and technologies for the vehicles of tomorrow in an international network of industrial and research partners. VIRTUAL VEHICLE is currently working in close collaboration with over 100 industrial partners (including Audi, AVL, BMW, Daimler, MAN, MAGNA, Porsche, Renault, Siemens and Volkswagen) and, in addition to our principle scientific partner,

Graz University of Technology, more than 45 international university research institutes (including KTH Stockholm, KU Leuven, Universidad Politécnica de Valencia, TU Munich, KIT Karlsruhe, University of Sheffield, or CRIM Centre de Recherche Informatique de Montreal). In corporate year 2014, VIRTUAL VEHICLE generated an operating income of 21 million Euros.

The COMET K2 program will provide the basis for funded research activities until at least the end of 2017. VIRTUAL VEHICLE directs and participates in more than 20 EU-projects and also offers a broad portfolio of contract research and services.

[www.vif.tugraz.at](http://www.vif.tugraz.at)



4a engineering GmbH is a technically oriented Research and Development company with a focus on plastics engineering and materials science. The core competence of 4a engineering GmbH resides in concept finding and optimization of product ideas based on the profound understanding and interpreting of physical and mechanical processes. 4a engineering GmbH works with a wide range of partially specially developed simulation software and analyzing methods. We are offering engineering and R&D services as well as our products **4a fibermap**, **4a micromec** and **4a impetus**.

4a impetus builds up an efficient and reliable process, using realistic testing methods and processing a validated material card. Recent developments of new test methods for 4a impetus satisfy the needs of complex material models as well as the expectations with regard to simple and favorable tests.

As final result 4a impetus is able to deliver a validated material card for LS-DYNA.

<http://www.4a-engineering.at>

<http://impetus.4a.co.at>



e-Xstream engineering is a software and engineering services company 100% focused on state-of-the-art multi-scale modeling of complex multi-phase composites materials and structures (PMC, RMC, MMC, nanocomposites, hard metals, etc).

Digmat coupled to LS-DYNA empowers the engineers to reduce the number of prototype iterations and to accurately model the crash behaviour of Fiber Reinforced Plastics components and systems. This solution help them to optimise the cost of toolings and the performance of their design.

[www.e-xstream.com](http://www.e-xstream.com)



GOM

**Gesellschaft für Optische Messtechnik**

GOM develops, produces and distributes software, machines and systems for 3D coordinate measuring technology and 3D testing based on latest research results and innovative technologies. With more than 60 sites and more than 1,000 metrology specialists, GOM guarantees profound advice as well as professional support and service. More than 10,000 system installations improve the product quality and manufacturing processes in the automotive, aerospace and consumer goods industries.

[www.gom.com](http://www.gom.com)



Das Haupttätigkeitsgebiet der LASSO Ingenieurgesellschaft mbH ist die Durchführung von Berechnungen und Simulationen mit Hilfe der Methode der Finiten Elemente. Dabei reicht das Spektrum von der reinen Netzerstellung über lineare und nichtlineare Statik und Dynamik bis zur Crashsimulation. Unsere Hardwareausstattung erlaubt auch die Crashsimulation von Gesamtfahrzeugmodellen im eigenen Haus. Ein weiteres Gebiet ist, im Auftrag der Firma BETA CAE Systems, der Vertrieb und die Betreuung des FE-Preprozessors ANSA, des FE-Lösers Epilysis und des FE-Postprozessors META. Die Hauptanwendungsbereiche liegen im Fahrzeugbau, im allgemeinen Maschinenbau und in der Luft- und Raumfahrttechnik. Speziell im Fahrzeugbau können wir auf eine langjährige Erfahrung zurückgreifen. Sei es bei der Berechnung von Fahrzeugkomponenten, bei der Erstellung von Gesamtfahrzeugmodellen, bei der Crashsimulation oder bei Sicherheitsnachweisen für Omnibusse nach ECE-R66, welche wir in Zusammenarbeit mit dem TÜV durchführen. Bei LASSO eingesetzte Software: ANSA, META, ABAQUS, LARSTRAN, NASTRAN, LS-DYNA3D und PAMCRASH

[www.lasso.de](http://www.lasso.de)



transtec, founded in 1980, with its headquarters in Tübingen, Germany, belongs to the leading European experts in High Performance Computing. We develop individual solutions according to the customer's requirements and we support our customers throughout life cycle of the solution. Small to medium-sized businesses as well as academic institutions value our intelligent, easy-to-manage HPC solutions.

transtec's competence does not only comprises in-depth knowledge with all current hardware & software technologies being used within the HPC ecosystem, but also includes a long-term expertise in numerous applications from Life Sciences, CAE, Physics, and various other areas of research. This helps us understand customers' workflows and provide the customer with an expert opinion regarding the deployment of new technologies like remote visualization or parallel filesystems.

transtec is a specialist in sizing and deploying high-performance and parallel filesystem storage solutions to customers, and looks a back upon a history of several petabytes of HPC storage deployed, including various open-source as well as commercial implementations.

[www.transtec.de](http://www.transtec.de)

4a engineering  
ARUP  
ASC(S)  
CPU 24/7  
DELL  
DYNAmore  
e-Xstream engineering  
Fujitsu  
GNS Systems  
GNS  
GOM - Gesellschaft für Optische Messtechnik  
Gompute (Gridcore)  
Ingenieurbüro Huß & Feickert  
Ingenieurbüro Loose  
Inprosim  
Intel  
Kompetenzzentrum Virtuelles Fahrzeug  
Lasso Ingenieurgesellschaft  
LSTC  
Nafems  
NEC Deutschland  
Rescale  
SCALE  
Transtec  
Universität Erlangen-Nürnberg



**KEYNOTE VORTRÄGE**


---

 Plenum, Montag, 10. Oktober, 13:30 – 15:40 Uhr Seite


---

**Recent Developments in LS-DYNA – Part I**

J. Hallquist, R. Grimes, J. Wang and other developers (LSTC)..... 27

**Modeling and Characterization of Continuous-Discontinuous Long Fiber-Reinforced Polymer Structures**

Prof. T. Böhlke, F. Henning, L. Kärgler, Prof. T. Seelig, K. A. Weidenmann (Karlsruhe Institut of Technology) ..... 29

**Status and Challenges of Safety CAE in Vehicle Development**

S. Frik (Adam Opel)..... 30

**Sponsorenvortrag: Enabling Effective and Easy to Access Simulation**

S. Gillich (Intel); E. Schnepf (Fujitsu Technology Solutions)..... 31

**Sponsorenvortrag: Dell HPC System for Manufacturing**

T. Vogt (Dell) ..... 32

---

 Plenum, Dienstag, 11. Oktober, 13:40 – 15:10 Uhr Seite


---

**Insassensimulation Kindersicherheit bei Mercedes-Benz**

H. Ipek, J. Fausel (Daimler)..... 33

**Historische Entwicklung Funktionssimulation bei der Porsche AG**

M. Geuther (Dr. Ing. h.c. F. Porsche) ..... 34

**Einsatz der Umformsimulation in der Modellierung und Verfahrensentwicklung von Blechumformprozessen**

Prof. M. Liewald (Universität Stuttgart)..... 35

---

 Plenum, Mittwoch, 12. Oktober, 13:30 – 15:15 Uhr Seite


---

**Recent Developments in LS-DYNA – Part II**

J. Hallquist, R. Grimes, J. Wang and other developers (LSTC)..... 27

**LS-OPT: Status and Outlook**

N. Stander, A. Basudhar, I. Gandikota (LSTC); K. Witowski (DYNAmore); Å. Svedin, C. Belestam (DYNAmore Nordic) ..... 36

**LS-DYNA in the Development Process of Occupant Restraint Systems**

K. Elsässer (ZF TRW)..... 38

**A New Versatile Tool for Simulation of Failure in LS-DYNA, and the Application to Aluminum Extrusions**

P. Du Bois (Consultant); M. Feucht (Daimler); F. Andrade (DYNAmore) ..... 39

**CRASH**Raum 1, Montag, 10. Oktober, 16:20 – 17:20 Uhr Seite

<b>Berücksichtigung des Bake Hardening Effekts bei umgeformten Blechteilen für die Crashsimulation</b> D. Riemensperger (Adam Opel) .....	40
<b>Virtuelle Produktentwicklung und Craschauslegung von Stahl-Werkstoffverbundsystemen</b> D. Pieronek, L. Kessler, H. Richter, S. Myslowicki (Thyssenkrupp Steel Europe) .....	41
<b>Influence of Submodel Size and Evaluated Functions on the Optimization Process of Crashworthiness Structures</b> S. Link, H. Singh, Prof. A. Schumacher (Universität Wuppertal) .....	42

**CRASH (BATTERIES)**Raum 1, Montag, 10. Oktober, 17:50 – 18:50 Uhr Seite

<b>Battery Abuse Analysis using LS-DYNA</b> P. L'Eplattenier, I. Çaldichoury (LSTC); J. Marcicki, A. Bartlett, X. G. Yang, V. Mejia, M. Zhu, Y. Chen (Ford Research and Innovation Center) .....	44
<b>Integration of Single Cells of Lithium Ion Traction Battery in Crash Simulation</b> M. Funcke (Forschungsgesellschaft Kraftfahrwesen Aachen); S. Lovski, L. Eckstein (RWTH Aachen University) .....	46
<b>Entwicklung eines optimierten Seitencrashkonzepts für das batterieelektrische Fahrzeugkonzept Urban Modular Vehicle</b> M. Schäffer, M. Münster, R. Sturm, H. E. Friedrich (DLR) .....	48

**CRASH (COMPOSITES)**Raum 1, Dienstag, 11. Oktober, 15:50 – 17:10 Uhr Seite

<b>Closed Simulation Process Chain for Short Fiber Reinforced Plastic Components with LS-DYNA</b> B. Lauterbach, M. Erzgräber (Adam Opel); C. Liebold, M. Helbig, A. Haufe (DYNAmore) .....	50
<b>Interactive Fracture Criterion for SGF-PP: Validation on Lower Bumper Support</b> M. Nutini, M. Vitali (LyondellBasell); M. Erzgräber, B. Lauterbach (Adam Opel) .....	52
<b>Crash Simulation of Long Fiber Reinforced Thermoplastics Considering Damage and Failure</b> L. Schulenberg, J. Lienhard (Fraunhofer IWM) .....	53
<b>Modeling Approaches for Endless-Fiber Reinforced Polymers in Crashworthiness Applications</b> G. Oberhofer, M. Vogler, H. Gese, H. Dell (Matfem Partnerschaft Dr. Gese & Oberhofer) .....	55

**SAFETY (AIRBAGS AND PRESSURE TUBES)**

Raum 2, Montag, 10. Oktober, 16:20 – 17:20 Uhr

Seite

**Simulation von Kaltgasgeneratoren unter Berücksichtigung des Joule-Thompson-Effekts**

T. Laufer, A. Heym (Takata) ..... 57

**Update on CPM for Airbag Modelling**

J. Wang (LSTC) ..... 59

**\*DEFINE\_PRESSURE\_TUBE: A Pressure Tube Sensor for Pedestrian Crash Simulation**

J. Karlsson (DYNAmore Nordic) ..... 61

**SAFETY (DUMMIES)**

Raum 2, Montag, 10. Oktober, 17:50 – 18:50 Uhr

Seite

**Correlation Studies for WorldSID-50 and Q10/Q6 Child Dummies in Latest Occupant Simulations**

T. Kotucha, E. Schneider (Adam Opel) ..... 63

**Dummy Models General Update**

F. Schüssler (Humanetics Europe) ..... 65

**News about the THUMS Human Model**

D. Fressmann, N. Lazarov (DYNAmore) ..... 67

**PROCESS (SHEET METAL FORMING)**

Raum 3, Montag, 10. Oktober, 16:20 – 17:20 Uhr

Seite

**Umformsimulationen, Schnittstellen und Prozesse**

M. Fleischer, J. Sarvas, H. Grass, J. Meinhardt (BMW) ..... 68

**Berücksichtigung von schergeschnittenen Blechkanten zur Auslegung von Formgebungsprozessen höherfester Stahlwerkstoffe in der FEM-Umformsimulation mit LS-DYNA**

T. Beier, S. Woestmann (Thyssenkrupp Steel Europe) ..... 69

**Sheet Metal Forming of Niobium RF Crab Cavities at CERN**A. Amorim Carvalho, S. Atieh, J-P. Brachet, O. Capatina, M. Toscan du Plantier,  
A. Dallochio, V. Gerbant, G. Favre, M. Garlaschè, L. Giordiano, R. Leuxe, M. Narduzzi,  
L. Prever-Loirii (CERN) ..... 71

**PROCESS (SHEET METAL FORMING)**

Raum 3, Montag, 10. Oktober, 17:50 – 18:50 Uhr

Seite

**Parameter Identification of Two Phenomenological Damage Models for Sheet Metal Forming**

S. Heibel, W. Nester (Daimler); T. Clausmeyer, Prof. E. Tekkaya (TU Dortmund)..... 73

**Analyse der zu einer verzögerten Rissbildung führenden umformtechnischen Randbedingungen**

M. Teschner, M. Schneider, M.Otto (Salzgitter Mannesmann Forschung) ..... 75

**Implementierung einer Netzwerkschnittstelle in LS-DYNA zur gekoppelten Simulation**

S. Kriechenbauer (Fraunhofer IWU)..... 77

**PROCESS (CONTINUOUS FIBER-REINFORCED POLYMERS)**

Raum 3, Dienstag, 11. Oktober, 9:00 – 10:20 Uhr

Seite

**Finite Element Simulation of Delamination During Side Milling of Cross-Ply Carbon Fiber Reinforced Polymer (CFRP) Boards**

H. Vazquez Martinez, P. Esch, K. Patel (Fraunhofer IPA) ..... 79

**BMBF MAI qfast:****Design and Validation with Ultrasim for Continuous Fiber Reinforced Parts**

S. Ebli, S. Glaser, A. Wüst (BASF)..... 81

**Berücksichtigung der umformbedingten Faser-Reorientierung bei der Verzugssimulation von CFK-Bauteilen**

C. Amann, S. Kreissl, H. Grass, J. Meinhardt (BMW); C. Liebold (DYNAmore); Prof. M. Merklein (Universität Erlangen-Nürnberg) ..... 85

**Forming Simulations in LS-DYNA using the Material Law 249**

B. Eck, G. Chambon (Faurecia Automotive Composite Technologies) ..... 87

**PROCESS (WELDING AND COOLING)**

Raum 3, Dienstag, 11. Oktober, 11:00 – 12:20 Uhr

Seite

**High Performance Computing Welding Analysis with DynaWeld and Parallelized LS-DYNA Solvers**

T. Loose (Ing.büro T. Loose); M. Bernreuther, B. Große-Wöhrmann, J. Herzer (Universität Stuttgart); Prof. U. Göhner (DYNAmore) ..... 89

**Simulation of Pulsed Water Cooling for Continuous Casting with LS-DYNA**

S. Scheibelhofer, J. Kronsteiner, S. Ucsnik (Leichtmetallkompetenzzentrum Ranshofen); P. Simon, H. Böttcher (AMAG Austria Metall) ..... 91

**Durability Assessment of Welded Structures Based on Welding Simulation with LS-DYNA**

A. Krasovskyy (DYNAmore Swiss); A. Virta (Winterthur Gas &amp; Diesel); T. Klöppel (DYNAmore)..... 93

**Recent Developments for Welding Simulations in LS-DYNA and LS-PrePost**

M. Schill, A. Jernberg (DYNAmore Nordic); T. Klöppel (DYNAmore) ..... 94

**PROCESS (SHEETMETAL FORMING)**Raum 3, Dienstag, 11. Oktober, 15:50 – 17:10 Uhr Seite

<b>Developments in LS-DYNA for Metal Forming Simulation</b> X. Zhu, L. Zhang (LSTC) .....	96
<b>Strategies to Improve the Efficiency of Sheet Metal Forming Simulations with LS-DYNA</b> W. Rimkus, M. Fritz (Hochschule Aalen); P. Vogel (DYNAmore) .....	99
<b>Advances in Characterization of Sheet Metal Forming in JSTAMP/NV</b> R. Liu, H. Fukiharu (JSOL) .....	100
<b>Updates in eta/DYNAFORM V.5.9.3</b> P. Vogel (DYNAmore); J. Du Bois (Engineering Technology Associates) .....	102

**MATERIALS (PARAMETER IDENTIFICATION)**Raum 2, Dienstag, 11. Oktober, 9:00 – 10:20 Uhr Seite

<b>Experimentelle Untersuchung des Probengeometrieinflusses auf das Deformationsverhalten amorpher thermoplastischer Kunststoffe</b> M. Helbig, D. Koch (DYNAmore); J. Irslinger, A. Hirth (Daimler) .....	103
<b>Calibration and Appliance of the Wilkins Damage Model for Aluminium Cast Aluminium</b> C. Mühlstätter (Leichtmetallkompetenzzentrum Ranshofen) .....	104
<b>4a impetus (part 1): Dynamic Material Characterization of Plastics – Development in the Past 10 Years</b> A. Fertschej, P. Reithofer, M. Rollant (4a engineering) .....	107
<b>4a impetus (part 2): Innovations – Test Methods, MAT_SAMP-1, Anisotropy, Composites and more</b> A. Fertschej, P. Reithofer, M. Rollant (4a engineering) .....	109

**MATERIALS (SHORT FIBER-REINFORCED POLYMERS)**Raum 2, Dienstag, 11. Oktober, 11:00 – 12:20 Uhr Seite

<b>Some Aspects on Characterizing and Modeling of Unreinforced and Short Fiber Reinforced Polymers in Crashworthiness Applications</b> M. Vogler, G. Oberhofer, H. Dell (Matfem Partnerschaft Dr. Gese & Oberhofer) .....	111
<b>Potential of MAT_157 for Short-Fiber-Reinforced Injection Molded Plastic Components</b> W. Korte, S. Pazour, M. Stojek (PART Engineering) .....	113
<b>Modeling of Fiber-Reinforced Plastics Taking into Account the Manufacturing Process</b> C. A. T. Reclusado (Fraunhofer EMI); S. Nagasawa (Fuji Heavy Industries) .....	116
<b>*MAT_4a_micromec – Micro Mechanic Based Material Model</b> A. Erhart, S. Hartmann (DYNAmore); B. Jilka, P. Reithofer (4a engineering) .....	118

**MATERIALS AND SIMULATION**Raum 2, Dienstag, 11. Oktober, 17:40 – 19:00 Uhr Seite

<b>Simulation and Optimisation of Functionally Graded Auxetic Structures</b> N. Novak, Prof. M. Vesenjak, Prof. Z. Ren (University of Maribor) .....	120
<b>Novel Approach to Model Laminated Glass</b> R. Böhm (Karlsruher Institut für Technologie); A. Erhart, A. Haufe (DYNAmore) .....	122
<b>Features in LS-DYNA R8.1 for Structural Mechanics – Part I + II</b> T. Erhart (DYNAmore) .....	124

**OPTIMIZATION AND ROBUSTNESS**Raum 1, Dienstag, 11. Oktober, 9:00 – 10:20 Uhr Seite

<b>LS-TaSC Product Status</b> K. Witowski (DYNAmore); W. Roux (LSTC) .....	125
<b>Finding the Best Thickness Run Parameterization for Optimization of Tailor Rolled Blanks</b> N. Klinke (Mubea Tailor Rolled Blanks); Prof. A. Schumacher (Universität Wuppertal) .....	127
<b>Automated Generation of Robustness Knowledge for Selected Crash Structures</b> C. Diez, C. Wieser, L. Harzheim (Adam Opel); Prof. A. Schumacher (Universität Wuppertal) .....	129
<b>Process to Improve Optimization with Combined Robustness Analysis Results</b> L. Jansen, D. Borsotto, C.-A. Thole (Sidact) .....	131

**CONNECTION MODELING**Raum 2, Mittwoch, 12. Oktober, 9:00 – 10:20 Uhr Seite

<b>Temperature Dependent TAPO Model for Failure Analysis of Adhesively Bonded Joints due to Temperature Induced Service Loading</b> P. Kühlmeyer, Prof. A. Matzenmiller (Universität Kassel) .....	133
<b>Charakterisierungsversuche und Parameterbestimmung für die Kohäsivzonenmodellierung von Polyurethan-Kleberverbindungen</b> M. Brodbeck, S. P. Sikora (DLR) .....	135
<b>Self-Pierce Riveting of Materials with Limited Ductility Investigated with the Bai-Wierzbicki Damage Model in GISSMO</b> M. Hofmann, R. Anderssohn, Prof. T. Wallmersperger (TU Dresden); M. Jäckel, D. Landgrebe (Fraunhofer IWU) .....	137
<b>Prozess- und Zerrei-Simulationen von punktförmigen Verbindungen im Automobilbau unter Berücksichtigung unscharfer Prozess-Parameter</b> I. Lepenies, A. Saharneau, P. Friedrich (SCALE) .....	139

**DROP TEST AND IMPACT**Raum 3, Dienstag, 11. Oktober, 17:40 – 19:00 Uhr Seite

<b>Simulation des Flugzeuganpralls auf Stahlbetonstrukturen</b> M. Grosse, R. Schlegel (Dynardo); H. Friedl (BKW) .....	140
<b>Comparing Predicted and Measured Accelerations from a Simple Drop Test Experiment</b> R. Boag (International Nuclear Services) .....	141
<b>Validation of a FEA Model of a Nuclear Transportation Package under Impact Conditions</b> C. Berry (International Nuclear Services) .....	143

**IMPACT, RUPTURE AND CONTAINMENT**Raum 3, Mittwoch, 12. Oktober, 11:00 – 12:20 Uhr Seite

<b>Some Observations on Artificial Bulk Viscosity in LS-DYNA: What Noh Knew in 1978</b> L. Schwer (Schwer Engineering & Consulting Services) .....	145
<b>Damping – Oscillation Elimination after Rupture</b> M. Dobes, J. Navratil (Robert Bosch / Brno University of Technology) .....	147
<b>Abbildung von Gußgehäusen und Schrauben in der Containment Simulation</b> S. Edelmann, C. Gross, H. Chladek (Inprosim); M. Marschner (KBB) .....	149
<b>Simulation of Containment-Tests at a Generic Model of a Large-Scale Turbocharger with LS-DYNA</b> S. Hennig, H. Honermeier, M. Jagic, M. Schönborn (Ingenieurbüro Huß & Feickert); Prof. A. Huß (Frankfurt University of Applied Sciences) .....	151

**NOISE, VIBRATION AND HARSHNESS**Raum 2, Dienstag, 11. Oktober, 15:50 – 17:10 Uhr Seite

<b>NVH Simulations for Car Seat</b> T. Kupczyk (Faurecia Grójec R&D Center); L. Guerin (Faurecia Automotive Seating) .....	154
<b>Model Set up and Analysis Tools for Squeak and Rattle in LS-DYNA</b> T. Fokolidis (Beta CAE Systems); M. Moridnejad (Volvo Car) .....	156
<b>Evaluation of Equivalent Radiated Power with LS-DYNA</b> Y. Huang, Z. Cui (LSTC) .....	158
<b>Eigensolution Technology in LS-DYNA</b> R. Grimes (LSTC) .....	160

**IMPLICIT SIMULATIONS**Raum 1, Mittwoch, 12. Oktober, 9:00 – 10:20 Uhr Seite

<b>Simulation with Implicit Time Integration of High Loaded Areas of a Forming Tool for Large Presses using LS-DYNA</b> F. Koch, P. Thumann, Prof. M. Wagner (OTH Regensburg); B. Suck, J. Meinhardt (BMW Group) .....	162
<b>Funktionssimulation: Deckelsimulation mit LS-DYNA</b> M. Geuther (Dr. Ing. h.c. F. Porsche); H. Abboud (GNS).....	164
<b>Funktionssimulation: Spoilersimulation mit LS-DYNA</b> M. Geuther (Dr. Ing. h.c. F. Porsche); B. Gajewski (Bertrandt).....	164
<b>Funktionssimulation: Dichtungssimulation mit LS-DYNA</b> M. Geuther (Dr. Ing. h.c. F. Porsche); I. Jurrmann (Bertrandt) .....	164

**SIMULATION AND CONTROL**Raum 1, Mittwoch, 12. Oktober, 11:00 – 12:20 Uhr Seite

<b>FE oriented Virtual Test of Closure Systems</b> C. Gembus, G. Büdding, W. Rieger (Brose Schließsysteme).....	165
<b>Simulation of Wear Processes in LS-DYNA</b> T. Borrvall, A. Jernberg, M. Schill (DYNAmore Nordic); L. Deng, M. Oldenburg (Luleå Technical University) .....	167
<b>Messung und Simulation von Verschleiß in einem anwendungsnahen tribologischen Prüfstand</b> A. Fertschej, B. Hirschmann, P. Reithofer (4a engineering) .....	169
<b>Control System</b> I. Yeh (LSTC); C. Keisser (DYNAmore France) .....	173

**MULTIPHYSICS**Raum 2, Mittwoch, 12. Oktober, 11:00 – 12:20 Uhr Seite

<b>Latest Developments in Automotive Aerodynamics using LS-DYNA</b> I. Çaldichoury, F. DelPin, R. Paz (LSTC) .....	174
<b>Recent Updates for the Structural Conjugate Heat Transfer Solver in LS-DYNA</b> T. Klöppel (DYNAmore).....	175
<b>Saving Calculation Time for Electromagnetic/Mechanical/Thermal Coupled Simulations using the New EM 2D/3D Capabilities</b> I. Çaldichoury, P. L'Eplattenier (LSTC) .....	177
<b>Towards a Multi-Physics Material Toolbox for LS-DYNA</b> M. Schenke, Prof. W. Ehlers (Universität Stuttgart) .....	178



**FINITE ELEMENT TECHNOLOGY**Raum 3, Mittwoch, 12. Oktober, 9:00 – 10:20 Uhr Seite

<b>Tests with a Sensitive Specimen Geometry Confirm Solid Elements when the Aspect Ratio is Below Four</b> T. Tryland (Sintef Raufoss Manufacturing).....	180
<b>Predictive Fracture Modeling in Crashworthiness: A Discussion of the Limits of Shell-Discretized Structures – Part I + II</b>	
A. Haufe, F. Andrade (DYNAmore); M. Feucht (Daimler); D. Riemensperger (Adam Opel); K. Schweizerhof (Karlsruhe Institute of Technology) .....	182
<b>Improved Robust Low Order Solid and Solid-Shell Finite Elements with Incompatible Modes / Enhanced Assumed Strains for Explicit Time Integration</b>	
C. Schmied, Prof. K. Schweizerhof (Karlsruhe Institute of Technology); S. Mattern (DYNAmore) .....	183

**ARENA 2036**Raum 1, Dienstag, 11. Oktober, 17:40 – 19:00 Uhr Seite

<b>ARENA2036 – Above and Beyond</b>	
J. Dittmann, P. Middendorf (Universität Stuttgart).....	185
<b>A Multiscale Approach for the Mechanical Investigation of Textile-Based Composite Structures within a Closed Process Chain</b>	
M. Vinot, M. Holzapfel (DLR); C. Liebold (DYNAmore).....	186
<b>Textile Process Simulation for Composite Structures</b>	
H. Finckh, F. Fritz, Prof. G. T. Gresser (ITV Denkendorf).....	188
<b>Closing the Simulation Process Chain using a Solver Independent Data Exchange Platform: The Digital Prototype</b>	
C. Liebold, A. Haufe (DYNAmore).....	190

**PERFORMANCE OF LS-DYNA ON NEW HARDWARE**Raum 4, Montag, 10. Oktober, 17:50 – 18:50 Uhr Seite

<b>Erkenntnisse aus aktuellen Performance-Messungen mit LS-DYNA</b>	
E. Schnepf, E. Kehl (Fujitsu Technology Solutions); C.-S. Kuo (ict information communication technology) .....	192
<b>LS-DYNA Performance auf NEC LX-Systemen</b>	
F. Unger (NEC).....	193

**LS-DYNA IN THE CLOUD**


---

Raum 4, Dienstag, 11. Oktober, 11:00 – 12:20 Uhr Seite


---

<b>How Cloud HPC Enables the Digital Transformation in Product Development</b> T. Smith (Rescale).....	194
<b>Hybrid Cloud HPC Cluster Solutions – Challenges, Impact and Industrial Use Cases</b> J. Tamm, A. Heine (CPU 24/7).....	195
<b>HPC in the Cloud: Gompute Support for LS-DYNA Simulations</b> R. Díaz (Gompute (Gridcore)) .....	196
<b>LSTC and DYNAmore Cloud Services</b> Prof. U. Göhner (DYNAmore).....	197

**SIMULATION DATA MANAGEMENT AND COMPRESSION**


---

Raum 1, Dienstag, 11. Oktober, 11:00 – 12:20 Uhr Seite


---

<b>LoCo - Multistage Assembly with a Wheel Generation Process Example</b> M. Thiele, A. Saharneau, D. Rentsch (SCALE).....	198
<b>Reducing Storage Footprint and Bandwidth Requirements to a Minimum: Compressing Sets of Simulation Results</b> S. Mertler, S. P. Müller (Sidact).....	200
<b>Compression Methods for Simulation Models in SDM Systems</b> J. Richter, W. Graf (TU Dresden); M. Büchse, M. Thiele, C. Löbner, M. Liebscher (SCALE) .....	202
<b>Managing a Global IT Infrastructure for CAE</b> C. Woll (GNS Systems).....	204

**RAUM FÜR NOTIZEN**

Seiten 206-208

# Recent Developments in LS-DYNA®

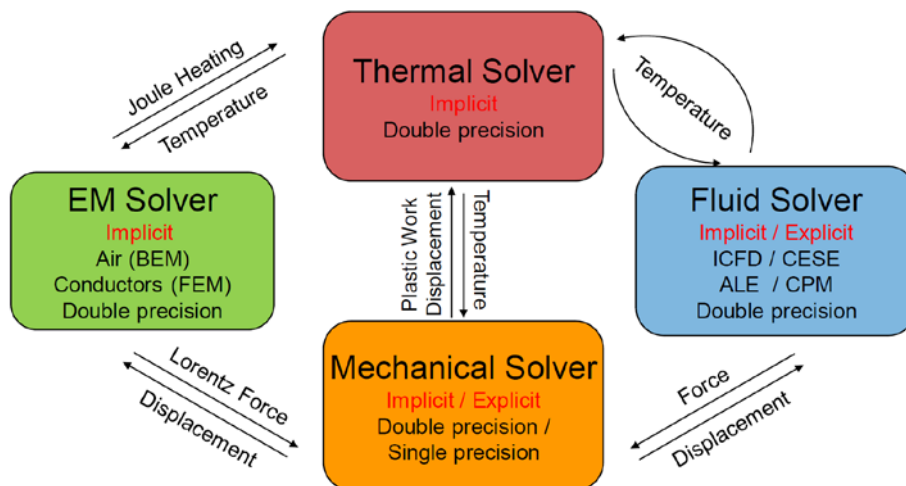
John Hallquist, Roger Grimes, Jason Wang,  
and many other developers

Livermore Software Technology Corporation (LSTC), Livermore, USA

## 1 Introduction

The goal of this presentation is to provide a brief overview of some recent, ongoing and future developments in LS-DYNA®, which is the general-purpose finite-element program of the Livermore Software Technology Corporation (LSTC).

In particular, LSTC follows a one-code strategy which combines multi-physics capabilities into one scalable code for solving highly nonlinear transient problems. These coupling possibilities are of great importance to enable out-of-the-box solutions for complex real-world problems that require multi-physics and multi-stage approaches. The following figure reveals the possible data exchange between the available implicit and explicit solvers in LS-DYNA®.



Moreover, besides its fully automated contact analysis capabilities that enabled users worldwide to successfully solve complex crash and forming problems, LS-DYNA® provides the following (uncomplete) list of features

- Manifold of 1-d, 2-d and 3-d finite-element discretizations
- Arbitrary Lagrange-Eulerian (ALE) discretization
- Mesh-free (particle) methods: EFG, SPH, SPG, CPM (“airbag particles”), DEM
- Acoustics, frequency response, modal methods
- Over 290 Material models
- Capabilities to parameterize loads and supports
- User Interfaces
- Rigid bodies

With these features at hand, LS-DYNA® provides the tools to solve applications in the fields of

- Crashworthiness & occupant safety
  - Airbags, seatbelts, pretensioners, retractors, slings, sensors, accelerometers
  - Connection models for spot welds, rivets, bolts and glues
- Aerospace
  - Bird strike (windshield and engine blade), blade containment and failure analysis
- Tank sloshing and hydroplaning

- Manufacturing
  - Metal Forming (hot & cold), hydroforming, forging, deep drawing and cutting
  - Electromagnetic forming, inductive heating
  - Welding and heat treatment
- Drop testing
- Blast and explosives modeling
- Earthquake engineering
- NVH and durability analysis
- Sports and consumer products (golf clubs, golf balls, baseball bats, helmets, diapers)
- Biomedical device and implant design

Finally, LS-DYNA<sup>®</sup> provides two parallel solution methods that are suitable for shared and distributed memory machines, respectively. Herein, the distributed memory solver for massively parallel processing (MPP) provides very short turnaround times on Unix, Linux and Windows clusters.

Besides LS-DYNA<sup>®</sup>, LSTC develops sophisticated tools to support the model creation and simulation process of large deformable structures. In particular, these are

- LS-PrePost<sup>®</sup>: Pre- and postprocessing
- LS-Opt<sup>®</sup>: Optimization and Workflow
- LS-TaSC: Topology optimization

## 2 Examples

This is a small selection of the many improvements that have been implemented in LS-DYNA<sup>®</sup>.

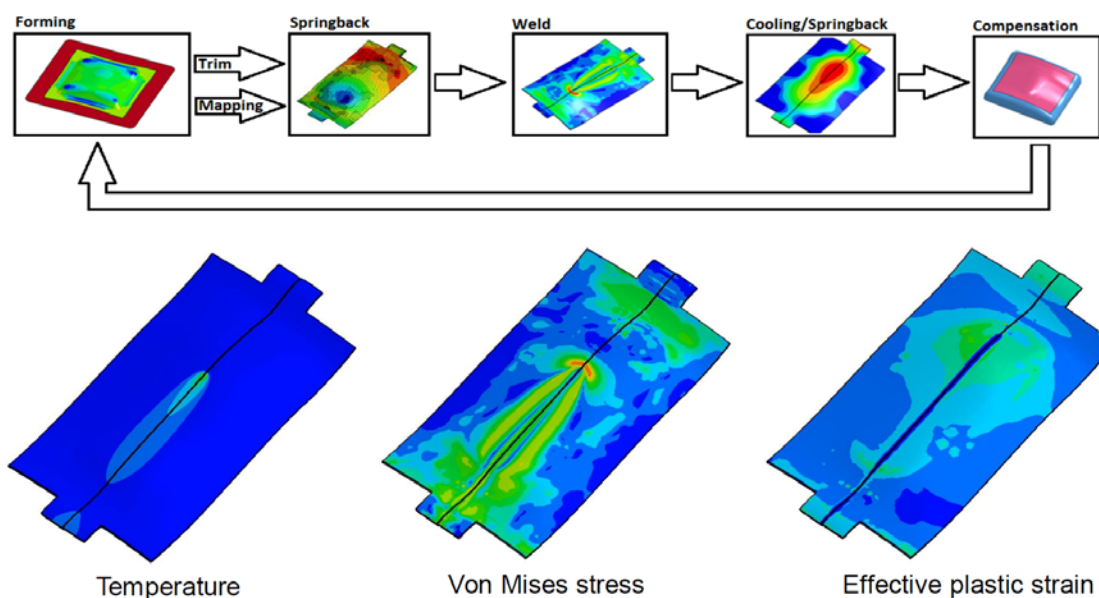


Fig.1: Welding process chain.

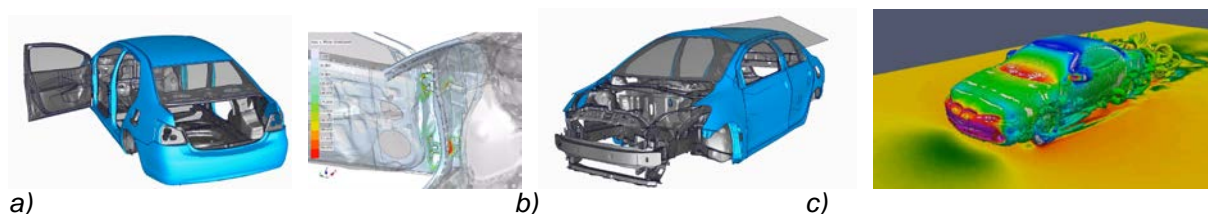


Fig.2: Improvements on implicit capabilities for a) door sag applications and b) roof crush. New turbulence models for the incompressible fluid solver ICFD for external aerodynamics.

## 3 Historical Review

LSTC was founded in 1987 by John O. Hallquist to commercialize as LS-DYNA the public domain code that originated as DYNA3D. DYNA3D was developed at the Lawrence Livermore National Laboratory, by LSTC's founder, John Hallquist.

---

# Modeling and Characterization of Continuous-Discontinuous Long Fiber-Reinforced Polymer Structures

T. Böhlke, F. Henning, L. Kärger, T. Seelig, K.A. Weidenmann,

Karlsruhe Institute of Technology (KIT)

[thomas.boehlke@kit.edu](mailto:thomas.boehlke@kit.edu)

Discontinuous long fiber reinforced polymer structures with local continuous fiber reinforcements represent an important and new class of lightweight materials. This class of materials has a significant potential for energy savings due to the high specific stiffness and strength as well as the variety of design options in diverse technical applications, e.g., in vehicle construction. In contrast to the continuous fiber-reinforced composites of non-crimp or woven fabrics, there is still a lack of integrated and experimentally proven concepts for the manufacturing, modeling and dimensioning of combinations of discontinuously and continuously reinforced polymer structures. Especially in the field of application of three-dimensional load-bearing structures, there is considerable demand for the enhancement of scientific methods.

In the talk, long fiber reinforced sheet molding compounds (SMC) and thermoplastics (LFT) are considered. The compression molding process is analyzed by in-mold rheological measurement and modeled by different (macroscopic) approaches for fiber interaction and viscosity. X-ray computed tomography is used for the analysis of the composite's microstructure as well as to determine fiber orientation tensors and fiber length distributions. Additionally, the data is used for both mean field homogenization as well as full-field simulations. The full-field modeling as well as experimental data are used to evaluate the different mean field approaches. The effective directional dependent material behavior of LFT and SMC is investigated by mechanical testing including biaxial loads.

Buck, F., Brylka, B., Müller, V., Müller, T., Weidenmann, K. A., Hrymak, A. N., Henning, F., Böhlke, T.: Two-scale structural mechanical modeling of long fiber reinforced thermoplastics. *Composites Science and Technology* 117, 159-167 (2015), DOI: 10.1016/j.compscitech.2015.05.020

Buck, F., Brylka, B., Müller, V., Müller, T., Hrymak, A. N., Henning, F., Böhlke, T.: Coupling of mold flow simulations with two-scale structural mechanical simulations for long fiber reinforced thermoplastics. *Materials Science Forum* 825-826, 655-662 (2015) DOI: 10.4028/www.scientific.net/MSF.825-826.655

Müller, V., Böhlke, T.: Prediction of effective elastic properties of fiber reinforced composites using fiber orientation tensors. *Composite Science and Technology* 130, 36-45 (2016)

Müller, V., Kabel, M., Andrä, H., Böhlke, T.: Homogenization of linear elastic properties of short fiber reinforced composites - A comparison of mean field and voxel-based methods. *International Journal of Solids and Structures* 67-68, 56-70 (2015)

Müller, V., Brylka, B., Dillenberger, F., Glöckner, R., Kolling, S., Böhlke, T.: Homogenization of elastic properties of short-fiber reinforced composites based on measured microstructure data. *Journal of Composite Materials*, published online before print (2015)

# Status and Challenges of Safety CAE in Vehicle Development

S. Frik

Adam Opel

# Enabling Effective and Easy to Access Simulation

S. Gillich  
Intel

E. Schnepf  
Fujitsu Technology Solutions

# Dell HPC System for Manufacturing

Tobias Vogt

Dell

Manufacturing and engineering customers need to focus on securely achieving results and breakthroughs — not troubleshooting system bottlenecks. The Dell HPC System for Manufacturing enables these users to run complex design simulations, including structural analysis and computational fluid dynamics, which combines the flexibility of customized HPC systems with the speed, simplicity and reliability of pre-configured systems.



# **Insassensimulation Kindersicherheit bei Mercedes-Benz**

Dr. Hakan Ipek, Joachim Fausel

Daimler AG

Die Fahrzeugsicherheit gehört zu den Kernwerten der Marke Mercedes-Benz. So auch die Kindersicherheit welche in einem eigenen Fachreferat vorangetrieben wird. Aktuell stellt die Insassensimulation einen wesentlichen Bestandteil der Entwicklungsarbeit für die Kindersicherheit dar. Der Vortrag befasst sich mit der Vorgehensweise und den verwendeten Methoden in der Insassensimulation Kindersicherheit. Erfahrungen mit aktuellen Ratinganforderungen und modernen Schutzsystemauslegungen werden ebenfalls vorgestellt.

# Historische Entwicklung Funktionssimulation bei der Porsche AG

M. Geuther

Dr. Ing. h.c. F. Porsche

# **Einsatz der Umformsimulation in der Modellierung und Verfahrensentwicklung von Blechumformprozessen**

Prof. M. Liewald

Universität Stuttgart

# LS-OPT<sup>®</sup>: Status and Outlook

Nielen Stander<sup>1</sup>, Anirban Basudhar<sup>1</sup>, Imtiaz Gandikota<sup>1</sup>,  
Katharina Witowski<sup>2</sup>, Åke Svedin<sup>3</sup>, Christoffer Belestam<sup>3</sup>

<sup>1</sup>Livermore Software Technology Corporation, Livermore, CA, USA

<sup>2</sup>DYNAmore GmbH, Stuttgart, Germany

<sup>3</sup>DYNAmore Nordic AB, Linköping, Sweden

## 1 Introduction

New features added to LS-OPT Version 5.2 are discussed. An outlook of the next version, which includes parameter identification based on Digital Image Correlation, support vector machine classification and interactive tables as a postprocessing feature, is given.

## 2 Digital Image Correlation

Digital Imaging Correlation (DIC) is an optical method which provides full-field displacement measurements for mechanical tests of materials and structures. It can be used to obtain temporal displacement, deformation or strain fields from an experimental coupon and can be combined with Finite Element Analysis to identify the constitutive properties of a material.

Fig. 1 shows an example of matching in time and space. Full field test results of a tensile test are used to identify material parameters.

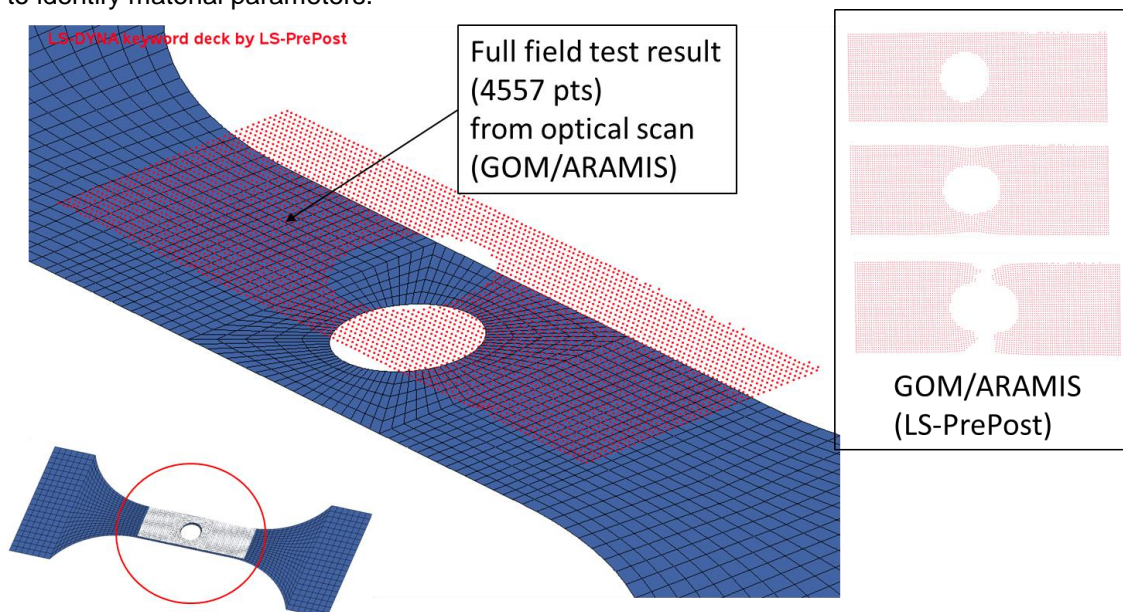


Fig.1: Full field test results and FE model of tensile test (Courtesy Martin Helbig, Andre Haufe, DYNAmore GmbH)

## 3 Support Vector Classification

Support vector classification (SVC) is a machine learning technique that classifies different data categories using a decision boundary. Unlike metamodels, which approximate the response values at design configurations, a decision boundary only classifies the design configurations (e.g. safe or failed). In the context of design optimization and reliability assessment, the boundary represents a constraint or a failure boundary. Only the classification information (e.g. pass or failed) at the sampled designs is needed for training an SVC boundary, unlike metamodels, which need the actual response values. As a result, SVC works equally well for continuous responses and for discontinuous or binary responses. Therefore, the classification-based approach is particularly useful for handling discontinuous or binary responses, which hamper the accuracy of metamodels. Fig. 2 shows a comparison between the classification approach and metamodeling.

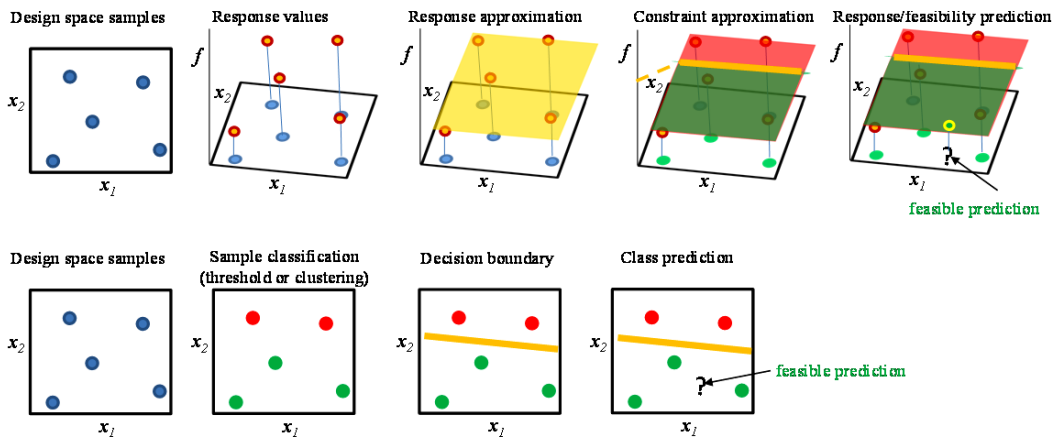


Fig.2: Summary of basic classification method (bottom) and comparison to metamodeling (top).

### 4 Interactive Tables

Interactive tables for postprocessing of optimization results are currently developed. New features are amongst others several filtering options, sorting with respect to selected columns and generation of virtual points including the possibility to run new simulations from the viewer. An example is displayed in Fig. 3.

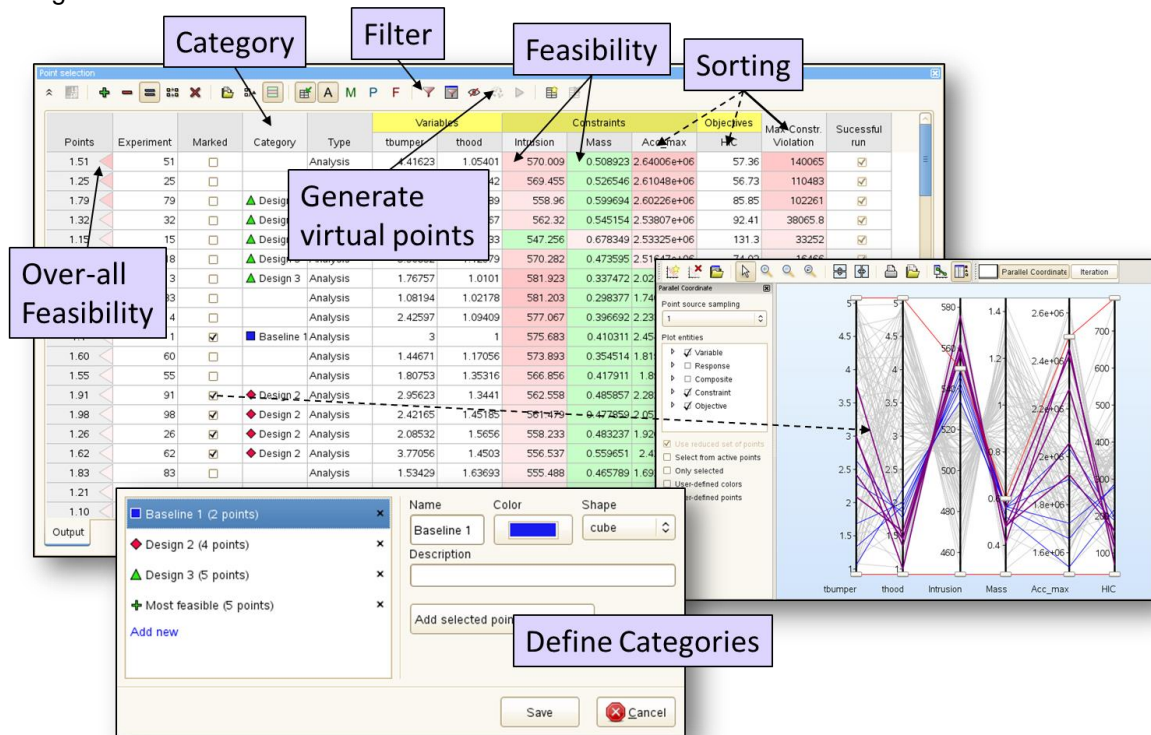


Fig.3: Interactive tables in LS-OPT; filtering and sorting of simulation results, generation of virtual points and running new simulations from the LS-OPT viewer.

### 5 Summary

The presentation summarizes new LS-OPT features in Version 5.2 and discusses major features under development. Features to use Digital Image Correlation results for parameter identification, SVC and interactive tables to evaluate optimization results will be available in Version 6.0.

### 6 Literature

[1] Stander, N., Basudhar, A.: "LS-OPT Status and Outlook", 14<sup>th</sup> International LS-DYNA Users Conference, 2016, Dearborn, MI

# **LS-DYNA in the Development Process of Occupant Restraint Systems**

K. Elsässer

ZF TRW

# **A New Versatile Tool for Simulation of Failure in LS-DYNA, and the Application to Aluminum Extrusions**

P. Du Bois  
Consultant

M. Feucht  
Daimler

F. Andrade  
DYNAmore

# **Berücksichtigung des Bake Hardening Effekts bei umgeformten Blechteilen für die Crashsimulation**

D. Riemensperger

Adam Opel



# Virtuelle Produktentwicklung und Craschauslegung von Stahl-Werkstoffverbundsystemen

D. Pieronek, L. Keßler, H. Richter, S. Myslowicki

thyssenkrupp Steel Europe AG

Durch Plattieren können Blechwerkstoffe mit unterschiedlichen Eigenschaften zu einem maßgeschneiderten Werkstoffverbund vereinigt werden. thyssenkrupp Steel setzt in einem patentierten Herstellungsverfahren das Warmwalzplattieren ein, um verschiedene Stähle miteinander zu verbinden und diese weiterführend als innovatives Sandwichprodukt vom Coil anzubieten. Dadurch kann weiterer Leichtbau mit Stahl im Karosseriebau ermöglicht werden.

Aufgrund der Vielzahl an möglichen Verbundkombinationen (Lagenanzahl, Stahlwerkstoffe, Schichtaufbau) wurde im Rahmen der Produktentwicklung eine modulare Simulationsmethode abgeleitet, um die resultierenden Verbundeigenschaften im Vorfeld numerisch prognostizieren zu können. Dadurch können verschiedenste Stahl-Sandwichvarianten am Computer effizient vorbewertet werden und der experimentelle Aufwand im Entwicklungsprozess deutlich reduziert werden. Aus dieser Produktentwicklung resultieren die dreilagigen Stahl-Werkstoffverbunde tribond® 1400 und tribond® 1200 für die Warmumformung, welche eine hohe Festigkeit mit hoher Duktilität unter Biegebelastung kombinieren und damit neue Anwendungsfelder in crashrelevanten Fahrzeugstrukturen erschließen können.

Die entwickelte Simulationsmethode wurde für tribond® 1400 und 1200 um eine geeignete Versagensmodellierung für den Verbund sowie Schweißpunkte ergänzt und auf Komponentenebene experimentell abgesichert. Dabei zeigte sich eine hohe Prognosegüte der erweiterten Simulationsmethode auch unter komplexer und dynamischer Belastung.

In virtuellen Potenzialanalysen an einer repräsentativen Gesamtfahrzeugstruktur konnten vielversprechende Leichtbaukonzepte identifiziert werden. Insbesondere Längsträger und die B-Säule scheinen für tribond® prädestiniert zu sein, um gegenüber dem derzeitigen Stand der Technik weitere 10-15% Gewichtseinsparungen zu erreichen. Im Rahmen des Vortrages werden die entwickelte Simulationsmethode für Stahl-Sandwichsysteme inklusive der Möglichkeiten zur Versagensmodellierung präsentiert sowie der virtuelle Produktentwicklungsprozess und potenzielle Anwendungen von tribond® diskutiert (Fig.1).

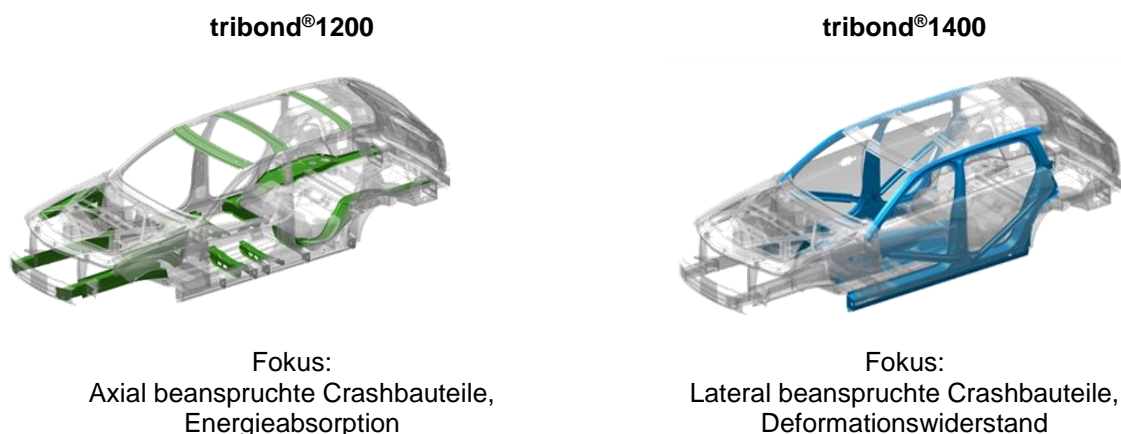


Fig.1: Potenzielle Anwendungsfelder von tribond® in der Karosserie.

---

# Influence of submodel size and evaluated functions on the optimization process of crashworthiness structures

Simon Link, Harman Singh, Axel Schumacher

University of Wuppertal, Faculty for Mechanical Engineering and Safety Engineering, Chair for Optimization of Mechanical Structures, Gaußstraße 20, 42119 Wuppertal, Germany

## 1 Introduction

Optimization of crashworthy structures is an influential aspect during the development of a vehicle body. Structural optimization is a procedure to enhance the mechanical properties of a structure with help of geometrical changes like size, shape and topology. This paper deals with the structural optimization of large crashworthy systems with modifications to its shape and topology using a submodel technique.

## 2 Submodel technique in the optimization process

A submodel is a region of interest cut out from the large system which is to be analyzed in detail. To optimize a submodel separately time dependent boundary conditions are required at the interfaces where the submodel region is cut. These boundary conditions are extracted during the first analysis of the large system and can be in form of displacements of nodes at the interfaces (nodal interface boundary conditions).

### 2.1 Influence of submodel size

In order to maintain the same mechanical behavior of the submodel region as in the large system an update of the boundary conditions is required during the optimization process. If the boundary conditions are exact, the submodel region will deform identical to the deformation of this region in the large system. Here the size of the submodel region and the update of the boundary conditions play a significant role in the optimization process and can have a negative influence on the optimization results. On the other side, the main advantage of the submodel technique is the smaller size of the submodel, which leads to a reduction of computation time, the usage of less computer storage space and the possibility to use finer mesh for higher resolution of critical areas.

### 2.2 Influence of evaluated functions

The development of large systems can be carried out using optimization in different levels. For example, level 1 is the large system and level 2 is a submodel of the large system. Both levels are coupled together with help of interface functions to form a multilevel optimization process using submodel technique. Here it is important to use an appropriate objective and constraint function in the submodel. The function described as an interface in the submodel remains unchanged during one complete iteration. Hence this function cannot be used as objective or constraint in that iteration of submodel optimization. Therefore a correlation between different potential objective functions is necessary in level 1 in order to choose a useful objective function for the submodel optimization. The influence of the size of submodel and the update of the submodel boundary conditions during the optimization process will be shown.

## 3 Application examples

The study is done with different application examples. One of them is the cantilever beam (Fig. 1) impacted by a solid sphere. Optimization functions are the intrusion of the sphere in the structure and the maximal internal energy of the submodel. The restriction is that the solid sphere must be stopped by the cantilever structure. The design variables are the position, the orientation and the size of the bead. The position of the submodel including a bead is optimized in level 1 and the orientation and size of the bead are optimized in level 2.

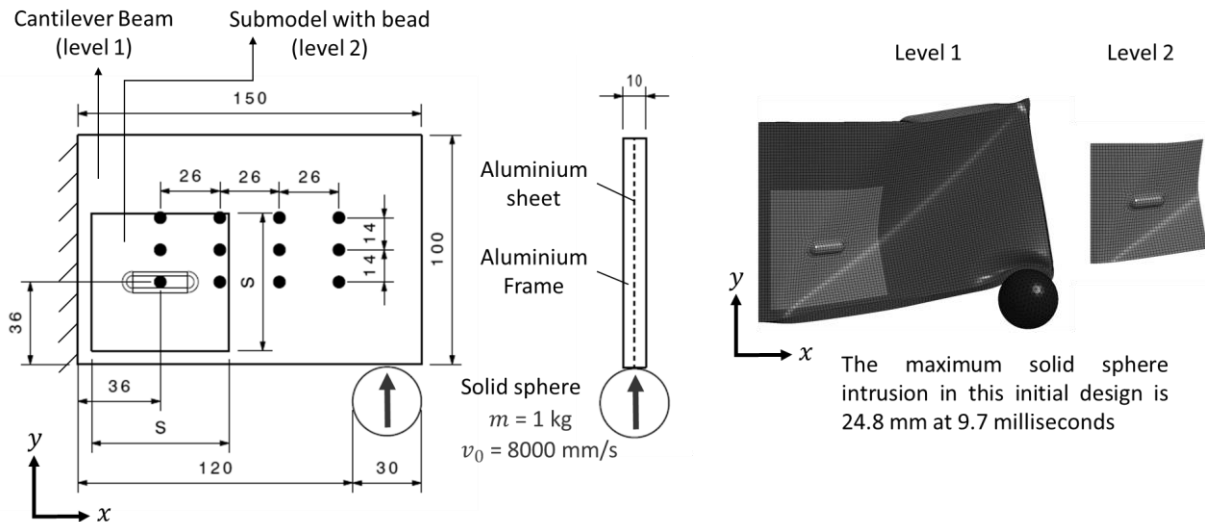


Fig. 1: A cantilever beam impacted by a solid sphere. Fig. 2: Exemplary Deformation in level 1 & 2.

The black dots in Fig. 1 show the 12 possible bead positions. An adjustable full factorial DOE with 12 function calls is used as strategy in level 1. For each function call in level 1, an optimization is conducted with 40 function calls in level 2 using differential evolution algorithm. The design parameters, the objective functions and the optimization results are shown in Table 1. Results show that the submodel size has an influence on the optimization results. It is found that the bead position in level 1 is different for each submodel size. The larger submodel shows better results for sphere intrusion in comparison to the smaller submodel in level 1. On the other hand, there are similarities seen in bead size in level 2. In both cases, the bead size tends to the upper limit during the optimization in order to maximize the internal energy of the submodel. In further research, the correlation between the objective functions of level 1 and level 2 will be shown.

	Level	Parameter Name	Start Value	Lower Limit	Upper Limit	Optimized Values for smaller submodel ( $s = 40$ )	Optimized Values for Larger submodel ( $s = 60$ )
Design parameters	1	Position $X_s$	75 mm	36 mm	114 mm	62 mm	62 mm
		Position $Y_s$	50 mm	36 mm	64 mm	36 mm	50 mm
	2	Bead Length $L_s$	20 mm	10 mm	30 mm	29.96 mm	29.96 mm
		Bead Radius $R_s$	3 mm	2 mm	5 mm	4.84 mm	4.84 mm
		Bead Angle $\theta_s$	0°	Constant in both levels		0°	0°
Objective functions	1	Maximum solid sphere intrusion				22.82 mm	19.51 mm
	2	Maximum internal energy of submodel				1080 N-mm	1455 N-mm

Table 1: Results of the optimization of the cantilever beam with two different submodel sizes.

The second example is a rocker beam in a pole impact load case. Here, the optimization functions are the intrusion of the pole and the mass. The optimization process is done with the “Graph and Heuristic based Topology optimization approach (GHT)” [1]. The design variables manage the topology, the shape and the sizes of the single components of the rocker.

#### 4 Acknowledgement

This research was supported by the "Bundesministerium für Bildung und Forschung" within the scope of the research project "Entwicklung von Softwaremethoden zur effizienten Ersatzmodell gestützten Optimierung für die Craschauslegung im Fahrzeugentwicklungsprozess (eEgO)". Beside the University of Wuppertal, the Automotive Simulation Center Stuttgart (asc(s)), the SCALE GmbH, the GNS mbH, divis GmbH and the Technical University of Munich are involved in the project.

#### 5 Literature

- [1] Ortman, C.; Schumacher, A. (2013): "Graph and heuristic based topology optimization of crash loaded structures", Journal of Structural and Multidisciplinary Optimization (2013) 47:839-854

---

# Battery Abuse Analysis using LS-DYNA

Pierre L'Eplattenier<sup>1</sup>, İñaki Çaldichoury<sup>1</sup>, James Marcicki<sup>2</sup>, Alexander Bartlett<sup>2</sup>, Xiao Guang Yang<sup>2</sup>,  
Valentina Mejia<sup>2</sup>, Min Zhu<sup>2</sup>, Yijung Chen<sup>2</sup>

<sup>1</sup>Livermore Software Technology Corporation, CA, USA

<sup>2</sup>Ford Research and Innovation Center, Dearborn, MI, USA

**\*KEYWORDS:** Battery abuse research and modeling, Spatially-resolved battery modeling, electro-thermal battery modeling

## 1 Introduction

As Lithium-ion batteries see increasing use in a variety of applications, anticipation of the response to abuse conditions becomes an important factor in designing optimized systems. Abuse scenarios with potential relevance to the automotive industry include crash-induced crush leading to an internal short circuit, external short circuit, or thermal ramp, and overcharge conditions. Simulating *each* of these abuse scenarios requires sophisticated modeling tools that span multiple physical and electrochemical phenomena, as well as handle complex geometries that accurately represent battery cells, modules, and packs.

## 2 Model

A distributed Randles circuit model has been added to the electromagnetics (EM) module in LS-DYNA. This model implements so called "1st order Randles circuits" connecting two vis-à-vis nodes on the positive and negative current collectors which define a unit cell. These circuits consist of a state-of-charge dependent voltage source, internal resistance, and RC loop for damping effects. They empirically model the electrochemical processes occurring between the current collectors during charge or discharge, such as electrochemical reactions, lithium transport through the electrodes and separator, and electron transport to reaction sites within the electrodes. The EM solver and Randle circuits are coupled to give the potential, current density, and heating distribution in the unit cell and connected conductors. The heat generation is transferred to the thermal solver, which then feeds back to the temperature dependent Randles circuit parameters.

Several unit cells can be connected together either by a connecting mesh or by applying EM boundary conditions, hence forming a complete battery cell. Similarly, several cells can be coupled together to form a module. The main purpose of this model is the additional capability to model the electrical and thermal response to battery abuse scenarios, such as crash-induced crush. Depending on the local mechanical deformation occurring during a crush scenario, some of the Randles circuits can be replaced by a short resistance (see fig. 1), hence triggering a local increase in the current flow and Joule heating which can lead to thermal runaway.

## 3 Results

Several battery abuse case studies are examined to verify the capability of the modeling tools. The impact of hardware size is investigated, as the thermal behaviour and corresponding severity of the abuse response changes depending on the number of cells and their configuration within a module. Experimental data are used to estimate parameters, confirm the model capability, and identify areas of future work to improve the fidelity and ease of implementation of the simulation tool. Multiple hardware types are compared to demonstrate the relationship between cell performance and module abuse response. As an illustration, fig. 2 shows experimental/numerical comparisons of an external short circuit on a module composed of 4 cells.

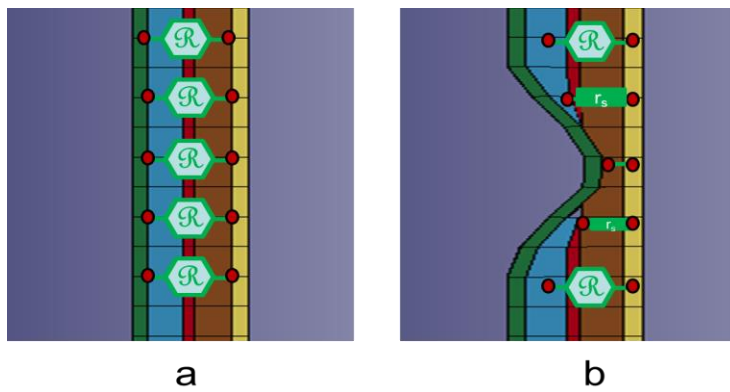


Fig.1: Illustration of the switch from Randles circuits (a) to resistances (b) when an internal short happens due to mechanical deformations.

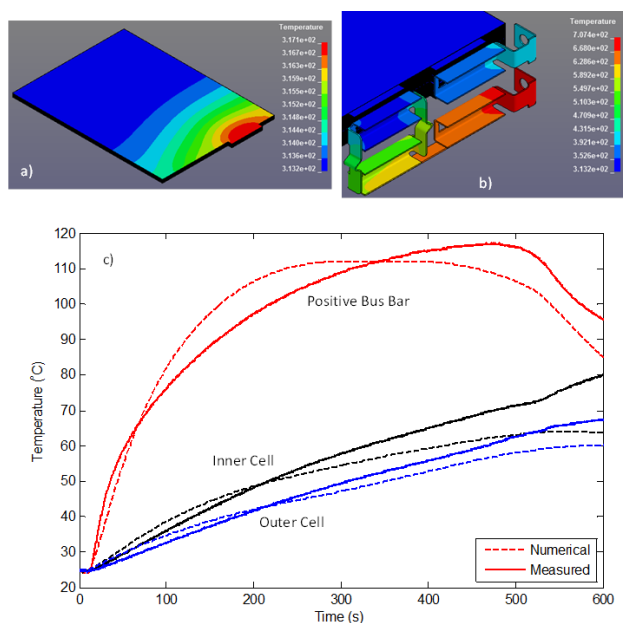


Fig.2: Thermal response of an external short circuit. a) Temperature fringe plot on the positive current collector surface for an outer cell. b) Temperature fringe plot on the bus bars. c) Comparison between experimental and simulated temperature time series data, where dashed lines indicate simulation results and solid lines are experimental measurements. Temperature fringe plots are shown at  $t = 267s$ , contain different scales due to the large temperature gradient between the bus bars and cells, and have units of Kelvin.

#### 4 References

- [1] P. L'Eplattener, I. Çaldichoury, J. Marcicki, A. Bartlett, X.G. Yang, V. Mejia, M. Zhu, Y. Chen, "A Distributed Randle Circuit Model for Battery Abuse Simulations Using LS-DYNA," presented at the 14th International LS-DYNA Conference, 2016.
- [2] J. Marcicki, A. Bartlett, X.G. Yang, V. Mejia, M. Zhu, Y. Chen, P. L'Eplattener, I. Çaldichoury, "Battery Abuse Case Study Analysis Using LS-DYNA," presented at the 14th International LS-DYNA Conference, 2016

---

# Integration of Single Cells of Lithium Ion Traction Battery in Crash Simulation

Dipl.-Ing. Michael Funcke<sup>1</sup>, Univ.-Prof. Dr.-Ing. Lutz Eckstein<sup>2</sup>, Dipl.-Ing. Sebastian Lovski<sup>2</sup>

<sup>1</sup>Forschungsgesellschaft Kraffahrwesen Aachen mbH

<sup>2</sup>Institut für Kraftfahrzeuge RWTH Aachen University

## 1 Motivation

The storage systems of an electric vehicle (EV) remain the central challenge for the successful, widespread introduction of EV, which are attractive to the customers and have a sufficient functionality (e.g. range). The current state of the art in electric vehicles is the lithium ion cell. This cell type requires a high level of security measures to ensure mechanical integrity of the cells. The resulting increase in vehicle mass, which results from these measures, reduces the vehicle efficiency. To meet the challenge of a light and safe energy storage as well as to be able making a reliable prediction on the safety at an early stage in the development process, an accurate knowledge of the mechanical behaviour of the cells and their simulation in the virtual development process is necessary. This is confirmed by the studies carried out concerning the simulation of lithium ion cells using the Finite Element Method (FEM).

The presentation represents the results generated within the project OSTLER (Optimised Storage Integration for the Electric Car), which was founded by European Union. The goal of the project was the development of a modular electrical storage system and to investigate the feasibility of active protection systems, such as inflatable elements. These elements are intended to protect the storage from mechanical hazards.

## 2 State of the Art

An analysis of the state of the art shows that the currently used approaches to evaluate the damage of the energy storage at a vehicle crash cause a conservative design of the structure since the behaviour of the single cells is not shown in the crash simulation and thus an assessment of the cell damage is not possible. During this investigation existing simulation models of individual cells are not suitable for crash simulations, due to their detailed structure and the resulting very small simulation time step. In addition, these models consider only partially the loads occurring in a vehicle crash, but are based on the standard abuse tests resulting from the current transportation standards.

## 3 Approach

To cover the existing research demand, a development methodology for building up a cell simulation model is set up. First, the crash loadcases causing the highest intrusions are identified from a dataset of the GIDAS accident analysis and statistic database. In the next step, these loadcases are carried out simulative for three different cell types using a modified version of the public Toyota Yaris model and simplified cell models, which represent the contour and the cell mass. In this model the energy storage is placed under the front seats in vehicle transverse direction. The deformation of the energy storage and the cells inside is used to determine a crash design loadcase for the given storage location. Due to the deformation resulting from the vehicle crash simulations the focus is set on the cell type pouch cell and a pole side impact. The analysis includes five impact points since the deformation in the pole impact is very localised. In addition, both the cell and the storage deformation are used to virtually derive loadcases on cellular level from the crash simulations, which then are carried out as real-life tests.

The selected simulation approach (see Fig. 1) consists of a layer structure of six shell and five solid element layers, which depict the electrically active cell components. The cohesion of the layers is realised by means of an element row connected to the outer shell layers. The edge area, which is characteristic for the analysed pouch cell and which is used for application of the clamping forces to fixate the cells in the installation position, is modelled as a shell element layer with a multi-layer (three layers) material. Via a constrained node contact the edge area is connected to one of the solid layers.

After performing a sensitivity analysis the model parameters are determined in a progressive process by comparison of the qualitative and quantitative cell behaviour in simulation and testing. As result of this process a cell model is available, which is validated on cell level. The virtual testing of the simulation model and the validation by a real life test is performed at system level using a loadcase derived from the full vehicle crash simulation. For this purpose, the simulation used for the derivation of cell load cases is analysed again. For the point of impact showing the highest energy storage deformation, the impact speed of the sill on the energy storage, the absorbed mechanical energy and the load representing impactor diameter are determined. Thus, the loadcase represents the loads acting in the vehicle crash. Both quantitatively and qualitatively a high correlation between the simulation and the testing is achieved, validating the admissibility of the selected simulation approach.

#### 4 Figures and Tables

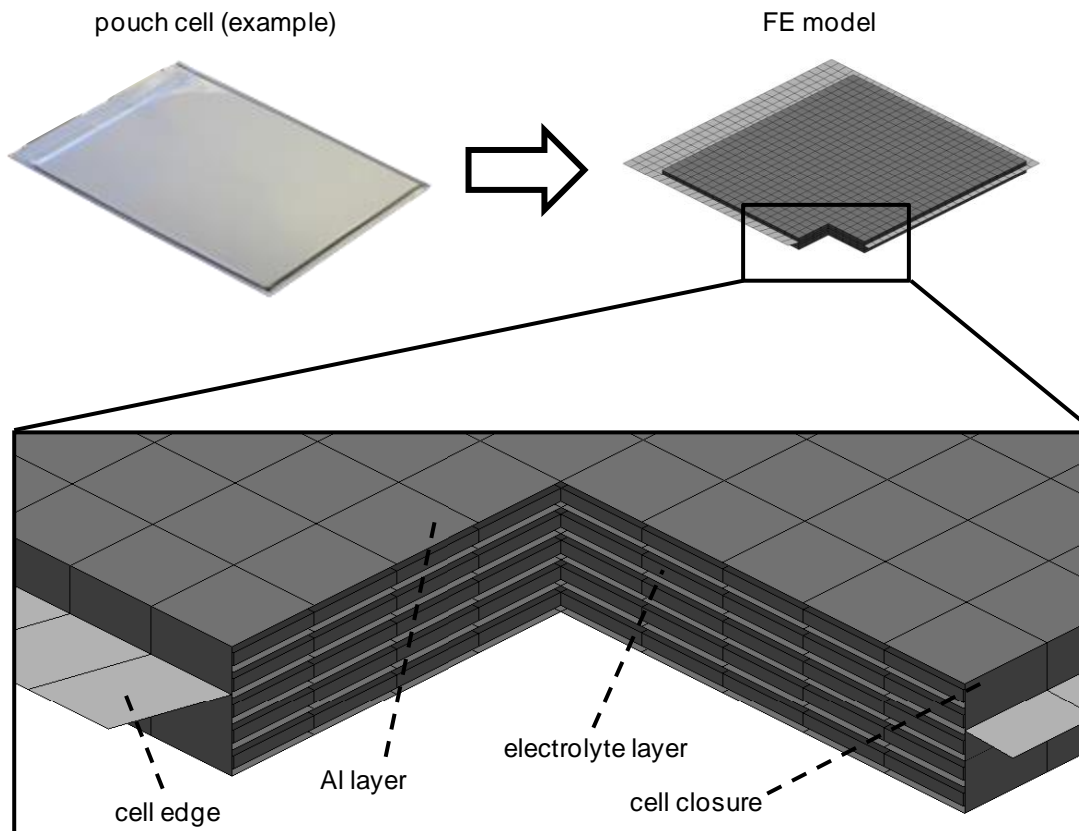


Fig.1: Selected simulation approach for the cell model

#### 5 Summary

Within the given presentation an approach for building up a cell simulation model for pouch cells, which is applicable to crash simulations, was given. Beside the basic model structure, the validation process was highlighted. The first step was the determination of a design loadcase for the given energy storage location within the vehicle, followed by the derivation of cell loadcases. These loadcases were performed as real tests as well as simulatively. Using a progressive approach the quantitative and qualitative comparison of simulation and test results were used to built up an on cell level validated simulation model. The final validation on system level, using a load case derived from the vehicle crash, showed the applicability of the simulation model.

#### 6 Literature

- [1] Sahraei, E.: Calibration and finite element simulation of pouch lithium-ion batteries for mechanical integrity, Journal of Power Sources, issue 201, 2012, pages 307-321

# Entwicklung eines optimierten Seitencrashkonzepts für das batterieelektrische Fahrzeugkonzept Urban Modular Vehicle

Michael Schäffer<sup>1</sup>, Marco Münster<sup>1</sup>, Ralf Sturm<sup>1</sup>, Horst E. Friedrich<sup>1</sup>

<sup>1</sup>Institut für Fahrzeugkonzepte, Deutsches Zentrum für Luft- und Raumfahrt e.V. (DLR), Stuttgart, Deutschland

## 1 Einleitung

Im Rahmen des DLR-Metaprojekts Next Generation Car (NGC) werden am Deutschen Zentrum für Luft- und Raumfahrt im Bereich Verkehr drei neuartige Fahrzeugkonzepte, Urban Modular Vehicle, Save Light Regional Vehicle und das Interurban Vehicle untersucht. Das NGC-Projekt vereinigt die Entwicklung von Tools, Methoden und Technologien für die verschiedenen Fahrzeugkonzepte aus dem gesamten Forschungsbereich Verkehr des DLR. In diesem Beitrag liegt der Fokus auf der Entwicklung eines optimierten Seitencrashkonzepts (Pfahlaufprall) für das batterieelektrische Fahrzeug Urban Modular Vehicle.

Durch die Elektrifizierung des Automobils ist es notwendig, Fahrzeugkonzepte und deren Karosseriestrukturen neu zu überdenken. Bei der Entwicklung von elektrifizierten Fahrzeugen stellen die Integration neuer Komponenten (z.B. die volumen- und masseintensive Batterie) Herausforderungen an die Gesamtfahrzeuggestaltung und an die Fahrzeugsicherheit.

## 2 Methodischer Ansatz

Für das Fahrzeugkonzept des Urban Modular Vehicle soll ein Seitencrashkonzept (Pfahlaufprall), bestehend aus einem Schwellerprofil mit integrierten energieabsorbierenden Aluminium-Sandwich-elementen, entwickelt werden. Bei der Auslegung des Konzepts werden unter anderem Lastpfadanalysen, Dimensionierungen und Formoptimierungen auf das Karosseriebodenkonzept angewendet, um die Crash-Performance zu erhöhen (siehe Abbildung 1).

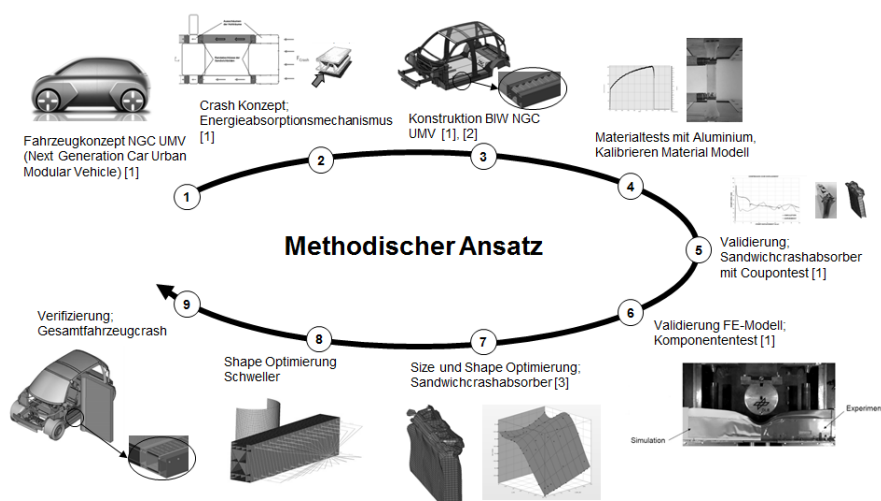


Fig.1: Gewählter methodischer Ansatz zur Entwicklung eines Seitencrashkonzepts für batterieelektrische Fahrzeugkonzepte

Bei der Formoptimierung des Sandwichelementes (Schritt 7 in Abbildung 1) werden durch „Morphing“ verschiedene Geometrien erzeugt, hierbei handelt es sich um Winkel- und Höhenänderungen des Sandwichkerns, die mit dieser Art der Modellmodifizierung mit akzeptabler Netzverzerrung realisiert werden kann. Zu den geometrischen Variationen des Crashabsorbers werden hierbei auch die Blechdicken der Decklagen und des Kerns variiert, um ein optimales Energieabsorptionsverhalten sicherzustellen.



Bei der anschließenden geometrischen Formoptimierung des Schwellerprofils (Schritt 8 in Abbildung 1) wird ein parametrisches Geometriemodell mit ANSYS APDL erstellt und über den Aufbau einer Prozesskette mit Python automatisiert (siehe Abbildung 2 „Inner Loop“). Die Simulationen und Optimierungen werden mit den LSTC -Produkten LS-DYNA und LS-OPT durchgeführt.

Die Optimierung ist als Multi-Level-Optimierung aufgebaut, um dem diskreten Optimierungsproblem Rechnung zu tragen, denn es werden nicht nur Positionen von Strukturen und Wandstärken optimiert, sondern es erfolgt auch eine Variation der internen Stützstrukturen. Diese Strukturen unterscheiden sich derart, dass nicht mehr von einem kontinuierlichen Optimierungsproblem ausgegangen werden kann.

Zu diesem Zweck ist die Optimierung in einen äußeren Loop, der die Variation der internen Stützstrukturen durchführt und einem inneren Loop zur Optimierung der jeweiligen internen Struktur unterteilt.

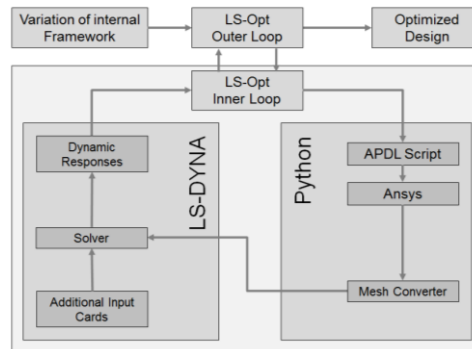


Fig.2: Multi-Level-Optimierungsloop für die geometrische Optimierung des Schwellerprofils

Da eine alleinige Schwelleroptimierung nicht zielführend ist, muss hierbei auch die dahinterliegende Struktur (Crashabsorber) berücksichtigt werden. Dies wird realisiert mit Elementen des Typs **\*ELEMENT\_BEAM** und dem Materialmodell **\*MAT\_GENERAL\_NONLINEAR\_6DOF\_DISCRETE\_BEAM**, welches die optimierte Kraft-Weg-Charakteristik aus der vorherigen Absorberoptimierung (Schritt 7 in Abbildung 1) besitzt. Zur Bewertung des jeweiligen Designvorschlags wird ein **\*ELEMENT\_DISCRETE** zur Messung der Intrusion in das Modell integriert. [4]

### 3 Zusammenfassung und Ausblick

Der gewählte Ansatz hat gezeigt, dass bei einfachen geometrischen Optimierungen Modelländerungen mit “Morphing” ausreichend sind, wenn die Qualität des FE-Netzes sichergestellt ist. Zudem hat die Multi-Level-Optimierung des Schwellerprofils, inclusive der Berücksichtigung der dahinterliegenden Crashstruktur über die Abbildung mit Beams, gezeigt, dass dadurch ein diskretes Optimierungsproblem sinnvoll angegangen werden kann und die Crash-Performance der Struktur gesteigert werden kann.

### 4 Quellen

- [1] Münster, M., Schäffer, M., Sturm, R., Friedrich, H.E.: “Methodological development from vehicle concept to modular body structure for the DLR NGC-Urban Modular Vehicle, 16<sup>th</sup> Stuttgart International Symposium, Stuttgart, Germany, 2016
- [2] Kopp, Gu., Kopp, Ge., Münster, M., Kriescher, M., Friedrich, H.E.: “Next Generation Car – Function Integrated Lightweight Structures”, Strategien des Karosseriebaus, Bad Nauheim, Germany, 2016
- [3] Schäffer, M., Münster, M., Sturm, R., Friedrich, H.E.: “Optimization of energy absorber for a novel electric vehicle concept”, 9<sup>th</sup> Graz Symposium Virtual Vehicle, Graz, Austria, 2016
- [4] Prem, A., Bastien, C., Dickison, M.: “Multidisciplinary Design Optimisation Strategies for Lightweight Vehicle Structures”, 10<sup>th</sup> European LS-DYNA Conference, Würzburg, Germany, 2015

# Closed Simulation Process Chain for Short Fiber Reinforced Plastic Components with LS-DYNA®

B.Lauterbach<sup>1</sup>, M. Erzgräber<sup>1</sup>, C. Liebold<sup>2</sup>, M. Helbig<sup>2</sup>, A. Haufe<sup>2</sup>

<sup>1</sup>Adam Opel AG  
<sup>2</sup>DYNAMore GmbH

## 1 Introduction

The mechanical properties of short fiber reinforced plastic (SFRP) components are highly dependent on the manufacturing process. Thereby, the fiber orientation within the component is depending on the injection molding process which defines the locally varying anisotropy of the manufactured part. Therefore, the consideration of the production process to predict the component's performance is necessary.

In [1], an overview over the homogenization and reverse engineering process being used within this work is already introduced, whereas the failure modeling which will be used here is a modified version of the one introduced in [6], using a strain based failure criteria in fiber direction and a stress based failure criteria in matrix direction in combination with the isotropic damage and failure model GISSMO. Within this work, a closed simulation process chain will be introduced and validated on a Lower Bumper Support (LBS). Using the mapping routine Envyo, validated Moldflow® analysis results will be homogenized and mapped onto LS-DYNA meshes and used for a parameter identification and reverse engineering of `*MAT_ANISOTROPIC_ELASTIC_PLASTIC (*MAT_157)`.

## 2 The process chain

The process chain which consists of a validated injection molding process, the parameter identification and mapping of homogenized elastic constants, and the validation on a component is shown in Fig. 1.

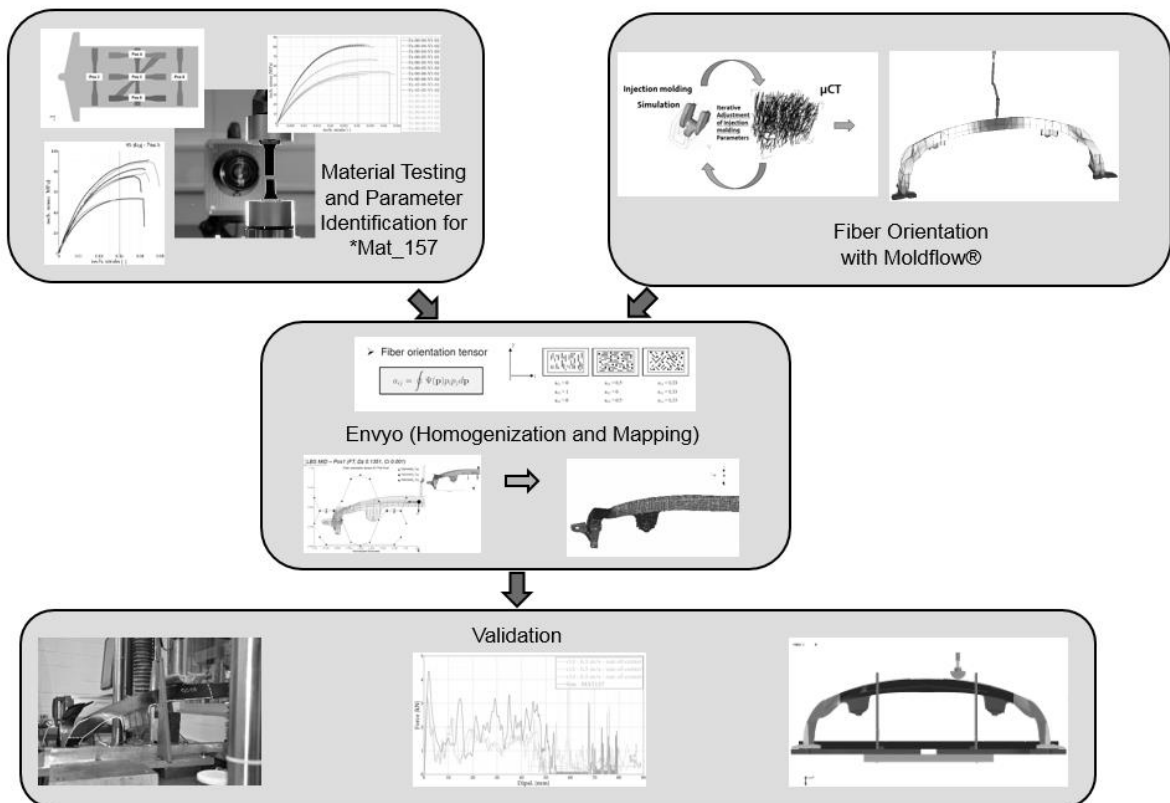


Fig. 1: Process chain for short fiber reinforced plastic components.

In order to perform a material parameter identification for **\*MAT\_ANISOTROPIC\_ELASTIC\_PLASTIC**, tensile specimen are taken in longitudinal (0°), transversal (90°), and diagonal (45°) direction compared to the direction of the flow of an injection molded plate. Quasi-static and dynamic tests are performed to consider the strain-rate dependency of the matrix material. With some adjustments of the matrix and fiber properties being used as an input for the homogenization of the elastic stiffness tensor in Envyo, the plasticity curves for these three directions can be reverse engineered as well as damage and failure parameters for the added isotropic GISSMO failure model. For a further mapping, linear interpolation is being used which allows to assign plasticity curves on each integration point in steps of 5° depending on the local orientation tensor's main direction compared to the element coordinate system.

The same plates are used to perform micro CT ( $\mu$ -CT) scans at several positions corresponding to the center of the used tensile specimen in order to validate and optimize the results of the Moldflow® analysis. Both methods being available within Moldflow®, the Folgar-Tucker approach and the reduced strain concentration (RSC) method are evaluated for their default values and an optimization is performed to fit the results to the data gained by the  $\mu$ -CT scans. The final injection molding process is simulated using the optimized parameters and also compared to CT scan results taken at supposedly characteristic positions of the LBS.

The mapping routines being implemented in Envyo for **\*MAT\_157** allow to consider the state-of-the-art Mori-Tanaka homogenization scheme [4] for the elastic regime, taking into account the inclusion shape being characterized by the aspect ratio which is the fiber length over its diameter according to [2], and a closure-approximation which allows to increase the size of the 2<sup>nd</sup> order orientation tensor to 4<sup>th</sup> order, as it is introduced in [3]. The user can define the matrix and fiber properties independently, using an ascii – based text file format. Material parameters will then be homogenized and defined for each integration point, using the **\*INITIAL\_STRESS\_{OPTION}** card. The routines are by now available for shell elements only. This also allows to consider direction and strain rate dependent plasticity curves using a tabular input. The direction dependent values  $q_0$  and  $q_1$  correspond to the main direction of the mapped orientation tensor in comparison to the element coordinate system.

### 3 Summary

A validation of the introduced method and the derived material parameters was performed on quasi-static and dynamic drop tests with the LBS for different velocities and at a center position of impact as well as at an out-of-center position. One can conclude that as an average, the prediction of the component's stiffness is acceptable whereas the damage and failure prediction is not accurate enough to allow a reliable forecasting of the component's behavior under crash loading. One reason for that is the restriction to isotropy within the GISSMO damage and failure model and therefore, future work will consider anisotropic failure using the Tsai-Hill or Tsai-Wu failure modeling such as it is already proposed by [5], the latter already being available in one of the recent LS-DYNA® releases.

Further investigations on the mapping strategy will have to be done as well. By now, the mapping only considers a nearest neighbor, or closest point search, so no averaging is performed for the tensorial data but this has to be investigated in future work.

### 4 Literature

- [1] Liebold, C., Erhart, A., Haufe, A: "The significance of the production process of FRP parts for the performance in crashworthiness", 14<sup>th</sup> International LS-DYNA Users Conference, Detroit, MI, USA, 2016.
- [2] Advani, S. G., Tucker, C. L., Journal of Rheology, The Use of Tensors to Describe and Predict Fiber Orientation in Short Fiber Composites, 31 (8), (1987), 751-784.
- [3] Dray, D., Gilormini, P., Regnier, G., Comparison of several closure approximations for evaluating the thermoelastic properties of an injection molded short fiber composite. Composites Science and Technology, Elsevier, (2007), pp.1601-1610.
- [4] Mori T, Tanaka K., Average stress in matrix and average elastic energy of materials with misfitting inclusions. Acta Metall (1973), 21:571-574.
- [5] Nutini, M., Vitali, M., Simulating anisotropy with LS-DYNA in glass-reinforced, polypropylene-based components. 9<sup>th</sup> LS-DYNA Forum, Bamberg (2010).
- [6] Hatt, A., Anisotropic modeling of short fibers reinforced thermoplastics materials with LS-DYNA. 13<sup>th</sup> LS-DYNA Forum, Bamberg (2014).

# **Interactive Fracture Criterion for SGF-PP: Validation on Lower Bumper Support**

M. Nutini, M. Vitali  
LyondellBasell

M. Erzgräber, B. Lauterbach  
Adam Opel

# Crash simulation of long fiber reinforced thermoplastics considering damage and failure

L. Schulenberg<sup>1</sup>, J. Lienhard<sup>1</sup>

<sup>1</sup>Fraunhofer Institute for Mechanics of Materials IWM, Wöhlerstr. 11, 79108 Freiburg

## 1 Abstract

An anisotropic visco-elasto-plastic material model for injection molded long fiber reinforced thermoplastics (LFT) is introduced. It considers local heterogeneities which are attributed to process induced variations of fiber orientation distributions and fiber volume fractions. These inhomogeneities have an effect on the mechanical properties and need to be considered in structural computations. In the material model this is realized through different steps of homogenization procedures. Firstly, an anisotropic stiffness tensor is approximated using mean field homogenization. Secondly, the plastic behavior is described using Hill's transversely isotropic yield criterion averaged over the three principal directions of the fiber orientation [1]. In the third step visco-elastic effects are taken into account through additional Maxwell elements within a parallel rheological network of the elasto-plastic and visco-elastic material model. The number of parameters describing the anisotropic visco-elasticity has been reduced by adopting a convenience hypothesis in the formulation of the generalized Maxwell model [2]. The advantage in combining these different approaches is a micro-mechanically based yet fast numerical calculation of the composite material behavior within LS-DYNA explicit. The damage model is decoupled from the material model and described in a tensorial form. The anisotropic material model is calibrated by simulating tensile tests on specimens taken in different directions from an injection molded plate of a fiber reinforced thermoplastic. The spatial variation of fiber orientation distribution and fiber volume fraction throughout the plate is determined from numerical mold filling simulations and is compared with computer tomography scans at different positions. A validation of the model is performed through simulating position dependent tensile tests as well as tests of different stress triaxialities, e.g. punch, shear and bending tests, which are well reproduced [1,2].

## 2 Experimental investigations

Injection molded plates of LFT out of polypropylene and 30 wt-% glass fibers (STAMAX 30YK270 SABIC) were examined. Microscopic computer tomography (CT) scans have been carried out to analyze the fiber orientation distribution at different positions in order to validate the injection mold filling simulation. To investigate the macroscopic material behavior including damage and failure different types of specimens with various sample geometries have been tested (Table 1) in order to generate various stress conditions and load path. All specimens are taken from different positions of injection molded plates to take into account the variation of the fiber orientation distributions. Six different strain rates from  $10^{-5} \text{ s}^{-1}$  up to  $200 \text{ s}^{-1}$  have been analyzed on the use of high-speed video imaging in combination with digital image correlation (DIC) and a high-speed infrared camera to determine material's properties including damage and fracture. [2].




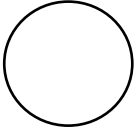


					
smooth tension	notched tension	shear	punch test	notched punch test	uniaxial pressure

Table 1: Schematic drawing of different specimen types to investigate damage and failure (not to scale).

### 3 Simulation results

The local fiber orientation distributions and fiber volume fractions are approximated in mold filling simulations and mapped to each Gauss point of the finite element calculation. To calibrate the material model and for separation of different nonlinear effects, e.g. plasticity and damage, uniaxial tensile tests with unloading has been simulated on the use of reverse engineering method (Fig. 1). The viso-elastic behavior is approximated on the use of anisotropic Maxwell elements in a parallel network to the elasto-plastic material model. As shown in Fig. 1 (right) the hystereses are well reproduced. In addition strain rate depended behavior for high strain rates which is relevant, e.g. in automotive crash simulations, can be approximated with this formulation.

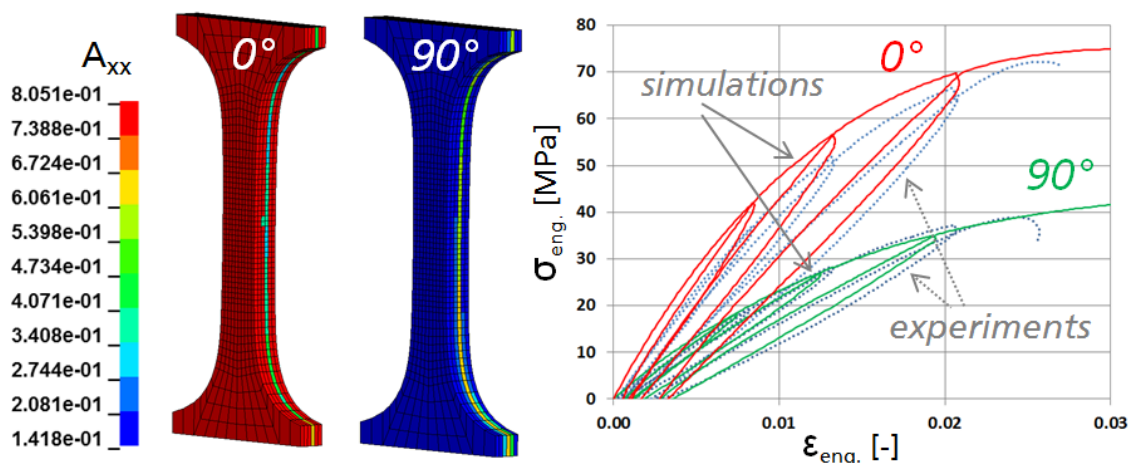


Fig. 1: Contour plot showing the content of fiber orientations  $A_{xx}$  orientated in flow direction for two tensile test specimens, taken in  $0^\circ$  and  $90^\circ$  to the injection molding flow direction (left). Experiments and simulations for loading-unloading tests with smooth tensile specimens at a strain rate of  $7 \cdot 10^{-4} \text{ s}^{-1}$  (right).

Failure is described as a load curve of failure strain versus stress triaxiality. Since interactions between different loading states and damaging effects are not fully understood, six independent damage variables are introduced. This leads to a tensorial formulation, where the damage evolution is considered separately for each component of the stress tensor. For convenience the same load curve of failure strain versus stress triaxiality and the same damage evolution formulation is assumed for all strain components. This has turned out to be sufficient when calculating failure strain from the experimental investigations on the use of reverse engineering method (Sec. 2).

### 4 Summary

The simulation results in this work show that the approach suggested here can be successfully employed to predict nonlinear anisotropic and strain rate dependent material behavior including damage and failure of injection molded long fiber reinforced composites in an explicit finite element calculation. Damage and failure have been considered within a rather simple approach and proved to be sufficient in the performed simulations. This is due to the fact that failure strains in  $0^\circ$  and  $90^\circ$  to the flow direction do not show significant differences. This might not be the case for stronger anisotropy (e.g. aligned fiber orientation) where anisotropic damage and failure criteria should be used.

### 5 Literature

- [1] Schulenberg, L., Seelig, Th., Andrieux, F., Sun, D.-Z.: An anisotropic elasto-plastic material model for injection molded long fiber reinforced thermoplastics accounting for local fiber orientation distributions, Journal of Composite Materials, accepted for publication.
- [2] Sun, D.-Z., Schulenberg, L., Lienhard, J., Andrieux, F., Huberth, F., Andrä, H., Niedziela, D., Shklyar, I., Steiner, K.; Wirjadi, O.: Entwicklung einer Methode zur Crashsimulation von Langfaserverstärkten Thermoplast (LFT) Bauteilen auf Basis der Faserorientierung aus der Formfüllsimulation. Forschungsvereinigung der Automobil-technik e. V., FAT-Schriftenreihe Nr. 284, 2016.

# Modeling Approaches for Endless-Fiber Reinforced Polymers in Crashworthiness Applications

G. Oberhofer, M. Vogler, H. Gese, H. Dell

MATFEM Partnerschaft Dr. Gese & Oberhofer, München

## 1 Introduction

In this presentation, current developments and capabilities for modeling endless-fiber reinforced polymers using the modular material and failure model MF-GenYld + CrachFEM are presented. A special class of these polymers which are of particular interest for automotive applications are organic sheets. Organic sheets consist of an endless fiber fabric (glass or carbon), embedded in a thermoplastic matrix (e.g. PP, PA). They offer high stiffnesses and high strengths in pre-defined directions. At elevated temperatures, organic sheets can be formed like a metal sheet. Fig.1: shows a schematic representation of polymers, starting from unreinforced polymers to highly oriented organic fabrics.

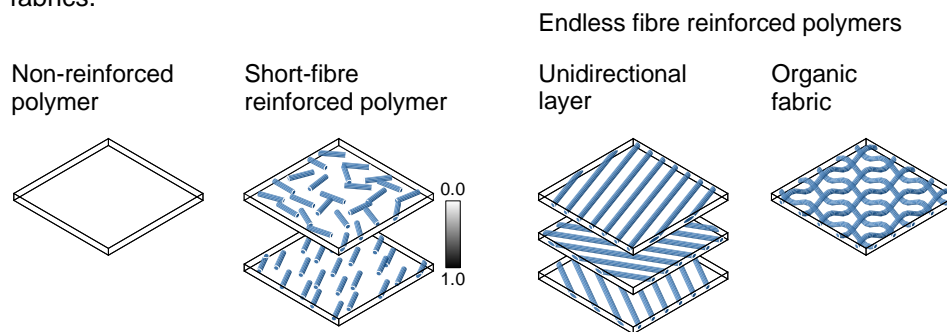


Fig.1: Different classes of polymers

Compared to unreinforced or short fiber reinforced thermoplastics (SFRT), the degree of anisotropy (elastic and plastic range, failure) is significantly higher in organic sheets. In fiber direction, nearly no nonlinearities are observed and the mechanical behaviour is dominated by the viscoelastic behavior of the fibers. In off-axis directions however, pronounced ductile behavior with low hardening can be observed. This behaviour is due to matrix yielding and rotations of the glass fibers in the matrix material. Although the material behavior of organic sheets is orthotropic in its initial condition, it can change locally from orthotropic to general anisotropic behavior after thermoforming or after extensive deformation in crash. Fig.2: shows the typical mechanical behavior of organic sheets under uniaxial tension under different orientations.

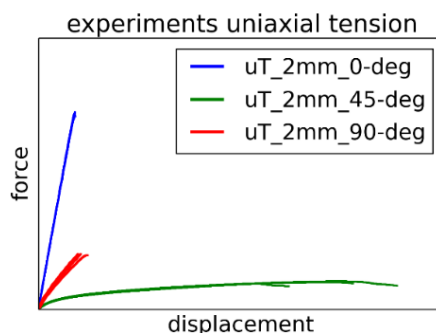


Fig.2: Mechanical behavior of the current organic sheet: results from uniaxial tensile tests in different orientations; organic sheet with twill weave 80% / 20% in thickness of 2 mm [1]

The specific behavior of organic sheets and unidirectional endless fiber composites in crash load cases imposes special demands on the material model. Only an appropriate material model allows to fully exploit the potential of organic sheets in lightweight design of hybrid components.

## 2 Modeling approach

Within this study, the modular material model MF-GenYld+CrachFEM was used in combination with LS-Dyna, whereby a similar characterization method compared to the implemented standard approach for short fiber reinforced thermoplastics (SFRT) has been used. An overview of the available tools of the modular material and failure model MF-GenYld+CrachFEM is given in Fig.3.

For the current organic sheet, the elastic anisotropy can be described with good accuracy using an orthotropic approach. The directionality of the yield strength is described by a Hill-1948 yield locus. Further investigations showed that the use of a further developed yield locus formulation according to Bron-Besson / Dell-2006 increases the accuracy of the hardening behavior for different orientations. The correct failure prediction was one of the challenging tasks due to the strong directionality and the different nature of failure. As already shown in Fig.2., the behavior can vary between brittle and ductile, depending on the loading directions. The combination of anisotropic stress based failure criteria accounting for brittle fiber failure and ductile strain based failure criteria for matrix dominated loadings turned out to be a suitable modeling strategy for organic sheets in crash load cases. In the presentation, the prediction of basic load cases and component tests will be shown and discussed.

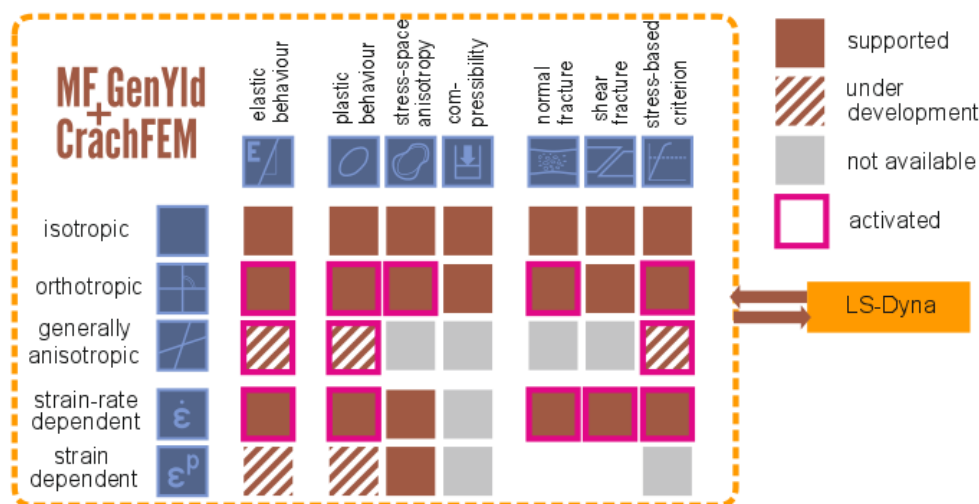


Fig.3: MF-GenYld+CrachFEM: Modules for modeling of polymers with endless fiber fabrics.

## 3 Summary and Outlook

The modeling approach using MF-GenYld+CrachFEM showed quite good results for the presented load cases whilst comparatively high performance with respect to calculation time and stability. It is therefore well suited for industrial applications.

In future work, further validation of the proposed modeling approach at component level is necessary. If organic sheets with thicknesses lower than 2 mm shall be used, the difference between membrane modulus (Young's modulus) and bending modulus has to be regarded. In some crash load cases with extensive deformations before failure, the exact consideration of the fiber rotations might be necessary. This is all the more the case if thermoforming should be addressed. In this case, the effect of evolving anisotropy due to fiber rotations and the exact tracking of the fiber directions during the deformation process is necessary.

Current developments are focused on the extension towards general anisotropy of elasticity and plasticity either based on the superposition of two yield loci or on the structural tensor approach according to the Ph. D. thesis of M. Vogler [2]. Both concepts will be briefly presented.

- [1] G. Oberhofer, H. Dell, M. Vogler, H. Gese: Current solutions and open challenges in modeling organic sheets, CAE Grand Challenge 2016, April 12-13, 2016
- [2] M. Vogler: „Anisotropic Material Models for Fiber Reinforced Polymers“, doctoral thesis, Institute of Structural Analysis, Leibniz Universität Hannover, 2014



# Simulation von Kaltgasgeneratoren unter Berücksichtigung des JOULE-THOMSON-Effekts

Tilo Laufer<sup>1</sup>, Axel Heym<sup>1</sup>

<sup>1</sup> Takata AG

## 1 Einführung

Die Einführung der Uniform Pressure Methode (UP-Methode) durch Nefske und Wang [1] im Jahr 1988 führte zu einer robusten und zuverlässigen Methode, um die Fluid-Struktur-Koppelung im automobilen Insassenschutz zu simulieren. Die UP-Methode ist heute in allen gängigen FE-Solvern implementiert und wurde bisher vielfach zur Simulation von Airbags verwendet.

Jedoch ist diese Methode nicht in der Lage, detaillierte Strömungsvorgänge oder komplexes Verhalten eines Gases abzubilden. Dadurch kann es bei Simulationen zum Insassenschutz zu Einschränkungen der Prognosefähigkeit kommen. Der Finite Element Solver LS-Dyna bietet hingegen mit der Corpuscular Particle Methode (CP-Methode) [2] eine realistischere Abbildung der Strömung. Dabei wird das Gas durch „Kügelchen“ diskretisiert, die durch ideal elastische Stöße miteinander und mit der Umgebung interagieren. Die reine Impulsübertragung durch elastische Stöße entspricht dem Verhalten eines idealen Gases, was in den meisten Anwendungsfällen eine hinreichende Modellierung von Strömungen in Airbags ermöglicht. Lediglich die Simulation von Kaltgasgeneratoren ist mit der Annahme eines idealen Gases oftmals nicht ausreichend. Hier kann sich das ausströmende Gas in Abhängigkeit von der Gaszusammensetzung bei der Expansion erwärmen oder abkühlen. Dieses Phänomen nennt sich JOULE-THOMSON-Effekt (J-T-Effekt) und ist ein Realgaseffekt.

In LS-Dyna ist es möglich, den J-T-Effekt bei der Simulation von Gasgeneratoren zu berücksichtigen. Dabei wird das Fluid beim Durchströmen von Drosseln (engen Querschnitten) aufgrund seiner Materialparameter (JOULE-THOMSON-Koeffizienten) künstlich erhitzt oder abgekühlt. Damit ist es möglich, in LS-Dyna das Abströmverhalten von Kaltgasgeneratoren realitätsgetreuer abzubilden und das Gasgeneratormodell im Tank-Test unter Berücksichtigung des J-T-Effekts zu validieren.

## 2 Bestimmung der JOULE-THOMSON-Materialparameter

Damit der J-T-Effekt berücksichtigt werden konnte, musste zunächst der entsprechende Materialparameter bestimmt werden. MAUL zeigt in "Der Joule-Thomson-Effekt" [3], wie sich der J-T-Koeffizient ( $\mu_{JT}(T)$ ) in Abhängigkeit von den VAN-der-WAALS-parametern  $a$  (Kohäsionsdruck) und  $b$  (Kovolumen) sowie der Wärmekapazität  $C_p$  berechnet.

$$\mu_{JT}(T) = \frac{b - 2a/RT}{C_p(T)} = \frac{b - 2a/RT}{C_{p0} + C_{p1}T + C_{p2}T^2 + C_{p3}T^3} \quad (1)$$

Da LS-Dyna die Temperaturabhängigkeit der Wärmekapazität durch ein Polynom n-ter Ordnung darstellt, wurde auch ein Polynom 3. Ordnung benutzt um den Verlauf der Wärmekapazität zu beschreiben (Gleichung (1), Zeile 2).

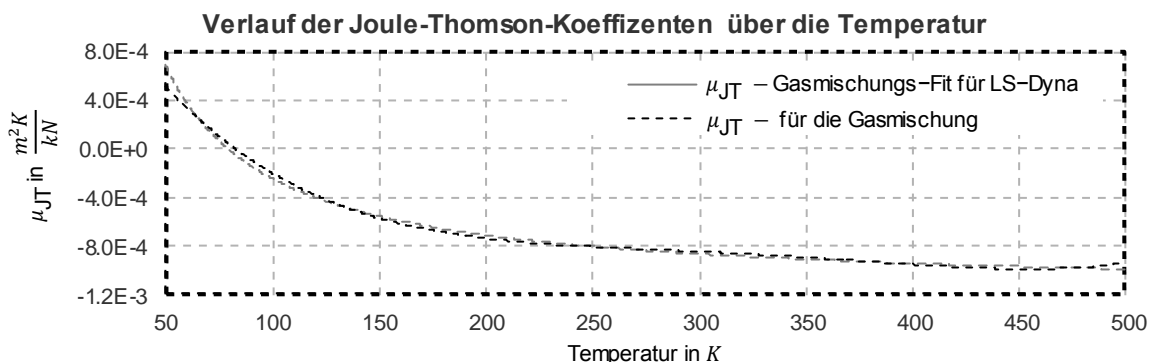


Fig.1: Verlauf des JOULE-THOMSON -Koeffizienten des Gases in Theorie und Polynom-Approximation

Weiterhin kann LS-Dyna den J-T-Koeffizienten nicht als Funktion verarbeiten, daher musste der Verlauf des J-T-Koeffizienten durch eine Polynom-Approximation angenähert werden. Nachdem ein Temperaturbereich für die Approximation gewählt wurde (50K-500K), konnten die Polynom-Koeffizienten mithilfe der Methode der kleinsten Quadrate bestimmt werden. Eine Gegenüberstellung zwischen dem J-T-Koeffizienten und der Approximation ist in Abbildung 1 dargestellt.

### 3 Umsetzung des JOULE-THOMSON-Effekts in LS-Dyna

Wie oben erwähnt, kann der J-T-Effekt in der CP-Methode Beachtung finden. Dafür wurden die Polynomkoeffizienten des J-T-Koeffizienten als Materialparameter des Gases eingeführt. Wie im nachfolgenden Code dargestellt, wurden die Koeffizienten in Karte 2 (Felder 1-5) des Keywords `*DEFINE_CPM_GAS_PROPERTIES` eingetragen.

```
*DEFINE_CPM_GAS_PROPERTIES
$      ID      Xmm      Cp0      Cp1      Cp2      Cp3      Cp4
      1301 0.0040026      20.8      0      0      0      0
$      mu_t0      mu_t1      mu_t2      mu_t3      mu_t4      Chm_ID      Vini
      111.809      -13.3453 0.0617413 -1.2798e-49 0.72665e-8
```

Die Bestimmung der Materialparameter (`mu_t1` - `mu_t4`) wurde im vorherigen Abschnitt 2 erläutert. Da die CP-Methode in der ihr zugrundeliegenden Theorie von einem idealem Gasmodell ausgeht, reichte das Hinzufügen der Materialparameter nicht aus, um den Einfluss des J-T-Effekts zu berücksichtigen. Zusätzlich musste mithilfe des Keywords `*DEFINE_CPM_VENT` eine Öffnung definiert werden, an der der J-T-Effekt angewandt wurde. Der Solver LS-Dyna hat alle durch die Öffnung fliegenden Partikel der CP-Methode aufgrund Ihrer J-T-Koeffizienten erwärmt oder abgekühlt. Damit ist die Energie des J-T-Effekts zusammen mit der in dem Gasgenerator gespeicherte potentielle Energie die gesamte in den Tank fließende Energie. Das Simulieren des Tank-Tests zeigte jedoch eine Abweichung zwischen dem gemessenen und dem simulierten Druck. Die Abweichung zwischen Versuch („Resultierende aller Versuchskurven“) und Simulation („J-T nach Theorie“) liegt bei ca. 20kPa und ist in Abbildung 2 dargestellt. Es ist nicht bekannt, ob noch weitere Realgaseffekte existieren, die einen zusätzlichen Energiebeitrag leisten, oder andere Einflussgrößen die Abweichung hervorrufen. Deshalb wurden die J-T-Koeffizienten validiert, so dass der fehlende Energieeintrag ausgeglichen wurde. Damit ergab sich eine gute Korrelation zwischen Versuch und Simulation (Abbildung 2, „Resultierende aller Versuchskurven“ vs. „J-T nach Validation“).

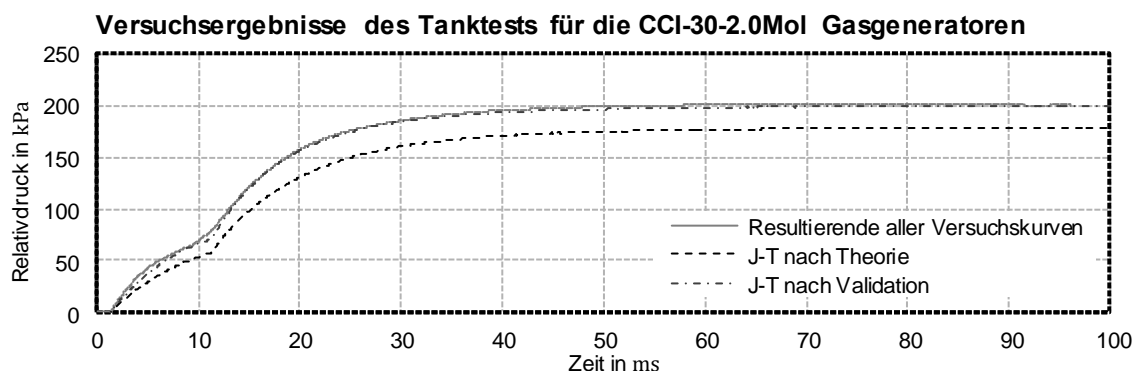


Fig.2: Vergleich von Versuch und Simulation bei Berücksichtigung des JOULE-THOMSON -Effekts

### 4 Literatur

- [1] Wang, J.T. and Nefske, D.J.: "A new cal3d airbag inflation model", SAE Technical Paper, 1988
- [2] Olovsson, L.: "Corpuscular method for airbag deployment dimulations in LS-DYNA", Impetus Afea Technical Publications, 2007
- [3] Maul, C.: "Der Joule-Thomson-Effekt", Praktikumsunterlagen Apparatives Praktikum Physikalische Chemie, 2009

# Update on CPM for Airbag Modelling

Jason Wang

LSTC, USA

## 1 Abstract

The out of position (OOP) airbag studies was initially conducted by traditional LS-DYNA FEM based FSI. Unfortunately, the method required lots of computing resources and encountered many limitations. Corpuscular particle method (CPM) was then introduced to avoid those problems about 10 years ago.

CPM is a meshless method based on the Kinetic Molecular Theory. Each particle represents many gas molecules. In general, it is a coarse grained multi-scale method for gas dynamics obeying ideal gas law. This method can predict well between OOP safety simulations and tests. Recently, airbag design gets more sophisticated which contains extra internal parts or separated compartments, etc. In order to catch the effect of those added features, CPM method is continuously improved and added new options to meet those challenges. In this paper, we will introduce few enhancements.

The first is the new feature for initial air option, `iair=1`. Originally, this option is only fill initial volume of the bag with UP air. During the initial deployment, the bag pressure may go under ambient pressure due to the huge impulse created by the inflator jets. The bag pressure is less than the environment and it makes the bag very hard to open. If this airbag has unblocked vents, those vents should allow ambient air into the bag in the real situation. This added energy will make the bag easier to deploy than without the effect as shown in Figure 1.

This feature is added in the recent LS-DYNA and simply sets `iair` option to `-1`. Based on the photo taken by using schlieren method, our customer showed the gas through the internal vent forms a jet instead random distribution, Figure 2. A new option is implemented under `*DEFINE_CPM_VENT` to allow rearranging particle release direction after passing through the internal vent, Figure 3. The particle distribution matches well with experiment using this new feature. The deployment shape and peak force are also matched well using the new method [1].

## 2 Figures

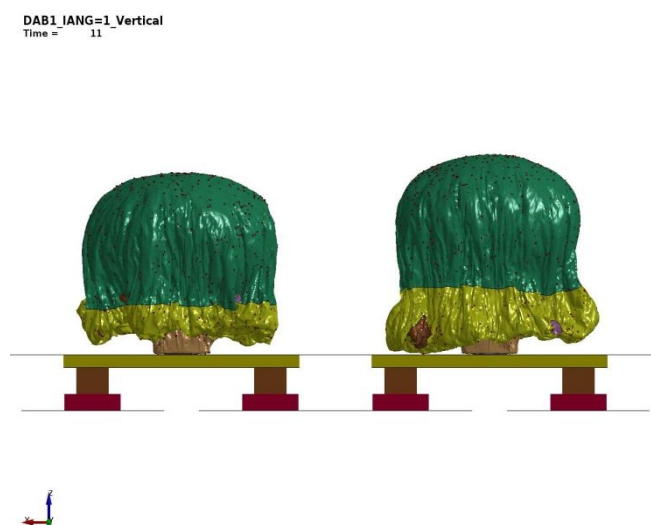


Fig.1: . Deployment with/without aspirated ambient air

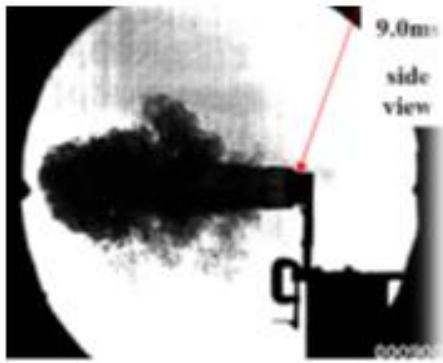


Fig.2: . Inflator as flow taken using schlieren method

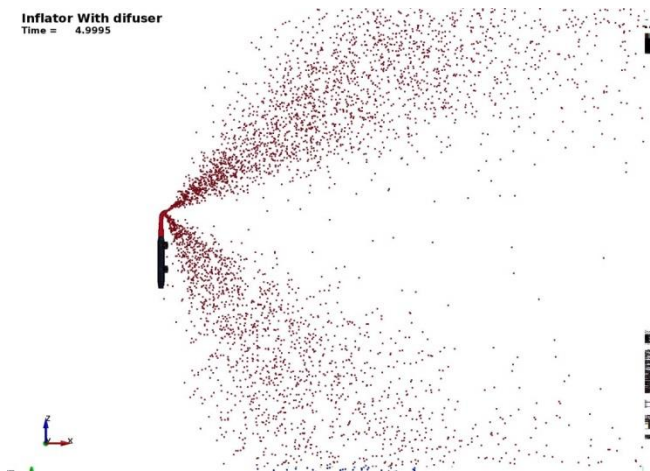


Fig.3: . Option with Jetting option

### 3 Literature

[1] H. Ida, M. Aoki, M. Asaoka, K. Ohtani, "A Study of gas flow behavior in airbag deployment simulation", 24th International Technical Conference on the Enhanced Safety of Vehicles (ESV). No. 15-0081, 2015.

# \*DEFINE\_PRESSURE\_TUBE: a pressure tube sensor for pedestrian crash simulation

Jesper Karlsson<sup>1</sup>

<sup>1</sup>DYNAmore Nordic AB

## 1 Background

Each year 1.25 million fatalities occur on the roads, with less than half being car passengers [1]. Although cars are becoming safer pedestrian fatalities are lagging behind, becoming an increasing share of road fatalities. Pedestrian safety is thus an increasingly important area in automotive safety.

In this talk I will present a new keyword, **\*DEFINE\_PRESSURE\_TUBE**, for simulating a passive safety system where traditional accelerometers are replaced by an air filled tube embedded in the front bumper with pressure sensors at the ends, see Figure 1. In the case of an impact the tube is compressed and a pressure wave travels to the sensors, enabling localization and extent of the impact. In recent years such systems have gained popularity in the automotive industry, posing a challenging task in efficient and accurate simulations.

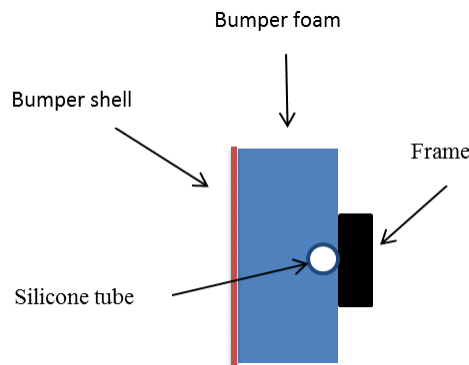


Fig. 1: Illustration of embedded pressure tube in cross section of a bumper.

## 2 Keyword usage and theory

The keyword **\*DEFINE\_PRESSURE\_TUBE** defines a closed gas filled tube using beam elements of element form 1,4,5 or 11 with **CST=1**, i.e. hollow circular beams. The gas volume is determined by inner area times initial length, and the pressure is calculated from area changes given by contact penetration from surrounding elements, currently supporting mortar contacts only. Note that the pressure calculation is not coupled to the deformation of beam elements.

The pressure tube is modeled using an acoustic approximation of the 1D compressible Euler equations for pipes with varying cross section area, given by

$$\frac{\partial p}{\partial t} + p_0 \left( \frac{\partial \ln A}{\partial x} u + \frac{\partial u}{\partial x} \right) + \frac{\partial \ln A}{\partial t} p = 0,$$

$$\frac{\partial u}{\partial t} + \frac{\partial \ln A}{\partial t} u + \frac{c_0^2}{p_0} \frac{\partial p}{\partial x} = 0,$$

where  $A = A(x, t)$  is the cross section area,  $p = p(x, t)$  is the pressure,  $u = u(x, t)$  is the velocity,  $p_0$  is the initial pressure, and  $c_0$  is the wave propagation speed in air. For constant area this is equivalent to the classical acoustic wave equation found in text books.

Given a part, **\*DEFINE\_PRESSURE\_TUBE** defines a pressure tube for each set of joint beam elements in that part and assigns a wave speed and initial pressure. Pressures and tube areas are consequently output through the keyword **\*DATABASE\_PRTUBE**, see Figure 2 and 3 for an example visualized in LS-PREPOST.

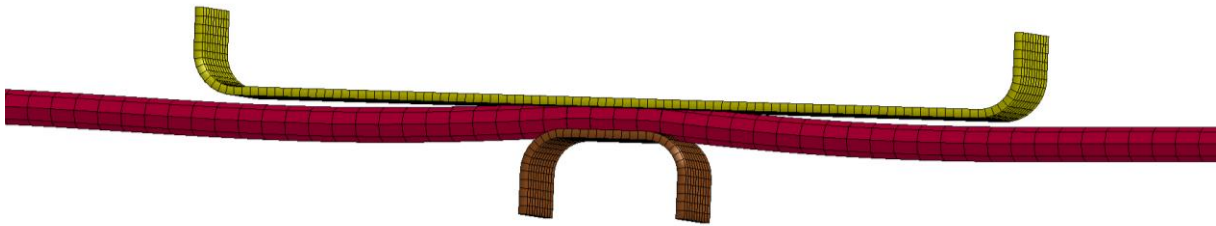


Fig.2: Simulation of compression of a 1.7m long silicone tube, shown right after impact. Only part of tube shown.

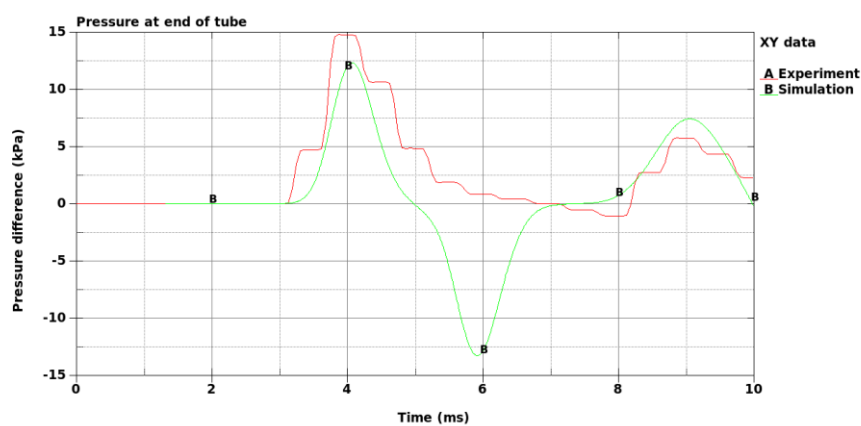


Fig.3: Pressure difference (with respect to sea level pressure) at end of tube. The undershoot at 6ms in the simulation may be caused by inaccurate mechanical response from the tube.

### 3 Future development

This keyword is still experimental (although available in R10) and may be enhanced in the near future by, e.g.

1. Solving the full 1D Euler equations to resolve shocks from supersonic flow.
2. Phenomenological model for cross section area as function of contact penetration. Currently, deformation of the tube cross section is not accounted for.
3. Phenomenological model for mechanical response of the tube. Currently modeled by contact stiffness only.

### 4 Summary

This talk presents the new keyword, `*DEFINE_PRESSURE_TUBE`, used to simulate pressure waves in an air filled tube. Such tube based systems equipped with pressure sensors are gaining attraction in the automotive industry as an alternative to traditional accelerometers. The keyword uses a 1D wave approximation making it vastly more efficient than traditional approaches using ALE or particle methods.

### 5 Literature

[1] WHO: Global Status Report on Road Safety 2015.

# Correlation Studies for WorldSID-50 and Q10/Q6 Child Dummies in Latest Occupant Simulations

Thomas Kotucha, Dr. Elena Schneider

Adam Opel AG

## 1 Abstract

Steadily growing demands on vehicle safety and occupant protection pose a continuous challenge for vehicle manufacturers. The virtual vehicle development process based on simulation requires well validated tools and methods to guarantee a reliable performance of the product. Correlation studies of different levels are used to prove component models and settings used in the simulation models. Among other changes, the latest Euro NCAP Protocol requires new occupant dummy models. Starting from 2016, WorldSID-50 driver dummy and Q6 / Q10 child dummies in the second seat row are applied. This paper demonstrates the results of dummy correlation studies performed in a full vehicle model including BiW, all interior components, child seats, and full restraint system.

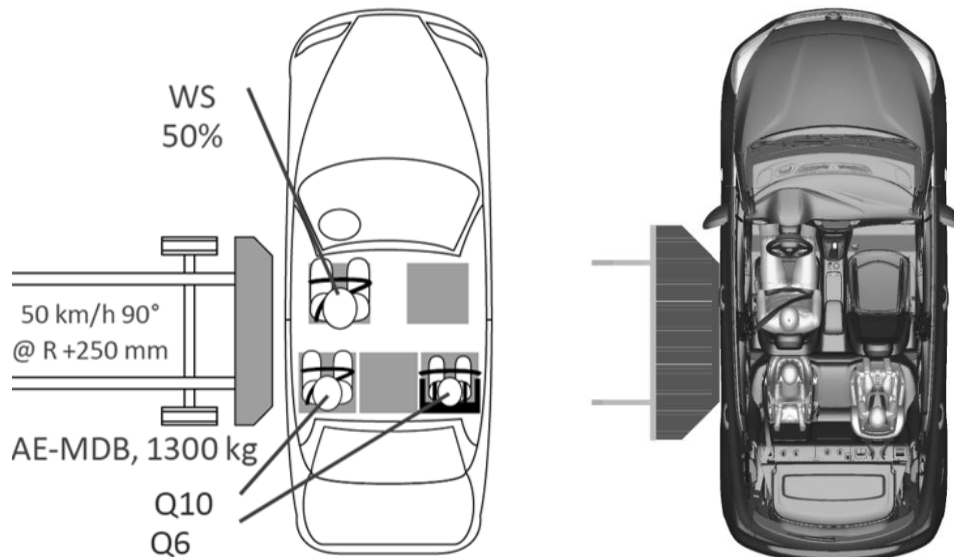


Fig. 1: Setup of Euro NCAP AE-MDB Side Impact with WSID-50 and Q10/Q6 Dummies

## 2 Summary

The document shows the latest results of the occupant simulation in a compact-size vehicle model including WorldSID-50 v3.5 dummy as well as Q6\_V2.0.3\_S3/Q10\_V1.3.1\_SK\_S3 dummies. Since the maturity of the models is quite high, an impressive correlation could be achieved for the side impact load cases as well as for the frontal crash.

Part of the correlation was a visual study of the dummy kinematics, the performance of the restraint system, and the vehicle kinematics. The occupant performance has been assessed by the ATD readings according to the latest crash test protocol and rating.

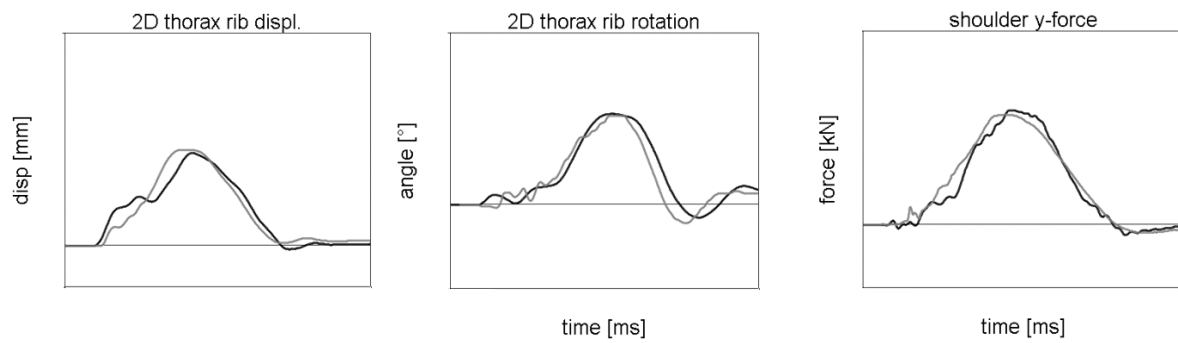


Fig.2: Extract from WorldSID-50 ATD Reading in AE-MDB Side Impact



Fig.3: Analysis of WorldSID-50 Dummy Kinematics Test vs. Simulation in AE-MDB Side Impact

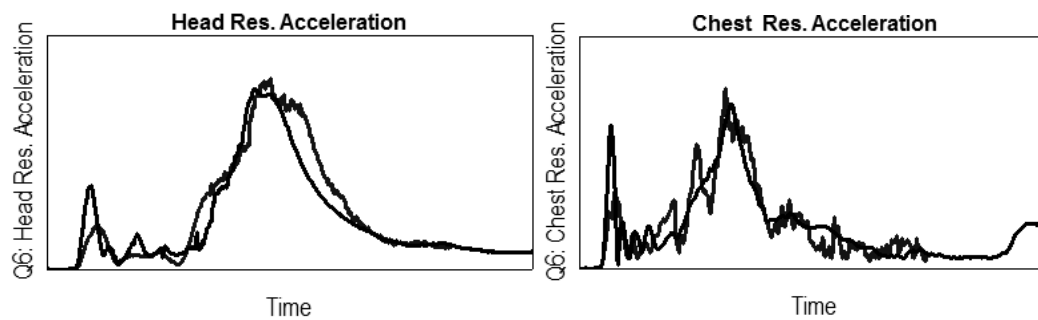


Fig.4: ATD Readings of Q6 according to Euro NCAP 2016 Protocol

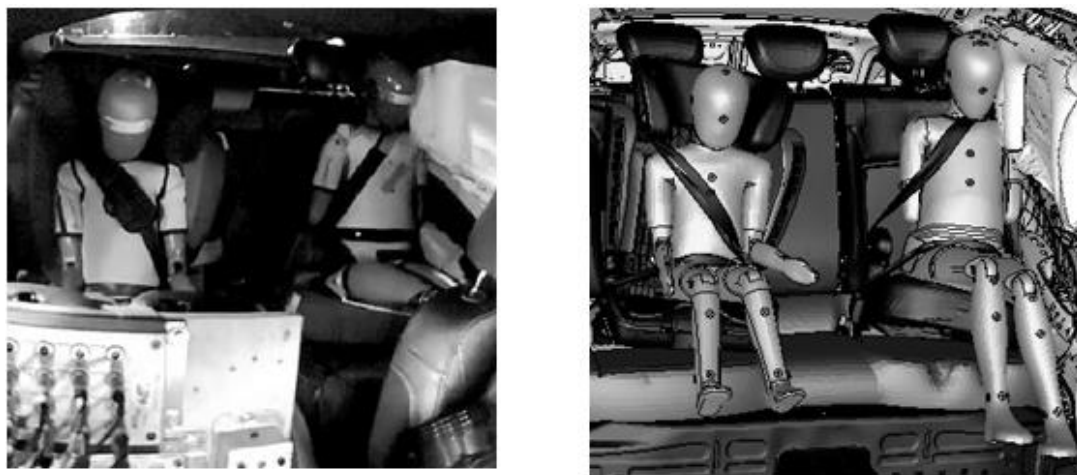


Fig.5: Analysis of Q6/Q10 Dummy Kinematics Test vs. Simulation in AE-MDB Side Impact



---

# Dummy models general update

Frank Schüssler

Humanetics Europe GmbH

## 1 Summary

Humanetics is committed to provide the industry with sophisticated crash test dummies and class-leading finite element models developed with state of art technology and unique engineering knowledge.

New regulations, have made it necessary to improve existing crash test dummies and introduce new dummies. Furthermore, harmonization and increasing quality requirements are responsible for modifications of existing crash test dummies as well.

Humanetics is working together with several OEM's, Tier-1 suppliers and engineering companies in the field of OOP, front crash, side crash, first row, second row and on topics like misuse load case, restraint system and airbag development.

Humanetics, would like to give an overview of the latest LS-DYNA finite element model developments of the HIII3YO, HIII6YO, HIII5th, HIII50th, HIII95th, Q6, Q10, Q10SK, SIDIIS, THOR-50M and Thor-5 and FLEX-PLI.

## 2 New Regulations

EURO NCAP and NHTSA will introduce in the next few years new test procedures and injury criteria which no dummy has seen before. This makes it necessary to set up new validation tests to prepare the FE dummy for these load cases.

## 3 New Hardware

The introduction of a new dummy like the THOR-50 M gives many new challenges for the industry. Car-developers wish to understand the consequences due to introduction of THOR-50 M as early as possible. Making first versions of high quality FE models available at a time that the latest hardware is not or only limited available, is helping to start preparation and get experience early in time.

Currently a new project within Humanetics is progressing aiming to develop a THOR-5 hardware dummy and a first industry FE model version is targeted to become available at the same time that the first hardware prototypes become available.

## 4 Hardware and Software Changes

Humanetics delivers harmonized hardware dummies and FE models representing these dummies.

Harmonization was undertaken to create a single brand of dummies, using select components from the two original manufacturers. This reduces dummy hardware variation which can help to reduce irrelevant influences during vehicle development. Some organizations take the opportunity to move to the more consistent product and specify only Harmonized hardware in there protocol.

Dummy hardware material replacement programs within Humanetics made it necessary to work on new material FE model development for the corresponding materials. Excellent material models have been achieved through new coupon level testing and modelling methods. The resulting material models have been implemented into the dummy models.

Over the years the FE requirements for elements, contacts and materials have changed and Humanetics has worked on these topics to provide the industry with sophisticated crash test dummies.

## **5 Dummy overview**

The HIII3YO and HIII6YO dummies are mostly used for Out Of Position load cases which made it necessary to work on parts which are influencing the Neck Injury criterion. The HIII5th and HIII50th dummies made a big hardware change geometrically and materially wise. The HIII95th is mostly used for severe misuse tests and therefore robustness is very important. The Q6, Q10 and Q10SK are the new kid dummies which will be used in the new regulations. The SIDIIS is a side test dummy where Humanetics has done new non certification tests for the Brain Injury Criteria. The THOR-50M and THOR-5 are the new frontal adult dummies which will be adopted in new regulation. The FLEX-PLI-GTR is a new Pedestrian Protection dummy which has been introduced during the past years.

## News about the THUMS Human Model

D. Fressmann, N. Lazarov

DYNAmore

# Umformsimulationen, Schnittstellen und Prozesse

M. Fleischer, J. Sarvas, H. Grass, J. Meinhardt

BMW

# Berücksichtigung von schergeschnittenen Blechkanten zur Auslegung von Formgebungsprozessen höherfester Stahlwerkstoffe in der FEM-Umformsimulation mit LS-Dyna.

T. Beier, S. Woestmann

<sup>1</sup>thyssenkrupp Steel Europe AG

## 1 Einleitung

Hochfeste, kaltumformbare Werkstoffe bieten ein großes Potenzial zur Erfüllung der gestellten wirtschaftlichen und sicherheitstechnischen Anforderungen für den Bereich der Kraftfahrzeuge. In Folge der inzwischen erzielbaren hohen Festigkeiten von bis zu 1200 MPa sollten bei der Planung mit diesen Werkstoffen einige Aspekte im Vorfeld analysiert und bewertet werden. Dabei ist neben einer frühzeitigen Bewertung des Crashvermögens auch die werkstoffgerechte Gestaltung des Umformprozesses von hoher Relevanz. Werkstoffe jenseits der Zugfestigkeit von 800 MPa zeigen mitunter ein deutlich erhöhtes Risiko im Hinblick auf das Kantenversagen bei der Umformung.

Bauteile aus höherfesten Stahlgüten weisen heutzutage anspruchsvolle Geometrien auf, um den hohen Anforderungen des Leichtbaus gerecht zu werden. Umformtechnisch hoch beanspruchte Bereiche bzw. Formelemente sind unter anderem kleine Radien und Bauteilkanten, Durchstellungen, Innen- und Außenecken, sowie Kanten an Entlastungslöchern und Flanschen. Gerade an Bauteilrändern hat der Werkstoff durch den vorrangegangenen Stanzprozess einen Teil seines Umformpotenzials eingebüßt.

## 2 Bewertung des Umformpotentials schergeschnittener Blechkanten

Es existiert inzwischen eine umfangreiche Anzahl an Versuchen zur Bestimmung der Kantenrissempfindlichkeit von Stahlwerkstoffen [2]. Lochaufweitungsversuche (HET) sind z.B. ein probates Hilfsmittel zur Abschätzung des Umformpotenzials eines Werkstoffes zur Herstellung von Durchstellungen [3]. Sie können aber auch als Bewertungshilfe zur Auslegung von Umformprozessen mit Kantenrissegefährdeten Flanscbereichen herangezogen werden [4]. Das maximale Lochaufweitungsverhältnis (HER) ist allerdings von mehreren Faktoren abhängig. Neben dem Werkstoffkonzept selbst und der natürlichen Streuung des Werkstoffes, spielt unter anderem das Schneidverfahren, als auch die Belastungssituation während der Umformung eine wesentliche Rolle. Die Belastungssituation wird z.B. beeinflusst durch Stempeltyp/ -geometrie, Ausgangslochung, Ziehring oder das Dehnungsniveau. Fig.1 zeigt die experimentell ermittelten HER für einen CP-Stahl und einem DP-Stahl ( $R_m \sim 800\text{MPa}$ ).

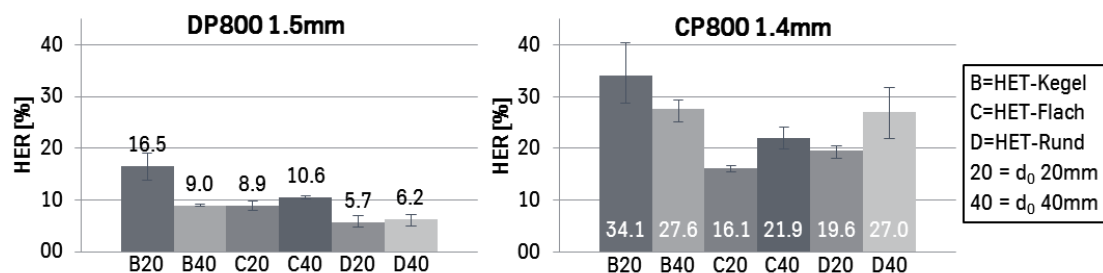


Fig.1: Mittlere HER für unterschiedliche Lochaufweitungstests DP800 & CP800

Es zeigt sich einerseits der Einfluss des Grundwerkstoffes, andererseits der Einfluss der Umformrandbedingungen. In diesem Fall wurden Werkzeuggeometrie (Kegel-, Nakajima- und Marciniakversuch) und Ausgangslochdurchmesser variiert. Die Lochungen wurden mit einem Schnittspalt von 10%, bezogen auf die Blechdicke, hergestellt. Durch Variation der Schneidparameter kann noch zusätzlich auf die Kantenrissempfindlichkeit Einfluss genommen werden [1].

Zur Untersuchung der Belastung durch die Umformung an der Kante und im kantennahen Bereich wurden mit LS-Dyna die einzelnen Versuche nachgerechnet. Zum Einsatz kommt ein 3D Schalenmodell. Die Anisotropie der Werkstoffe wird durch den Fließort Barlat 2000 dargestellt. Für das Fließver-

halten bei hohen Dehnungen wird die Fließkurvenextrapolation durch den Bulgetest abgesichert. Vergleicht man z.B. die Lochaufweitung mit Flachbodenstempel mit der Lochaufweitung mit Kegelstempel, nimmt der Anteil des beteiligten Materials ab und der Biegeanteil an der Umformung nimmt zu. Dies kann unter anderem durch den orthogonalen Dehnungsgradienten beschrieben werden, siehe Fig. 2 rechts. Hierzu wurde die Zunahme der Dehnung zur Kante hin, bezogen auf 5 mm Kantenabstand, in der Simulation ermittelt. Fig. 2 links zeigt die gefundenen Zusammenhänge für die beiden untersuchten Werkstoffe.

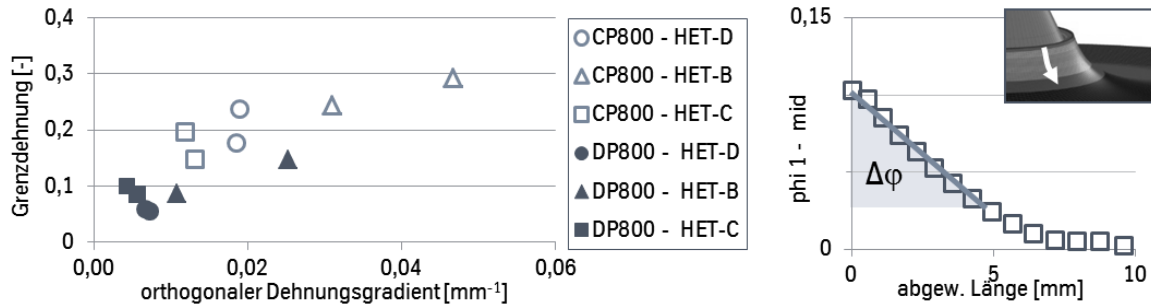


Fig.2: Maximalen Kantendehnung vs. orthogonalem Dehnungsgradienten für DP800 und CP800

Diese Belastungen lassen sich auch an Tiefziehteilen z.B. aus dem automobilen Karosseriebau ermitteln. Niedrige Dehnungsgradienten findet man in Umformprozessen an tiefziehbeanspruchten Platinenrändern unter dem Niederhalter wieder. Höhere Gradienten liegen bei Durchzügen vor. Fig. 3 zeigt beispielhaft den Dehnpfad kritischer Bereiche an Platinenrändern. Dargestellt wird dieser durch die Entwicklung des orthogonalen Dehnungsgradienten und der Hauptformänderung, für eine Durchstellung und einen Platinenrand unter dem Niederhalter im Einflussbereich einer Kofferecke.

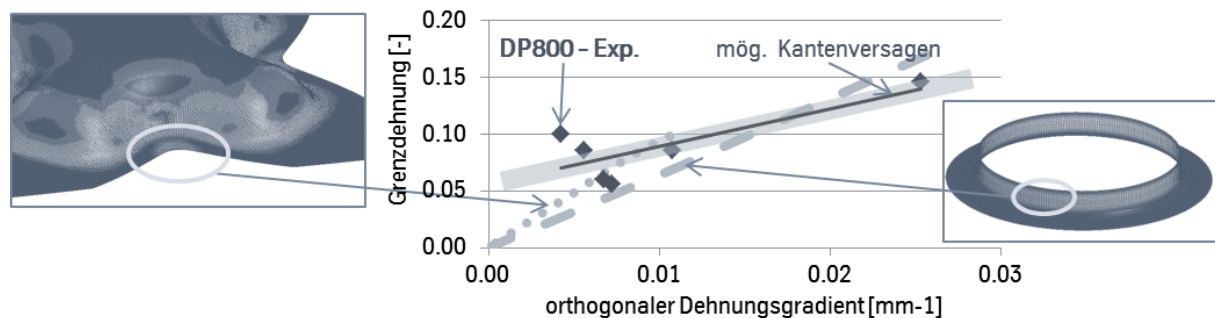


Fig.3: Kritischer Dehnpfad Kofferecke und Durchstellung

### 3 Zusammenfassung & Fazit

Es lässt sich zusammenfassen, dass das Umformpotential von höherfesten Stahlwerkstoffen neben dem Beschnittverfahren, insbesondere vom Werkstoffkonzept und von der Belastungssituation an der Kante um im kantennahen Bereich abhängt. Der orthogonale Dehnungsgradient bietet die Möglichkeit die unterschiedlichen Lochaufweitungsversuche zu differenzieren. Zur Bewertung der Machbarkeit von Realbauteilen ist für kritische Bereiche ein Ersatzversuch mit vergleichbaren Gradienten heran zu ziehen

### 4 Literatur

- [1] Beier, T.; Gula, G.; Woestmann, S.; Kessler, L.: „Eine Bewertung des Umformpotenzials von Schnittkanten zur Auslegung von Formgebungsprozessen mit höherfesten Stahlwerkstoffen.“ EFB-Kolloquium Blechverarbeitung, Bad Boll, Deutschland, 2015
- [2] Schneider, M.; Geffert, A.; Peshekhodov, I.; Vucetic, M.; Behrens, B.-A.: „Overview and comparison of various test methods to determine formability of a sheet metal cut-edge and approaches to the test results application in forming analysis.“ Material Science and Engineering Technology, 46, p. 1196-1217. 2015
- [3] Goncalves, J.; Fouques, D.; Bellut, X.; Zhang, L.; Huang, M.; Van Deventer, J.; Far-rand, B.: „More fruitful and robust hole expansion testing conditions“, IDDRG 2014, Paris, France, 2014
- [4] Iizuka, E.; Urabe, M.; Yamasaki, Y.: „Effect of strain gradient on stretch flange deformation limit of steel sheets – Prediction method of cut edge failure“ Umformen im Karosseriebau, Bad Nauheim, Deutschland 2015

# Sheet Metal Forming of Niobium Crab Cavities at CERN

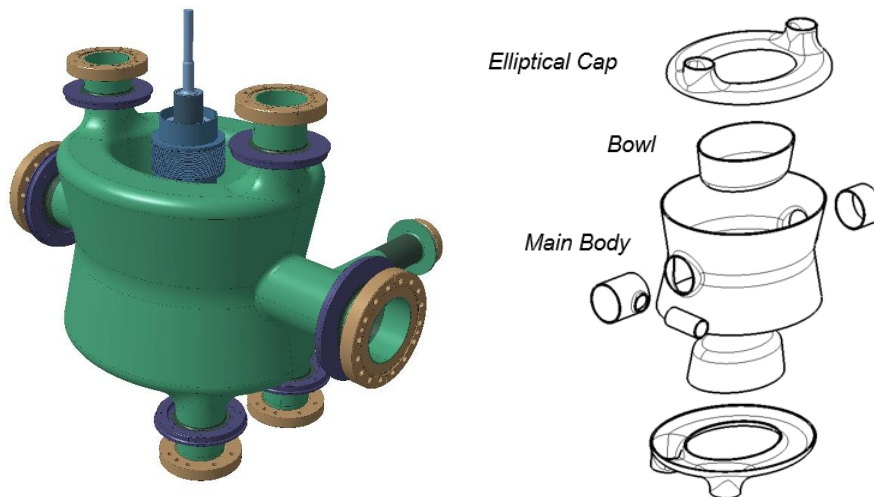
Alexandre Amorim Carvalho, S. Atieh, J-P. Brachet, O. Capatina, M. Toscan du Plantier, A. Dallochio, V. Gerbant, G. Favre, M. Garlaschè, L. Giordiano, R. Leuxe, Manuele Narduzzi, L. Prever-Loiri

CERN

## 1 Introduction

The installation of superconducting Radio Frequency (RF) Crab Cavities is one of the key upgrades in the framework of the High-Luminosity Large Hadron Collider (HL-LHC) at CERN. These devices – built out of niobium sheets – are shaped and joined into a complex geometry entailing very tight tolerances, in order to comply with strict RF requirements.

For production purposes, the so-called Double Quarter Wave (DQW) Crab Cavity was sub-divided in three major sub-elements: *elliptical cap*, *main body* and *bowl* (Fig. 1). These sub-elements were formed in multi-step shaping processes, ranging from deep-drawing to extrusion and bending.



**Fig. 1:** DQW and its main subelements: Elliptical Cap, Bowl and main Body. Overall envelope of the cavity is 660x411x510(mm).

The forming of 4mm thick niobium sheets into the final cavity shape is a demanding process given the high aspect ratio of the different pieces and their tolerances, which are in the order of 0.1mm. This made clear the necessity of better understanding the behavior of the material itself and also of the shaping processes themselves.

In response to this need, LS-DYNA simulations were performed throughout the R&D and production phases. The objective of this study is to present the numerical model set up, to show the results obtained and to analyze their capacity of prediction and of steering production choices.

## 2 Numerical approach

An initial modelling of niobium elasto-plastic properties has been performed via `*MAT_PIECEWISE_LINEAR_PLASTICITY` [1] and the adoption of data from past structural tests performed at CERN; despite the sheet typical dimensional ratios and production processes, isotropic properties have been assumed. Few literature may be found regarding the mechanical aspects and numerical modeling of niobium; the authors thus felt the necessity to improve the initial material model employed, via an extended test campaign which is currently ongoing.

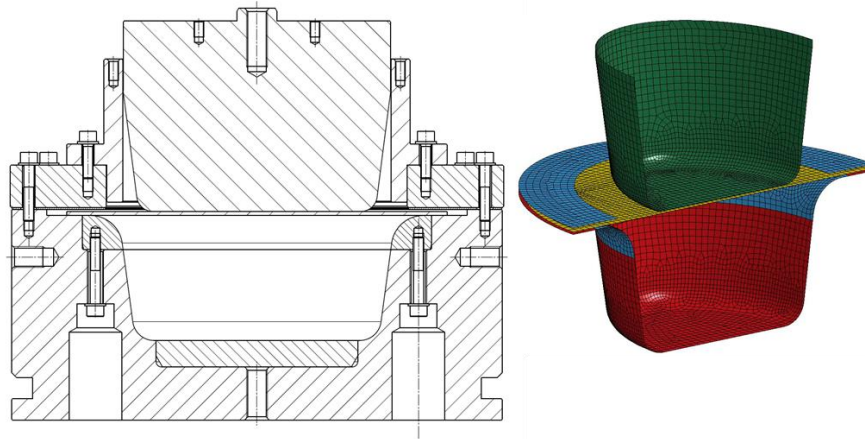
For all studied processes, the behavior of the 4mm-thick niobium sheets, has been modelled via fully integrated shell formulation ELFORM 16 (with 7 through thickness integration points).

For all the rigid parts: punches, pads and molds, the standard rigid body model was employed.

Contacts between the different tool parts and the sheets were defined with `*CONTACT_FORMING_ONE_WAY_SURFACE_TO_SURFACE` [2]. The boundary conditions were imposed

with `*BOUNDARY_PRESCRIBED_MOTION_RIGID` and `*LOAD_RIGID_BODY` for displacement-based simulations and load-based simulations respectively.

Figure 2 shows a cross section view of the tool used for shaping of the Bowl (Left) and the corresponding numerical model (right). A pseudo-elliptical punch deep-draws the niobium sheet into the dual mold. Press-pads are used to guide the sheet during the process.



**Fig. 2:** Tool for deep-drawing of the Bowl sub-element (Left) and its corresponding numerical model (Right).

### 3 Benchmarking

Punch load and displacement data was collected during the different forming processes, in order to provide an evaluation means of the model accuracy. Such data has been obtained via an ad-hoc system of optical and pressure sensors embedded in the hydraulic press.

Each formed piece has also undergone thorough metrology of its surfaces. Shape results have been compared between reality and model.

A script has also been developed, which allows to extract data from metrology results and determine thicknesses at given sections. Such thicknesses have also served as comparison between the numerical and the real process.

The synergy of the above-mentioned methods has allowed insightful benchmark of the numerical model versus the real process, to an accuracy deemed satisfactory for the project's needs. The finite element model has thus served as a powerful tool in understanding the physics of the shaping processes and in steering tool design choices.



**Fig. 3:** Metrology of the Bowl.

### 4 Literature

- [1] LS-DYNA Keyword user's manual Volume II, LSTC, February 2013
- [2] LS-DYNA Keyword user's manual Volume I, LSTC, February 2013



# Parameter identification of two phenomenological damage models for sheet metal forming

S. Heibel<sup>1</sup>, W. Nester<sup>1</sup>, T. Clausmeyer<sup>2</sup>, A. E. Tekkaya<sup>2</sup>

<sup>1</sup>Process Development and Materials, Mercedes-Benz Cars, Daimler AG

<sup>2</sup>Institute of Forming Technology and Lightweight Construction, TU Dortmund University

## 1 Motivation

In modern car body manufacture, the widespread high-strength steels are less ductile. They are more sensitive to damage effects than conventional deep-drawing steels due to their multiphase microstructure and various inclusions. For example, voids nucleate in dual-phase steels at the phase-boundaries between martensite and ferrite at low plastic strains. The voids grow and coalesce during further loading and thus the material fails without severe necking. The Forming Limit Curve (FLC) as the classic failure criterion in forming simulation is only partially suitable for this class of steels. Besides ductile failure without severe necking shear fracture cannot be predicted using the FLC. An improvement can be obtained by using damage mechanics. The objective of this contribution is the comparative assessment of the Enhanced Lemaitre Damage Model and GISSMO (Generalized Incremental Stress State dependent Model) for the application in sheet metal forming simulation.

## 2 Damage modeling – Enhanced Lemaitre Damage Model and GISSMO

Damage indicator models as well as models formulated in the framework of Continuum Damage Mechanics (CDM) introduce a damage variable  $D$  based on Kachanov's idea of a reduction in the load carrying cross section as a result of the formation of voids. Assuming an initial damage value of  $D = 0$ , damage indicator models like the Modified Hosford-Coulomb criterion predict the onset of failure reaching a critical damage value ( $D_{crit} = 1$  for most models). CDM based models like the Enhanced Lemaitre Model and GISSMO compute effective stresses and thus link the scalar damage parameter with the stress tensor. The damage mechanisms are described in a phenomenological manner depending on the triaxiality (void growth) and the Lode-parameter (void shape and inter-void linking). Experimental investigations for various multiphase steels show porosities of about one percent of the undamaged material [1]. This amount of porosity is within such a low range that the computation of effective stresses is not mandatory. However, to compensate the shortcoming of shell elements in the post necking area, the coupling between damage and plasticity model may be reasonable.

The classical Lemaitre Model ([2]) was enhanced in past and recent research works to account for the "void closure effect" under hydrostatic pressure ( $h$ ) and the dependency of the failure strain on the Lode-parameter to better predict shear-dominant fractures ( $2\tau_{max}/\bar{\sigma}$ ) [3], [4].

$$\dot{D} = \left(\frac{2\tau_{max}}{\bar{\sigma}}\right)^\theta \left(\frac{Y-Y_0}{S}\right)^s \left(\frac{\dot{\epsilon}_{pl}}{(1-D)^\beta}\right) \quad \text{with} \quad Y = \frac{1+\theta}{E} \left(\sum_{i=1}^3 (\sigma_i)^2 + h(-\sigma_i)^2\right) - \frac{\theta}{2E} ((\sigma_m)^2 - h(-\sigma_m)^2) \quad (3)$$

The onset of failure is obtained when  $D$  reaches a material specific critical damage value  $D_{crit}$ . Results of [4] and [5] reveal that this damage model with seven parameters shows sufficient flexibility to fit complex fracture curves.

The basis of GISSMO is an incremental damage accumulation which depends on a failure curve. The failure curve itself depends on the stress triaxiality. The damage parameter  $D$  intrinsically incorporates the influence of non-proportional loading paths. The damage accumulation is driven by the evolution of equivalent plastic strain and can be influenced by a damage exponent  $n$ . The damage parameter is coupled to the stress tensor after reaching the so-called instability curve. The "magnitude" of coupling depends on the fading exponent  $m$ . For further information regarding GISSMO see reference [6].

## 3 Parameter identification

In the course of these investigations, both damage models are calibrated inversely for a dual-phase and complex-phase steel with a tensile strength of 1 GPa. The experimental basis for the parameter identification consists of the classical mechanical properties as well as the force-displacement curves of a shear tension, a uniaxial tension, a plane-strain tension and an equi-biaxial tension test to cover a triaxiality range between 0 and 0.67. The uniaxial and plane-strain tension specimens, in particular, exhibit non-proportional loading paths. The plastic material behavior is modelled with Hill48's yield criterion and with a tabulated flow-curve for isotropic hardening. The flow-curve is determined with a

multiplicative Hockett-Sherby - Swift approach, which is approximated via reverse-engineering to all four experiments.

The optimization software LS-Opt is used for the parameter identification of the Enhanced Lemaitre Damage Model. To reduce the number of parameters for the optimization process  $Y_0$  and  $D_{crit}$  are calculated with formulas proposed by Lemaitre [2],  $h$  is assumed to be 0.2 and  $S$  is kept constant with a value of 0.5 GPa. Hence  $\theta$ ,  $s$  and  $\beta$  are determined via LS-Opt.

The material card for GISSMO is generated via reverse engineering. To fit the experimental force-displacement curves the failure strains of the failure curve are adjusted for respective triaxialities, the position of the instability curve is determined and suitable values for  $n$  and  $m$  are chosen.

For both steels, the numerically determined curves computed with GISSMO lay in good accordance with the experimental ones. For DP1000, the onset of failure is determined slightly too early with the Lemaitre Model. The highest deviation between the experimental and numerical curves can be found for the Nakajima specimen representing the equi-biaxial tension stress-state. For CP1000, on the other hand, the onset of failure is overestimated for the shear tension and equi-biaxial tension test.

#### 4 Validation

Two principle parts are used to validate the calibrated models. A cross-die cup is used for failure with underlying triaxialities between uniaxial and equi-biaxial tension. The failure for lower triaxialities is represented with a curved cup. Figure 1 shows an example of simulations with GISSMO and the respective fractured cups for DP1000.

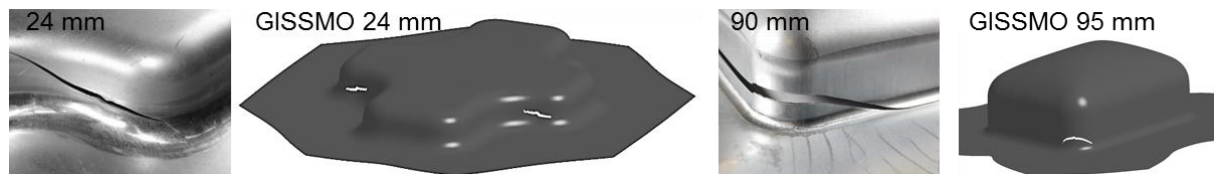


Fig.1: GISSMO: Comparison of experiment and simulation for DP1000 (left: cross-die cup; right: curved cup)

For the cross-die cup the drawing depth predicted by the GISSMO model lies within the experimental scattering and the onset of failure is predicted in the frame of the cup. The Enhanced Lemaitre Damage Model predicts a drawing depth of 19 mm. The onset of failure takes place at the die corner due to the premature onset of failure in the equi-biaxial tension stress state. With an experimental drawing depth of about 90 mm for the curved cup and a numerically computed drawing depth of 95 mm GISSMO slightly overestimates the onset of failure for lower triaxialities. With the Lemaitre model no failure is observed till a drawing depth of 100 mm. This can be explained by the strong influence of considering the "void closure effect" on damage accumulation for negative triaxialities.

#### 5 Summary

In this contribution it is shown that GISSMO can be calibrated via reverse engineering and that the model is able to predict the failure behavior of high-strength steels in sheet metal forming simulation. With the strategy used for identification of the Enhanced Lemaitre Damage Model, there were slight deviations for the force-displacement curves in the shear and equi-biaxial stress state. This influences the predictability of failure in simulation of the forming process of the cross-die and curved cup.

#### 6 Literature

- [1] Heibel, S.; Nester, W.; Clausmeyer, T.; Tekkaya, A. E.: "Damage characterization of high-strength multiphase steels", IDDRG, 2016
- [2] Lemaitre, J.: "A Course on Damage Mechanics", Springer-Verlag Berlin Heidelberg, 1996
- [3] Tekkaya, A. E.; Soyarslan, C.; Isik, K.; Doig, M.: "FOSTA P 853 – Entwicklung eines anwenderorientierten Versagensmodells für die Blechumformsimulation", 2014
- [4] Isik, E.; Doig, M.; Richter, H.; Clausmeyer, T.; Tekkaya, A. E.: "Enhancement of Lemaitre Model to Predict Cracks at Low and Negative Triaxialities in Sheet Metal Forming", Key Engineering Materials Special Issue SheMet, 2015, 427-434
- [5] Soyarslan, C.; Richter, H.; Bargmann, S.: "Variants of Lemaitre's Damage Model and Their Use in Formability Prediction of Metallic Materials", Mechanics of Materials, 2015
- [6] Andrade, F.; Feucht, M.; Haufe, A.: "On the Prediction of Material Failure in LS-DYNA: A Comparison Between GISSMO and DIEM", 13<sup>th</sup> International LS-DYNA Users Conference, 2014

---

# Analyse der zu einer verzögerten Rissbildung führenden umformtechnischen Randbedingungen

M. Teschner<sup>1</sup>, M. Schneider<sup>1</sup>, M. Otto<sup>1</sup>

<sup>1</sup>Salzgitter Mannesmann Forschung GmbH

Der verstärkte Einsatz höchstfester Stähle für sicherheitsrelevante Bauteile im Automobilbau ermöglicht die Umsetzung von Leichtbauzielen, bevorzugt bei gleichbleibender bzw. idealerweise nochmals gesteigerter Crash-Performance. Die erfolgreiche Produktentwicklung verlangt hierzu auch die Einbeziehung von zusätzlichen Einflussgrößen, deren Extremwerten sowie ihren Auswirkungen an Prozessgrenzen. Das Thema Wasserstoffbeladung oder wasserstoffinduzierte verzögerte Rissbildung nach der Umformung ist ein solches Merkmal, dass aktuell unter Experten für Stahlsorten mit Zugfestigkeiten oberhalb 1000 MPa diskutiert wird. Es besteht die Hypothese, dass der Werkstoff unter besonders ungünstigen Umständen empfindlich auf den durch das Herstellungs- und Weiterverarbeitungsverfahren eingebrachten diffusiblen Wasserstoff reagieren könnte. Neben der Menge an diffusiblen Wasserstoff scheinen sehr große plastische Formänderungen sowie anliegenden Spannungen ursächlich zu wirken. Damit das Potenzial moderner Stähle - höchstfest bei maximaler Umformbarkeit - voll ausgeschöpft werden kann, ist die Kenntnis über die Randbedingungen wichtig, unter denen mit verzögerter Rissbildung ggf. zu rechnen ist.

Im Rahmen der Untersuchung werden in verschiedenen experimentellen Versuchsreihen aus Ronden Rundnäpfe geformt, mit denen analysiert wird, inwieweit unter extrem ungünstigen Laborbedingungen eine verzögerte Rissbildung auftreten könnte. Ziel ist es zum einen, ein Grenzziehverhältnis bezüglich des Auftretens von verzögerter Rissbildung zu ermitteln und zum anderen den Einfluss verschiedener Schnittkantenqualitäten zu untersuchen. Weiterhin werden umfangreiche, numerische Versuchsreihen zur Napfumformung durchgeführt, bei denen sowohl unterschiedliche Ziehverhältnisse als auch Napfdurchmesser berücksichtigt werden. Die dabei verwendeten Materialmodelle werden zur Nachbildung der anisotropen Eigenschaften des Materials durch virtuelle Zugversuche entsprechend der Realversuche kalibriert. Zur Validierung der Ergebnisse der virtuellen Napfumformung werden sowohl Vergleichsmessungen der Wanddicke an verschiedenen Positionen durchgeführt, als auch ein Abgleich zwischen einem virtuellen und einem optisch vermessenen Rundnapf hinsichtlich der über der Abwicklung vorliegenden Formänderungen vorgenommen. Im Anschluss werden die Umformsimulationen durch entsprechende Postprocessing-Makros automatisch ausgewertet. Betrachtet werden hierbei vor allem die plastische Dehnung und die im Bauteil verbleibenden Zugspannungen an der Schnittkante. Die mithilfe der Makros exportierten Daten werden durch weitere Excel-Makros importiert und analysiert. Sowohl die daraus resultierenden Spannungs-Dehnungs-Verhältnisse als auch die Ergebnisse der experimentellen Versuchsreihen dienen der Entwicklung einer Grenzkurve, auf deren Basis das Auftreten von verzögerter Rissbildung abgeschätzt werden könnte. Die Anwendbarkeit der Grenzkurve wird durch Abgleich der Ergebnisse einer Umformsimulation eines Sitz-Lehnen-Seitenteils mit den experimentellen Untersuchungen bestätigt. Zur weiteren Absicherung sind dennoch zusätzliche experimentelle Untersuchungen sinnvoll.

# Implementierung einer Netzwerkschnittstelle in LS-DYNA zur gekoppelten Simulation

S. Kriechenbauer<sup>1</sup>

<sup>1</sup>Fraunhofer IWU, Nöthnitzer Str.44, 01187 Dresden

## 1 Einleitung

Zur Simulation von Blechumformprozessen werden im industriellen Einsatz einfache Modelle verwendet. Damit werden Machbarkeitsstudien durchgeführt und Blechzuschnitte ausgelegt. Mit der Simulation werden Tiefziehwerkzeuge entwickelt, die nach der Fertigung eingearbeitet werden müssen. Da in den vereinfachten Modellen nicht alle qualitätsbeeinflussenden Faktoren berücksichtigt werden, entstehen Defizite bei der Entwicklung der Werkzeuge [1]. Beispielsweise werden die Durchbiegung der Werkzeuge und die Auffederung der Pressmaschine nicht abgebildet. Diese Nachgiebigkeiten führen beim Tiefziehen zu einer Druckverteilung am Niederhalter, die den Werkstofffluss bestimmt. In der Simulation werden nur starre Wirkflächen abgebildet, womit abweichende Flächenpressungen im Flansch prognostiziert werden. Bei hohem Druck wird das Blech am Hineinfließen in die Umformzone gehindert. Bei der Einarbeitung werden die Kräfte durch manuelles Ab- oder Auftragen der Niederhalterfläche korrigiert. Dieser Prozess muss mehrmals wiederholt werden bis das Ergebnis stimmt, da nur Erfahrungen und Handarbeit zum Erfolg führen.

Mit modernen Servo-Pressen können die Bewegungen von Stößel und Ziehkissen frei programmiert werden. Diese Flexibilität kann mit den starren Randbedingungen in den einfachen Prozessmodellen nicht abgebildet werden. Bei der Modellierung werden keine realen Massenverhältnisse abgebildet, um die Rechenzeit zu beschleunigen. Die dynamischen Verhältnisse werden somit falsch beschrieben. Neuere Entwicklungen von Prozessen auf modernen Servo-Pressen, die z.B. eine deutliche Abhängigkeit von der Bewegung der Werkzeugteile zeigen, können mit den einfachen Modellen nicht abgebildet werden.

In vorhergehenden Arbeiten wurden bereits Ansätze entwickelt, um die Prozessmodelle um charakteristische Maschineneigenschaften zu erweitern. Das Spektrum der Erweiterungen reicht in der Simulation mit finiten Elementen von vereinfachten Ersatzmodellen wie z.B. Feder-Dämpfer-Elementen bis hin zur Modellierung gesamter Pressen [2]. Dadurch erhöht sich die Komplexität der Modelle deutlich. Es wird schwieriger, die Modelle aufzubauen und zu parametrieren. Häufig dauert der Modellfindungsprozess länger. Die Berechnung der Umformvorgänge verlängert sich bei den erweiterten Modellen um ein Vielfaches. Die Interaktion von Prozess und Maschine lässt sich auch durch die Kopplung zweier unterschiedlicher Simulationsumgebungen abbilden [3]. Dabei werden die Vorteile der zwei Umgebungen wie z.B. FEM (Finite-Elemente-Methode) und DBS (Digitale Blocksimulation) verbunden und Nachteile der einzelnen Programme beseitigt. Mit der zuletzt genannten Simulationsumgebung kann das dynamische mechatronische Systemverhalten erfasst werden. Durch die Kopplung erweitert sich auch der Funktionsumfang. Die Prognosegenauigkeit nimmt bei gekoppelten Simulationen zu, da Prozessgrößen wie z.B. die Kräfte während der Umformung in beiden Umgebungen aktualisiert und ausgetauscht werden. Beispielsweise können durch diesen Austausch asymmetrische Effekte aufgrund der Stößelkipfung wie einseitige Faltenbildung oder lokal stärkerer Blecheinzug erklärt werden [1].

## 2 Softwarekonzept zur gekoppelten Simulation

In der vorliegenden Veröffentlichung wird beispielhaft eine Kopplung zwischen Matlab-Simulink (DBS) und LS-DYNA (FEM) vorgestellt. Die entwickelte Software kann auch mit anderen Simulationsumgebungen gekoppelt werden. Zunächst soll das Konzept der Kopplung näher erläutert werden. Der Aufbau der gekoppelten Simulation ist beispielhaft für die zwei Clients in Fig.1: dargestellt. Die Kommunikation mit dem Server kann um beliebig weitere Simulationsumgebungen erweitert werden. Die Clients arbeiten unabhängig voneinander in verschiedenen Threads.

Der Datenaustausch ist bei gekoppelten Simulationen nicht standardisiert. Daher muss jeweils eine Schnittstelle geschaffen werden, die den Ablauf der gekoppelten Simulation kontrolliert. Sinnvollerweise wird für den Datenaustausch auf das Netzwerkprotokoll TCP/IP (Transmission Control Protocol/Internet Protocol) zurückgegriffen. Dieses Konzept ermöglicht maximale Flexibilität bei der Wahl der Programme und Standorte der Simulation. So lassen sich über das Internet Daten zwischen mehreren Simulationsumgebungen austauschen. LS-DYNA und MATLAB melden sich als Clients am

Server an, der den Datenaustausch zentralisiert und überwacht. In der jetzigen Form wurde der Server in C/C++ programmiert und als Konsolenprogramm gestartet. Eine Benutzeroberfläche soll in weiteren Arbeitsschritten folgen. Die Funktionalität ist so verpackt, dass die Programmerroutinen als Bibliothek exportiert und in andere Programmiersprachen leicht eingebunden werden können. Der Umfang ist auf wenige Funktionen für das Senden und Empfangen von Daten oder Anweisungen beschränkt. Daher können leicht Schnittstellen zu anderen Programmiersprachen wie z.B. Python oder Fortran realisiert werden. Falls eine Simulationsumgebung keine offenen Programmierschnittstellen bietet, kann ein externes Programm die Austauschgrößen erfassen und an den Server weiterleiten. Die Steuerung der Simulation wird dadurch allerdings erschwert.

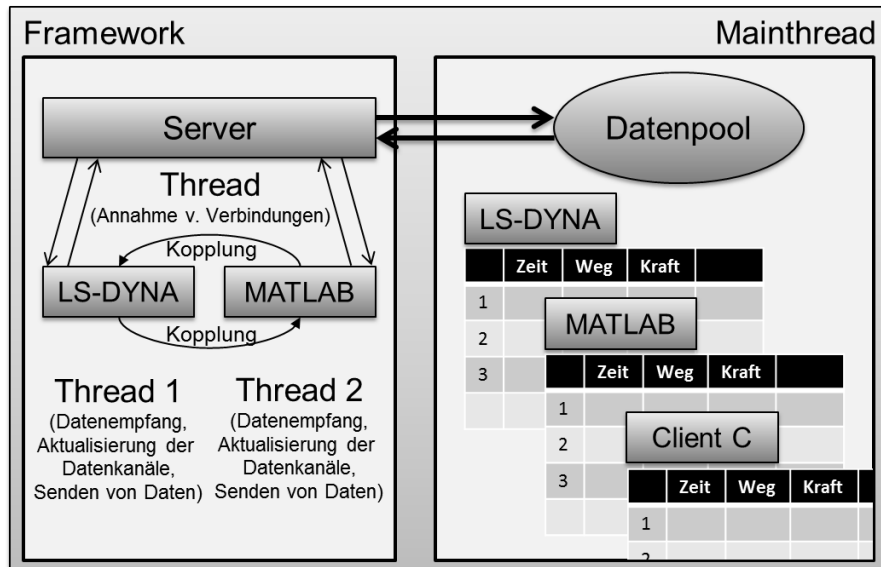


Fig.1: Softwarekonzept zur gekoppelten Simulation basierend auf dem Netzwerkprotokoll TCP/IP am Beispiel zwischen LS-DYNA und Matlab Simulink

In LS-DYNA wurde das Netzwerkprotokoll in die User-Subroutine uctrl1 in der Programmierschnittstelle dyn21.F implementiert. Vorteil ist dabei, dass LS-DYNA in jedem Berechnungsschritt mit dem Server kommuniziert und während der Simulation auch auf Freigaben des Servers wartet. In der expliziten Version von LS-DYNA werden die Austauschgrößen für den nächsten Zeitschritt direkt in die Vorgaben der Randbedingungen geschrieben. Diese Vorgehensweise funktioniert für kinematische Größen und Kräfte. Zur Aktivierung und Steuerung der Schnittstelle wird eine separate Datei beim Start des Solvers eingelesen. Damit wird sichergestellt, dass bestehende Umformsimulationen nicht beeinflusst werden. In der Datei wird die IP-Adresse des Servers hinterlegt, die Zeitschrittweite für das Empfangen und Senden von Daten und die ID's für **\*DEFINE\_CURVE** bzw. **\*DEFINE\_CURVE\_FUNCTION**. Der Datenaustausch ist asynchron, d.h. die Zeitschrittweite für das Senden kann sich von der für das Empfangen unterscheiden. Die Daten aus der Empfangsrichtung werden direkt in die Arrays für die entsprechenden Kurven geschrieben bzw. in der Senderichtung ausgelesen. Bei jedem Austauschschritt zum Datenempfang wartet der Client auf Antwort vom Server, um die Simulation mit den aktuellen Daten eines anderen Clients fortsetzen zu können. Durch diese Abfolge wird gewährleistet, dass alle Simulationsumgebungen mit aktuellen Datensätzen weiterrechnen. Die berechneten Austauschdaten werden im Server in Datenkanälen zwischengespeichert. Fordert nun ein Simulationsprogramm zu einem bestimmten Zeitschritt Daten an, werden diese interpoliert und weitergegeben. Die Zeitschritte für den Datenaustausch dürfen nicht zu weit auseinander liegen, um die Stabilität der gekoppelten Simulation zu gewährleisten.

In LS-DYNA steht mit dieser Implementierung in Fortran eine voll funktionsfähige Netzwerkschnittstelle zum Datenaustausch bereit. In Matlab Simulink wurde die Funktionalität mit einer S-Function implementiert. Die S-Function ist eine C/C++ Programmierschnittstelle. In Fig.2: ist die Schnittstelle in einem Matlab-Simulink-Modell zusammen mit einem Beispielprozess dargestellt. Die aktuellen Daten von LS-DYNA kommen an der Client-Schnittstelle an. Im Beispiel wird die Kraft als Austauschgröße weitergeleitet an das Matlab-Simulink-Modell. Im Beispiel wird ein Kraftsprung simuliert. Die Reaktion des Systems gemessen an den kinematischen Größen wird wieder über die Client-Schnittstelle und den Server weitergeleitet an LS-DYNA oder an andere Simulationsumgebungen. Ähnlich wie beim Tiefziehen wird die Prozesskraft aus dem Umformmodell der FEM-

Umgebung ausgelesen und im Modell der Pressmaschine in der DBS-Umgebung vorgegeben. Die resultierende Verlagerung wird zurück an das Umformmodell gegeben. Diese Art der Kopplung basiert auf dem Austausch von Kraft- und kinematischen Größen wie Weg, Geschwindigkeit oder Beschleunigung.

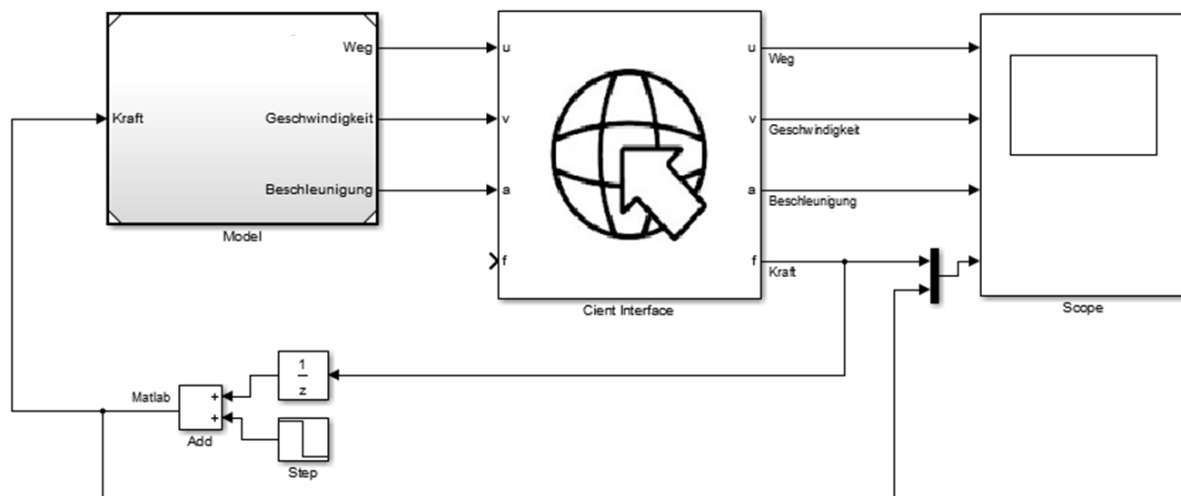


Fig.2: Darstellung des Matlab-Simulink-Modells mit Beispielprozess in der FEM (links) der Client-Schnittstelle (mitte) und der Auswertung (rechts)

### 3 Zusammenfassung

Mit einer gekoppelten Simulation kann die Wechselwirkung zwischen einem Umformprozess und der Pressmaschine berechnet werden. Der Werkstofffluss ist beim Tiefziehen abhängig von der Druckverteilung am Niederhalter, die wiederum von der Verformung des Werkzeuges und der Auffederung der Pressmaschine bestimmt wird. Bei Berücksichtigung der Effekte in einer gekoppelten Simulation können Tiefziehwerkzeuge entwickelt werden, die eines geringeren Einarbeitungsaufwands bedürfen.

Zur Kopplung mehrerer Programme entstand eine Software, die zum Zweck des Datenaustausches auf dem Netzwerkprotokoll TCP/IP basiert. Damit können verschiedenste Simulationsprogramme gekoppelt werden. Am Beispiel von LS-DYNA und Matlab Simulink erfolgte eine direkte Implementierung in die Programme. Das Netzwerkprotokoll kann dabei durch eine Eingabedatei aktiviert und gesteuert werden.

### 4 Literatur

- [1] Hardtmann, A.: "Entwicklung und Bewertung eines erweiterten Blechumformprozessmodells unter besonderer Berücksichtigung der elastostatischen Wechselwirkungen zwischen Maschine und Prozess", Dissertation TU Dresden, 2010
- [2] Geimer, M.; Krüger, T.; Linsel, P.: „Co-Simulation, gekoppelte Simulation oder Simulatorkopplung“, O+P 11-12, 2006, S. 572-576
- [3] Weber, J.; Schulze, T.; Großmann, K.; Penter, L.; Schenke, C.-C.: Simulationsgestützte Abstimmung von Ziehkissen, EFB-Forschungsbericht Nr. 412, Hannover, 2015

# Finite Element Simulation of Delamination during Side Milling of Cross-Ply Carbon Fiber Reinforced Polymer (CFRP) Boards

H. Vazquez Martinez<sup>1,2</sup>, P. Esch<sup>2</sup>, K. Patel<sup>2</sup>

<sup>1</sup> Fraunhofer Institute of Manufacturing Engineering and Automation IPA, Stuttgart Germany

## 1 The machining of CFRP components

Carbon fiber reinforced polymers (CFRP) are lightweight materials widely used in aerospace, automobile, machine components and sport equipment. CFRP components are mostly manufactured in such a way, that if possible, no additional treatments after their production are required. However, different finishing or drilling steps are inevitable to maintain the flexibility on manufacturing chains. Due to the inhomogeneity of CFRPs, machining operations can induce different type of damages such as delamination, fiber pullout, fiber-matrix interface cracking and matrix cracking on the structures. These damages can induce further crack propagations especially in the fiber direction [1]. In this sense, the machining of composite materials can be considered to be quite different compared to common metal cutting operations. The present study intends to determine operational parameters for preventing delamination to take place with the use of finite element (process) simulations for the side milling of CFRP laminates.

## 2 Modelling approaches

Apart from empirical or analytical methods, numerical methods have made it possible to study machining processes. Numerical methods include finite element method (FEM), molecular dynamics and multiscale modeling methods. The FE-method is used for modelling cutting processes at macro scale, where continuum mechanics principles are applicable [2]. The three main approaches used to model the behavior of composite materials are: multi-phase modeling approach (micromechanical approach), an equivalent homogeneous material (EHM) approach (macromechanical approach) and combination of the two approaches [2]. The FE software LS-Dyna offers several material cards to model the behavior of composite materials with use of EHM models.

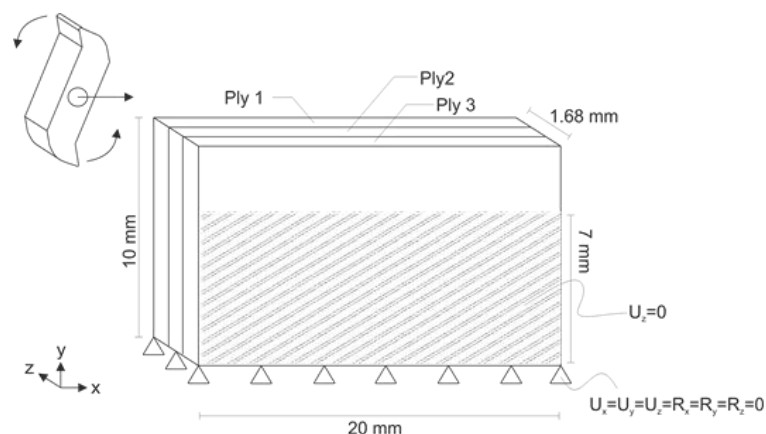


Fig.1: Schematic representation of the simulation setup.

## 3 Experimental and simulation work

An experimental setup has been designed in order to measure the delamination induced through side milling operations. In this case a unidirectional CFRP structure made up from the prepreg with the fiber orientations [0/90] has been used. The laminate is made up of 9 plies each with the thickness of 0.56 mm. A carbide cutting tool has been used for the edge milling of the CFRP laminate. The tool has two cutting edges with straight flute and is made up of EMT 100 carbide material. The figure 1 shows the schematic representation of the simulation model. Material card 54 in LS-Dyna (MAT54: Enhance composite damage) has been used to model the behavior of the CFRP work piece. This material card

uses *Chang-Chang* failure criteria, which is a modified version of the *Hashin* failure criterion. The *Hashin* failure criterion considers the failure of fiber and matrix in tension and compression separately. The *Chang-Chang* criterion expands on the *Hashin* failure criterion by including the non-linear shear-stress behavior of laminas and defining the post-failure degradation rule so that the behavior of the laminate can be analyzed after each successive lamina failure [3].

#### 4 Results

The figures 2 and 3 show exemplary experimental and simulation results obtained in this work.

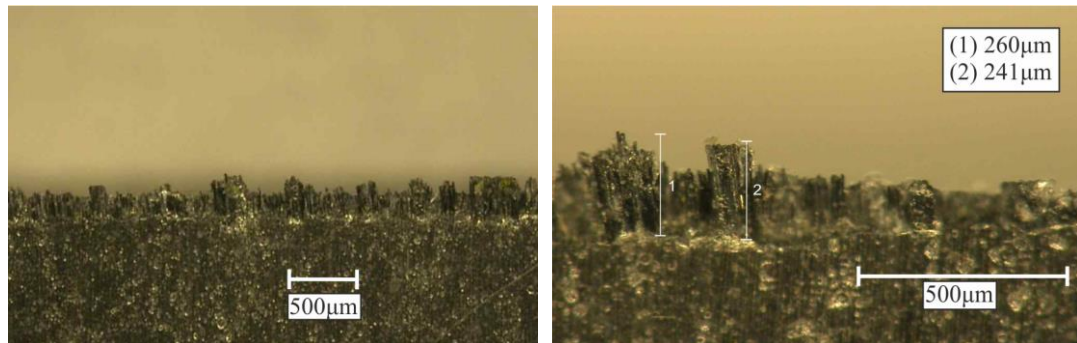


Fig.2: Experimental results: Surface delamination presented on CFRP laminates after side milling with a feed velocity of 233 mm/sec.

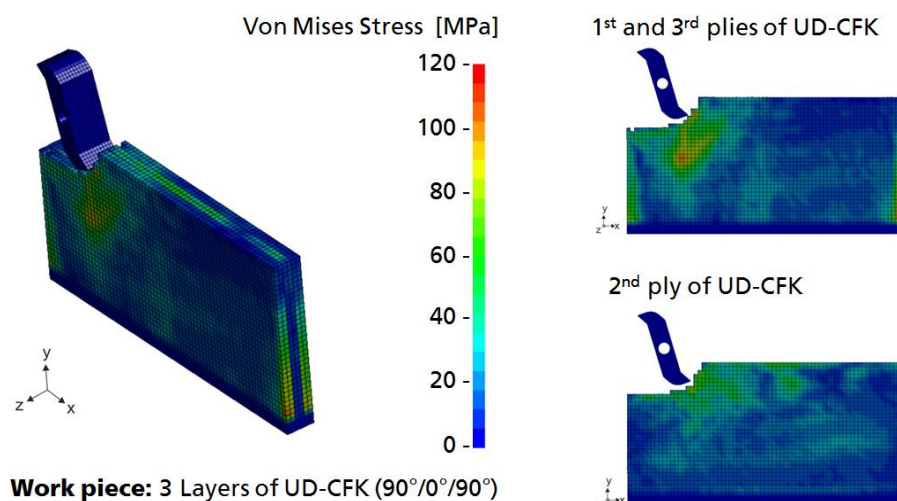


Fig.3: Simulation results: Calculated stress distribution by the simulation of side milling UD-CFK at time = 0.0219 sec.

#### 5 Summary

A 3D finite element model of side milling process of CFRP laminate made up of 3 cross-plyes [90°/0°/90°] has been developed with use of LS-Dyna. Experimental milling tests on cross-ply CFRP laminate have been performed to determine parameters inducing delamination. The simulated model shows plausible responses concerning to the stress distribution along the fiber directions due to the action of the mechanical loads. The model is capable to reproduce interlaminar delamination and no surface delamination. Both experimental and simulation results show that the increase of the feed rate induces higher delamination levels on the CFRP laminate.

#### 6 Literature

- [1] Ramulu, M.: Machining and surface integrity of Fiber-Reinforced Plastic Composites. *Sadhana*, Vol. 22(3), 1997, p. 449-472.
- [2] Anania D., Colt-Stoica M., Mohora C., Stoica D.: Defects in composite material caused by drilling in manufacturing Process, University Politehnica from Bucharest.
- [3] Roy K.: Numerical modeling of impact damage on carbon fiber reinforced polymer laminates, Master's thesis, Ryerson University, Canada, 2014.



# BMBF MAI qfast: design and validation with ULTRASIM® for continuous fiber reinforced parts

Sebastian Ebli, Stefan Glaser, Andreas Wüst

BASF SE, Ludwigshafen

## 1 Introduction

MAI qfast was one project of the leading-edge cluster MAI Carbon, which is promoted by the Federal Ministry for Training and Research (BMBF).

Finished in 2015, the goal of this project was to design a generic continuous fiber reinforced part (CFRP) with focus on a high-scale automotive production.

Together with AUDI and BMW, a design space for a smaller, generic structure based on a body in white underfloor structure was defined. After the definition of generic load cases, two designs were defined for different matrix systems (PA/SMC and PU/EP) in combination with carbon fiber in different manufacturing processes.

## 2 Design

BASF's ULTRASIM approach tries to calculate the part right (material modelling), but also to calculate the right part (design optimization). In addition to classical optimization methods like topology, topography and free-size optimization a special composite optimization method is used in the project. With the three-step composite method developed by Altair (Optistruct Composite), an optimum sequence for the layup with respect to manufacturing constraints can be defined, see Fig.1.

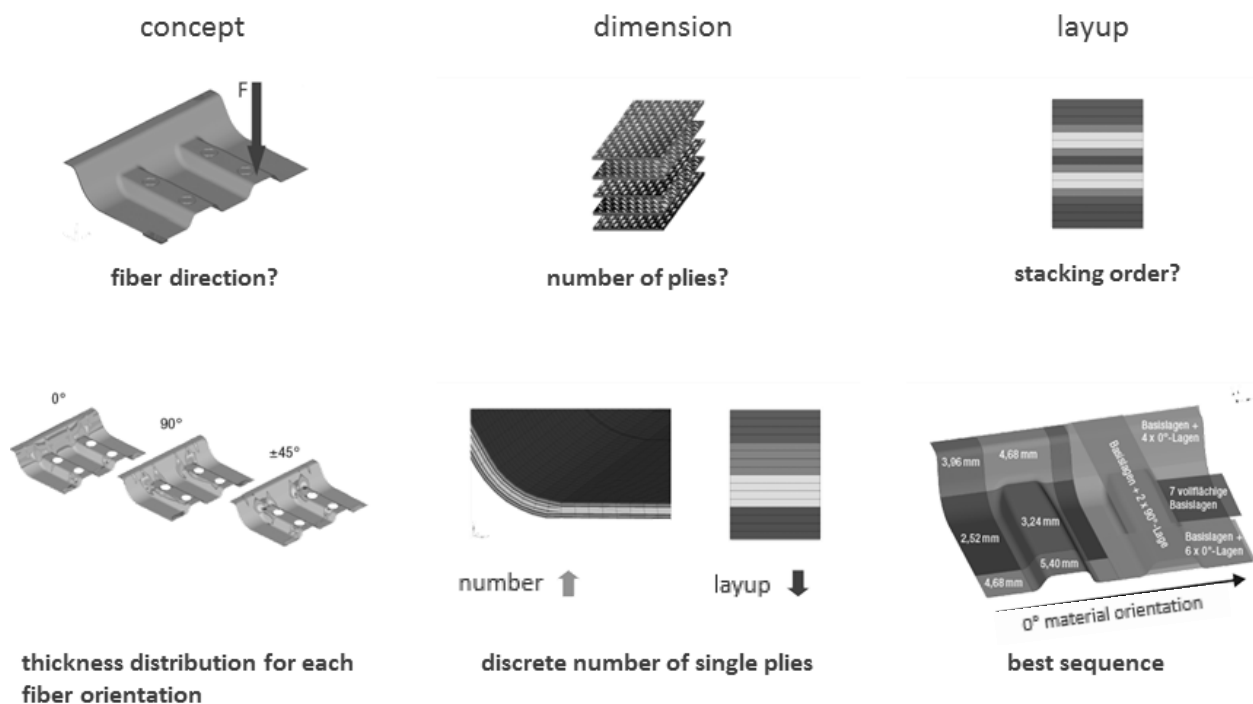


Fig.1: Three-step composite optimization: Find the best fiber direction – Find the adequate no. of plies – Find the best stacking order

### 3 Simulation and Testing

After production of 100 parts at Fraunhofer ICT in Pfinztal, different load cases were tested focussing on static, dynamic, NVH and crash load. After “calculating the right part” by means of the above described optimization schemes, the simulations were performed for load cases “Twisting load”, “Operating load” and “Impact load”, see Fig. 2.

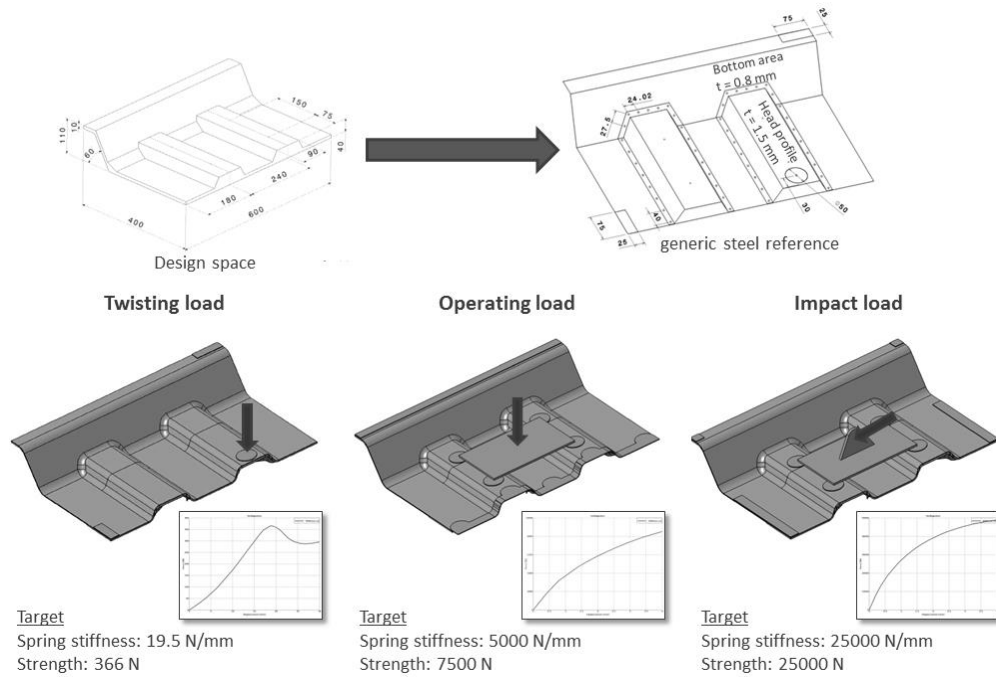


Fig.2: Load cases

This was done based on the Ultrasim material model, which has been developed for CFRP parts (“calculating the part right”) see Fig. 3. LS-Dyna coupled with Ultrasim user-material model was used for all mechanical simulations needed. Draping simulations, also based on LS-Dyna, were done to model the fiber direction change during the manufacturing process. For the draping simulation \*Mat\_249 was used.

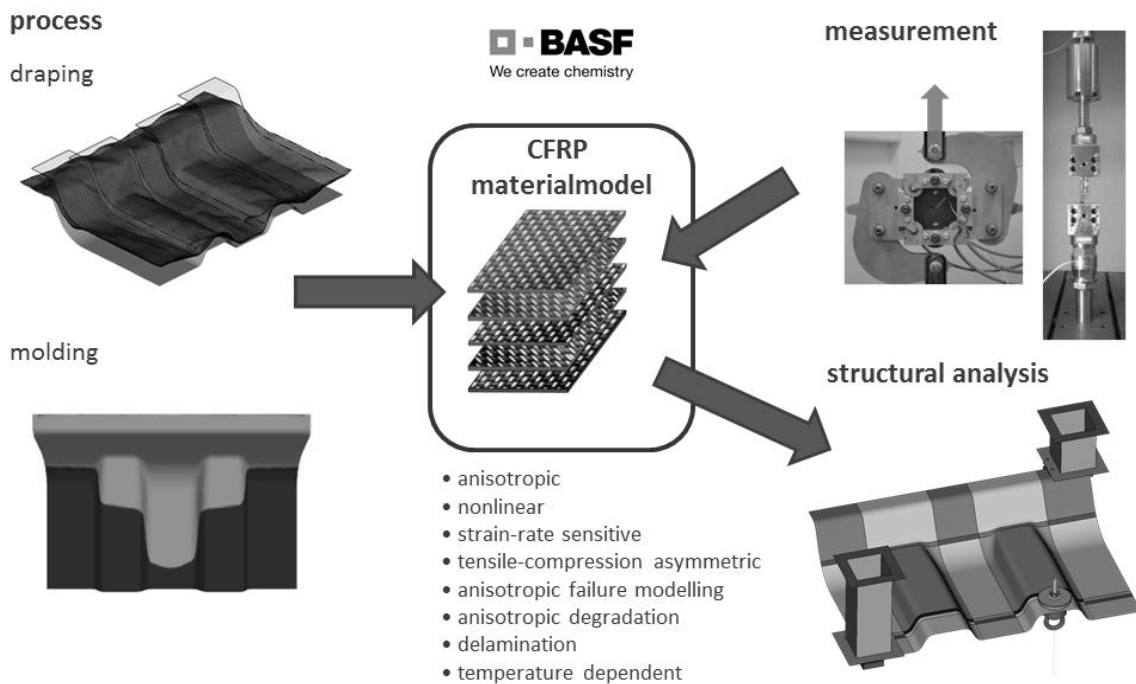


Fig.3: BASF ULTRASIM User material model and workflow

Figure 4 shows a full calculation and post processing for load case “Twisting load”. Standard results like deformation or von Mises stress is plotted and additionally two ULTRASIM failure indices (global failure for matrix/fibre and delamination) are visualized.

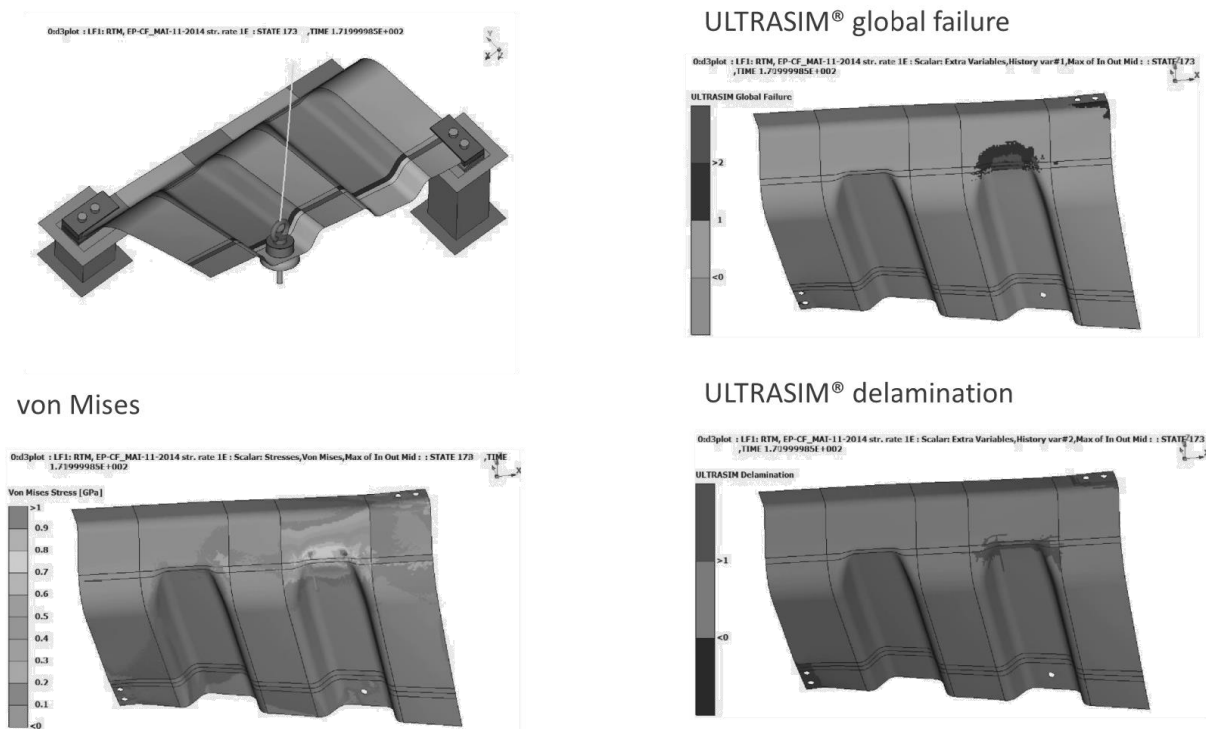


Fig.4: Load case “Twisting load”

This information is used to detect problem areas in the part. For every single element, the layup definition is known and damage propagation as a function of time can be plotted. Additional information, separate for fiber and matrix failure as well a stress vectors, is also available, see Fig. 5.

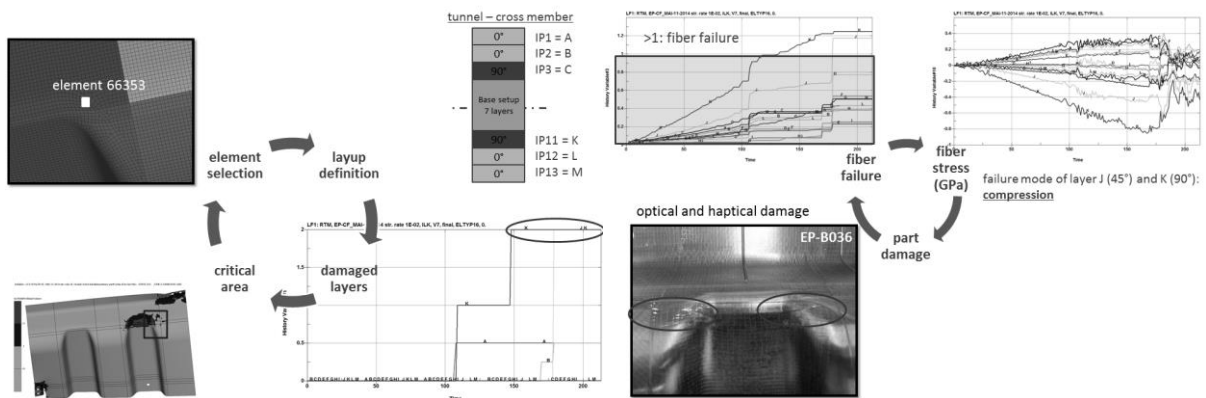


Fig.5: Extraction of damaged layer, fiber failure and stress

The calculated simulation results, based on the method described, fit very well to the experiment. Overall stiffness as well as measured force drops due to delamination could be predicted by the simulation very close to the experimental results, see Fig. 6.

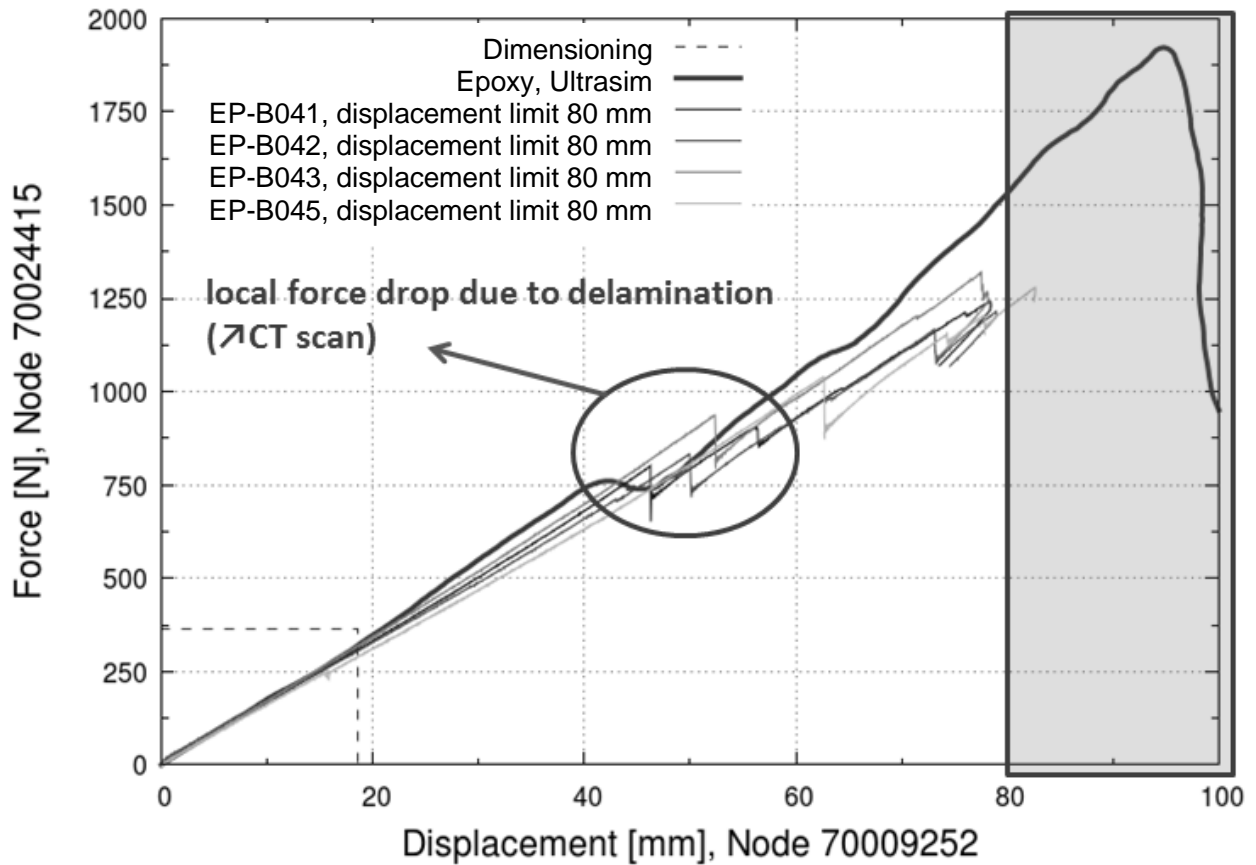


Fig.6: Force vs. Displacement curve – Simulation compared to measurement

#### 4 Summary

During the project MAI qfast, a CFRP Part was developed using composite optimization techniques. Four load cases have been tested. As an example the load case “Twisting load” is presented and the comparison between simulation and measurement is shown. All the simulations were done with LS-Dyna based on a CFRP material model developed by BASF (Ultrasim) which includes delamination effects.

The results of all investigation done in the project are published at “Technische Informationsbibliothek (TIB) – Leibniz-Informationszentrum Technik und Naturwissenschaften und Universitätsbibliothek” in 2015 via Audi AG with the working title “MAI qfast: Abschlussbericht für alle Projektpartner: Vergleichende Prozess- und Eigenschaftsbewertung für potentielle FVK-Strukturanwendungen in der automobilen Großserie”.

# Berücksichtigung der umformbedingten Faser-Reorientierung bei der Verzugssimulation von CFK-Bauteilen

Christoph Amann<sup>1</sup>, Christian Liebold<sup>2</sup>, Sebastian Kreissl<sup>1</sup>, Hannes Grass<sup>1</sup>, Josef Meinhardt<sup>1</sup> und Marion Merklein<sup>3</sup>

<sup>1</sup>BMW Group, 80788 München, Deutschland

<sup>2</sup>DYNAmore GmbH, 70565 Stuttgart, Deutschland

<sup>3</sup>Friedrich-Alexander-Universität Erlangen-Nürnberg, 91058 Erlangen, Deutschland

## 1 Einleitung

Den steigenden Ansprüchen an aktive und passive Sicherheit sowie an den Komfort heutiger Automobile steht die Forderung nach einer Reduktion des Fahrzeuggewichtes zur Verringerung des CO<sub>2</sub>-Ausstoßes entgegen. Zur Erfüllung dieser Aufgabe können innovative Leichtbaukonzepte beitragen. Die Verwendung von kohlenstofffaserverstärkten Kunststoffen (CFK) empfiehlt sich dabei aufgrund ihrer hohen spezifischen Steifigkeiten und Festigkeiten. Für den Großserieneinsatz von CFK sind Herstellungsprozesse wie z.B. das Nasspressen erforderlich, welche hohe Stückzahlen bei reproduzierbarer Bauteilqualität ermöglichen. Die Sicherstellung der Bauteilqualität erfordert den Einsatz von Experimenten unterstützt durch simulative Methoden. Zu letzteren zählt die simulative Abbildung des Herstellungsprozesses mit Hilfe der Methode der finiten Elemente (FEM).

Durch die Teilprozesse Umformung, Imprägnierung und Solidifikation werden insbesondere die Charakteristika Faserorientierung, Beharzungszustand und Endgeometrie des CFK-Bauteils festgelegt, welche es durch geeignete FE-Simulationen vorherzusagen gilt [1]. Da die verschiedenen Teilprozesse unterschiedlichste Anforderungen an eine Simulation stellen, wäre eine ganzheitliche Simulation des Fertigungsprozesses mit zu großem rechnerischem Aufwand verbunden. Daher wird häufig jeder Teilprozess durch eine eigene Simulation abgebildet, d.h. Umform-, Imprägnier- und Verzugssimulation.

Ziel dieses Beitrags ist es, eine Möglichkeit der Kopplung von Umform- und Verzugssimulation aufzuzeigen. Dabei wird mit der Faserorientierung eine Ergebnisgröße der Umformsimulation in der Verzugssimulation berücksichtigt. Anhand der optischen Vermessung einer Schwellerverstärkung aus CFK wird die Auswirkung dieser Implementierung auf die Vorhersagegenauigkeit der Verzugssimulation untersucht.

## 2 Methodik

Mit Hilfe der Umformsimulation auf Basis der Arbeit von Senner [2] wird die Drapierbarkeit von CFK-Gelegen sichergestellt, indem umformbedingte Merkmale wie Falten und Welligkeiten sowie die Faser-Reorientierung vorhergesagt werden. Der in [2] beschriebene modulare Modellierungsansatz umfasst die Verwendung von Schalenelementen zur Abbildung des Fasermaterials.

Zur Berechnung von Maß- und Formänderungen von CFK-Bauteilen wurde in [3] ein Ansatz entwickelt, welcher das im FE-System LS-DYNA implementierte, linear elastisch orthotrope Materialmodell \*MAT\_21 [4] nutzt. Konventionelle Schalenelemente scheiden für die Modellierung des Spring-In-Effektes [5] aus, da sie auf der Annahme eines ebenen Spannungszustandes beruhen. Für die Verzugssimulation werden daher Volumenelemente verwendet, wobei sowohl dicke Schalen vom Typ 3 und 5 als auch Solidelemente in Frage kommen. Die initiale Faserorientierung wird unter Verwendung der AOPT-Projektionsmethoden [4] definiert. Für komplex geformte Geometrien kann das bedeuten, dass im Preprocessing eine aufwändige Partitionierung des FE-Netzes durchgeführt werden muss. Dieser Prozessschritt entfällt, wenn die Information der Faserorientierung aus einer vorangegangenen Umformsimulation auf das Volumennetz übertragen wird. Darüber hinaus kann damit der bei einer Umformung über doppelt gekrümmte Geometrien stattfindenden Faser-Reorientierung Rechnung getragen werden. Dies hat in Abhängigkeit von Geometrie und Materialeigenschaften Auswirkungen auf die Genauigkeit der Verzugssimulation.

Um die Information zur Faserorientierung aus der Umformsimulation für die Verzugssimulation zugänglich zu machen, wird in dieser Arbeit das Mapping-Programm Envyo® verwendet [6]. Hierbei wird eine Nachbarschaftssuche zwischen den Elementen des Quell- (Umformsimulation) und Zielnetzes (Verzugssimulation) durchgeführt, wobei die Informationen des am nächsten liegenden

Elementes übertragen werden. Das Quellnetz ist im vorliegenden Fall ein Modell mit mehreren Schichten, wobei die einzelnen Schichten nicht miteinander verbunden sind. Das Zielnetz besteht aus geschichteten und über die Knoten verbundenen Volumenelementen. Ergebnis des Mapping-Prozesses sind sogenannte \*ELEMENT\_SOLID\_ORTHO-Elemente, welche die Information der Faserorientierung beinhalten. Zur Beschleunigung des Mapping-Prozesses ist ein Bucket-Sort-Algorithmus implementiert.

### 3 Ergebnisse

Zur Untersuchung des Einflusses der Faser-Reorientierung auf die Endgeometrie wurden im Nasspressverfahren hergestellte Versuchsbauteile einer CFK-Schwellerverstärkung optisch vermessen. Aufgrund der zahlreichen Verprägungen des Bauteils werden im Rahmen der Umformsimulation insbesondere in den Bereichen doppelter Krümmung Faserumorientierungen prognostiziert, welche erhebliche Auswirkungen auf die Verzugsvorhersage haben. In Fig. 1 sind die Abgleiche zweier Simulationen mit dem Ergebnis der optischen Messung eines repräsentativen Bauteils abgebildet. Dabei ist im linken Teil der Abbildung der Abgleich mit der Simulation mit der konventionellen Definition der Faserorientierung zu sehen. Im rechten Teil ist der Abgleich mit jener Simulation abgebildet, welche die Information der Faserorientierung durch ein vorangegangenes Mapping erhielt. Durch die Berücksichtigung der Faser-Reorientierung verbessert sich die Vorhersagegenauigkeit hierbei von ca. 1,4 mm auf ca. 0,6 mm.

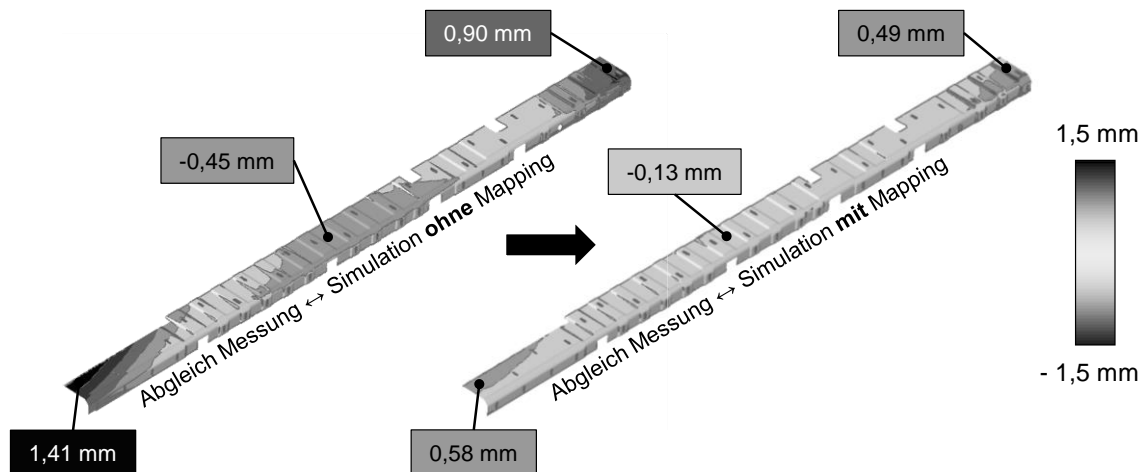


Fig.1: Abgleich von optischer Messung mit Simulation ohne (links) und mit (rechts) gemappter Faserorientierung der Umformsimulation

### 4 Zusammenfassung und Ausblick

Durch die Verwendung des Mapping-Tools Envyo® kann die umformbedingte Faserorientierung in zukünftigen Verzugsimulationen berücksichtigt werden. Zum einen kann dadurch das Preprocessing erleichtert werden und zum anderen ein Beitrag zur Verbesserung der Vorhersagegenauigkeit geleistet werden. Die Berücksichtigung weiterer Ergebnisgrößen der Umformsimulation wie z.B. der Faservolumengehalte bietet das Potential, die Genauigkeit der Verzugsimulation weiter zu steigern.

### 5 Literaturverzeichnis

- [1] Neitzel, M.; Mitschang, P.: Handbuch Verbundwerkstoffe, Hanser Verlag, 2004, S. 155-161
- [2] Senner, T.; Kreissl, S.; Merklein, M.; Meinhardt, J.; Lipp, A.: A modular modeling approach for describing the in-plane forming behavior of unidirectional non-crimp-fabrics, Production Engineering 8/2014 (5), S. 635-643
- [3] Amann, C.; Kreissl, S.; Grass, H.; Meinhardt, J.; Merklein, M.: Industrial Distortion Simulation of Fibre Reinforced Plastics – A Study on Finite Element Discretisation, In: Advanced Materials Research 1140 (WGP Congress 2016), S. 272-279
- [4] Livermore Software Technology Corporation (Hrsg.): LS-DYNA KEYWORD USER'S MANUAL, VOLUME II, Material Models, Version 971 / Release 6. Livermore Software Technology Corporation, 2012
- [5] Radford, D.; Diefendorf, R.: Shape Instabilities in Composites Resulting from Laminate Anisotropy, Journal of Reinforced Plastics and Composites 12/1993 (1), S. 58-75
- [6] Envyo® User's Manual, DRAFT, DYNAMore GmbH, Germany, 2016.

# Forming simulations in LS-DYNA with the new material law 294

Dr. Benedikt ECK<sup>1</sup>, Guillaume CHAMBON<sup>1</sup>

<sup>1</sup>FAURECIA Automotive Composite Technologies  
2 rue des Salines  
35400 Saint-Malo, France

## 1 Automotive composites forming

The reduction of car fuel consumption by proposing lightweight parts is one of the main strategic goals of Faurecia. Composites as fiber reinforced plastic materials (FRP) provide an important lightweight potential and Faurecia Automotive Composite Technologies (FACT) is specifically dedicated to the development, industrialization and fabrication of FRP-parts.

Fiber reinforced composites are however more complex compared to standard engineering materials due to possible anisotropies in the material. The latter is induced or, depending on the fiber structure, at least reinforced during processing and impacts largely the product performances [1].

One of the process steps which modifies largely the material structure is the shaping of the generally flat composite plies into a complex 3D geometry. These plies can be organosheets, used in the Thermoforming process or dry fabrics, used to produce preforms for the RTM process. Due to the complex behavior of the fiber materials, prior simulations and optimizations of the forming process are mandatory to avoid cost- and time-consuming trials to obtain a part without faults.

## 2 Forming simulations

### 2.1 Material model

Multiple software programs can be used to simulate the forming process. After a small in-house benchmark which showed only small differences between the tested codes, LS-DYNA has been selected for the quality of results and the ongoing advances in the domain of forming simulation. Additionally, similar models can be used for following mechanical simulations in LS-DYNA, which is one of the standard codes at FACT. This implies a reduction of the not-negligible translation effort between different software codes.

A successful forming simulation implies the use of a predictive material law with realistic material parameters. Up to now the material law Mat-34 was used successfully for low- to mid-complex preforming process simulations. However, this material law reaches its limits when it is applied in complex forming situations as it neglects some physical phenomena. In figure 1 an unrealistic element-rippling is depicted, which can occur during forming simulations with Mat-34.

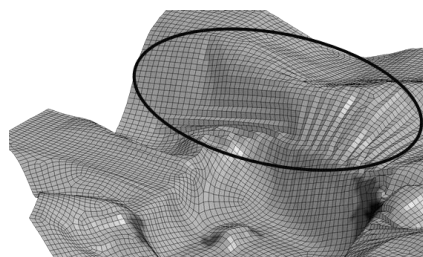


Fig.1: Element-rippling in a forming simulation with Mat 34 due to a missing shear-distortion coupling

This material behavior can lead to an error abortion of a simulation and, more critical, it can provide non-representative results when simulating more complex forming scenarios as a sequential stamping. Thus a simulation campaign with the newly developed material law Mat-294 has been started at FACT.

## 2.2 Material characterization

Before applying a new material law, a methodology had to be developed which allows a correct identification of the material parameters. Some material parameters can be determined directly with the outcome of characterization-trials. For non-physical ones, as for example the bending stiffness in the studied material laws, a reverse engineering approach is necessary. This implies to create models corresponding to the trials and to do parameter optimizations using LS-Opt.

## 2.3 Example – Lamp-pod geometry of the Fraunhofer ICT

The goal of the here presented project is to evaluate dry fabrics preforming on the preforming center developed by the Fraunhofer ICT together with Dieffenbacher [2]. The main particularity of this preforming center is the possibility to do sequential stamping. The idea is to form the material step by step in order to reduce the occurrence of fiber wrinkles. Additionally different clamping configurations can be used to increase locally the fiber tensions and reduce thereby also the wrinkle formation.

By these two means it is possible to modify largely the forming kinematics of the part. These are fundamentally linked to the induced local stress state which is at the origin of local defects. Thus it is possible to enhance the final forming result and to reduce occurring defects as wrinkle development by optimizing the forming kinematics. In order to avoid a time consuming trial and error determination of the optimal forming kinematics, process simulations were realized.

Using the correct material characteristics, a high grade of correlation between the outcome of the simulation and real forming trials can be obtained which is independent of the selected stamping sequence, as illustrated for 1 part in figure 2. This enables the optimization of the forming kinematics prior to starting costly and time-intensive trials

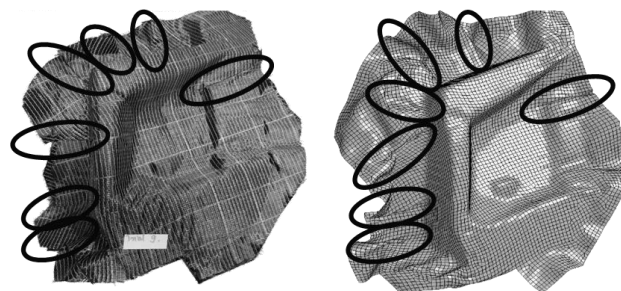


Fig.2: Comparison between a formed preform and simulation with Mat-294

## 2.4 Transition to crash simulations

Once the forming simulation is finished, its outcome can be integrated into the mechanical simulation. This is very important as even small modifications in the forming process, for example a modification of the stamping sequence, can influence largely the outcome of the mechanical behavior. This has been demonstrated in a second phase of the project where produced parts have been challenged in drop-tower trials regarding their resistance to crash.

## 3 Conclusions

Having determined the corresponding material parameters, Mat-249 allowed the optimization of the forming kinematics for complex shapes as for a lamp-pod geometry in the here presented project. These results can thereafter be integrated in mechanical simulations in order to have more predictive results. Other applications for this new material law, as the thermoforming process are currently under investigation at FACT.

## 4 Literature

- [1] Nardari C. et al.; Simultaneous engineering in design and manufacture using the RTM process. Composites Part A, Applied Science and Manufacturing; 33(2); 2002; p. 191–196
- [2] Henning F. et al.; Cost-efficient preforming as leading process step to achieve a holistic and profitable RTM product development; 1st International Composites Congress (ICC); 2015



---

# High Performance Computing Welding Analysis with DynaWeld and Parallelized LS-DYNA Solvers

Tobias Loose<sup>1</sup>, Martin Bernreuther<sup>2</sup>, Bärbel Große-Wöhrmann<sup>2</sup>, Jörg Hertzner<sup>2</sup>, Uli Göhner<sup>3</sup>

<sup>1</sup> Ingenieurbüro Tobias Loose, Herdweg 13, D-75045 Wössingen, [www.tl-ing.eu](http://www.tl-ing.eu)

<sup>2</sup> Universität Stuttgart, Höchstleistungsrechenzentrum, Nobelstraße 19,  
D-70569 Stuttgart, [www.hlrs.de](http://www.hlrs.de)

<sup>3</sup> DYNAMore Gesellschaft für FEM Ingenieurdienstleistungen mbh, Industriestraße 2,  
D-70565 Stuttgart, [www.dynamore.de](http://www.dynamore.de)

## 1 Abstract

As an integral part of the PRACE SHAPE project “HPC Welding” [1] the parallel solvers of LS-DYNA were used by Ingenieurbüro Tobias Loose to perform a welding analysis on the Cray XC40 “Hazel Hen” at the High Performance Computing Center Stuttgart (HLRS).

A variety of test cases relevant for industrial applications have been set up with DynaWeld, a welding and heat treatment pre-processor for LS-DYNA, and run on different numbers of compute cores. The explicit mechanical solver was tested on up to 4080 cores with significant scaling. As far as we know, it was the first time that a welding simulation with the LS-DYNA explicit solver was executed on 4080 cores.

## 2 Welding simulation

Welding structure simulation is a highly sophisticated finite element (FE) application [2]. It requires a fine mesh discretization in the weld area so that, in combination with large assemblies and long process times, welding simulation models are very time consuming during the solver run.

HPC with massively parallel processors (MPP) can provide a solution to this issue. In crash applications and forming analysis, it is known that the commercial finite element code LS-DYNA, using the explicit solution algorithm, provides good performance on HPC systems. However, at the authors' knowledge, performance benchmarking of LS-DYNA for welding simulations have never been performed prior to this study. This project has analyzed the feasibility of welding analysis with parallelized LS-DYNA solvers and its performance.

In this project a Cray-specific LS-DYNA mpp double precision (I8R8) version has been used. The version used, named as revision 103287, was compiled by Cray using the Intel Fortran Compiler 13.1 with SSE2 enabled. The Extreme Scalability Mode (ESM) was used.

In addition, the commercial pre-processor DynaWeld [3,4] is used to set up the welding simulation models for the solver.

## 3 Welding tasks

The welding technique covers a very wide range of weld types, process types, clamping and assembly concepts and assembly dimensions. For example: arc weld, laser weld, slow processes, high speed processes, thin sheets, thick plates, single welds, multi-layered welds, unclamped assemblies, fully clamped assemblies, prestress and predeformations. This shall illustrate that there is not only one "welding structure analysis" but a wide range of modelling techniques to cover all variants of welding. In consequence, welding simulation cannot be checked in general for HPC, but every variant of modelling type has to be checked separately.

This project considers several representative modelling variants for welding structure with the aim to cover a range as wide as possible. Fig. 1, for example, shows a model of a gas metal arc welded curved girder. This model covers a complex and large industrial case with many welds. A high speed laser welded thin sheed was the test case for the explicit analysis of the project (Fig. 2). This case was modelled with 200 000 shell elements (EDB) and 1 million shell elements (MDB).

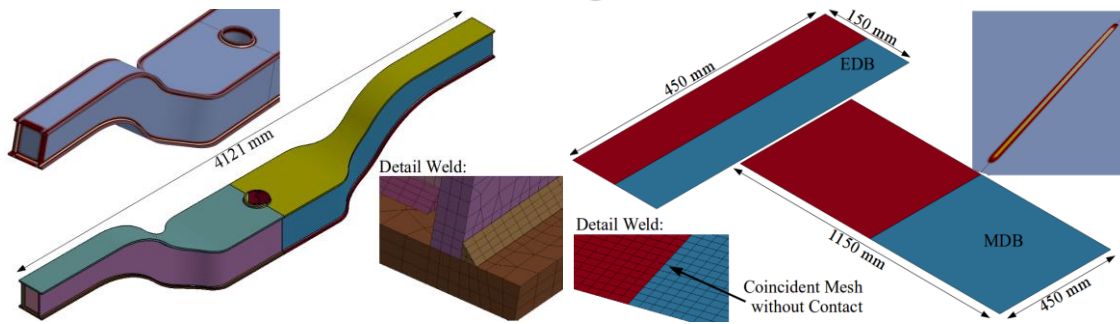


Fig. 1: Model of arc welded curved girder

Fig. 2: Models of high speed laser welded sheet

#### 4 Results of the project

The results of the test cases with explicit analysis provided the following results: The scaling behaviour in the double-logarithmic scale is linear with nearly constant gradient up to 4080 cores (Fig. 3). Above 96 cores the model MDB with 1 million elements provides a better scaling than the model EDB with 200 000 elements due to the fact that the number of elements per core domain is larger in this case. Regarding the parallel efficiency (the ratio of speedup and number of cores), the larger model has a ratio of 0.45 at 768 cores, and at the highest number of cores (4080) a ratio of 0.4.

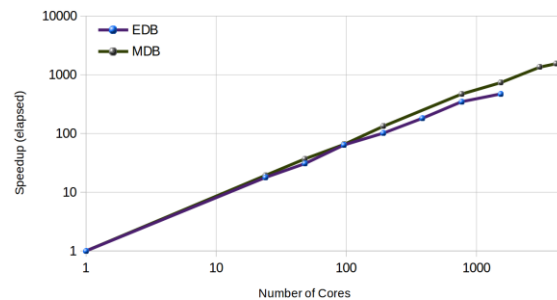


Fig. 3: Speedup of elapsed time for the explicit analysis

As a result of the project in general, recommendations for the number of cores in order to obtain the optimal performance are provided and the expected speedup is given. Both the number of the cores and the speedup depend on the model type.

The overall effort for welding analysis on HPC is now much better known with the help of this SHAPE project [1], leading to the ability of a more accurate cost estimate of welding consulting jobs.

This project provides a good basis for further investigations in high performance computing for welding structure analysis.

#### 5 Acknowledgements

This work was financially supported by the PRACE project funded in part by the EU's Horizon 2020 research and innovation programme (2014-2020) under grant agreement 653838.

#### 6 Literature

- [1] Loose, T. ; Bernreuther, M. ; Große-Wöhrmann, B. ; Göhner, U.: SHAPE Project Ingenieurbüro Tobias Loose: HPCWelding: Parallelized Welding Analysis with LS-DYNA, SHAPE White Paper, 2016, <http://www.prace-ri.eu/IMG/pdf/WP220.pdf>
- [2] Loose, T.: Einfluß des transienten Schweißvorganges auf Verzug, Eigenspannungen und Stabilitätsverhalten axial gedrückter Kreiszyinderschalen aus Stahl, Dissertation, Universität Karlsruhe, 2007
- [3] Loose, T. ; Mokrov, O. ; Reisgen, U.: SimWeld and DynaWeld - Software tools to set up simulation models for the analysis of welded structures with LS-DYNA. In: Welding and Cutting 15, pp. 168 - 172, 2016
- [4] <http://www.dynaweld.eu>; <http://www.tl-ing.eu>

# Simulation of pulsed water cooling for continuous casting with LS-DYNA

Stefan Scheiblhofer<sup>1</sup>, Johannes Kronsteiner<sup>1</sup>, Stephan Ucsnik<sup>1</sup>, Peter Simon<sup>2</sup>, Holm Böttcher<sup>2</sup>

<sup>1</sup> LKR Leichtmetallkompetenzzentrum Ranshofen GmbH, Ranshofen, Austria

<sup>2</sup> AMAG Austria Metall AG, Ranshofen, Austria

## 1 Introduction

Continuous Casting Processes (CCP) are used for the production of metal billets and the semi-finished material for further processing of metal sheets. In CCP water cooling is a critical feature (figure 1). In the casting process, high cooling rates are triggered by the contact of the cast material with the starting head at the start of process. Only a limited amount of water is necessary to obtain the desired cooling effect. In the later stage of the casting process, the thermal mass of the already cast material is limiting the cooling effect. Therefore, additional and increased water cooling is required to obtain further cooling of the billet. There are two possibilities to increase the cooling rates by water cooling. One way is to increase the flow rate, the other way is to use high flow rates from the beginning of the CCP but to pulse the water to reduce the cooling rates at the start of the CCP. Consequence of the cooling process at the start of the cast is shrinkage leading to thermal stresses in the cast material. Pulsed water cooling can help to release those stresses for the later stage of the casting process.

The modelling of the Pulsed Water Cooling (PWC) is thus an important feature for an accurate simulation of the CCP in order to capture the thermal evolution of the billet over time. Although the modelling of such cooling schemes is originally not supported by LS-DYNA® keywords, it is possible to consider them by extending the solver through user-defined interfaces and routines.

## 2 Modelling approach

One way to describe water cooling in finite element simulations is through the use of heat transfer coefficients (HTC) in contact definitions. These definitions can be expanded to further model PWC. For this the HTC is described via parameters like water flow rate, the pulse rate, the temperatures of both water and billet and the timeline of the casting process. These parameters are critical for the continuous casting process and depend on time, as they vary during the process. In general, PWC is characterised by a square wave signal as illustrated in figure 2.



Fig.1: Water flow in a CC mould

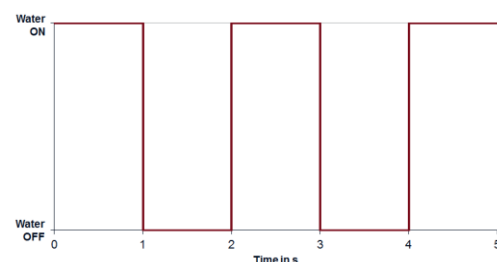


Fig.2: Square wave signal for PWC

To implement such a signal into LS-DYNA®, a mathematical formulation has been developed by means of Fourier series of order N. This approximation is capable of including the dependencies on the time, the magnitude of the signal and the duty cycle. The thermal energy exchange between cast billet and the surrounding environment is modelled by contacts and the implementation of HTC definitions. LS-DYNA® naturally supports the HTC definition of constant values and also functions of temperature, pressure and time. The detailed description is possible with the keyword `*CONTACT..._THERMAL_FRICTION...`, whose description can be found in the LS-DYNA® manual.

PWC can be modelled through `*DEFINE_FUNCTION` or by using a user-defined subroutine for calculating the HTC. The `*DEFINE_FUNCTION` keyword is able to include source codes in C, enabling the implementation of the derived Fourier series. However, the more efficient way is to implement the

user-defined subroutine, which is able to reduce the calculation time and to allow an easier definition within the keyword input file for the end-user. The user-defined subroutine can be called by an option within `*CONTACT... _THERMAL_FRICTION...`, allowing the input of several user-defined parameters.

### 3 FE-Model and results

A simple FE-model was setup to study the functioning of the PWC model definitions through implemented Fourier series and to show the influence of the PWC. The FE-model used for the evaluation of the pulsed water cooling is basically a quarter model of the CCP in steady state conditions. For this evaluation case, the geometric features were simplified and reduced. The simplifications resulted in a small and flat ingot, surrounded by shell elements on the outside faces which were needed for the simulation of the water cooling (figure 3). The modelled aluminium ingot has had an initial temperature of 500°C and was cooled by water with constant temperature of 20°C.

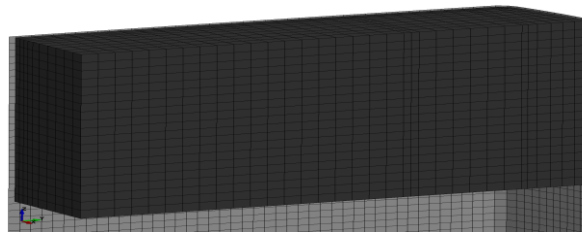


Fig.3: 1/4-model for the evaluation of PWC, with the simplified ingot (dark grey) surrounded by shell elements (light grey)

The results displayed in figure 4 and 5 show the influence of the individual cooling methods for the Constant Water Cooling (CWC) and PWC respectively. The temperature graphs are plotted for the billet surface and for different inside positions away from the ingot surface. On the ingot surface the effects of pulse water can directly be seen at the corresponding cooling curve. The PWC effect is highest at the surface and decreases with increasing distance from the surface. When the distance is more than 27 mm from the surface, almost no effect is visible anymore. Furthermore, the cooling curves show a smaller cooling rate for the PWC as the temperature after 50 seconds of casting is higher than CWC case.

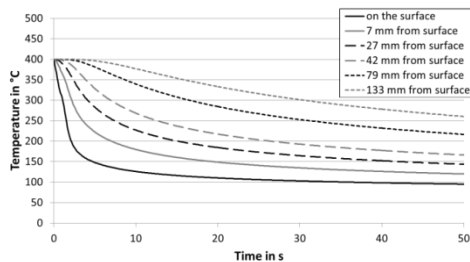


Fig.4: Cooling curves for CWC

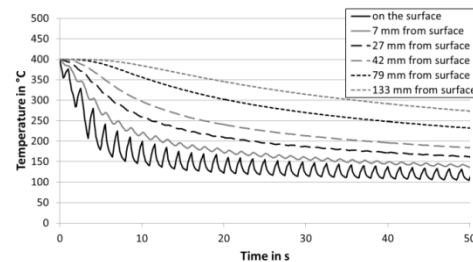


Fig.5: Cooling curves for PWC

### 4 Summary

This paper presents a modelling approach for pulse water cooling within LS-DYNA®. For the implementation, the conventional square wave signal of the cooling method is approximated by a fourier series of order N, which can be addressed by LS-DYNA® within the user-defined subroutine for the heat transfer coefficient. The results of the simulation show the impact of pulse water cooling on the cooling curve, as this is an efficient way to control the water flow and therefore the cooling rate of the process without limiting the amount of water towards the end of the process.

### 5 Acknowledgement

The authors would like to thank the Austrian Research Promotion Agency (FFG), the Federal Ministry for Transport, Innovation and Technology (BMVIT) and the State of Upper Austria for sponsoring this research work in the framework of COMET. This work has been supported by the European Regional Development Fund (EFRE) in the framework of the EU-program "IWB Investition in Wachstum und Beschäftigung Österreich 2014-2020", and the federal state Upper Austria.

# Durability assessment of welded structures based on welding simulation with LS-DYNA®

Andriy Krasovskyy<sup>1</sup>, Antti Virta<sup>2</sup>, Thomas Klöppel<sup>3</sup>

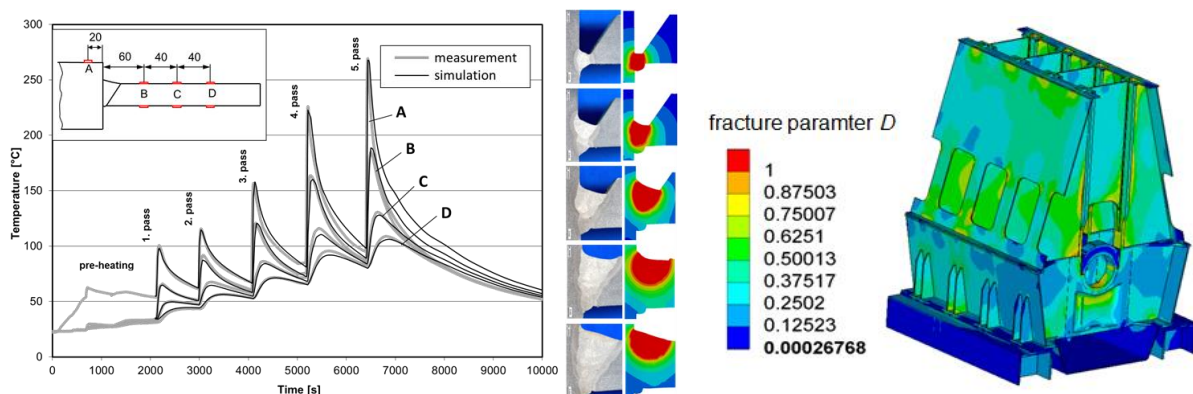
<sup>1</sup>DYNAmore Swiss GmbH

<sup>2</sup> Winterthur Gas & Diesel Ltd

<sup>3</sup>DYNAmore GmbH

## Abstract

The importance of welding for modern structural engineering cannot be emphasized enough. Different techniques are currently applied in the industrial environment offering almost unlimited possibilities regarding manufacturability with high cost effectiveness. At the same time the requirements on welded structures are increasing and so the requirements on the design methods. This paper presents an advanced calculation method for fatigue assessment of welds based on the simulation of a welding process in LS-DYNA®, thermophysical material modeling and fracture mechanics. The proposed method considers the most important aspects for durability prediction of welds. Applying worst-case assumptions, fatigue limits derived by the weight function method can be used in the lifetime assessment of complex welded structures together with the critical plane approach in order to consider a multiaxial nonproportional loading.



courtesy of Winterthur Gas & Diesel Ltd.

---

# Recent Developments for Welding Simulations in LS-DYNA® and LS-PrePost®

Mikael Schill<sup>1</sup>, Anders Jernberg<sup>1</sup>, Thomas Klöppel<sup>2</sup>

<sup>1</sup>DYNAmore Nordic AB, Linköping, Sweden

<sup>2</sup>DYNAmore GmbH, Stuttgart, Germany

## 1 Introduction

The multi-physics capabilities of LS-DYNA® makes it ideal for simulating the welding process where the mechanical and thermal physical regimes are combined to simulate the resulting part tolerance and residual stresses. Welding capabilities are continuously being added to LS-DYNA®, e.g. the material models **\*MAT\_CWM** and **\*MAT\_CWM\_THERMAL** which are tailored for CWM simulations. The CWM material models include e.g. ghost element and anneal functionality. However, the challenge when performing this type of simulations is not only related to the solver. The pre-processing quickly becomes a daunting task where the user needs to assign weld paths, weld power and clamping for several weld passes. To accommodate for this, a novel welding GUI has been added to LS-PrePost®. The GUI includes e.g. a welding process planner, welding path selection using the graphical interface and welding heat source definition and visualization. Further, the welding process setup is written to an ASCII input file that can be combined with an optimization software to optimize the process with respect to e.g. welding deformations. This paper will present the recent developments in the mechanical and thermal solvers in LS-DYNA® to accommodate for welding simulations. Also, the novel Welding GUI in LS-PrePost® will be presented together with some application examples

## 2 Material modelling

The material models tailored for CWM modeling in LS-DYNA has two distinctive features apart from full mechanical and thermal coupling. The first feature is that it can be assigned different material states. Namely,

- Solid material: Material that is always solid or a weld pass that has been previously activated
- Liquid material: Material that is in a ghost state but will be activated during the current weld pass.
- Ghost material: Material that will not be activated during this weld pass. But it will be activated in a subsequent pass.

The second feature is the annealing functionality. This simulates the limit temperature when the material will recover to a novel state. Thus, above this temperature, the material histories are zeroed out and the material will behave as ideal plastic. Today, two material models have CWM functionality. It is the **\*MAT\_CWM/#270** and the phase kinetics model **\*MAT\_UHS/#244**.

## 3 Heat source modelling

A novel keyword has been implemented denoted **\*BOUNDARY\_THERMAL\_WELD\_TRAJECTORY**. The implementation involves improvements in many areas. Firstly, the heat source modelling is implemented in the thermal solver only. Thus, it can be run as a thermal only simulation. Secondly, the heat source movement can now be defined by a consecutive node set. This means that the weld path will follow the deformation of the structure. Further, since the heat source is an incremental thermal load, there will in practice be a dependency between the element size, heat source movement velocity and the time step. This resulted in severely distorted elements if a too high time step was used. This issue has been addressed by introducing sub stepping of the heat source within each thermal time step. Lastly, the new keyword includes a number of heat source shapes. Apart from the well known Goldak double ellipsoid heat source, it is now possible to use a conical and a double conical shape.

## 4 LS-PREPOST® welding GUI

When setting up a CWM simulation, several tasks has to be addressed including e.g. defining the weld path, weld characteristics, mechanical and thermal boundary conditions. This quickly becomes

complicated for a multistage analysis, especially if the process order or directions are varied. To remedy this, a Welding GUI is implemented in LS-PrePost®. The welding sequence is presented in a table like manner where weld passes, mechanical and thermal boundary conditions can be combined to form a process order, see Fig 1. Within the GUI, each welding pass characteristics are defined and the weld paths are easily identified by clicking.

Sequence	Welds	Struct. B.C.	Therm. B.C.					
		1	2	3	4	5	6	7
== Welds ==								
4 WELD 1								
5 WELD 2								
6 WELD 3								
7 WELD 4								
8 WELD 5								
9 WELD 6								
10 WELD 7								
== Struct. B.C. ==								
1 prescribed temp								
2 spc table								
== Therm. B.C. ==								
Air segm.								
1 clamp set 1								
2 Clamp set 2								
3 Clamp set 3								
4 Clamp set 4								
5 tied 3 1								

Load Save Export Desktop

Fig.1: Process sequence folder

## 5 Summary

The recent developments in CWM simulations in LS-DYNA® involves material modeling and heat source modeling. Together with the well-established multiphysics capabilities, this makes LS-DYNA® suitable for welding simulations. Further, LS-PrePost® now includes a welding GUI to ease the pre-processing of the welding process.

# Developments in LS-DYNA® for Metal Forming Simulation

Xinhai Zhu and Li Zhang

Livermore Software Technology Corporation

## 1 Introduction

Selected major developments for stamping simulation in LS-DYNA are discussed. These developments are:

- Improvements to \*ELEMENT\_LANCING
- Checking fixture clamp definition and simplification of FORMING contact definition
- New options in \*INTERFACE\_BLANKSIZE
- Trimming of solids, laminates and TSHELL
- New features in \*CONTROL\_FORMING\_OUTPUT
- Damage is added to \*CONTROL\_FORMING\_ONESTEP
- Automatic offset of tool element/node IDs with \*INCLUDE\_AUTO\_OFFSET

## 2 Developments

### - Improvements to \*ELEMENT\_LANCING

1. A part set is now allowed, which enables lancing across tailor-welded blanks.
2. IGES format curves can now be used as input to define the lancing route.
3. Meshes along the lanced boundary is now automatically adapted to provide a smooth edge.
4. Trimming now can be defined after lancing to remove the scrap. This is done with the new keyword \*DEFINE\_LANCE\_SEED\_POINT\_COORDINATES.
5. Lancing activation distance can now be defined using a new variable CIVD.

### - Checking fixture clamp definition and simplification of FORMING contact definition

Clamping of formed/trimmed panel on a checking fixture is sometimes used for springback prediction. The new feature, implemented in keywords \*DEFINE\_FORMING\_CLAMP and DEFINE\_FORMING\_CONTACT:

1. eliminate the need to use auto-position cards between the formed panel and clamps;
2. do away with prescribed rigid body motion (\*BOUNDARY... and \*DEFINE\_CURVE);
3. simplify the contact definition between the panel and the clamps.

### - New options in \*INTERFACE\_BLANKSIZE

1. The option SCALE\_FACTOR allows user to include or exclude a target curve in the calculation of the initial curve. It also allows user to scale up or down in size of a target curve involved in the calculation.
2. The option SYMMETRIC\_PLANE allows user to define a symmetric plane by specifying a point on the symmetric plane with X, Y, Z coordinates, and vector components for the normal of the plane.

### - Trimming of solids, laminates and TSHELL

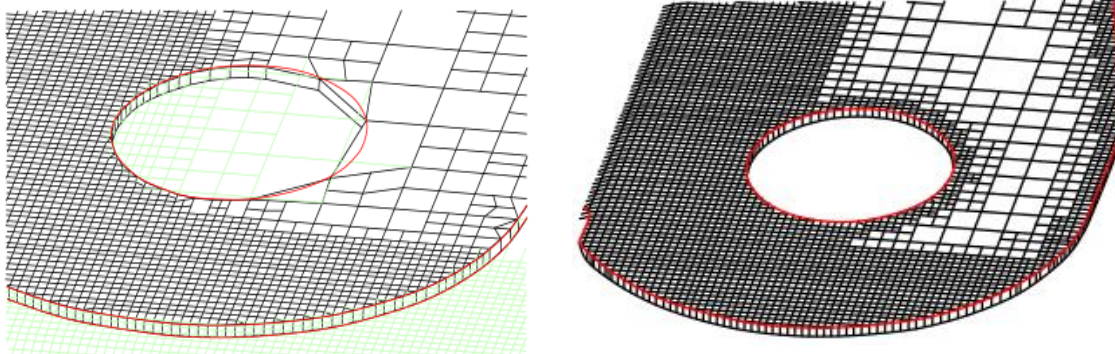
New capabilities are added and summarized in the following table:

	2D (along one direction)	3D (element normal)	2D & 3D Double Trim	Adaptive mesh
<b>Shell</b>	Yes	Yes	Yes	Yes
<b>Solids</b>	Yes	Yes	Yes	N/A



<b>Laminates</b>	Yes	Yes	Yes	One layer of solids only; Multiple layers of solids okay for non-adaptive mesh.
<b>TSHELL</b>	Yes	N/A	N/A	N/A

Improvements are also done to the meshes around trim edges, which are now automatically adapted, resulting in a much smoother trim edge, see figure below, where the left is without adaptivity and the right is with mesh adaptivity.



#### - New features in \*CONTROL\_FORMING\_OUTPUT

A new variable CIDT is added to allow definition of state outputs according to simulation time specified. The new state outputs will be in addition to the state outputs according to punch distance from home (bottom), specified by the existing variable LCID.

#### - Damage is added to \*CONTROL\_FORMING\_ONESTEP

Damage accumulation  $D$  is calculated based on (refer to manual section \*MAT\_ADD\_EROSION):

$$D = \left( \frac{\varepsilon_p}{\varepsilon_f} \right)^{DMGEXP}$$

A load curve can be defined for plastic failure strain vs. stress triaxiality relationship and DMGEXP can be input. The calculated damage accumulation is written into a file called "onestepresult" as history variable #6, and can be plotted in LS-PrePost.

#### - Automatic offset of tool element/node IDs

Incoming element and node IDs of the tooling mesh files such as the punch, die, and binder, can be overlapped with each other, or overlapped with those on the sheet blank (especially after adaptive trimming). Multiple \*INCLUDE\_AUTO\_OFFSET can be used to include punch, die, binder separately, if desired. For example, four different components of the tooling, upper die, lower punch, binder and gage pins can be included and their element and node IDs properly offset after those of a gravity-loaded sheet blank:

```
*INCLUDE
gravity.dynain
*INCLUDE_AUTO_OFFSET
upperdie.k
*INCLUDE_AUTO_OFFSET
lowerpunch.k
*INCLUDE_AUTO_OFFSET
binder.k
*INCLUDE_AUTO_OFFSET
pins.k
```

### 3 Summary

Various features related to metal forming have been developed to meet the requirements of our stamping users. Selected developments are discussed. LSTC is committed to working with our stamping users to advance the metal forming simulation technology, and will continue to improve to lead ahead.

### 4 Reference

[1] LS-DYNA User's Manual (I) DRAFT.

---

## Strategies to improve the Efficiency of Sheet Metal Forming Simulations with LS-DYNA

Dr. Wolfgang Rimkus, Hochschule Aalen - Technologiezentrum Leichtbau  
Melanie Fritz, Hochschule Aalen - Technologiezentrum Leichtbau  
Peter Vogel, DYNAmore GmbH

The production of arbitrary complex geometries in forming processes requires a certain effort of production planning. This includes cost and time aspects. In this context simulation is an essential point to minimize development cycles. Within simulations an optimization potential can be generated.

Therefore the paper deals with strategies of improvements in efficiency of forming processes under the usage of LS-DYNA. The parameters which can be adjusted may have an influence in respect of duration and accuracy of the results.

The paper describes in which way afore identified parameters on the chosen forming simulation have an effect. Also it indicates the impact of a variation of some parameters.

---

# Advances in Characterization of sheet metal forming in JSTAMP/NV

R. LIU<sup>1</sup>, H.FUKIHARU<sup>1</sup>

<sup>1</sup>JSOL Corporation Harumi Center Bldg. 2-5-24, Chuo-ku, Tokyo 1040053

## 1 Introduction

Lightweighting material, especially high strength materials are very common in Asia comparing hot stamping and aluminum parts in European automobile industry. Sheet metal forming simulation has been widely applied with the developing of automobile industry during last decades. JSTAMP/NV[Fig.1], an integrated sheet metal forming system developed by JSOL, is rapidly increasing in Asia area these years because of its capability of accurate springback prediction. Three items are important to predict springback accurately. First is manufacturing condition in simulation should be close enough with real manufacturing. Then is proper material model to identify real materials stress-strain behavior. Finally it is accurate material parameters for the material in mass production. JSTAMP/NV provides a sophisticated pre-processor to catch real stamping machine condition. The latest material model, material databases are always developed so as to get complicated stress-strain behavior in sheet metal forming. This material will introduce JSTAMP/NV's characterization of sheet metal forming. A typical material model developed by JSOL, named Yoshida-Uemori material model to do springback simulation for high strength steel and aluminum. To identify material parameters for Yoshida-Uemori model, a material identification tool MatPara is also introduced. In addition, using Yoshida-Uemori model and MatPara, a benchmark example of NUMISHEET2016 will be included so as to verify its capability.

## 2 Yoshida-Uemori material model

Yoshida-Uemori[2] proposed a model of large-strain cyclic plasticity that well describes the stress-strain responses in reverse deformation [Fig.2], as well as cyclic hardening characteristics, such as:

- two stages of the Bauschinger effect: (i) the transient Bauschinger deformation characterized by early re-yielding and smooth elastic-plastic transition with a rapid change of workhardening rate; and (ii) the permanent softening characterized by stress offset observed in a region after the transient period;
- plastic strain dependent Young's modulus;
- the workhardening stagnation appearing at a certain range of reverse deformation;
- strain-range and mean-strain dependency of cyclic hardening, e.g., the larger the cyclic strain range the larger the saturated stress amplitudes.

Yoshida-Uemori model assumes the kinematic hardening of the yield surface, describes the transient Bauschinger deformation characterized by early re-yielding and the subsequent rapid change of workhardening rate.

JSOL developed a subroutine based on Yoshida-Uemori model and proposed to Japanese customers. It has been extremely evaluated since its outstanding accuracy comparing traditional isotropic hardening material model.

## 3 What is MatPara?

MatPara[Fig.3] is a tools to identify a set of material parameters of several elasto-plasticity constitutive models, e.g. Yoshida-Uemori model, from stress-strain experimental data by means of an optimization technique. It offers a GUI environment for stress-strain data-input, calculation of stress-strain responses, as well as displaying experimental/calculated results and output numerical data and graphic data; MatPara can prepare appropriate experimental data by smoothing noisy and find strain reversal points. Additionally, it calculates the stress-strain response with a selected constitutive model for a given cyclic straining condition. Furtherly, by minimizing the difference in stress between experimental and the corresponding numerical results, MatPara identifies material parameters for different models. It helps JSTAMP/NV customers to get material database and conduct springback simulation easily and accurately even without uniaxial and cyclic experimental data. JSOL is distributing MatPara to customers in the world.

### 4 Figures

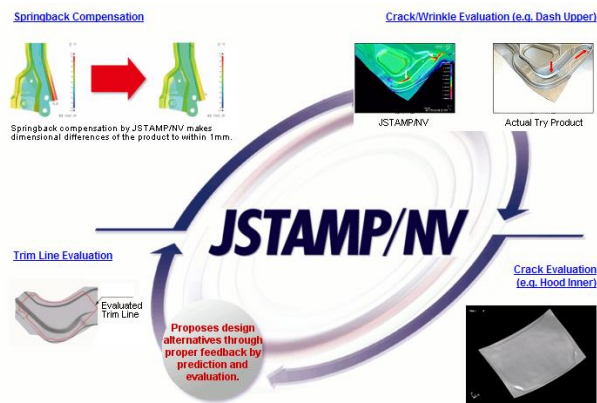


Fig.1: General description of JSTAMP/NV

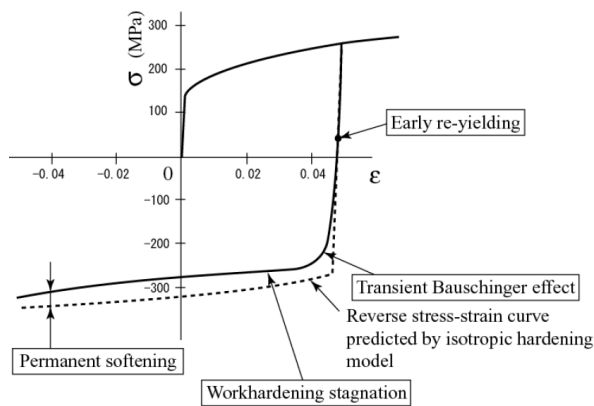


Fig.2: An example of stress-strain response in a forward-reverse deformation

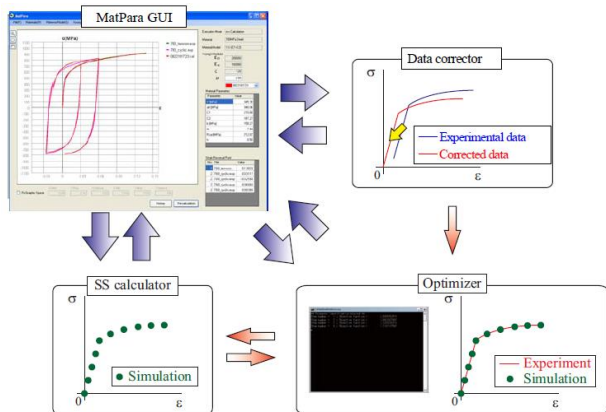


Fig.3: MatPara's schematic illustration structure.

### 5 Summary

To satisfy the high strength steel forming needs in Asia area, a sheet metal forming system, JSTAMP/NV which provides an accurate springback prediction solution has been introduced. A well-known sheet metal forming material model, Yoshida-Uemori model and related parameter identification tool, MatPara are also included. A Numisheet2016 benchmark model was introduced.

### 6 Literature

- [1] <http://www.jstamp.jp/en/index.html> JSTAMP URL , JSOL Corporation
- [2] Yoshida, F. and Uemori, T.: *Int. J. Mechanical Sciences*, 45, 2003, 1687-1702
- [3] MatPara theory manual CEM 2012

## Updates in eta/DYNAFORM V.5.9.3

P. Vogel  
DYNAmore

J. Du Bois  
Engineering Technology Associates

# Experimentelle Untersuchung des Probengeometrieinflusses auf das Deformationsverhalten amorpher thermoplastischer Kunststoffe

M.Helbig<sup>1</sup>, D.Koch<sup>1</sup>, Johannes Irslinger<sup>2</sup>, Andreas Hirth<sup>2</sup>

<sup>1</sup>DYNAMore GmbH

Thermoplastische Kunststoffe werden zunehmend in crashrelevanten Bauteilen verwendet. Dazu ist eine Charakterisierung des Deformationsverhaltens dieser Werkstoffe notwendig, um Crashesimulationen durchführen zu können. Die Anforderungen an eine Zugprobengeometrie ist nicht trivial, sowohl statische als auch dynamische Versuche sollten nach Möglichkeit mit der gleichen Geometrie durchgeführt werden können, ein möglichst homogener einachsiger Spannungszustand sollte vorherrschen, optische Verzerrungsauswertung sollte ausführbar sein, höhere nominelle Dehnraten sollten realisierbar sein und die Geometrie sollte sowohl für duktile als auch für spröde Kunststoffe geeignet sein [1].

Bei der Entwicklung einer optimalen Probengeometrie z.B. [1] wurde bisher meist nur ein Werkstoff betrachtet, während im Simulationsalltag sowohl spröde, duktile sowie modifizierte und verstärkte Polymere verwendet und verglichen werden müssen. Deswegen ist eine optimale Zugprobengeometrie, welche für alle thermoplastischen Kunststoffe geeignet ist, bisher Gegenstand von Diskussionen.

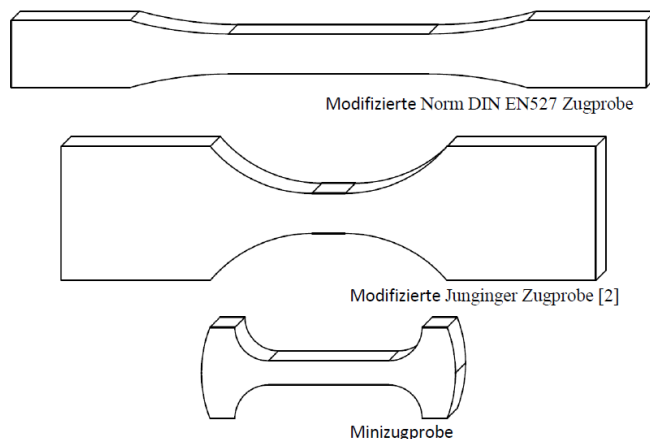


Fig.1: : Zugprobengeometrien.

Es werden zunächst zwei unterschiedliche Zugprobengeometrien sowie der Einfluss der Verzerrungsermittlung auf das inelastische Deformationsverhalten experimentell untersucht. Im nächsten Schritt wird ein möglicher Einfluss des Probenherstellungsprozesses auf das Deformationsverhalten experimentell untersucht.

Schließlich wird das Deformationsverhalten von gegossenen Zugproben und Minizugproben die aus einem Serienbauteil entnommen wurden verglichen.

## 1 Literature

- [1] Becker, F. 2009. Entwicklung einer Beschreibungsmethodik für das mechanische Verhalten unverstärkter Thermoplaste bei hohen Deformationsgeschwindigkeiten. Dissertation an Universität Halle-Wittenberg
- [2] Junginger, M 2002. Charakterisierung und Modellierung unverstärkter thermoplastischer Kunststoffe zur numerischen Simulation von Crashvorgängen. Dissertation an Universität der Bundeswehr München

# Calibration and Appliarence of the Wilkins Damage Model on Cast Aluminium

Christian Mühlstätter

LKR Leichtmetallkompetenzzentrum Ranshofen GmbH, Austrian Institute of Technology

## 1 Introduction

The application of Aluminium cast alloy in automotive fields faces increasing interest. The advantages of cast alloys are well-established manufacturing processes, the function integrity and a relatively low weight. In contrast, some challenges are related to cast alloys, e.g. the presence of pores and shrinkage defects. These voids may be involved in the mechanism of ductile fracture, which is an accumulation of the micromechanical phenomena as void nucleation, void growth and coalescence. Modelling the behaviour of materials in numerical finite element models composes the constitution of stress-strain relationship through material laws. This leads to stress data, which allows an evaluation of material damage. Therefore, a strategy for material characterisation and the application of material models to upcoming materials needs to be developed. The material evolution and consideration of new materials is a key issue in light weight design.

The theory of material damage are micromechanical modelling of ductile fracture introduced by Gurson [1] and subsequent works of Tvergaard and Needleman [2]. The original approach of Gursen captures material damage caused by hydrostatic stress but does not consider material failure in shear dominated load cases. The modification of the Gurson Model by Nahshon and Hutchinson [3] overcomes this weakness.

Additional, phenomenological approaches for damage modelling of metallic materials are proposed, e.g. by Johnson and Cook [4]. These consider the influence of strain rate effects and temperature effects on the damage behaviour. A further approach is called Generalized Incremental Stress State dependent Damage Model (GISSMO) and is implemented in LS-Dyna [5]. The damage consideration in GISSMO is assumed as function of plastic equivalent strain, stress triaxiality and the Lode Stress Parameter. Since GISSMO is developed for describing a wide range of different material behaviours, a high amount of phenomenological parameters has to be calibrated. Thus, a comprehensive knowledge of material modelling is necessary for the calibration of GISSMO.

An advanced Material Damage Model, introduced by Wilkins [6], is investigated in this paper. In this study, the Wilkins Damage Model is calibrated for an AlSi-cast alloy by means of tensile test coupons with different geometries. Furthermore, a validation test in application of hat profiles subjected to crushing load is performed.

## 2 Wilkins Damage Model

The approach of Wilkins [6] considers the actual stress state and the corresponding equivalent plastic strain  $\varepsilon_{pl,equ}$ . This information is taken into account by the damage evolution variable  $D$  as follows:

$$D = \int \omega_1 \omega_2 d\varepsilon_{pl,equ} \quad (1)$$

Both parameters  $\omega_1$  and  $\omega_2$  contain stress data and are determined as

$$\omega_1 = \left( \frac{1}{1-\gamma \sigma_H} \right)^\alpha \quad (2)$$

and

$$\omega_2 = (2 - A_D)^\beta. \quad (3)$$

These two parameters denote the main characteristic of the approach of Wilkins, which is a separated consideration of the hydrostatic stress  $\sigma_H$  and the deviatoric stresses  $s_1$ ,  $s_2$  and  $s_3$  through  $A_D$ . The parameter  $A_D$  in Equation 3 is composed by the deviatoric principal stresses (Equation 4), which obeys the condition  $s_1 > s_2 > s_3$ . Furthermore, phenomenological parameters, denoted by  $\alpha$ ,  $\beta$  and  $\gamma$ , included in Equation 2 and 3.



$$A_D = \max\left(\left|\frac{s_2}{s_3}\right|, \left|\frac{s_2}{s_1}\right|\right) \quad (4)$$

The Wilkins Damage Model is included in *LS-Dyna*, keyword **\*MAT\_082** or synonymous as **\*MAT\_PLASTICITY\_WITH\_DAMAGE\_ORTHO (\_RCDC)**.

### 3 Simulation results and experimental validation

The calibration of the Wilkins Damage Model is carried out for an AISi cast alloy by tensile test coupons of different geometries. The strategy for the characterization of the damage behaviour includes surveys of notch, shear and tension test geometries. Additionally, tensile tests with Merklein geometry [7] are conducted. The entire test series is performed on a tensile test rig, which ensures a low effort on tool configuration.

After calibration, the material model is applied on a crushing simulation of hat profiles. An associated simulation result represented in visual scheme is depicted in Figure 1. A well accordance to the experimental deformation behaviour (Figure 1, left) is observed. Furthermore, the damage incidence during the crushing process is captured in an appropriate manner. The comparison of energy absorption values shows a deviation of only 3 % of the numerical model to the experiments.

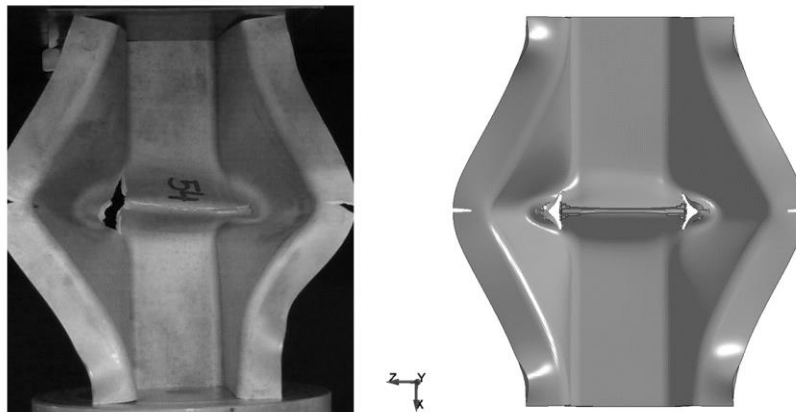


Fig. 1: Experimental result of hat profiles (total length, x: 250 mm, width, z: 117 mm and depth, y: 91 mm) with a subjected crushing displacement of 30 mm (left) and the corresponding simulation in application of the Wilkins Damage Model (right)

### 4 Summary

The intention of this paper is the investigation on a Material Damage Model introduced by Wilkins. This model is calibrated for an AISi cast alloy by different test coupons for various triaxiality regimes. After model calibration, a 3D validation simulation is performed through crushing of a hat profile. The evaluation of this test shows a well accordance of simulation results with respect to experimental tests.

### 5 Acknowledgement

This work has been supported by the European Regional Development Fund (EFRE) in the framework of the EU-program "IWB Investition in Wachstum und Beschäftigung Österreich 2014-2020", and the federal state Upper Austria.

### 6 References

- [1] Gurson A. L., "Porous rigid-plastic materials containing rigid inclusions-yield function, plastic potential and void nucleation," *The Physical Metallurgy of Fracture*, 1978.
- [2] Tvergaard, V.; Needleman, A., "An analysis of ductile rupture in notched bars," *Journal of the Mechanics and Physics of Solids*, 1984.
- [3] Hutchinson, J.; Nahshon, K., "Modification of the Gurson Model for shear failure," *European Journal of Mechanics and Solids* 27, 2008, 1-17.

- [4] Johnson, G. R.; Cook, W. H., "Fracture characteristics of three metals subjected to various strains, strain rates, temperatures and pressures," *Engineering Fracture Mechanics*, 1985, pp. 31–48.
- [5] Corporation Livermore Software Technology; (LSTC), "LS-Dyna Keyword User's manual Volume 2 Material models R 7.1," 2014.
- [6] Wilkins, M. L.; Streit, R. D.; Reaugh, J. E., "Cumulative-strain-damage model of ductile fracture: Simulation and prediction of engineering fracture tests," 1980.
- [7] Yin, Q.; Zillmann, B.; Suttner S.; Gerstein G.; Biasutti, M.; Tekkaya A.; Wagner M.; Merklein, M.; Schaper, M.; Halle, T.; Brosius, A., "An experimental and numerical investigation of different shear test configurations for sheet metal characterization," *International Journal of Solids and Structures*, 2014, pp. 1066-1074.

# 4a impetus (PART 1): Dynamic material characterization of plastics – development in the past 10 years

A. Fertschej, P. Reithofer, M. Rollant

4a engineering GmbH

## 1 Introduction

In recent years plastics have been used more and more in automotive industry primarily

- for cost reasons in complex design,
  - for safety reasons in the area of occupant and pedestrian safety application and
  - for CO<sub>2</sub> reduction reasons in lightweight applications with regard to structural performance needs.
- Therefore simulation of the application load cases is an indispensable must have in the product development. Based on the successful usage of simulation tools in the metallic section, the standard simulation methods and material models can't represent the plastic material behavior. Many developments and improvements in the crashcode LS-DYNA especially for plastics and composites have been seen in the past 10 years, with the necessity to consider the deformation (viscoelasticity, viscoplasticity, anisotropy) as well as damage and failure behavior in the material model.

## 2 Retrospect

New developments in the testing and material characterization have been going along with requirements of these new models [1]. The classic testing methods ideally with mechanical understanding (tension, compression and shear) with local strain measurements (for example by DIC) are one approach to deal with this topic.

Another approach is to use the bending load case and its many advantages:

- this is the most frequently occurring load case in reality,
- the geometry of the test specimens can be very simple and
- tests can be performed very quickly and accurate using 4a impetus (see fig. 1).

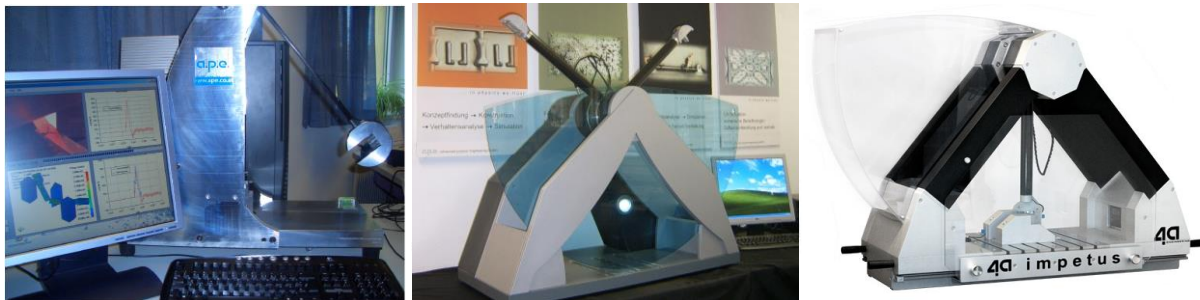


Fig. 1: Prototype of 4a impetus (2004 [2]), first commercial version (2006 [3]) and the current version (2015 [4])

In the presentation we will give an exemplary overview of the development in the field of plastic materials testing in the past 10 years

- starting with simple \*MAT\_024 and high-speed tensile tests compared to the easy 4a impetus bending approach,
- showing the reverse engineering process with LS-OPT and the normal and clamped bending as alternative to high speed tensile tests,
- considering different loading situations (e.g. \*MAT\_187), needed test specimens and methods to characterize the material,
- including temperature and moisture dependencies for thermoplastics and
- concluding with current developments in considering the process influence and in failure prediction.

### 3 State of the art

In the field of old school material characterization static and dynamic tensile tests are the base for a \*MAT\_024 material card generation. For plastics and composites there is no high-speed tensile testing standard method available. Considering complex yield surfaces (tension, shear, compression, ...) or anisotropy is often a known issue and well researched in several public founded projects, but cannot be seen as standard in automotive simulation applications.

4a impetus stands for the new solution, starting from measurement data handling up to an automatic material parameter identification process (MPIP) based on reverse engineering. The hardware and software products are used by automotive OEMs and their suppliers, material suppliers, research institutes and engineering service providers. Meanwhile 4a offers standards to generate simple material cards like \*MAT\_024, considering anisotropy \*MAT\_054/058/157, compression/tension behavior \*MAT\_124/187.

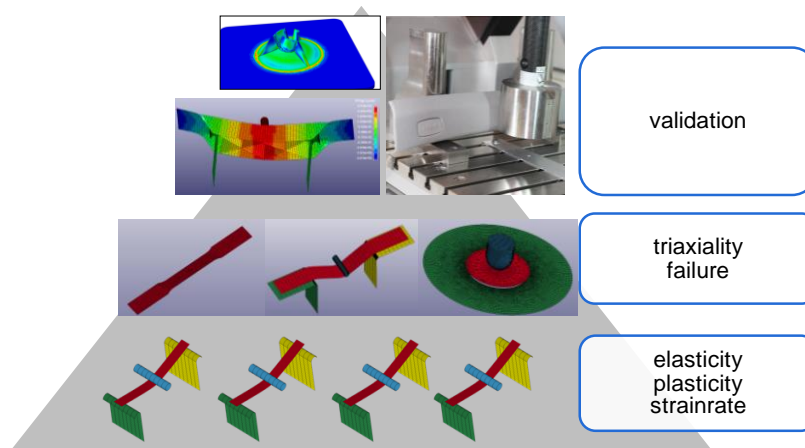


Fig.2: 4a impetus material characterization pyramid for plastics [5], [6],[7]

### 4 Summary & Outlook

Driven by the increasing requirements of the industry to predict not only the "average" deformation behavior, the simulation methods and the therefore needed material models as well as the testing methods have to be improved continuously. 4a impetus is the first approach, closing the gap between the simulation and testing fractions.

Due to lightweight applications and the mechanical structural relevance of plastic and composite materials especially damage and failure prediction as well as considering process induced inhomogeneity (e.g. short and long fiber reinforced materials, foamed plastics, ...) will be R&D topics in the next years.

### 5 Literature

- [1] Kolling, St. et.al.: *SAMP-1: A Semi-Analytical Model for the Simulation of Polymers*, 4. LS-DYNA Anwenderforum, Bamberg 2005
- [2] Hafellner, R. et. al: *Neue flexible Methoden der Materialdatenermittlung für die dynamische Simulation*, 3. LS-DYNA Anwenderforum, Bamberg 2004
- [3] Fritz, M. et. al: *Kunststoffcharakterisierung mit Impetus II - Der effiziente Weg zu validierten dynamischen Materialdaten*, LS-DYNA Forum, Frankenthal 2007
- [4] <http://impetus.4a.co.at>
- [5] Reithofer, P. et. al: *Dynamic Material Characterization Using 4a impetus*, 29th Regional Conference of the Polymer Processing Society, Graz 2015
- [6] Fertschej, A. et. al: *Failure models for thermoplastics in LS-DYNA*, 29th Regional Conference of the Polymer Processing Society, Graz 2015
- [7] Reithofer, P. et. al: *Zeitabhängiges Materialverhalten von Kunststoffen*, 4a. Technologietag, Schladming 2016

# 4a impetus (PART 2): innovations – test methods, MAT\_SAMP-1, anisotropy, composites and more

A. Fertschej, P. Reithofer, M. Rollant

4a engineering GmbH

## 1 Introduction - Characterizing plastics and composites using 4a impetus

In recent years plastics are substituting other materials mostly to reduce the weight of the part. As they are also carrying the same applied loads it is necessary to consider the deformation behavior (plasticity) as well as damage and failure in the material model. To characterize the dynamic deformation behavior dynamic bending tests on 4a impetus (fig. 1 left) are a cost-efficient alternative or extension compared to standard dynamic test methods. Furthermore many plastic materials have a huge difference in the tension and compression behavior. Consequently a material card generation of simple elastic-viscoplastic material models (e.g. \*MAT\_024) based on static and dynamic bending tests, which takes both into account, will be near to reality [1].

As a result of the processing unreinforced as well as reinforced plastics have different mechanical properties at the outer surface compared to the inner core. The bending properties (stiffness, failure behavior ...) are usually favorably higher. Due to the stress distribution in bending load cases the outer highly orientated layer carry most of the load compared to the tension case. Engineering judgment based on bending material properties is therefore the better choice.

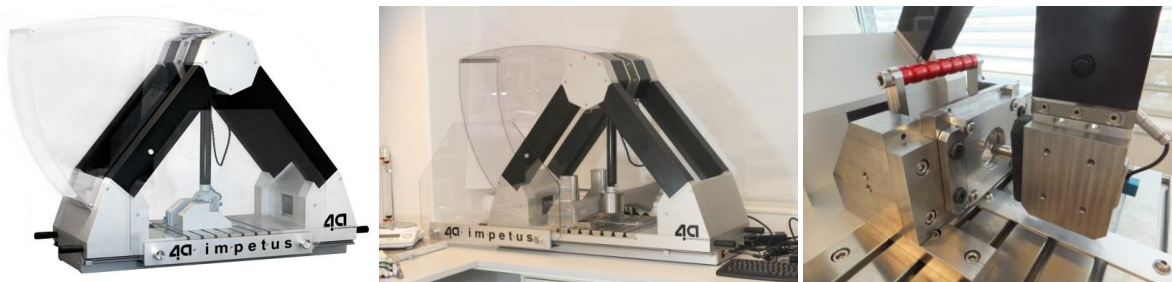


Fig.1: The actual version of 4a impetus (left); component testing in 4a impetus (middle); new puncture test and pendulum arm (right)

Nowadays more detailed material models considering complex yield surfaces (e.g. \*MAT\_124 or \*MAT\_187 for plastics), anisotropy (e.g. \*MAT\_157 or \*MAT\_215 for reinforced plastics) or complex failure models (e.g. \*MAT\_ADD\_EROSION) are available. The objective is of course a better description of the material behavior [2, 3, 4]. The newest 4a impetus developments regard these needs - always with the focus to offer an efficient material parameter identification process (MPIP).

## 2 Innovations in 4a impetus - hardware

The design of 4a impetus and the pendulum arm was improved. Now it's possible to test even parts and composite materials up to an impact energy of 50J (fig. 1 middle). To characterize the dynamic behavior and failure under biaxial loading a new puncture test method was designed (fig. 1 right). It also allows testing under low or high temperatures. The implementation of a high-speed-camera (newest accessory kit) allows the visualization of dynamic behavior of the material during test (crack initiation and propagation in detail, see fig. 2).

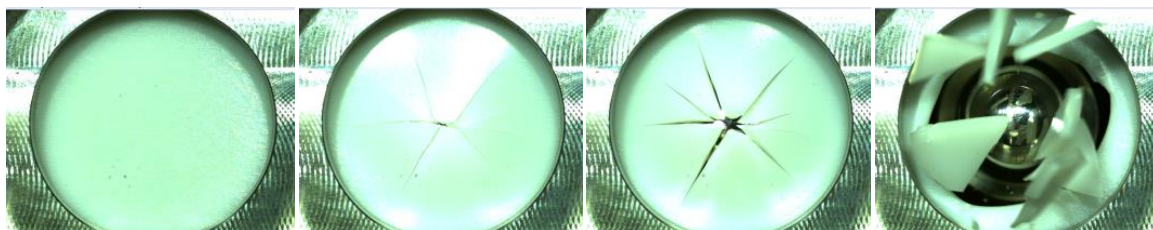


Fig.2: High speed pictures of the dynamic puncture test of a POM at different time steps

### 3 Innovations in 4a impetus - software

In the presentation many new features will be shown, exemplary two of them are described in this abstract in detail.

The above mentioned complex material models (fig. 3 left) as well as the most common failure models are implemented in 4a impetus GUI. The describing parameters can be directly evaluated in the material parameter identification process. For standard material cards (e.g. \*MAT\_024) an automated workflow on 3-point-bending-tests was developed and implemented as AUTOFIT process. Within a few clicks and some simulation/optimization time an accurate material card is generated by 4a impetus (fig. 3 right).

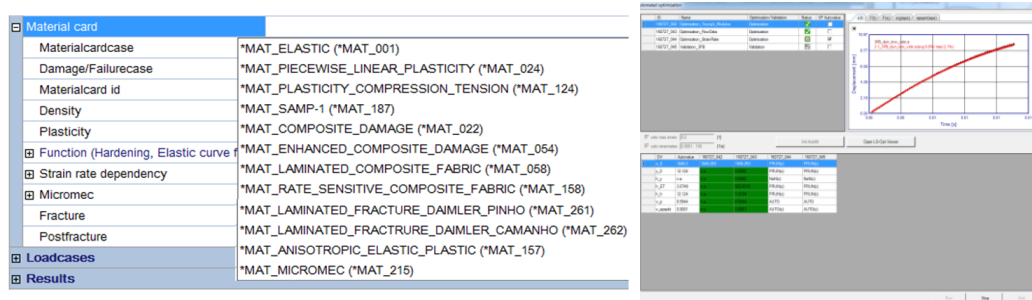


Fig.3: Available LS-DYNA material cards in 4a impetus (left); AUTOFIT process – creating material cards within a few clicks automatically (right)

For fiber reinforced plastics and composites 4a micromec is implemented as library in 4a impetus. 4a micromec is based on the Mori Tanaka Meanfield Theory and allows the user to calculate automatically the thermo elastic mechanical properties of a composite based on the information of the matrix and filler [5]. As a consequence less material parameters have to be determined in the MPIP; so the micro mechanics reduce the effort of testing and material card generation remarkable (fig. 4).

The image shows a screenshot of the 4a impetus software interface. The left panel shows the 'Micromec' library with a table of material parameters. The right panel shows the 'Composite Density' table with a list of material parameters. The parameters are grouped into 'matrix data', 'filler data', and 'orientation data'. Three parameters are marked in red: 'y\_0', 'h\_ET', and 'v\_p'.

Strain rate dependency	Table	Composite Density	Value	Unit
Strain rate dependency	Johnson Cook	c_C11	6172	[MPa]
Micromec	User defined	c_C12	1808	[MPa]
Matrix		c_C13	1231	[MPa]
Density of the matrix	900	c_C14	0	[MPa]
E-Modulus	1500	c_C15	0	[MPa]
Poisson's ratio	0.3	c_C16	0	[MPa]
Yield strength	15	c_C22	4135	[MPa]
Strength at Break	17	c_C23	1181	[MPa]
Failure strain	0.05	c_C24	0	[MPa]
Fiber		c_C25	0	[MPa]
Fillerlength	1000	c_C26	0	[MPa]
Fillerdiameter	20	c_C33	2616	[MPa]
Phi or Psi	φ	c_C34	0	[MPa]
Phi	12.9	c_C35	0	[MPa]
Psi	30.1	c_C36	0	[MPa]
Fillermaterial	E-Glas	c_C44	1554	[MPa]
Orientation		c_C45	0	[MPa]
Fillerorientationtype	CA lin. OF	c_C46	0	[MPa]
Fillerorientationvalue 1	0.6	c_C55	888.6	[MPa]
Fillerorientationvalue 2	0.33	c_C56	0	[MPa]
		c_C66	957.5	[MPa]
		y_r00	1	[1]
		y_r45	0.5105	[1]
		y_r90	0.2865	[1]
		y_scalematrix0	9.076	[1]

Fig.4: Calculation of the material parameters for \*MAT\_157 using the 4a micromec library, this reduces the unknown material parameters down to 3 (marked in red) [5]

### 4 Innovations in 4a impetus - future

In future 4a impetus hardware and software developments will continue to focus on testing and simulation trends. We will work hard to set further trend standards to ensure that the user can generate very easy, quick and cost efficient accurate validated material cards.

### 5 Literature

- [1] Reithofer, P. et. al: *Dynamic Material Characterization Using 4a impetus*, 29th Regional Conference of the Polymer Processing Society, Graz 2015
- [2] Reithofer, P. et. al: *4a impetus (PART 1): Dynamic material characterization of plastics – development in the past 10 years*, 14. LS-DYNA Anwenderforum, Bamberg 2016
- [3] Fertschej, A. et. al: *Failure models for thermoplastics in LS-DYNA*, 29th Regional Conference of the Polymer Processing Society, Graz 2015
- [4] Staack, H. et. al: *Application oriented failure modeling and characterization for polymers in automotive pedestrian protection*, 8. Complasp, Barcelona 2015
- [5] Reithofer, P. et. al: *Material characterization of composites using micro mechanic models as key enabler*, automotive CAE Grand Challenge, Hanau 2016

# Some Aspects on Characterizing and Modeling of Unreinforced and Short Fiber Reinforced Polymers in Crashworthiness Applications

M. Vogler, G. Oberhofer, H. Dell

MATFEM Partnerschaft Dr. Gese & Oberhofer, München

## 1 Introduction

The specific behavior of unreinforced and short fiber reinforced polymers in case of crashworthiness, drop test and misuse load cases demands special requirements both on the material modeling approach and on the material parameter characterization. Polymers in general show a strongly stress state dependent yielding and fracture behavior. Furthermore, viscous effects are observed both in the elastic and in the plastic regime and fracture strongly depends on the strain rate. Initial or evolving anisotropy is due to fiber reinforcements or reorientation of molecule chains. Furthermore, most polymers exhibit a compressible behavior under tensile stress states due to the nucleation and evolution of micro voids. This complex mechanical behavior of polymers makes it quite challenging both in terms of material characterization and in terms of finding a good constitutive representation.

In the presentation, the modular material and failure model MF-GenYld + CrachFEM and the underlying material characterization concept for polymers will be introduced. Furthermore, some particular aspects will be discussed in detail: localization effects in uniaxial tension and the so called ductile-brittle transition of fracture.

## 2 Modeling polymers using the modular material model MF-GenYld+CrachFEM

Fig. 1 shows an overview of the available features in the modular material and failure model MF-GenYld+CrachFEM. The different elasticity laws, yield loci, failure criteria etc. can be combined in a modular way in order to meet the needs of the respective material. For short fiber reinforced thermoplastics, both the elastic and the plastic anisotropy can be described with good accuracy using an orthotropic approach. Whereas in most cases the principal axes of the elasticity tensor and of the yield surface are coaxial, the fracture behavior can be generally anisotropic and the main anisotropy axes do not necessarily coincide with the main anisotropy axes of the elasticity tensor and of the yield surface, respectively. In order to account for the general anisotropic nature of failure, various discrete directions are probed for the maximum fracture risk in the modular material model MF-GenYld+CrachFEM. Furthermore, different fracture scenarios like shear fracture and ductile normal fracture are regarded.

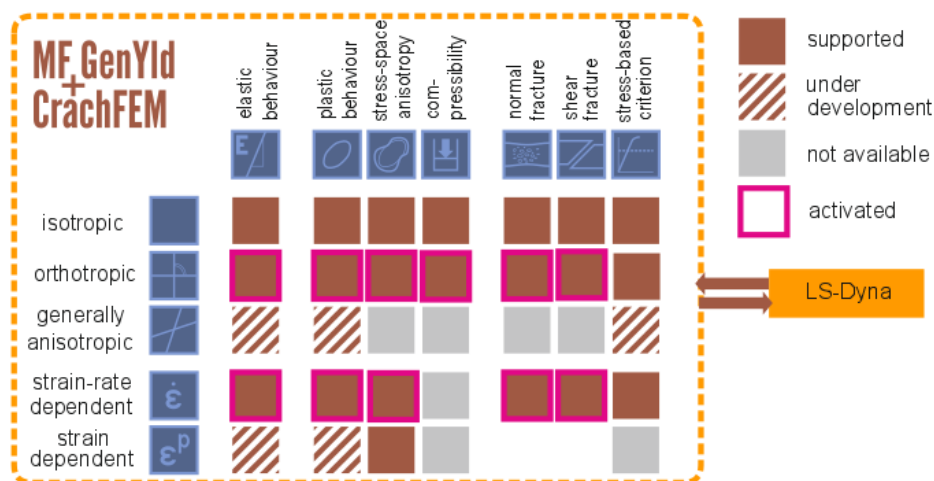


Fig. 1: MF-GenYld+CrachFEM: Modules for modeling unreinforced and fiber-reinforced polymers.

A prerequisite for a reliable prediction of fracture is the exact prediction of the stresses and strains in various stress states prior to failure. Considering that, different modules are available in order to modify the respective basic yield surface [1]. In order to account for a different hardening behavior under shear, the waist module can be activated and a waist function can be input. In the same way, the usually observed different hardening in tension and compression can be regarded via the asymmetry module and the asymmetry function. Biaxial hardening behavior can be controlled via the biaxial scaling factor. These yield locus modifications can be chosen for all available yield loci in MF-GenYld. This enables a precise prediction of hardening in all relevant stress states. Compressibility (dilatancy) can be regarded via the compressibility module and the evolution of the plastic Poisson ratio can be input as a function of the equivalent plastic strain [2]. In order to regard anisotropy, the fiber orientation tensor can be directly processed in the material model MF-GenYld+CrachFEM for the calculation of the principal directions of anisotropy as well as the degree of fiber orientation. Different methods are available in order to obtain the required orientation tensor for the target mesh. The forthcoming release of software "Converse" [3] can be used in order to provide the orientation tensor based on the results obtained with different form filling simulation tools.

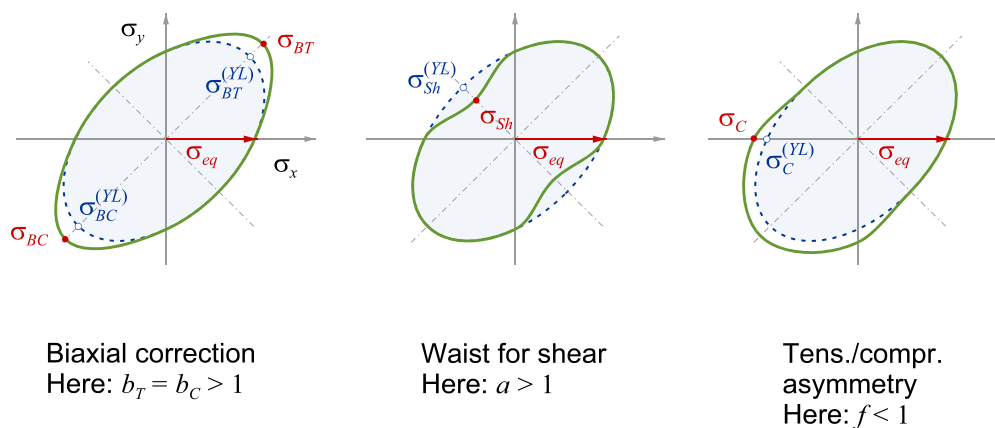


Fig.2: Modular material model MF-GenYld+CrachFEM: Modifications of the basic yield surface.

In the presentation, both the modeling concept using MF-GenYld+CrachFEM and the underlying characterization concept will be introduced, whereby two aspects will be given special consideration: strain localization in uniaxial tension and ductile-brittle transition of failure.

As an example, an ABS polymer (Acrylonitrile butadiene styrene) will be discussed, exhibiting a strong tendency to localization in uniaxial tension, but showing a stable hardening behavior in plane strain and biaxial stress states. For such materials prone to localization it is essential to distinguish between localization and fracture by refinement of the evaluation range of the ARAMIS system.

Another aspect often observed in polymers is the so called ductile-brittle transition. Some thermoplastics exhibit a pronounced ductile behavior with high failure strains at lower strain rates and a very brittle glass-like behavior under high strain rates. This transition from ductile to brittle behavior can occur gradually or abrupt – depending on the material. The challenges both for characterization and for modeling of this effect will be discussed.

### 3 Summary and Outlook

In general, a quite good prediction of the mechanical behavior for a variety of polymeric materials can be achieved with the current MF-GenYld+CrachFEM material model. Current developments are focused on the extension of the model with respect to strain dependent evolution of the plastic yield locus allowing for completely independent strain hardening in different orientations and for changing of the Lankford parameter with increasing plastic strain.

- [1] H. Dell, H. Gese, G. Oberhofer: ADVANCED YIELD LOCI AND ANISOTROPIC HARDENING IN THE MATERIAL MODEL MF GENYLD + CRACHFEM, Numisheet 2008, Interlaken, Switzerland
- [2] H. Dell, V.Yelisseyev, G. Oberhofer: Failure prediction for non-reinforced and short fiber reinforced polymers. German LS-DYNA Forum 2014, 6. - 8. October 2014, Bamberg, Germany
- [3] N.N.: CONVERSE, <http://www.partengineering.com/software/converse/>, PART Engineering GmbH, Bergisch Gladbach, 08.09.2016



# Potential of MAT157 for Short-Fiber-Reinforced Injection Molded Plastic Components

Dr.-Ing. Wolfgang Korte, Dipl.-Ing. (FH) Sascha Pazour, Dr.-Ing. Marcus Stojek

PART Engineering GmbH

## 1 Introduction

The injection molding process causes a local anisotropic material behavior within the molded part due to the alignment of the fibers dependent on the local flow conditions in the part (Fig. 1). The fiber orientation varies not only at different locations in the part but also across the wall thickness. The laminar flow of the melt in combination with the velocity profile in the flow channel lead to a characteristic fiber orientation across the wall thickness. The fibers are mainly aligned parallel to the flow direction in the outer so-called shear layers and fibers mainly aligned transverse to the flow direction in the mid layer.

It is evident that the structural analyst is interested in considering these effects. Such a consideration may result in a more precise prediction of the mechanical behavior of the investigated component.

In this paper, a strategy is described to predict stiffness and strength of injection-molded short-fiber-reinforced (SFR) plastic components.

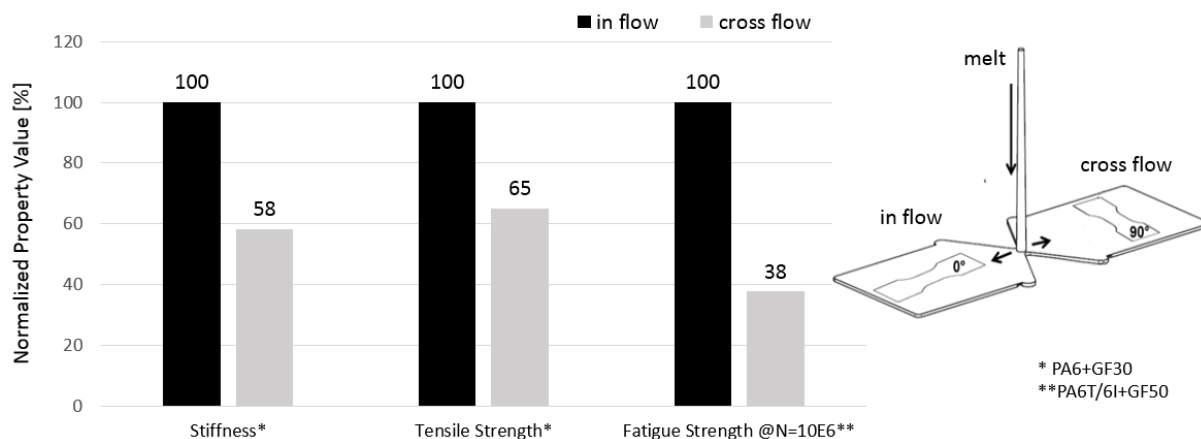


Fig. 1: Direction Dependent Material Properties

## 2 Material Modeling of Short-Fiber-Reinforced Plastics

In general the specific material behavior of SFR plastics requires an anisotropic elasto-plastic material description, at least if an evaluation of the ultimate component strength is considered. In this case the deformation of the material exceeds the linear respectively linear-viscoelastic range and irreversible plastic deformation occurs. Such an anisotropic elasto-plastic material description is available; in most FEM solvers the so-called Hill potential [1] is implemented. The Hill potential was originally defined for the anisotropic plastics behavior of metals based on Mises plasticity. In fact the Hill potential is an anisotropic von Mises stress taking into account the deviatoric stresses. In practice it is used e.g. for the simulation of deep drawn sheet metals where anisotropy as well as plastics deformation occur due to the stretching of the material. However, the Hill potential is defined for unidirectional conditions, this is that it is assumed that three anisotropy axes as well as three anisotropy planes of the material exist. Whereas in injection molded SFR parts there is a fiber orientation distribution instead of ideally aligned fibers. This means there exist principal anisotropy axes and planes but additionally each of them is superimposed with a fiber orientation distribution function (ODF) giving the information how many fibers are aligned exactly in these anisotropy axes and how many in certain discrete angles to them. Which in turn influences the mechanical behavior of the material significantly (Fig. 2).

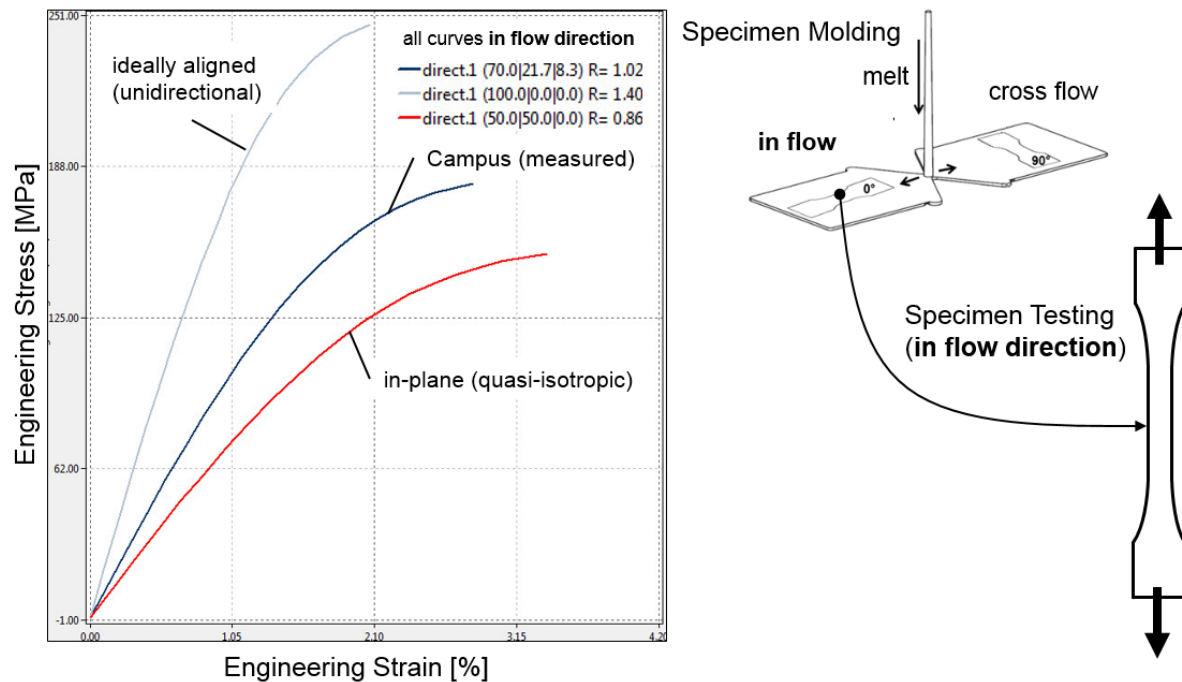


Fig.2: Influence of local ODF on stress/strain-curve

If one aims to simulate the mechanical behavior of SFR parts this has to be taken into account. For this a so-called orientation averaging can be applied (Advani and Tucker [2]). The unidirectional mechanical properties, here initially the elastic stiffnesses are meant, are weighted with their local degree of orientation. E.g. for a narrow distribution the degree of orientation is close to unity and for a very broad distribution close to zero (quasi-isotropic). The information about the local degree of orientation can be extracted from the orientation tensor which is provided as standard output by most injection molding solvers. Additionally, the plastic part of the material description has to be defined dependent on the ODF. Therefore the classic unidirectional Hill formulation is modified in such a way that the yield ratios are not anymore constant rather than defined as a function of the local ODF.

Additionally to the consideration of the local ODF the anisotropic material properties themselves have to be determined. Basically this could be done by testing. However, there are at least two problems with an experimental approach. First, there are 9 anisotropic material properties needed for the linear-elastic part of the material model (tensile, shear moduli, Poisson ratios) and additionally 6 yield ratios for the Hill potential for the plastic part of the model. These required 15 material parameters would lead to an extensive test scheme linked to high testing costs alike. Second, in general it is not possible to manufacture test specimen with a particular ODF.

In order to overcome these problems it is possible to compute the required parameters and not to determine them experimentally. This can be conducted by utilizing a micro-mechanical model. Such a model applies a so-called homogenization scheme, it is capable to determine the anisotropic material properties of an unidirectional ideally aligned unidirectional representative volume element (RVE) only based on the constituents of the composite. That are the properties of the matrix, the fiber, the aspect ratio (fiber length vs. diameter ratio) and the volumetric fiber fraction (Mori and Tanaka [3]). After that is done the ODF is taken into account by applying the orientation averaging scheme on the determined unidirectional material properties. By applying this strategy a minimum of experiments is required in order to calibrate the material model. Typically two tests, in-flow and cross-flow, are sufficient. If even these tests are not accessible a reasonable estimation can be made by using only a Campus [4] test specimen.

In order to conduct the described procedure automatically and efficiently the software "Converse" [5] is available, that incorporates all described algorithms, including a micro-mechanical model. It is stressed here that the micro-mechanical model applied is only used in order to provide all required anisotropic

elastic and elasto-plastic material properties. The whole process works in pre-processing. For the analysis of the actual component at hand only solver built-in material models are used. As they are available in LS-Dyna as well. This is described in detail in the next chapter.

### 3 Analysis of SFR Plastic Components in LS-Dyna with Material Type 157

In the past the procedure outlined was in LS-Dyna only applicable with shell elements with material type 108. Since LS-Dyna Version 8, Material Type 157 (\*MAT\_ANISOTROPIC\_ELASTIC\_PLASTIC) provides the capability to describe the anisotropic elasto-plastic material behavior of short-fiber-reinforced plastics for solid elements as well. The material type 157 is a combination of the anisotropic elastic material model (MAT\_002) and the anisotropic plastic material model (MAT\_103\_P) [6]. The stiffness has to be defined in a  $6 \times 6$  anisotropic constitutive matrix where 1 corresponds to the so-called “a”-material direction (in fiber-direction), 2 to the “b”-material direction and 3 to the “c”-material direction (transverse fiber-directions). Here an orthotropic system can be used and due to partly symmetry only 9 values are needed. These 9 material properties, as already mentioned, describe the anisotropic linear-elastic material behavior. For the plastic part of the material model, described by MAT\_103\_P additionally the 6 anisotropic parameters for the Hill yield criterion and a load curve id that refers to the materials reference stress/strain-curve have to be provided. So far these 15 parameters describe the anisotropic unidirectional behavior of the material.

The required incorporation of the ODF is done by defining 45 different sets of those 15 parameters for particular local ODFs. The elements in the component to be analyzed then are classified in those 45 classes respectively according to their belonging local ODF. The provision of the ODF for each element as well as their classification is done by “Converse”. Which provides as well all 45 required sets of material parameters.

By using this approach for a strength assessment it is assumed implicitly that the Hill yield surface describes not only the yield but the failure location as well. So far this approach has been applied for real components under loading which lead to local plastic straining in notch roots. A subsequent failure occurred mainly due to tension stresses up to a maximum of the ultimate breaking stress of the stress/strain-curve. To what extent this approach is suitable for the post-failure range of the stress/strain-curve, typically of interest for crash analysis is not yet validated. It might be the case that here more complex yield and failure criteria are necessary. Especially this might hold true if the stress in the component does not only occur in locally limited areas under tension stress but in complete cross sections and/or under compression stresses. This is typically the case in crash analysis for that more complex models are available via a subroutine as user-defined material, to mention here is the software “MF-GenYld+CrachFEM” [7]. In the forthcoming Converse Release exists an interface to “MF-GenYld+CrachFEM” in order to provide the orientation tensor from an injection molding simulation for a subsequent mechanical analysis of the SFR component. This opens up a way to apply seamlessly and efficiently such models as well.

### 4 References

- [1] Hill, R.: A theory of the yielding and plastic flow of anisotropic metals. Proc. Roy. Soc. London, 193 (1948), p. 281–297
- [2] Advani, S.G. and Tucker, C.L., The use of tensors to describe and predict fiber orientation in short fiber composites, J. of Rheology Vol. 31 (1987) No. 8, p. 751-784
- [3] Mori, T.; Tanaka, K.: Average Stress in Matrix and Average Elastic Energy of Materials with Misfitting Inclusions, Acta Metallurgica 21 (1973), p. 571-574, Tokyo
- [4] N.N., CAMPUS, <http://www.campusplastics.com/campus/>, 08.09.2016
- [5] N.N.: CONVERSE, <http://www.partengineering.com/software/converse/>, PART Engineering GmbH, Bergisch Gladbach, 08.09.2016
- [6] Livermore Software Technology Corporation, \*MAT\_ANISOTROPIC\_ELASTIC\_PLASTIC, LS-Dyna Keyword User’s Manual Volume 2, p. 823-828
- [7] Vogler, M.; Dell, H., Oberhofer, G.; Gese, H.: Beschreibung von unverstärkten, kurzfaserverstärkten und endlosfaserverstärkten Kunststoffen in der Crashsimulation, Proc. Kunststoffe + Simulation, Hanser Tagung, München, 2016

# Modeling of Fiber-Reinforced Plastics Taking into Account the Manufacturing Process

Cherry Ann T. Reclusado<sup>1</sup>, Sumito Nagasawa<sup>2</sup>

<sup>1</sup>Fraunhofer Institute for High-Speed Dynamics, Ernst-Mach-Institut, EMI

<sup>2</sup>Fuji Heavy Industries Ltd.

## 1 Motivation

Injection molded glass fiber-reinforced plastics (GFRP) play an important role as modern lightweight construction materials, used for example for interior or exterior parts in the automotive industry. They combine high-strength glass fibers with a shaping polymer matrix. A suitable distribution of the fiber orientation and the degree of anisotropy within a component can contribute positively to its resistance against deformations. But finding the optimum design and process parameters can be challenging, because development costs and times are usually limited.

## 2 Integrative simulation

Aim of this study is to reduce the time and effort and to exploit the advantages of GFRPs to the full potential. For this purpose, a method is developed to take into account the fiber orientation distribution when modeling the mechanical behavior of GFRPs (Fig.1). In doing so the fiber orientation and degree of anisotropy are calculated in an injection molding simulation and subsequently mapped to the structural simulation. This approach is called integrative simulation.

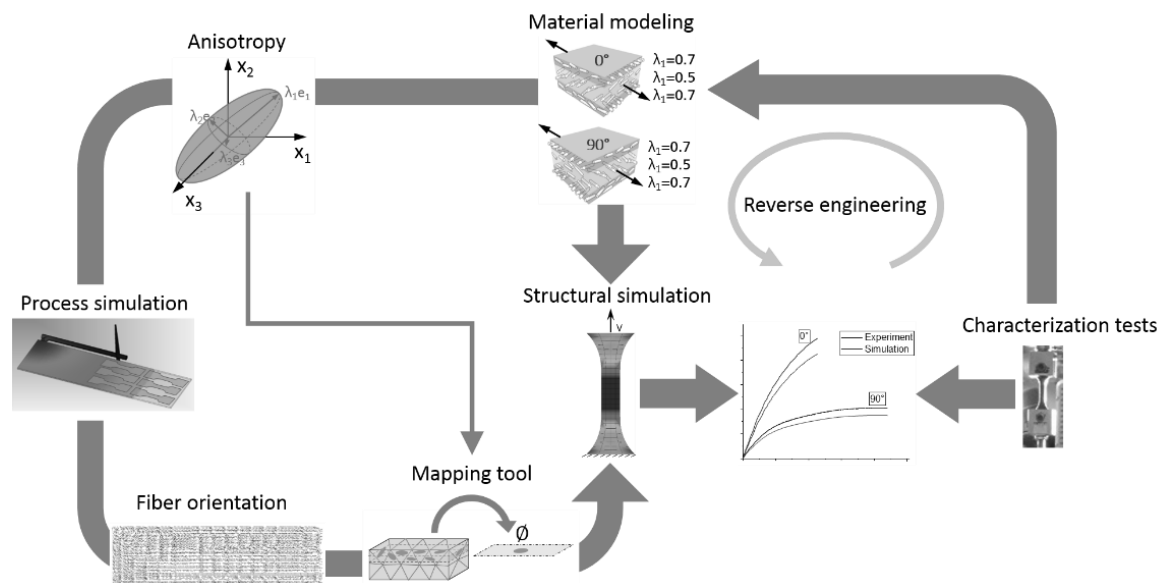


Fig. 1: Methodology of the realized integrative simulation.

## 3 Material modeling

In a first step an injection molding simulation is performed, which provides information about the orientation state at discrete material points in terms of an orientation tensor. By means of the eigenvalues and the respective eigenvectors of the orientation tensors the degree of anisotropy and the principle fiber direction are defined. Similar to the described approach by Gruber et al. [1] several material classes are declared to cover different degrees of anisotropy. But other than in [1], where two material cards (**\*MAT\_54** and **\*MAT\_98**) were overlapped, only one material card (**\*MAT\_108**) is generated for each material class. The material cards are assigned with the keyword **\*ELEMENT\_SHELL\_COMPOSITE**. For the present study it is assumed that at least five significant

layers (two outer, two transition and one central layer) are formed in the thickness direction of a composite and therefore three material classes are used for the current material modeling.

Advani and Tucker **Fehler! Verweisquelle konnte nicht gefunden werden.**2] proposed an approach to calculate the engineering constants of a material with arbitrary fiber distribution by means of the engineering constants in the uni-directional state. However, from the tensile tests we get a combined Young's and shear modulus because the fiber distribution in the tested specimens are arbitrary. The approach proposed by Advani and Tucker is therefore reversed. In Fig.2 the determination of the engineering constants is illustrated.

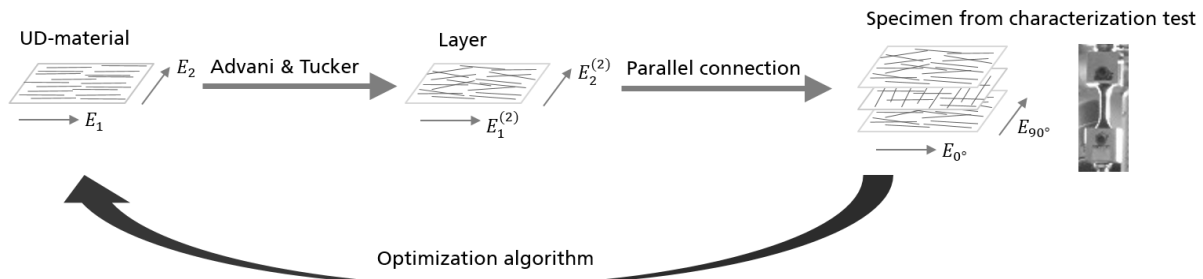


Fig.2: Schematic illustration of the determination of the engineering constants.

To calculate the Young's and shear moduli for the three specified material classes the Young's moduli and the in-plane shear modulus determined from tensile and shear tests in 0°- and 90°-direction are used. It is assumed, that the Young's moduli and the in-plane shear modulus of the investigated GFRP are composed as follows:

$$E_{0^\circ} = \eta E_2^{(3)} + (1 - \eta) E_1^{(2)} \quad (1)$$

$$E_{90^\circ} = \eta E_1^{(3)} + (1 - \eta) E_2^{(2)} \quad (2)$$

$$G_{0^\circ/90^\circ} = \eta G_{12}^{(3)} + (1 - \eta) G_{12}^{(2)} \quad (3)$$

$\eta$  is the share of the central layer's thickness and it is assumed to be 0.2.

The upper index indicates the material class and the lower index indicates the mainly involved direction of the orthotropic material.

First the engineering constants of the uni-directional material are calculated using an optimization algorithm. For each of the three material classes one **\*MAT\_108** material card is then created. While the calculated engineering constants can be inserted directly for the elastic parameters, the plastic parameters are calibrated using LS-OPT.

#### 4 Validation and further investigations

To evaluate the predictive power of the prepared models and the introduced approach, dynamic three-point bending tests and a structural simulation of these tests have been performed using a component with a ribbed structure. Judging from the force-displacement curves and the analysis of the deformation the experiments could be represented well by the generated structural simulation model. Considering the degree of anisotropy in a gradual manner by defining several material classes is a very time consuming approach, because for each material class, one set of parameters has to be calibrated iteratively. The impact of considering the degree of anisotropy on the simulation results has therefore been investigated as well. Another crucial aspect within this work was the development of a mapping tool to automatically translate and map the injection molding simulation results to appropriate variables in the structural simulation model.

#### 5 Literature

- [1] G. Gruber, A. Haimerl, S. Wartzack: *Consideration of Orientation Properties of Short Fiber Reinforced Polymers within Early Design Steps*, 12th International LS-DYNA Conference, 2012
- [2] S.G. Advani, C.L. Tucker: *The Use of Tensors to Describe and Predict Fiber Orientation in Short Fiber Composites*, Journal of Rheology, 31(8), 1987, 751-784

# \*MAT\_4A\_MICROMECH – micro mechanic based material model

A. Erhart<sup>1</sup>, A. Fertschej<sup>2</sup>, S. Hartmann<sup>1</sup>, B. Jilka<sup>2</sup>, P. Reithofer<sup>2</sup>

<sup>1</sup>Dynamore GmbH

<sup>2</sup>4a engineering GmbH

## 1 Introduction

Nowadays a great number of short and long fiber reinforced thermoplastics play a decisive role in the automotive industry to ensure affordable lightweight design and availability in large quantities. The properties of these materials are especially highly influenced through the manufacturing process (typically injection molding for SFRT and LFRT). Due to the short filling times high speeds and pressures are necessary in those processes, This leads to a a development of a significant fiber orientation by the extensional and shear flows in the mould. Integrative simulation is considering this manufacturing-induced distribution in the structural simulation by mapping the fiber orientation from the process simulation to the structural analysis.

## 2 State of the art

Until now there are two approaches to consider the local process induced anisotropy. The first one is to use an additional external software library (like ULTRASIM®, DIGIMAT®, ...), which is typically linked as **USERMATERIAL** providing a high sophisticated micro mechanical material model that can handle the local anisotropy. The gain in accuracy however means an increase of needed CPU time and additional license costs combined with less flexibility in daily work (e.g. sharing input decks between project partners, library must be available, ...).

The second possibility is to consider the local anisotropy in LS-DYNA with standard available material models or composite layups. The first attempts to describe the anisotropic behavior can be found in these publications:

- [Reithofer2008] : **\*MAT\_108** only orthotropic elastic plastic
- [Nutini2010] : **\*MAT\_103** only orthotropic visco plasticity
- [Schöpfer2011] : **\*MAT\_108 + \*MAT\_054** approach combining material models

Later approaches considered the fiber orientation by using composite layups or initialization methods (**\*INITIAL\_STRESS\_SHELL(SOLID)**) [Haufe2014]. Figure 1 shows the current simulation process chain to include the local mechanical anisotropy [Reithofer2015].

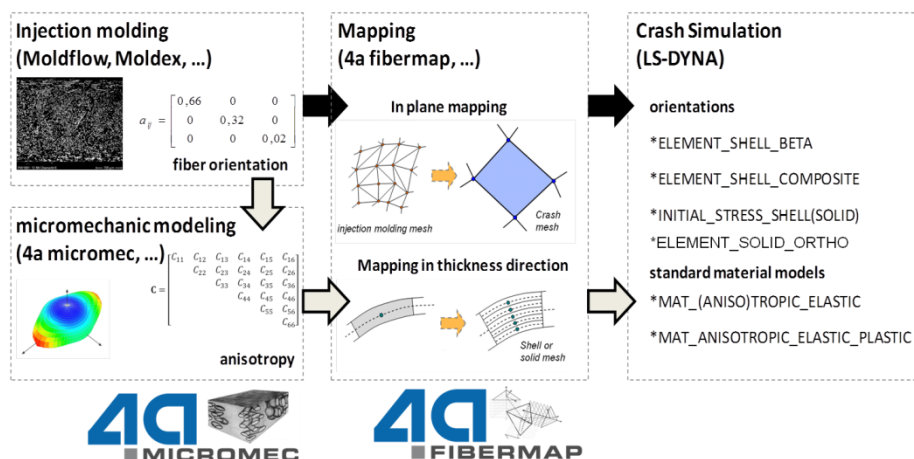


Fig.1: Available simulation process chain for injection molded parts [Reithofer2015].

The later approaches exhibits mainly two drawbacks:

- The used material models are based on a phenomenological description of the whole composite . This prevents the possibility to describe the mechanical behavior based on matrix and fiber dominant mechanical aspects, which can really be helpful in failure prediction and propagation.

- The pre- and post-processing of all these local material properties at each integration point may be cumbersome. A reasonable usage of these simulation methods stops at the mapping of local directional cosines.

### 3 New developments in LS-DYNA

To improve the current state of the art 4a provided DYNAmore a LS-DYNA usermaterial to be implemented as a standard LS-DYNA material model. Based on [Mlekusch1997] the core functionality to calculate the thermoelastic composite properties using the Mori Tanaka Meanfield Theory, can be found in the software product 4a micromec. Based on the material knowledge of fiber reinforced plastics in the past 15 years this model was extended to an elasto-viscoplastic matrix behavior.

The developments focused on the essential known mechanical material behavior, which leads to a fast and robust material model. The matrix failure is considered by a damage initiation and evolution model and fiber failure may be considered with a simple maximum stress criterion. The needed keyword input properties can be seen in fig. 2. Starting with R10 the presented material model shall be available as **\*MAT\_215/ \*MAT\_4A\_MICROMECC**, implemented for shell, thick shell and solid elements.

	*MAT_4A_MICROMECC									
<b>header</b>	\$01	mid	mmopt	bupd	--	--	failm	failf	NUMINT	
	1000000		1.0	0.01			0.	0.	-65.	<b>options</b>
	\$02	aopt	macf	xp	yp	zp	a1	a2	a3	<b>direction</b>
<b>composite</b>	\$03	v1	v2	v3	d1	d2	d3	beta	--	
		0.0	0.0	0.0	0.0	0.0	1.0	45.	--	
<b>fibre</b>	\$04	fvf	--	f1	fd	--	a11	a22	--	<b>definition</b>
		.115		53.	1.0		.7	.25		
<b>matrix</b>	\$05	rof	e1	et	glt	prtl	prtt	--	--	<b>transversal i. elasticity</b>
		2.5899e-09	70000.	70000.	28759.	0.217	0.217			<b>failure</b>
<b>matrix</b>	\$06	xt	--	--	--	--	--	SLIMXT	NCYRED	
		2800.						0.01	10	
	\$07	rom	e	pt	--	--	--	--	--	<b>isotropic elasticity</b>
<b>matrix</b>	\$08	sigyt	etant	--	--	eps0	c			<b>viscoplasticity</b>
	\$09	LCST	--	--	--	LCDI	UPF			<b>damage</b>
	1000000					1000020	-1000026			

Fig.2: Typical keyword input for **\*MAT\_215/\*MAT\_4A\_MICROMECC**.

### 4 Verification / Validation / CPU consumption

In the presentation some simulation verification (e.g. matrix only, fiber only, DOE on fiber content/-orientation/aspect ratio, ...) and validation results on coupon level of PP fiber reinforced material will be shown. The model calibration [Reithofer2016] and usage in the simulation process chain will be roughly described. Also results on CPU time consumption and current experiences on large models will be discussed. Finally an outlook to further possible developments and improvements will be given.

### 5 Literature

- [Reithofer2008] Reithofer, P. et. al: *Kurzfaserverstärkte Kunststoffbauteile Einfluss der prozessbedingten Faserorientierung auf die Strukturmechanik*, 7. LS-DYNA Anwenderforum, Bamberg 2008
- [Nutini2010] Nutini, M. et. al: *Simulating anisotropy with LS-Dyna in glass-reinforced, polypropylene-based components*, 9. LS-DYNA Forum, Bamberg 2010
- [Schöpfer2011] Schöpfer, J.: *Spritzgussbauteile aus kurzfaserverstärkten Kunststoffen: Methoden der Charakterisierung und Modellierung zur nichtlinearen Simulation von statischen und crashrelevanten Lastfällen*, Dissertation, Institut für Verbundwerkstoffe GmbH 2011
- [Haufe2014] Haufe, A. et. al: *Zum aktuellen Stand der Simulation von Kunststoffen mit LS-DYNA*, 11. 4a Technologietag, Schladming 2014
- [Mlekusch1997] Mlekusch, B. A.: *Kurzfaserverstärkte Thermoplaste*, Dissertation, Montanuniversität Leoben (1997)
- [Reithofer2015] Reithofer, P. et. al: *Short and long fiber reinforced thermoplastics material models in LS-DYNA*, 10th European LS-DYNA Conference, Würzburg 2015
- [Reithofer2016] Reithofer, P. et. al: *Material characterization of composites using micro mechanic models as key enabler*, NAFEMS DACH, Bamberg 2016

# Simulation and optimisation of functionally graded auxetic structures

Nejc Novak<sup>1</sup>, Matej Vesenjajk<sup>1</sup>, Zoran Ren<sup>1</sup>

<sup>1</sup> Faculty of Mechanical Engineering, University of Maribor, Maribor, Slovenia

## 1 Auxetic materials

Auxetic cellular materials are modern materials which have some unique and superior mechanical properties. As a consequence of their internal structure deformation, they exhibit a negative Poisson's ratio, i.e. they get wider when stretched and thinner when compressed. The effect of negative Poisson's ratio can be useful for many different applications to enhance properties in density, stiffness, fracture toughness, energy absorption and damping [1].

This work presents mechanical analysis of auxetic cellular structures built from tetrapods (Fig. 1) fabricated from the Ti-6Al-4V powder by the selective electron-beam melting method (SEBM) at the Institute of Materials Science and Technology (WTM), University of Erlangen-Nürnberg, Germany [2].

## 2 Numerical model

Compressive testing of auxetic specimens in two orthogonal directions was performed to determine complete mechanical behaviour of these structures. The results of experimental testing were used to validate developed discrete computational models built with the beam finite elements as well as homogenised computational models by using the crushable foam material model (**MAT\_063**). The difference in post yielding behaviour in the case of numerical model built with the beam finite elements between material models **MAT\_024** and **MAT\_153** in LS-Dyna was investigated. Description of the geometry, results of experimental testing and comparison with the numerical model (discretised with beam finite elements, material model **MAT\_153**) in the direction X2 are shown in Fig. 1.

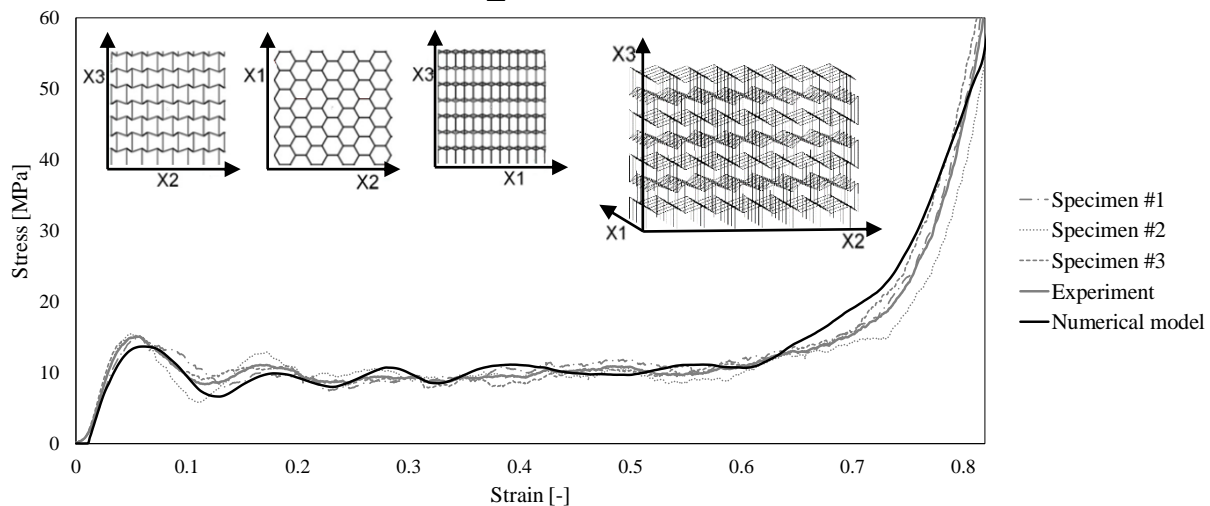


Fig.1: Comparison between experimental results and results from numerical model built with beam finite elements

## 3 Optimisation of functionally graded auxetic structures

Validated computational models were used for further optimisation of auxetic structure geometry to obtain user defined response during compression loading by applying functionally graded porosity. The optimised geometries of new auxetic lattice structures with functionally graded porosity were developed by using the Ls-Opt curve matching option [3]. Newly developed geometries of auxetic structures (Fig. 2) offer the possibility to tailor the response of the structure for particular loading conditions (e.g. degressive, linear, progressive or any other arbitrary function).



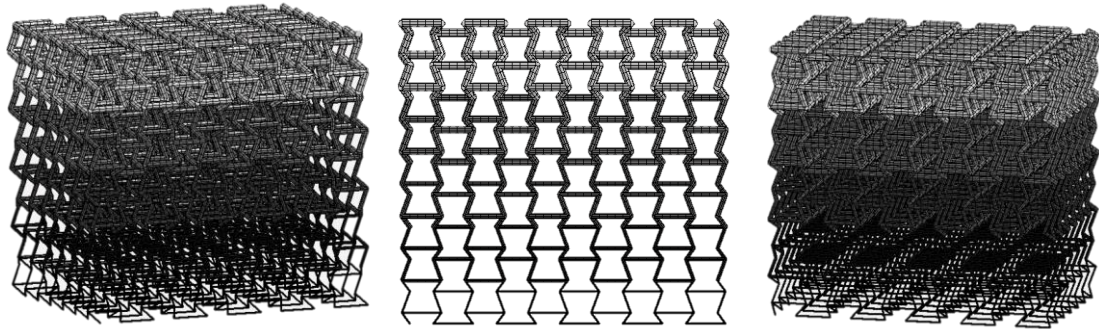


Fig.2: Numerical model of auxetic structure with functionally graded porosity

#### 4 Summary

Two different numerical models of auxetic structure were developed and validated. Using validated numerical model discretised with beam finite elements and Ls-Opt software new auxetic structures with functionally graded porosity were developed. The response of these structures can be tailored using arbitrary density distribution in structure, which can be achieved using different geometries. Newly developed functionally graded auxetic geometries will be experimentally tested at different strain rates and compared with results from numerical simulations for further validation of numerical models and to validate the concept of response optimisation of the auxetic structures.

#### 5 Literature

- [1] Novak, N., Vesenjok, M., Ren, Z.: "Auxetic Cellular Materials - a Review". *Strojniški Vestnik - Journal of Mechanical Engineering*, vol. 62, no. 9, 2016, p. 485–493
- [2] Schwerdtfeger, J., Heintz, P., Singer, R.F., Körner, C.: "Auxetic cellular structures through selective electron beam melting". *Physica Status Solidi (B) - Basic Solid State Physics*, vol. 247, no. 2, 2010, p. 269–272
- [3] Stander, N., Roux, W., Basudhar, A., Eggleston, T., Goel, T., Craig, K.: "LS-OPT User's Manual 5.2", 2015.

# Novel Approach to Model Laminated Glass

A. Haufe<sup>2</sup>, R. Böhm<sup>1</sup>, A. Erhart<sup>2</sup>

<sup>1</sup>Karlsruher Institut für Technologie, Karlsruhe, Germany

<sup>2</sup>Dynamore GmbH, Stuttgart, Germany

## 1 Motivation

Nowadays, car manufacturers are using glass not only for windows, but also as a design element like panoramic sunroofs, so that the glass parts are having a large influence on the stiffness of the car. Therefore, the material behaviour of the glass panes is getting more and more important in crashworthiness. As glass has a purely brittle damage behaviour with nearly random cracking patterns, the numerical treatment in simulations of the glass itself would be challenging. The fact that windshields are usually made of laminated safety glass (two glass layers separated by a PVB interlayer) is making it even more complex.

## 2 Common approach

The common discretization method of the laminated safety glass with finite elements is to model the layers separately, using shell elements for glass and solid elements for the PVB interlayer, both coupled by shared nodes. A common approach for the glass' material in crashworthiness applications is to use a linear elastic model with failure, where elements are deleted if a certain failure criteria is reached. This leads to a physically incorrect post cracking behaviour (no residual stiffness if elements are deleted, see Fig. 1) and crack patterns that depend on the element orientation. Therefore, correct material response is only obtained by adjusting the material parameters (unphysically) for individual load cases (e.g. head impact).

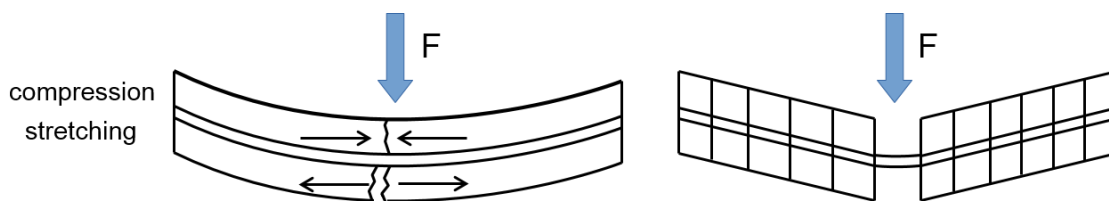


Fig.1: Post cracking behaviour

## 3 Novel approach

### 3.1 Theoretical background

In need of a more general and physically correct approach, which could also be used in industrial crashworthiness applications, a new material model was developed. This is a more sophisticated approach, which basically depends on a smeared fixed-crack model and takes crack closure effects into account. If a failure criteria (e.g. Mohr-Coulomb (see Fig. 2), several other approaches are implemented) is met in an element, the corresponding element won't be deleted, but is considered as cracked from now on and changes its material behaviour to orthotropic with the material axes oriented according to the crack direction (Fig. 3). The stiffness in each direction depends on whether the crack is closed or open. It is possible that a second crack occurs in the direction orthogonal to the first crack.

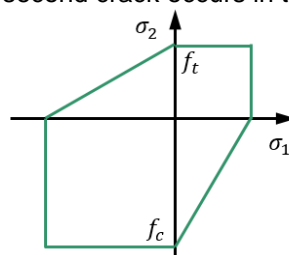


Fig.2: Mohr-Coulomb failure criteria

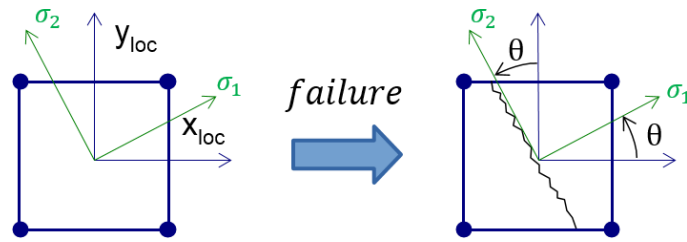


Fig.3: Orthotropic axes in element

### 3.2 Simulation results

In Fig. 4 the development of the cracks in a head impact test on a windshield, using the new material model for both glass layers, can be seen. The windshield was discretized with a regular mesh with 4-node elements. The fringe plot shows the value of the crack flag, which is equal to the number of cracks occurred in each element. It clearly shows that the cracks are developing independently from the mesh orientation.

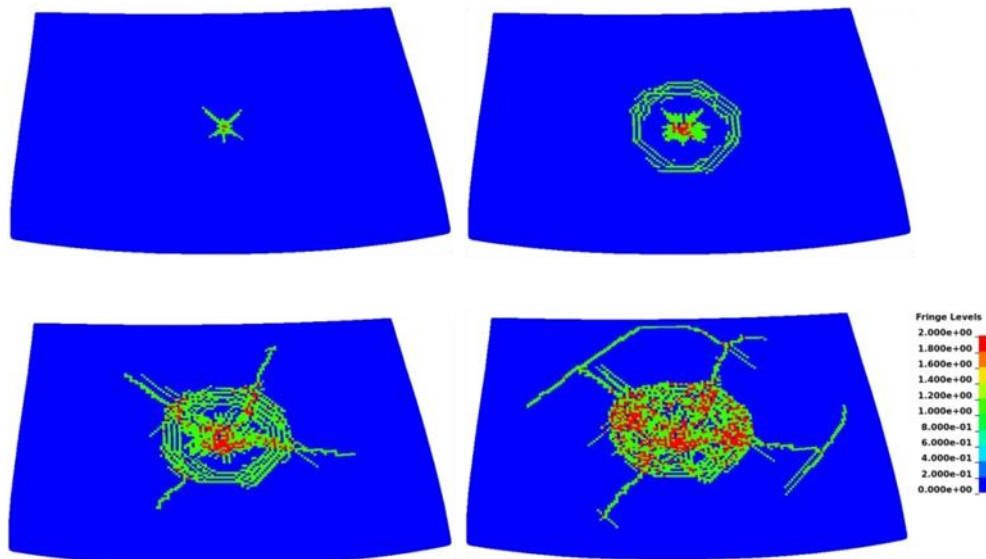


Fig.4: Development of cracks

## 4 Conclusion

The material model was implemented in version R9 of LS-DYNA as `*MAT280/*MAT_GLASS`. To give a clearer understanding of how the new material model is working, an overview about the theoretical background is given in this contribution. Additionally, first results of its application in simulations based on real experiments with car windshields are shown.

# Features in LS-DYNA R8.1 for Structural Mechanics

Tobias Erhart

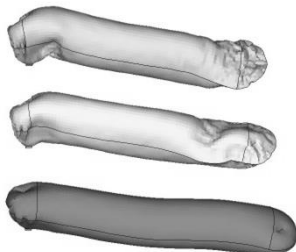
Dynamore GmbH, Stuttgart, Germany

## Abstract

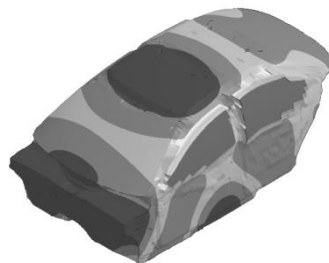
An overview of new capabilities in LS-DYNA version R8.1 will be given. This release was published in February 2016 and contains several new features in the areas of solid mechanics and the multiphysics solvers. The presentation will mainly focus on the major changes since version R7.1.2 in the area of Structural Mechanics.

Topics of discussion will include (with related keywords):

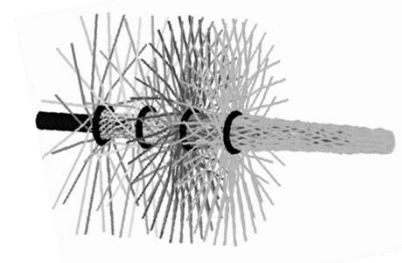
- Airbag related subjects (\*AIRBAG\_OPTION, \*AIRBAG\_PARTICLE)
- Blast simulation (\*PARTICLE\_BLAST)
- Various contact options (\*CONTACT\_ERODING\_... , MORTAR, WEAR, etc.)
- Connection techniques (\*CONSTRAINED\_JOINT, \*CONSTRAINED\_SPR2, etc.)
- Frequency domain solvers (\*FREQUENCY\_DOMAIN\_...)
- Element technologies (\*ELEMENT\_BEAM\_SOURCE, \*ELEMENT\_DISCRETE, etc.)
- Isogeometric analysis (\*ELEMENT\_SHELL\_NURBS\_PATCH)
- Forming related features (\*CONTROL\_FORMING, \*ELEMENT\_LANCING, etc.)
- Implicit analysis (\*CONTROL\_IMPLICIT\_ROTATIONAL\_DYNAMICS, etc.)
- Material models (\*MAT\_034, \*MAT\_058, \*MAT\_157, \*MAT\_244, \*MAT\_249, etc.)
- MPP, Miscellaneous, Bug fixes



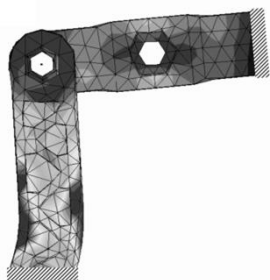
Airbag inflation



Sound pressure distribution



Braiding process



Pre-stressing of joints



Pre-preg forming



Rotordynamics

# LS-TaSC™ Product Status

Katharina Witowski<sup>1</sup>, Willem Roux<sup>2</sup>

<sup>1</sup>DYNAmore GmbH

<sup>2</sup>Livermore Software Technology Corporation

## 1 Introduction

The latest innovation in LS-TaSC is the multi-point scheme which is for the constrained topology design of highly nonlinear structures. These highly nonlinear structures are designed for multiple load cases and multiple constraints, which means that the final design should have load paths for each load case as well as satisfy the constraints. This is done here by using two sets of variables: the local variables describing the part topology on the element level and the global variables consisting of the load case weights and part masses.

## 2 Multi-point constrained topology optimization

The design variables are considered in two groups and the best design process is used for each group. The variables are partitioned into:

- The **local variables**  $\mathbf{x}$ . These are the classical topology variables describing the layout or local design of the structure; for example, the amount of material in an element. These variables therefore describe the load paths in the structure.
- The **global variables**  $\xi$ . These describe a global quantity such as the mass fraction of a part, or a load case weight. These global variables are set to satisfy the constraints, and the derivatives of the constraints with respect to the global variables are computed using a multipoint method such as finite differences or metamodels.

If the global variables are chosen such that  $\mathbf{x} = \mathbf{x}(\xi)$ , then the relationship between a response  $R$  and the variables can be written as

$$R = R(\mathbf{x}(\xi))$$

which allows the numerical computation of the derivative of  $R$  with respect to  $\xi$ .

There are two optimization problems: one for the global variables and one considering the local variables. The optimization problem considering only the global variables  $\xi$  can be written as:

$$\min_{\xi} f(\xi) \text{ with } \xi = (M_1, \dots, M_p, w_1, \dots, w_L),$$

subject to

$$g_i(\xi) < 0 \text{ with } i = 1, \dots, m$$

$$\xi_i^L \leq \xi_i \leq \xi_i^U$$

with  $\xi$  the global variables bounded by  $\xi^L$  and  $\xi^U$ ,  $M$  the part mass fractions for  $p$  parts,  $w$  the load case weights for  $L$  load cases, and  $f$  and  $g$  the objective function and constraints respectively.

The optimization problem considering the local variables  $\mathbf{x}$ , for each design part, is solved using the existing methodology.

## 3 Multi-disciplinary example problem

The structure as shown in **Fehler! Verweisquelle konnte nicht gefunden werden.** is subject to an impact and two linear load cases as well as required to be symmetric around the XY and ZX planes. The objective is the minimum mass of the structure, while the load cases and constraints are:

1. *Impact* An impactor hits the structure as shown in the Fig. 1 with a constraints of

$$\text{Reaction force}_{\text{impact}} \leq 200e6$$

$$\text{Energy absorbed}_{\text{impact}} \leq 11.2e6.$$

2. *Bending* A linear analysis of the bending load as shown in Fig. 1 with a constraint of

$$\text{Displacement}_{\text{bending}} \leq 0.3125.$$

3. *Torsion* A linear analysis of a torsion load as shown in Fig. 1 with a constraint of

$$\text{Displacement}_{\text{torsion}} \leq 0.075.$$

Note that the reaction force constraint conflicts with the displacement constraints, because the one needs a compliant structure and the other a stiff structure.

The problem has three global design variables: the part mass fraction, the crash load case weight, and the torsion load case weight. Using central differences to compute the derivatives with respect to the global variables, six variations of the design must be analyzed per load case, resulting in twenty-one FEA analyses per design iteration.

The final design is shown in **Fehler! Verweisquelle konnte nicht gefunden werden..**

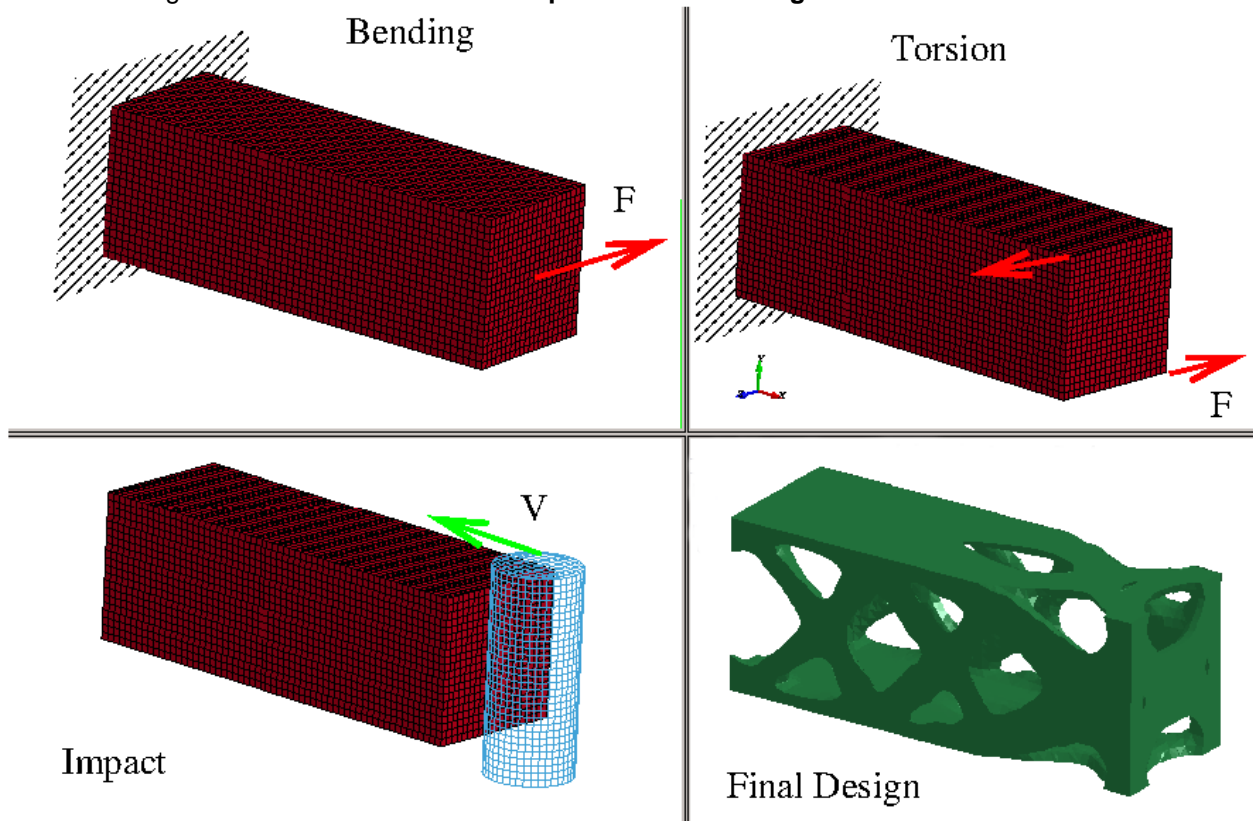


Fig.1: Three load cases together with the final design

#### 4 Summary

The results are encouraging for the constrained topology design of structures for which analytical design sensitivity information is not available.

Numerical derivatives of the constraints with respect to the global variables can be computed. These were used to construct approximations used together with mathematical programming to satisfy the constraints.

The methodology has the advantage of allowing general constraints – a constraint can depend on different parts and load case weights, or the constraint can be a complex computation of results extracted from the FEA analysis.

It should be noted that the results are for a relatively recent and growing method with only two years of research and development completed. With time the results should improve.

#### 5 Literature

[1] Roux, W.: "The LS-TaSC™ Multipoint Method for Constrained Topology Optimization", 14<sup>th</sup> International LS-DYNA Users Conference, Dearborn MI, 2016

# Finding the best thickness run parameterization for optimization of Tailor Rolled Blanks

Niklas Klinke<sup>1</sup>, Axel Schumacher<sup>2</sup>

<sup>1</sup> Mubea Tailor Rolled Blanks GmbH, TRB Product Development, P.O. Box 472, D-57428 Attendorn, Germany, niklas.klinke@mubea.com, +49 (0)2722 62 6170

<sup>2</sup> University of Wuppertal, Faculty 7, Chair for optimization of mechanical structures, Gaußstraße 20, D-42119 Wuppertal, Germany, schumacher@uni-wuppertal.de, +49 (0)202 439 2386

## 1 Introduction

Typical Body in White (BiW) parts are subjected to numerous loadcases from different disciplines (Crash, NVH, and Durability). In combination with several design boundaries like design spaces, manufacturability and cost, the resulting parts mostly show inhomogeneous material utilization. Together with the interest in reducing CO<sub>2</sub> emissions by saving weight in structural parts tailored blank technologies help to increase material utilization and therefore reducing part masses [1].

Tailor Rolled Blanks (TRB) are an established lightweight application for highly stressed structural parts in automotive industry. By varying the rolling gap, parts with load adapted thickness profiles and continuous transitions are manufactured (Fig.1). Typical benefits of using TRB are weight reduction, part integration or fine tuning of performance. Different to other tailored blank technologies the number of different thicknesses in a part does not drive the part cost. Compared to Tailor Welded Blanks (TWB) the stress distribution in transition areas doesn't show any inconstancy due to the sudden increase in thickness. Also it was shown that TRB has good forming characteristics because of the removal of the weld seam and the heat affected zone [2]. The rolling process itself is subjected to several manufacturing constraints like the maximal thickness reduction or the maximal slope which have to be taken into account in the design optimization.

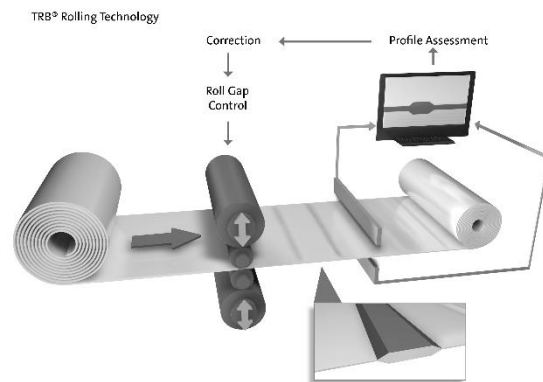


Fig.1: Flexible Rolling

In order to design the thickness run and efficiently find lightweight potentials optimization techniques are used. The publications [3] and [4] show the potential of TRB for BiW application by using optimization techniques. Different parametrization approaches were used to control the part thickness distribution. The question arising here is: What is the best thickness run parameterization for a given problem? Therefore, we compare different parametrization approaches.

The optimization problem is formulated for the use in typical automotive development processes. LS-OPT is used for metamodel-based optimization of a hotformed sheet metal profile subjected to different dynamic bending loadcases. Radial Basis Functions (RBF) are used as metamodels in conjunction with adaptive simulated annealing (ASA) as optimization algorithm. Results are compared on behalf of performance, mass and function calls. As a result we present recommendations for the best thickness run parametrization.

## 2 Approach

Since the parametrizations used in literature can roughly be separated in those with fixed plateau boundaries (FPB) and moving plateau boundaries (MPB), we want to compare those with different number of thickness areas. Since both parametrizations have different dependency on the number of thickness variables, only parametrization with the same number of design variables (4, 7 and 10) are compared.

A sequential metamodel-based optimization scheme is used in conjunction with a reduction of the sampling domain (SRSM).  $1.5(n + 1) + 1$  design points are added sequentially in each iteration by space filling sampling. Since the location of the sampling points is depending on a random number generator, the resulting metamodel might be significantly different in the early stages. The SRSM

subdomain is depending on the predicted optimum on the specific Metamodel, hence it can be shown that the whole optimization evolution is strongly depending on the random number seed. To reduce the influence on the results, every optimization is done ten times with different seed values.

### 3 Application example

A hotformed w-profile of 1000 x 165 x 35 mm dimensions is analyzed in a dynamic three point bending loadcase. A cylindrical rigid impactor with 150 mm diameter, weighting 180 kg is dropped with 20 km/h in the middle of the profile. At the ends the part is laying on two fixed cylindrical rigid walls. Gravity is applied to the whole model.

Initial design is a 2 mm constant thickness part with weight of 3.75 kg. The functional constraint is derived from the maximum impactor displacement of this design (approx. 100 mm).

The Optimization task can be formulated as follows:

$\min_{mass}$ ,  $d_{impactor} \leq 100 \text{ mm}$ . As a restriction the thickness run is set to be symmetric.

Fig.3 and Fig.4 show the results of two optimization with 7 design variables.

It can be shown that both parametrization types lead to a comparable weight reduction of approx. 26 % (0.975 kg). The MPB parametrizations show a slightly higher weight reduction of 1 % but at a significantly higher number of runs (up to 3 times as many).

MPB parametrization is recommended to be used for applications where the number of plateaus and their approximate position is known a priori. This could be due to a specific loadcase setup, design constraints or a sufficient number of previous iterations done by an engineer.

If the number of plateaus is unknown or subjected to change the FPB parametrization is more useful because different thickness run scenarios could be evaluated. Also the number of function calls needed to end up at a converged optimum is lower.

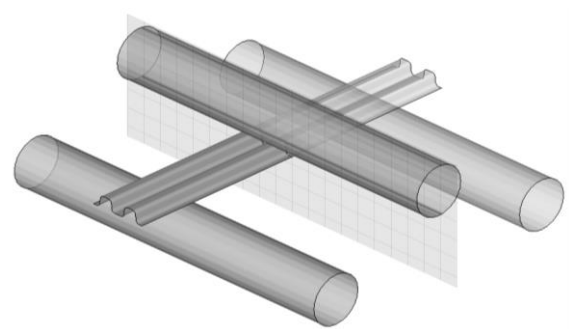


Fig.2: Loadcase setup (A) with symmetry plane at  $x = 0 \text{ mm}$

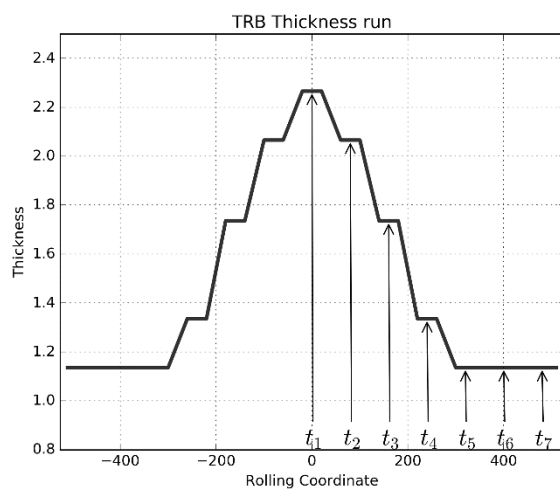


Fig.3: Fixed plateau boundaries (FPB) parametrization with 7 design variables (7 thicknesses)

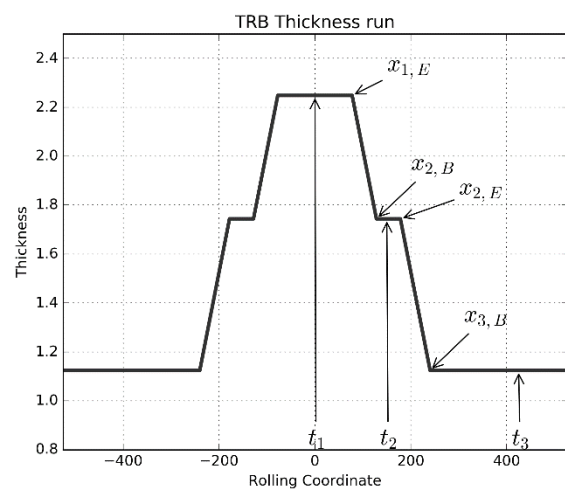


Fig.4: Moving plateau boundaries (MPB) parametrization with 7 design variables (3 thicknesses and 4 positions)

### 4 References

- [1] M. Merklein, M. Lechner, Manufacturing Flexibilisation of Metal Forming Components by Tailored Blanks, 2013.
- [2] R. Kopp, C. Wiedner, A. Meyer, Flexible rolling for load adapted blank, International Sheet Metal Review, (4) (2005) 20–24.
- [3] C.H. Chuang, R.J. Yang, G. Li, K. Mallela, P. Pothuraju, Multidisciplinary design optimization on vehicle tailor rolled blank design, Struct Multidisc Optim 35 (6) (2007) 551–560.
- [4] L. Duan, G. Sun, J. Cui, T. Chen, A. Cheng, G. Li, Crashworthiness design of vehicle structure with tailor rolled blank, Struct Multidisc Optim 53 (2) (2016) 321–338.



# Automated Generation of Robustness Knowledge for selected Crash Structures

Constantin Diez<sup>1</sup>, Christian Wieser<sup>1</sup>, Lothar Harzheim<sup>1</sup>, Axel Schumacher<sup>2</sup>

<sup>1</sup>Adam Opel AG

<sup>2</sup>University of Wuppertal

## 1 Introduction

Maintaining or even improving vehicle safety whilst vehicle mass is reduced and safety regulations are tightened is a key challenge in vehicle design. Mastering scatter of material properties, manufacturing tolerances and load condition variations requires sophisticated robustness analysis, in order to gain knowledge about the behavior of the car under typical uncertainties. In order to condensate the knowledge in the crash simulation data much better than just doing casual statistics, advanced pattern recognition techniques are needed.

Uncertainties are usually modeled with probabilistic distributions, which are then used in a robustness analysis. The most common first step is to observe the scatter of the critical responses and check whether an unacceptable violation occurred. In case of a violation, it can be very difficult and time demanding to find the causes for the violation due to high nonlinearity, bifurcations and concatenation of effects. Even though humans are having extremely flexible pattern recognition capabilities in combination with the usage of previous knowledge, the mind itself still struggles with recognizing patterns within large amounts of data, namely "Big-Data".

In order to face these challenges, a new knowledge generating approach was developed. This process is outlined in Figure 1 and comprises geometric model reduction, results mapping, similarity calculation and finally knowledge generation through visualization, outlier detection, clustering and cluster importance ranking.

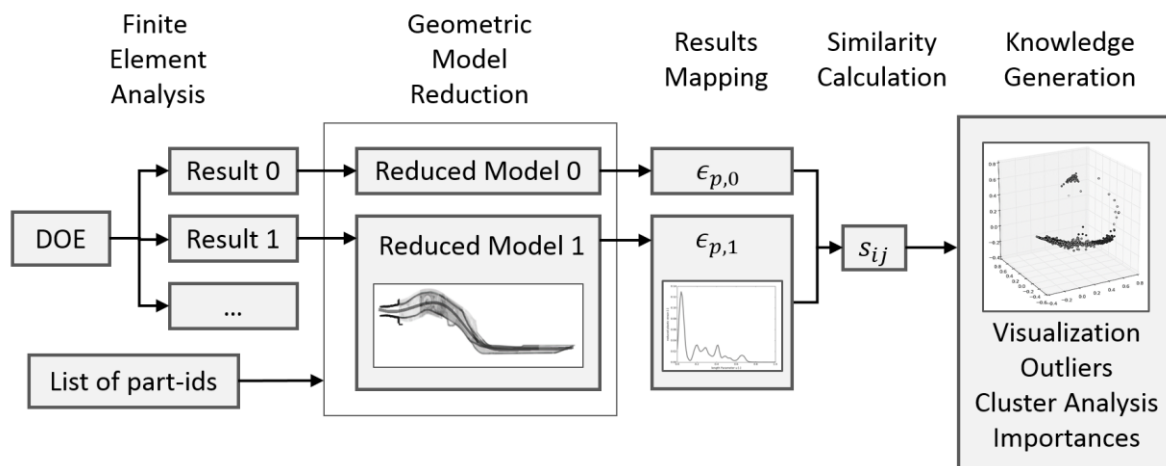


Fig. 1: Proposed process flow

## 2 Data Reduction and Knowledge Generation

The first step in the process flow of Figure 1, after the Finite Element Analysis (FEA), is a geometric model reduction. Various techniques have been proposed [1-3,7], but these are either computationally expensive, need to be adjusted to the specific problem or need recalculation if new data is added. To mitigate these disadvantages, an own technique for geometric model reduction was developed, which simplifies a selected group of parts to either a 1D line or 2D plane, which generically reflect beam or sheet structures in technical applications (see Figure 1). The line or plane is fitted to the geometry with a parametric Bézier-Polynomial.

Thereafter the results of the individual FEA runs, such as plastic strain, are mapped to the reduced geometry. The equivalent plastic strain was chosen as it describes large deformations well. Since the

mapping is done with a smoothing kernel, the result is a continuous function of reduced plastic strain along the parametric coordinates of the reduced model geometry (Figure 1).

In the next step, the similarity of two individual FEA runs represented by the above functions of reduced plastic strain needs to be quantified. The metric  $\langle \cdot | \cdot \rangle$  for calculating the similarity  $s_{ij}$  between two functions of reduced plastic strain is the dot product for continuous functions [6]

$$s_{ij} = \frac{\langle \mathcal{F}_i | \mathcal{F}_j \rangle}{\sqrt{\langle \mathcal{F}_i | \mathcal{F}_i \rangle \langle \mathcal{F}_j | \mathcal{F}_j \rangle}} \quad (1)$$

Since the comparison is computationally cheap, it can be applied to all runs of the robustness study, resulting in a symmetric similarity matrix, which contains the similarities of all runs to each other.

Finally the knowledge intrinsically hidden/embedded in the data needs to be extracted. For data visualization and cluster analysis, the similarity matrix is fed to machine learning algorithms. Visualization of the similarities enables recognizing patterns in the data, such as clusters of similar behavior, and hence enables the extraction of the underlying knowledge. The non-geometrical nature of the similarity data requires lower dimensional embedding techniques [4,5] to generate plots (see Fig. 1). Here Multidimensional Scaling (MDS) was used. Outlier detection in order to find statistically conspicuous samples, and cluster analysis to find groups of similar behavior has been implemented as well. The clustering is hierarchical, so that finer substructures may be analyzed too. The association of a simulation sample with clusters represents knowledge and is saved in a knowledge database.

Eventually, importance ranking of parameters, realized by decision tree algorithms [8], and association with individual clusters allows for identifying sensitive parameters with regard to cluster occurrence. Parameters responsible for generating undesired clusters may represent sensitive knobs to turn, in order to make a specific design robust to input variations.

### 3 Outlook

An important bottleneck for meaningful statistical analysis is the large number of samples. This is particularly true for the huge computational effort for full vehicle crash simulations. Hence, knowledge derived from previous studies by the above process needs to be utilized such that future DOEs can be set-up smartly with less required samples. Furthermore, importance ranking may enable automatic solution proposals as a next step. Lastly a modification of the process may enhance the segmentation of different bending directions, which cannot be treated easily with plastic strain.

### 4 Literature

- [1] Reuter, M: "Laplace–Beltrami spectra as ‘Shape-DNA’ of surfaces and solids", Computer-Aided Design 38, 2006, 342-366
- [2] Mitra, N: "Algorithms for Comparing and Analyzing 3D Geometry", PhD Thesis Stanford University, 2006
- [3] Teran, R: "Enabling the Analysis of Finite Element Simulation Bundles", International Journal for Uncertainty Quantification 4, 2014, 95-110
- [4] Borg, I: "Modern Multidimensional Scaling – Theory and Application", Springer Series in Statistics, 1997
- [5] van der Maaten, L: "Visualizing Data using t-SNE", Journal of Machine Learning Research 9, 2008, 2579-2605
- [6] Kimmerle, W: "Lineare Algebra fuer Ingenieure, Mathematiker und Physiker", edition delkhofen verlag, 2007
- [7] Thole, C-A: "Advanced Mode Analysis for Crash Simulation Results", 9. LS-DYNA Forum Bamberg, 2010
- [8] Criminisi, A: "Decision Forests: A Unified Framework for Classification, Regression, Density Estimation, Manifold Learning and Semi-Supervised Learning", Foundations and Trends in Computer Graphics and Vision 7, 2011, 81-227

---

# Process to improve optimization with combined robustness analysis results

Lennart Jansen, Dominik Borsotto, Clemens-August Thole

SIDACT GmbH

## 1 Introduction

Today's engineers are facing the challenge of creating both robust and optimized solutions to fulfil a variety of requirements. While being able to create designs that can handle parameter variability and still produce predictable results, the models also need to be optimized with respect to lower production and development costs.

Thus following the growing demand to create robust and optimized solutions, new processes and techniques are needed allowing engineers to improve their CAE models. Not only to speed up the development process but also to improve the quality of the model.

## 2 Process

To manage the above mentioned challenge a new process is introduced creating a direct link from a Principal Component Analysis (PCA) driven robustness analysis towards an LS-OPT driven metamodel-based optimization.

### 2.1 PCA - based robustness analysis

Based on a set of simulation runs a PCA based robustness analysis is performed, revealing the dominating deformation modes. These represent the most important events regarding result variation in the dataset [1]. Being able to compute these modes now allows us to use them as an input parameter for the metamodel-based optimization. As the modes represent deformation behaviour, they contain valuable information that can be transferred to the metamodel either as an objective, a constraint or as an argument. Based on this there are different levels of improvement for the metamodel.

### 2.2 Metamodel - based optimization

The LS-OPT metamodel-based optimization can now be initialized with the PCA results. Thus incorporating the PCA results, the objectives and constraints are:

- Maximizing the distance between firewall and seat (based on node distance)
- Minimizing the sum of thicknesses (constraint: keeping single thicknesses above a certain threshold)
- Restricting the firewall deformation mode towards a certain preferred crash deformation shape

Due to the incorporation of PCA results it is shown that a mode can be an adequate replacement of the node distance objective. Additionally the metamodel including PCA modes shows an improvement of the quality/accuracy compared to the standard metamodel without taking PCA modes into account. The metamodel accuracy comparison can be seen in Fig. 1 and Fig 2.

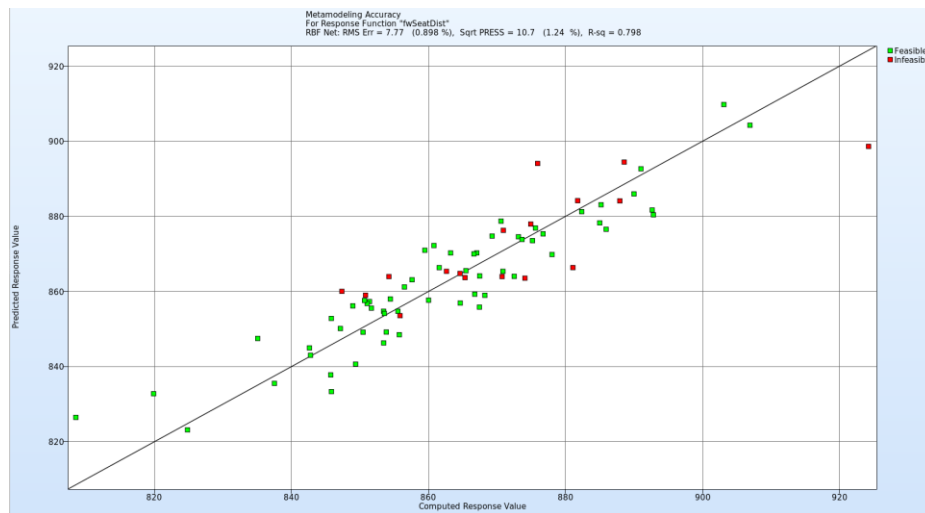


Fig.1: Accuracy of the standard metamodel

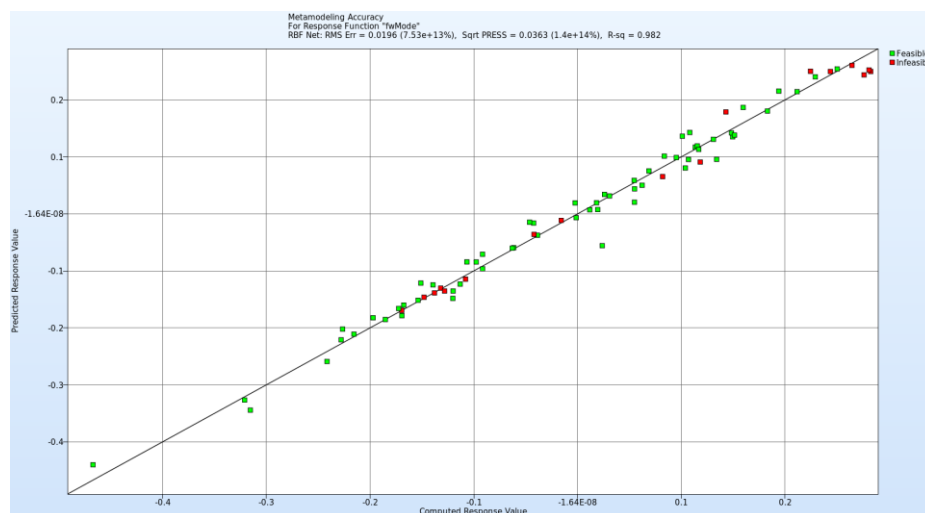


Fig.2: Accuracy of the PCA mode improved metamodel

### 3 Example case

For illustration the publicly available Chevrolet Silverado model from the NCAC is analyzed by means of robust design and optimization of the crash model. Therefore 77 simulation runs were performed based on random thickness variations of 12 parts and analyzed with the above mentioned methods.

### 4 Summary

To manage the challenge of creating robust and optimized models a new process is introduced creating a direct link from a Principal Component Analysis (PCA) driven robustness analysis towards an LS-OPT driven metamodel-based optimization. It is shown that the results of the robustness analysis can be directly fed into the optimization task to improve both the quality of the metamodel as well as the therewith calculated optimization results.

### 5 Literature

- [1] Thole C.A., Nikitina Lialia, Nikitin Igor, Clees T.: “Advanced Mode Analysis for Crash Simulation Results”, 9. LS-DYNA Forum, Bamberg, 2010

# Temperature dependent TAPO model for failure analysis of adhesively bonded joints due to temperature induced service loading

Patrick Kühlmeyer<sup>1</sup>, Anton Matzenmiller<sup>1</sup>

<sup>1</sup>Institute of Mechanics, Department of Mechanical Engineering, University of Kassel, Mönchebergstr. 7, 34125 Kassel, Germany

## 1 Introduction

The Toughened Adhesive Polymer (TAPO) material model is available in LS-DYNA with the keyword **\*MAT\_TOUGHENED\_ADHESIVE\_POLYMER (\*MAT\_252)** since the revision R7.1.1. It describes the mechanical behaviour of crash optimised high-strength adhesives under crash conditions by taking elasticity, viscoplasticity and damage due to plastic deformation into account—see [1,2]. Here, the model is implemented for a solid element into LS-DYNA and can be used for the cohesive elements (19) and (20) in **\*SECTION\_SOLID** with the option **\*MAT\_ADD\_COHESIVE**. Also, the equations of the TAPO model are reduced to the interface theory in [2]. In this contribution, the reduced TAPO model in [2] is extended by temperature dependent viscoelasticity, plasticity and damage considering rate and temperature effects below and beyond the yield strength. Here, the focus of the material model is to predict failure of joints, which are bonded with ductile-modified adhesives and subjected to service loading with low strain rates due to temperature changes. The equations of the extended TAPO model are implemented into LS-DYNA as a “user defined cohesive model” for the eight node cohesive elements (19) and (20) in **\*SECTION\_SOLID** assuming a thin adhesive layer between the adherends [3]. Thus, the local interface traction  $\mathbf{t}$  is described as a functional of the local separation vector  $\mathbf{\Delta}$ .

## 2 Thermo-viscoelastic-plastic model with damage

For the thermo-viscoelastic extension of the TAPO model, a generalised MAXWELL model and a thermal element are arranged in series—see Fig. 1. Thus, the separation  $\mathbf{\Delta}$  is additively decomposed into a viscoelastic  $\mathbf{\Delta}^{ve}$ , a plastic  $\mathbf{\Delta}^{pl}$ , and a thermal part  $\mathbf{\Delta}^{th}$ —see Fig. 1. The temperature dependency of the relaxation times  $\hat{\tau}_i^{n,s}$  of the MAXWELL chains is taken into account with the reduced time  $\xi$ , which depends on the shift function  $a_T(\theta(t))$  and the temperature  $\theta(t)$  in the theory of thermorheologically simple materials. The relaxation functions in the convolution integral are DIRICHLET-PRONY series in normal and tangential direction:

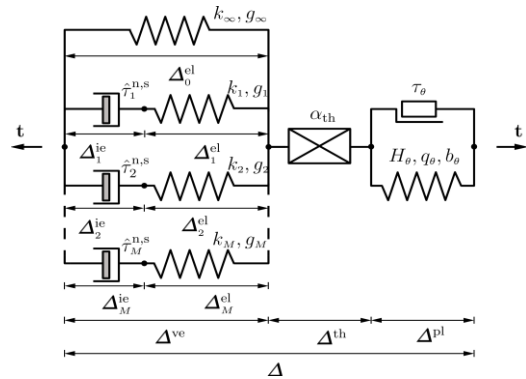


Fig.1: Rheological network of the model

$$\begin{pmatrix} t_n \\ t_t \\ t_b \end{pmatrix} = \int_{-\infty}^{\xi(t)} \begin{bmatrix} R_n(\theta_0, \xi(t)-\tau) & 0 & 0 \\ 0 & R_s(\theta_0, \xi(t)-\tau) & 0 \\ 0 & 0 & R_s(\theta_0, \xi(t)-\tau) \end{bmatrix} \frac{d(\mathbf{\Delta} - \mathbf{\Delta}^{th} - \mathbf{\Delta}^{pl})}{d\tau} d\tau \quad (1)$$

Furthermore, the yield stress  $\tau_\theta$ , the parameters of the nonlinear isotropic hardening stress  $H_\theta, q_\theta, b_\theta$ , and the critical and failure strain in the damage approach of the TAPO model [1,2] are empirical functions of the temperature  $\theta$ . The thermo-viscoelastic integral (1) is numerically integrated using a recursive algorithm and solved with the equations of plasticity by a predictor corrector scheme [3].

## 3 Parameter identification, model verification and validation

The parameters are inversely identified by fitting the model response to the related test data of the thick adherend shear specimen (TASS) and the butt joint specimen (BJS) by means of the optimisation program LS-OPT—see Fig. 2 a) and b). For the validation, a bimetallic specimen is tested, which

consists of a steel and an aluminium sheet bonded with a ductile-modified structural adhesive. The test provides the deflection at the tip due to temperature loading, which is compared to the result of the related FE simulation. In the FE model, both sheets are spatially discretised by means of the enhanced solid element (-2) in `*SECTION_SOLID` and characterised by `*MAT_001` as well as `*MAT_ADD_THERMAL_EXPANSION`. The adhesive between the sheets is discretised using the cohesive element (19) in `*SECTION_SOLID` and is described by the extended TAPO model with `*MAT_USER_DEFINED_MATERIAL_MODELS`. For the FE simulation of the bimetallic specimen, the mean of the experimental temperature-time course is prescribed to the nodes using `*LOAD_THERMAL_LOAD_CURVE`. The deflection at the tip  $u_z$  of the FE simulation is compared to the test data in Fig. 2 c). As a result, the FE simulation is in good agreement with the measured test data.

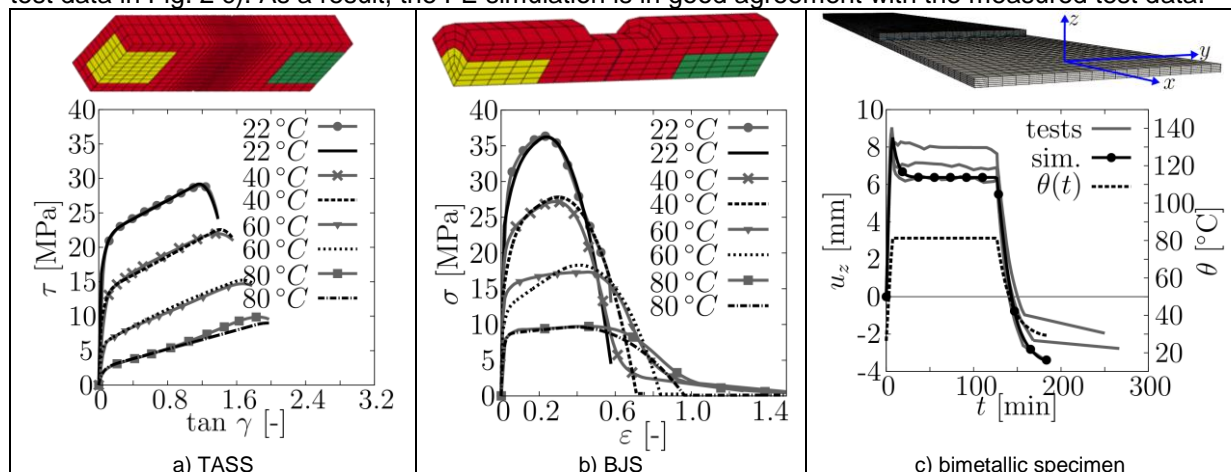


Fig.2: Comparison of test data (symbols) and FE simulation (dotted/dashed lines) of TASS a) and BJS b) with the identified material parameters. Validation of deflection at tip of the bimetallic specimen by means of FE simulation and test data c)—see [3,4]

#### 4 Summary

The reduced TAPO model in [2] is extended with a thermo-viscoelastic model and functions of temperature for the isotropic hardening as well as for the ductile damage approach. Further, the implementation of the constitutive equations into LS-DYNA is verified with the test data of the TASS and the BJS and is validated with the bimetallic specimen for a temperature induced mechanical deformation.

#### 5 Acknowledgements

We thankfully acknowledge financial support of the Federal Ministry for Economic Affairs and Energy through the AiF (Arbeitsgemeinschaft industrieller Forschungsvereinigungen "Otto von Guericke" e.V.) by grant P 878 / 369 ZN of the Forschungsvereinigung Stahlanwendung e. V.

#### 6 References

- [1] Brede, M. and Hesebeck, O. (Eds.): *Robustness and reliability of methods to simulate adhesive joints with high strength steel sheets at crash conditions*. Report of project P 828, Forschungsvereinigung Stahlanwendung e. V. (FOSTA), Sohnstr. 65, 40237 Düsseldorf, in press<sup>1)</sup>
- [2] Burbulla, F.: *Kontinuumsmechanische und bruchmechanische Modelle für Werkstoffverbunde*, PhD thesis, Berichte des Instituts für Mechanik 2/2015, Department of Mechanical Engineering, Institute of Mechanics, Department of Numerical Mechanics, University of Kassel, 2015
- [3] Kühlmeyer, P. and Matzenmiller, A.: *Materialmodell zur Abbildung der Klebschichteigenschaften unter Betriebslasten*. In: *Development of methods for simulation and evaluation of damage in adhesive layers due to thermal cyclic loadings during manufacturing and operation*. Report of project P 878, Forschungsvereinigung Stahlanwendung e. V. (FOSTA), Sohnstr. 65, 40237 Düsseldorf, in press<sup>1)</sup>
- [4] Kühlmeyer, P. and Matzenmiller, A.: *Validierung der konstitutiven Gleichungen an der Bi-Metall-Probe unter Betriebsbelastung*. In: *Development of methods for simulation and evaluation of damage in adhesive layers due to thermal cyclic loadings during manufacturing and operation*. Report of project P 878, Forschungsvereinigung Stahlanwendung e. V. (FOSTA), Sohnstr.65, 40237 Düsseldorf, in press<sup>1)</sup>

<sup>1)</sup> Download author-created reports of the Institute of Mechanics, University of Kassel at: [www.uni-kassel.de/maschinenbau/institute/mechanik/fachgebiete/numerische-mechanik/publikationen.html](http://www.uni-kassel.de/maschinenbau/institute/mechanik/fachgebiete/numerische-mechanik/publikationen.html)

# Charakterisierungsversuche und Parameterbestimmung für die Kohäsivzonenmodellierung von Polyurethan-Kleberverbindungen

Marcel Brodbeck<sup>1</sup>, Sebastian P. Sikora<sup>2</sup>

<sup>1</sup>Deutsches Zentrum für Luft- und Raumfahrt (DLR), Institut für Bauweisen und Strukturtechnologie

<sup>2</sup>Deutsches Zentrum für Luft- und Raumfahrt (DLR), Institut für Fahrzeugkonzepte

## 1 Einleitung

Im Automobil-Leichtbau werden neben epoxidharzbasierten (EP) Klebstoffen verstärkt auch polyurethanbasierte (PU) Klebstoffe für die Verbindung struktureller Komponenten eingesetzt. Besonders für die Multi-Material-Bauweise, bei der Werkstoffe mit unterschiedlichen Wärmeausdehnungen eingesetzt werden, ist die größere Nachgiebigkeit der PU-Klebstoffe von Vorteil. In der Crashtestsimulation größerer Strukturen wird das Materialverhalten der EP-Klebstoffe aufgrund ihrer Effizienz hinsichtlich Rechenzeit bevorzugt mit sogenannten „Kohäsivzonenmodellen“ abgebildet. Die Klebung wird hierbei als bruchmechanische Ersatzmodellierung mit einem Element in Dickenrichtung modelliert. Im Rahmen des DLR-Projektes „Next Generation Car“ werden Modellierungsansätze für verschiedenartige Klebstoffsysteme untersucht. Die zunehmende Bedeutung der PU-Klebstoffe für strukturell relevante Komponenten erfordert es, PU-Klebstoffe hinsichtlich ihres Crashverhaltens zu charakterisieren und in der Verbindung zu modellieren.

## 2 PU-Charakterisierung

Der zugrunde liegende Ansatz ist, zu untersuchen, inwieweit eine Simulationsmethodik mittels Kohäsivzonenmodellierung und die korrespondierenden Methoden zur Kennwertermittlung von EP-Klebstoffen auf PU-Klebstoffe übertragen werden können.

### 2.1 Modellierungsansatz „Kohäsivzonenelemente“

Für die Kohäsivzonenmodellierung in LS-DYNA wurde u.a. das Materialmodell „cohesive mixed mode elastoplastic rate“ (MAT\_240) entwickelt [1]. Dieses energiebasierte Materialmodell berücksichtigt die Dehnratenabhängigkeit der Bruchenergie und der Fließspannung. Bei MAT\_240 wird zwischen den beiden bruchmechanischen Belastungsrichtungen Mode-I (Schälzug) und Mode-II (Scherzug) unterschieden. Zur Gewinnung von Materialparametern für MAT\_240 sind neben Dichte, Elastizitätsmodul und Schubmodul die Energiefreisetzungsrate  $G_{IC}$  (für Mode-I) und  $G_{IIC}$  (für Mode-II) sowie die Versagensspannungen  $\sigma_I$  und  $\sigma_{II}$  zu ermitteln. MAT\_240 wurde insbesondere für zähmodifizierte Klebstoffe mit dünner Klebschicht entwickelt. Die modellseitige Einstellbarkeit des Spannungs-Verformungsverlaufs ermöglicht es zudem, das Versagenverhalten elastischer Klebungen mit dicker Klebschicht, wie z.B. PU-Klebstoffe, abzubilden.

### 2.2 Versuche zur Parameteridentifikation

Anhand eines ausgewählten PU-Klebstoffs wurde untersucht, welche Versuche zur Charakterisierung von EP-Klebstoffen aus [2] und [3] auf PU-Klebstoffe übertragen werden können und welche Prüfkörper bzw. Prüfungen modifiziert oder neu konzipiert werden müssen (Fig. 1).

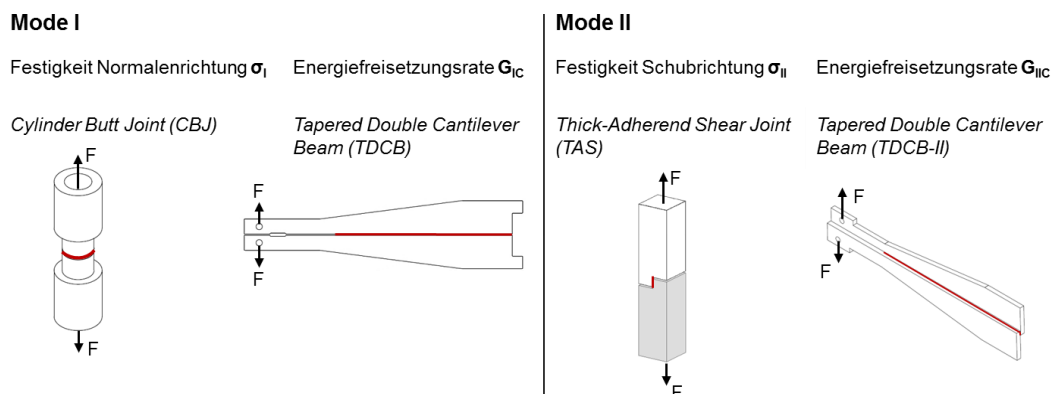


Fig. 1: Charakterisierungsversuche für PU-Klebstoffe (Kohäsivzonenmodell MAT\_240)

Zur Ermittlung der Energiefreisetzungsrate  $G_{IC}$  konnten die sog. TDCB-Versuche (Tapered Double Cantilever Beam) nach dem Vorbild der EP-Klebstoffe mit Anpassungen übernommen werden. Bei der Ermittlung der Energiefreisetzungsrate  $G_{IIc}$  hat sich gezeigt, dass die für EP-Klebstoffe bewährten Versuche nicht für PU-Klebstoffe geeignet sind. Die vergleichsweise großen Schubverformungen, die bis zum vollständigen Versagen der PU-Klebung auftreten, sind nicht mit den vorgesehenen Verformungsgrenzen bekannter Probekörper vereinbar und somit für die Charakterisierung von PU-Klebstoffverbindungen nicht zielführend. Deshalb wurde zur Ermittlung der bruchmechanischen Kennwerte unter Schub eine modifizierte Probengeometrie (TDCB-II) entwickelt und getestet, die die Mode-II-Charakterisierung auf Basis einer Mode-III-Beanspruchung vorsieht. Zur Ermittlung der Versagensspannungen  $\sigma_I$  und  $\sigma_{II}$  wurden der Kopfzugversuch und der einfach überlappte Scherzugversuch (jeweils mit geometrischen Anpassungen) verwendet. Die Versuche zur Materialcharakterisierung wurden bei verschiedenen Belastungsgeschwindigkeiten durchgeführt, wodurch ein dehnratenabhängiges Materialverhalten des PU-Klebstoffs identifiziert werden konnte.

### 3 Simulationsergebnisse

Es wurde ein Parametersatz unter Berücksichtigung der Dehnrateneffekte für MAT\_240 ermittelt, womit das Materialverhalten des untersuchten PU-Klebstoffs für die bruchmechanischen Versuche nachgebildet werden kann. Für die TDCB-Versuche zeigt sich eine gute Übereinstimmung der Kraftweg-Kurven mit den Simulationsergebnissen (Fig. 2 links).

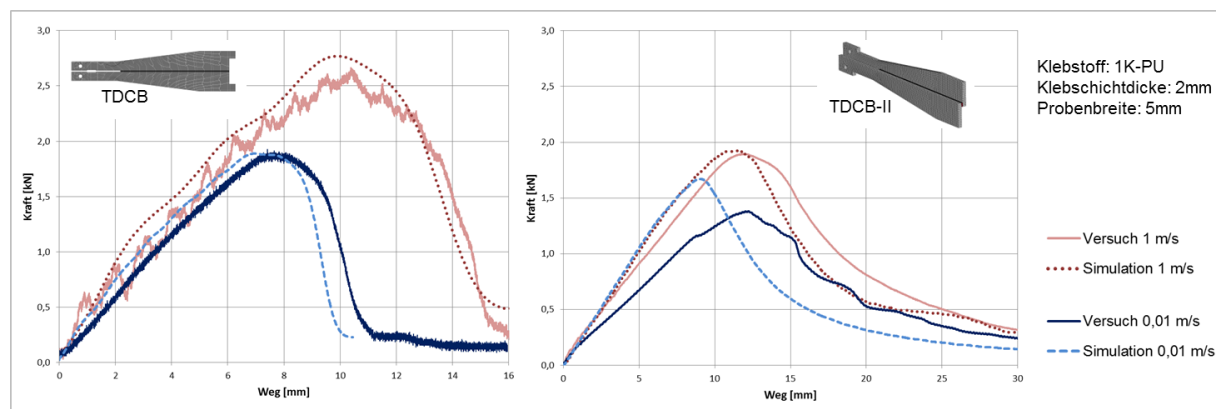


Fig.2: Simulationsverifikation TDCB- (links) und TDCB-II-Versuch (rechts) bei zwei verschiedenen Versuchsgeschwindigkeiten

Für die TDCB-II-Versuche zeigt sich in der Simulation eine steifere Probenantwort als im Experiment (Fig. 2 rechts). Dies könnte darauf zurückzuführen sein, dass in MAT\_240 ein linear elastischer Spannungs-Verschiebungs-Zusammenhang angenommen wird. PU-Klebstoffe verhalten sich jedoch nicht-linear elastisch und zeigen hierbei veränderliche Elastizitäten in Abhängigkeit der Dehnraten.

### 4 Zusammenfassung und Ausblick

Die Untersuchungen zeigen, dass die Kohäsivzonenmodellierung in Form des MAT\_240 neben EP-Klebstoffen auch für PU-basierte Automobil-Klebstoffe und damit auch für Klebungen über eine große Bandbreite mechanischer Eigenschaften berücksichtigt werden kann. Die Simulationsergebnisse für die vorgeschlagenen Mode-II-Versuche zeigen noch Abweichungen. Diese sind zum einen dadurch begründet, dass die Steifigkeiten in MAT\_240 nicht dehnratenabhängig hinterlegt werden können. Zum anderen sind Diskretisierungseinflüsse zu bewerten. Weiter gilt es zu prüfen, wie sich der gewählte Modellierungsansatz unter kombinierter (mixed-mode) Belastung verhält.

### 5 Literatur

- [1] Marzi, S.: "Ein ratenabhängiges, elastoplastisches Kohäsivzonenmodell zur Berechnung struktureller Klebverbindungen unter Crashbeanspruchung", Dissertation, 2010
- [2] Brede, M.: „Methodenentwicklung zur Berechnung von höherfesten Stahlklebverbindungen des Fahrzeugbaus unter Crashbelastung“ Forschungsvorhaben P676, Forschungsvereinigung Stahlanwendung e.V., 2008
- [3] Brede, M.; Hesebeck, O.: „Robustheit und Zuverlässigkeit der Berechnungsmethoden von Klebverbindungen mit hochfesten Stahlblechen unter Crashbedingungen“ Forschungsvorhaben P828, Forschungsvereinigung Stahlanwendung e.V., 2014



# Self-pierce riveting of materials with limited ductility investigated with the Bai-Wierzbicki damage model in GISSMO

Martin Hofmann<sup>1</sup>, Robert Anderssohn<sup>1</sup>, Thomas Wallmersperger<sup>1</sup>, Mathias Jäckel<sup>2</sup>, Dirk Landgrebe<sup>2</sup>

<sup>1</sup>TU Dresden, Institut für Festkörpermechanik

<sup>2</sup>Fraunhofer-Institut für Werkzeugmaschinen und Umformtechnik

## 1 Introduction

The application of mechanical joining techniques is nowadays a common practice in automotive industry. But when self-pierce riveting lightweight materials, such as aluminum die castings, due to the limited ductility cracks in the closing head of the joint can occur. For the numerical optimization of these difficult joining tasks it is necessary to find suitable damage models, which can predict the cracking in the lightweight materials with limited ductility.

## 2 Model

Advanced damage models like the one of Bai and Wierzbicki [1] have been already used for sheet metal forming. They take into account that the strain at damage depends on the stress state itself. The model of Bai and Wierzbicki [1] is based on a Coulomb-Mohr hypothesis in stress space and therefore considers two of the three invariants of the stress tensor. Together with the hardening law, it is possible to describe the effective plastic strain at failure depending on triaxiality  $\eta$  and lode angle  $\theta$ .

The application of their model to self-pierce riveting of material with limited ductility however involves some challenging tasks. Experimental data for the strain at failure from sheet specimen is only available in a small range of triaxiality from shear to biaxial tension. During the joining process a much higher range of triaxiality occurs. For materials with limited ductility it is difficult to measure the strain at failure due to very small localization bands.

The parameters of the damage model were retrieved from notched tensile and notched shear specimen using digital image correlation. Direct evaluation of the failure strain was not possible, since the notched tensile specimens violated the plain stress assumptions. The critical points are located in the bulk material and the triaxiality reaches values up to one, see the calculated strain path of the specimens in Fig.1 left. Therefore a correction had to be done, resulting in the damage surface of Fig.1 right, where the triaxiality dependence is reduced compared to the original data. The damage model is included using the GISSMO option of `*MAT_ADD_EROSION`.

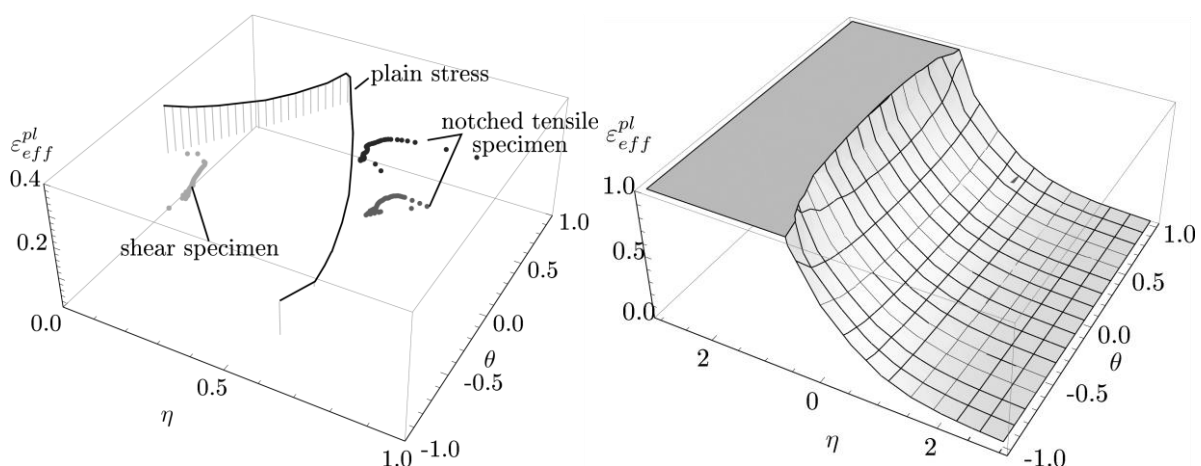


Fig.1: Left: Strain paths of the used shear and notched tension specimens compared to plane stress conditions. Right resulting damage surface (clipped at  $\epsilon_{eff}^{pl} = 1$ ).

### 3 Results

At the considered material combination the aluminum sheet EN AW-6016 T4 ( $t = 2.0$  mm) is positioned punch-sided and the non heat-treated aluminum die casting AISi9Mn F ( $t = 2.0$  mm) is positioned on the die side. In the investigation ball-shaped dies in different die depths  $h_{m1} = 1.0$  mm and  $h_{m2} = 1.5$  mm are considered. Only when using the deeper die geometry cracking in the aluminum die casting was observed. Since the focus was on the occurrence of cracks in the die casting, a geometrical cutting criteria for the upper sheet has been used.

Some problems arise during the simulation. One important is that the element deletion that occurs due to damage can lead to zig-zag boundaries. Subsequent contact of these regions yields either to convergence problems or remeshing failures. Currently these problems preclude complete simulation of the joining process. But at least it is possible to predict, if cracking occurs and determine where the crack starts. This can be seen by the cross sections for the two different ball-shaped die geometries as shown in Fig.2 and Fig.3.

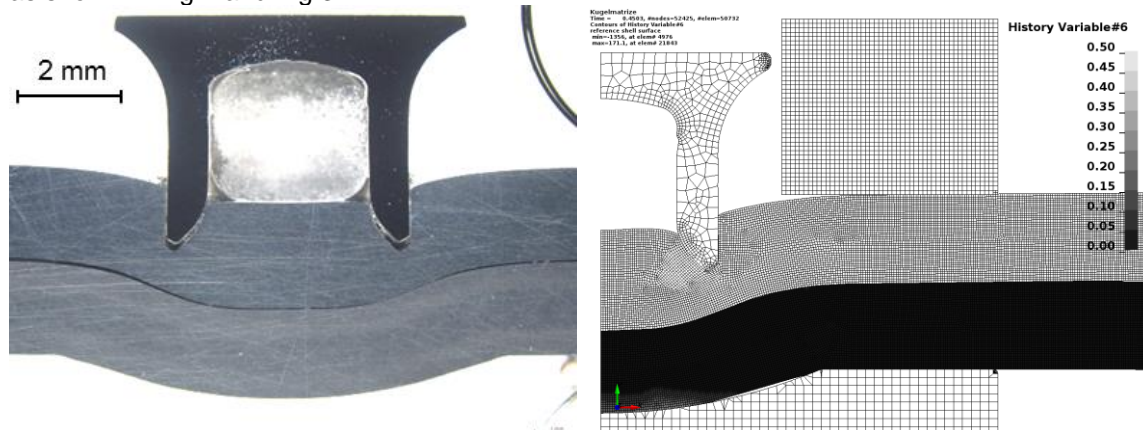


Fig.2: Joint with flat ball-shaped die. Left: Cross section showing no cracks, right: Damage values of the model in the lower sheet with comparable rivet position without crack.

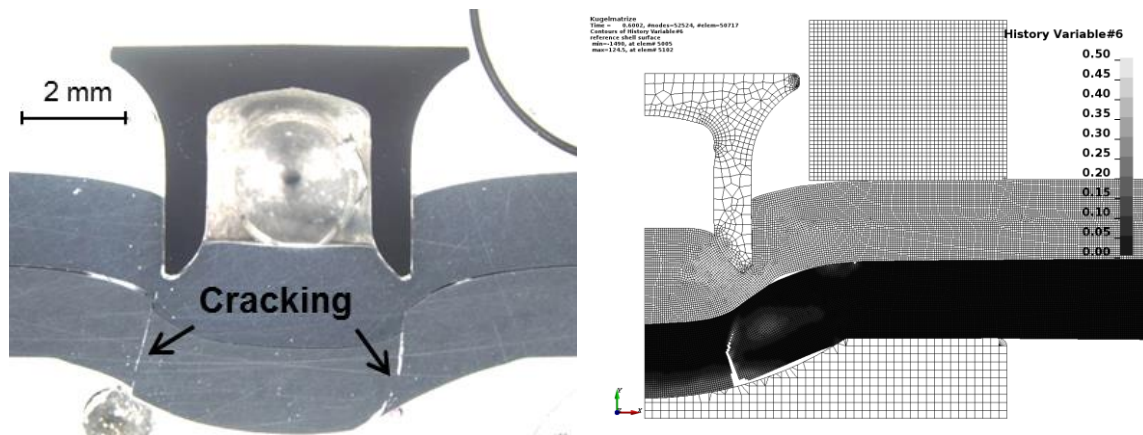


Fig.3: Joint with deep ball-shaped die. Left: Cross section showing radial cracks, right: : Damage values of the model in the lower sheet at error termination with crack at correct position.

### 4 Summary

The advanced damage model of Bai and Wierzbicki [1] has been applied to model self-pierce riveting for aluminum die casting with different die geometries. Currently only start and location of cracking can be predicted. The element deletion due to damage leads to convergence problems resulting from contact or to aborts at remeshing. Therefore further investigations have to be done. Possibly it might be more suitable using other methods than finite elements like smooth particle hydrodynamics (SPH), because there no remeshing will be needed and the blurry boundaries of the particles will reduce convergence problems during contact.

### 5 Literature

[1] Bai, Y.; Wierzbicki, T.: A new model of metal plasticity and fracture with pressure and Lode dependence. *International Journal of Plasticity*, 24, 2008, 1071 – 1096

---

# Prozess- und Zerreis-Simulationen von punktförmigen Verbindungen im Automobilbau unter Berücksichtigung unscharfer Prozess-Parameter

Ingolf Lepenies (SCALE), Alexandru Saharnean (SCALE), Peter Friedrich (SCALE\*)

Thema des Vortrages ist die virtuelle Charakterisierung von punktförmigen Verbindungen am Beispiel von Halbhohlstanzniet- und Clinch-Verbindungen. Der Fügeprozess zur Herstellung der Verbindungen wurde unter Berücksichtigung der Unschärfe einer Vielzahl von Prozess-Parameter aufgebaut. Dazu wurde ein Prozess entwickelt, welcher die Prozessmodelle parametrisch generieren, simulieren und auswerten kann.

Damit sind Sensitivitäts- und Robustheitsanalysen möglich, welche den Einfluss der Geometrien vom Blech, Niet, Matrize, Stempel und Niederhalter sowie Material- und Prozess-Parameter berücksichtigen.

Wesentlicher Bestandteil des entwickelten Prozesses ist die automatisierte Auswertung der Vielzahl an Füge- und Zerreis-Simulationen. Hierzu werden u.a. für jeden Belastungsschritt der Fügesimulation die Konturen der Verbindungssituation automatisiert vermessen. Somit lassen sich nicht nur die charakteristischen Größen (z.B. Hinterschnitt) für die final erzeugte Verbindung angeben, sondern es wird auch die Entwicklung der Verbindungseigenschaften während des Fügens quantitativ ermittelt.

Nach der geometrischen Charakterisierung der Verbindung aus dem Fügeprozess werden mit Zerreis-Simulationen die richtungsabhängigen Verbindungsfestigkeiten unter Berücksichtigung der Materialzustände aus dem Fügeprozess prognostiziert.

Diese Methodik erlaubt z.B. das Bestimmen von Zusammenhängen zwischen Hinterschnitt und der erreichbaren Verbindungsfestigkeiten.

# Simulation des Flugzeuganpralls auf Stahlbetonstrukturen

M. Grosse, R. Schlegel  
Dynardo

H. Friedl  
BKW

---

# Comparing Predicted and Measured Accelerations from a Simple Drop Test Experiment

Rhianne Boag<sup>1</sup>,

<sup>1</sup>International Nuclear Services Ltd

## 1 Abstract

The objective of this paper is to present the results from a series of simple drop test experiments compared with the equivalent Finite Element Analysis (FEA) models. There are several methods of obtaining acceleration-time histories in LS-DYNA. The experiments looked to demonstrate the validity of utilising predicted acceleration-time histories through nodal output, and to understand how comparable the predicted and measured accelerations could be.

## 2 Introduction

Measured accelerations are used in drop testing and crashworthiness to validate FEA models. It is a common practice to utilise accelerations for limits in design calculations. Accelerations of objects are often recorded through accelerometers, but often little is understood about the associated signal processing to determine the accuracy of the data. This work compared the use of accelerations predicted from nodal output to measured accelerations recorded from an attached accelerometer.

In order to simplify the tests, a small section of standard stainless steel 304 pipe was located on a stationary plate, fitted with a load cell, and a rigid cylindrical impactor (OD=150mm, L=1000mm) weighing 140kg was raised to achieve a drop height of 3.88m above the 100mm long sample. An accelerometer was attached to the top of the impactor to produce acceleration-time history data. The tests were reproduced using LS-DYNA R7.1.2 [1] FEA software to extract acceleration-time histories from four nodal outputs in order to compare these with the results from the physical tests.

## 3 Experiment Set-Up

The physical drop tests were performed on a test rig by a contractor. The pipe samples were selected from standard 2½" Schedule 5 pipe. The ends of the pipes were machined to be square to the side of the pipe in a lathe prior to testing. The acceleration of the impactor was measured using a piezoelectric accelerometer attached to the upper free surface that was mounted off-centre to accommodate the hoist attachment.

In the FEA model an initial acceleration representing the equivalent drop height was applied to the impactor. The acceleration-time histories from four nodes around one element face in a similar location to test were recorded using `*DATABASE_HISTORY_NODE` and the output was defined using `*DATABASE_NODOUT`. A sufficient sampling rate had to be chosen to avoid clipping or aliasing the data, which was based upon the minimum timestep of the model.

## 4 Comparison between FEA and physical tests

### 4.1 Time Domain – Elastic Effects

The nodal output for the accelerations was averaged across the four nodes to provide one mean signal. In order to compare the acceleration-time histories from FEA and from test, both signals had to be filtered consistently at 4.7kHz and the FEA acceleration-time history had to be down-sampled from 6MHz to 1MHz to reduce the number of data points and improve filter stability. All signal processing was carried out using HyperMath [2].

Only the magnitude of the first acceleration peak was compared between test and FEA. This was because the oscillations produced by the undamped FEA model are not attenuated as they are in reality. In shock analysis it is common to assume that the first peak occurs so rapidly that damping has

a very small affect. When compared to the FEA signal, the initial peak magnitude predicted in the 2 1/2" Sch5 samples differed by 4.5% (FEA peak 349.1g, test 365.4g), see below in Figure 1.

#### 4.2 Time Domain – Rigid body Effects

In order to compare the rigid body acceleration of the impactor for FEA and test, these accelerations need to be passed through a second low-pass Butterworth filter at 1kHz to remove the elastic effects.

Figure 2 compares the acceleration-time histories for both FEA (solid line) and 2 1/2" Sch5 pipe (dashed line) together to see how closely the predicted filtered accelerations were with the measured filtered accelerations. The curves follow a similar profile, but with the measured filtered acceleration returning to 0g quicker than the FEA filtered acceleration. The initial peaks of the rigid body acceleration are within 10% of each other, making this a good indication of the consistency of the filters applied to the accelerations.

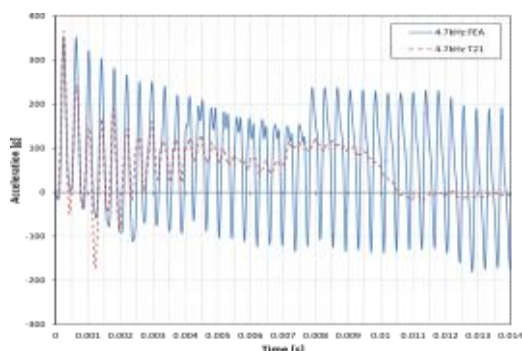


Fig.1: Elastic accelerations- filtered at 4.7kHz

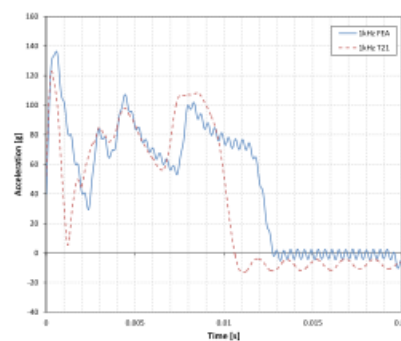


Fig.2: Rigid body accelerations- filtered at 1kHz

#### 4.3 Frequency Domain

Due to the excess energy contained in the elastic acceleration-time histories in the time domain, both FEA and test signals were also compared in the frequency domain by converting to FFT. In this case because the FEA signals were undamped it was unrealistic to compare magnitudes; the purpose of this comparison was to match the frequency content. As shown below in Table 1, this proved to be a good match.

	1st Peak	2nd Peak	3rd Peak	4th Peak
FEA	67 Hz	2577 Hz	5154 Hz	7663 Hz
2 1/2" Sch5	67 Hz	2848 Hz	4815 Hz	6758 Hz
Eigenvalue	N/A	2521 Hz	5021 Hz	7477 Hz

Table 1: Comparison of dominant frequencies contained in acceleration-time history for 2 1/2" Sch5 pipe samples

### 5 Conclusions

This study was to validate accelerations predicted using FEA with acceleration measurements from an impact drop experiment. This study highlighted the importance of selecting a sampling rate small enough to reflect the smallest time step within the model to avoid clipping or aliasing recorded data, and having a suitable sampling rate and filter frequency in the data acquisition equipment used in the physical tests. It was found the filters applied to the FEA and measured accelerations had a varying effect on the initial peaks.

Overall the acceleration-time histories still contained significant excess noise so was deemed inaccurate to compare beyond the first peak. Both the initial acceleration peak for the elastic and rigid body matched favourably, confirming that for essentially a 1-D impact, nodal output accurately replicated the test conditions.

### 6 References

- [1] Livermore Software Technology Corporation (LSTC). LS-DYNA Keyword User's Manual, 2014
- [2] Altair Engineering Inc. Hyperworks, 2014

---

# Validation of a FEA Model of a Nuclear Transportation Package under Impact Conditions

Chris Berry<sup>1</sup>,

<sup>1</sup>International Nuclear Services Ltd

## 1 Abstract

This paper discusses the process of validating a Finite Element Analysis (FEA) model of an entire nuclear transport package, known as M4/12, and presents the results obtained from impact simulations using the explicit analysis tool, LS-DYNA. The analytical results were compared with actual recorded impact deformation damage from physical drop testing under regulatory conditions. The purpose of the validation was to achieve a FE model that can be used in future design assessments involving impact conditions. The successful validation of the FE model is qualified by obtaining close agreement between the analytical results and the measurements recorded from the physical drop testing.

## 2 Introduction

Measured impact deformations of the M4/12 test specimen from a series of drop tests were used to compare the simulated deformations of the FE model. The testing was undertaken by AEA Technology between November 2004 and January 2005 and the findings were reported in the Package Design Safety Report (PDSR) [1]. All analyses were performed using LS-DYNA [2].

Analytical predictions were performed of four different drop tests of the M4/12 package corresponding to the physical drop test specifications. Two drops to survey the impact damage to the base end with a further two drops at the lid end. The level of the deformation damage to the package external shock absorbers formed the basis for the validation. The impact damage to the shock absorbers was the primary focus in the comparison between the simulation results versus the physical tests.

## 3 Modelling approach

The FE model was setup to simulate the different drops from a 9m height onto a rigid surface using the \*RIGID\_WALL keyword in LS-DYNA. This corresponds to the physical drop test specimen being dropped an equivalent height onto an unyielding surface. Each analysis was run for a specific time duration, measured in milliseconds, until almost all of the kinetic energy of the package decreased to a minimum. The number of impacts that are involved over the total duration of the analysis can vary depending on the initial drop orientation. A primary impact may only be considered if the drop angle is steep in relation to the longitudinal axis of the package, otherwise a shallower drop orientation may incur a primary impact followed by a secondary (slap-down) impact.

### 3.1 FEA model and verification checks

The M4/12 package is a complex assembly containing many subassemblies of a large number of different components. The FE model was constructed based on using geometry from a three-dimensional computer generated model. The geometry was thoroughly checked against drawings that were used to manufacture the test specimen. The weight of the package was also compared to the test package used in the physical drop testing.

### 3.2 Material assignment and material modelling checks

All materials were verified for the correct assignment to the individual components over the entire FE model. The M4/12 assembly contains a large percentage of materials that are isotropic. These are straight forward in that there is no requirement to specify properties in different directions. As the package has external shock absorbers containing wood as the main impact energy absorbing material, which is naturally an anisotropic material, its mechanical behavior is different in two

directions, i.e. along the grain and across the grain. The assembly of the shock absorbers contain an array of wood blocks which are stacked in different directions - one set orientated in the radial direction and another in the axial direction.

Achieving the correct wood grain alignment in the FE model is not always easy to get right, especially if the drop orientation angle of the package varies due to performing a number of different impact analyses. So, it is important to capture the correct alignment of the grain directions accurately and it is prudent to carry out checking of them so the impact behaviour of the shock absorbers resemble the design intent.

#### 4 Comparison between FEA and physical testing

An initial drop orientation of the package with primary impact to the lid end is shown in Figure 1. The angle of the package in relation to its axial reference longitudinally and its center of gravity means most of the energy from the inertia of the package is in the direction vertically down. Comparison between the results from simulation and physical testing was carried out to quantify the level of closeness of the amount of deformation damage. Figure 2 shows the difference in results between analysis and test.

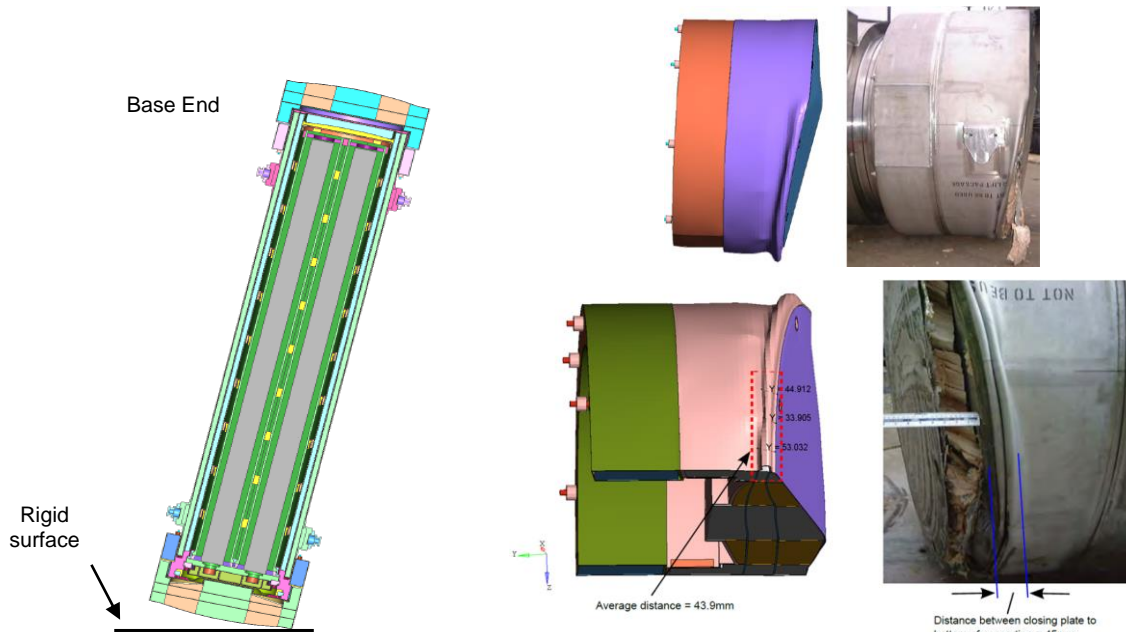


Fig.1: Lid End drop orientation of M4-12 package. Fig.2: Comparison of simulated damage vs. test.

#### 5 Conclusions

This work was to perform validation of the M4/12 FE model by following a process of comparing the deformations predicted using FEA with the actual deformation damage from physical testing.

Overall the deformations show good agreement predicted in the shock absorbers yielding a close match with the deformation from test. The work confirms that the FE model has successfully qualified as being validated.

#### 6 References

- [1] Jones, W: Package Design Safety Report for the M4/12 Package, Technical Report No.113 Revision 2, INS Ltd, May 2011.
- [2] Livermore Software Technology Corporation (LSTC): LS-DYNA, 2014.



## Some Observations on Artificial Bulk Viscosity in LS-DYNA: What Noh Knew in 1978

Co-author Len Schwer,

<sup>1</sup>Schwer Engineering & Consulting Services, USA I

A review of the development background for artificial bulk viscosity is presented with a focus on the development implemented in LS-DYNA and similar to other explicit codes. The analytical solution and benchmark calculation results presented by Noh (1978) for a one dimension shock problem are used to indicate errors in the simulation results attributed by Noh to artificial bulk viscosity. Noh identifies and demonstrates three types of artificial bulk viscosity errors: (1) excess shock heating, (2) non-uniform meshing and (3) due to spherical geometries. The LS-DYNA Multi-Material ALE solver is used to model Noh's shock problem and the results are reported for plane strain, axisymmetric (cylindrical) and spherical geometries; the latter being of practical importance in modeling free air bursts.

Several appendices are include that cover closely related topics: the role of bulk viscosity in time step stability calculations, solution of the Rankine–Hugoniot Jump Conditions for Noh's plane strain case, and a comparison of four explicit solver results for the spherical geometry case.

Perhaps the most lucid discussion of shock viscosity, a.k.a. artificial bulk viscosity, is Section 2.8 "The shock viscosity in one dimension" in the paper by Benson (1992), from which this manuscript borrows, in part. Calculations involving shocks have long used the numerical artifice of shock viscosity to obtain reasonable solutions in a numerical continuum mechanics framework for the discontinuities associated with shocks. The role of the shock viscosity is to spread out the shock thickness (discontinuity) over several elements. Thus the mesh refinement must be fine enough to allow for this approximation.

Strong shocks in gases are dissipative due to both the gas heating caused by the large and rapid compression of the gas and viscosity among the gas molecules in the densified shock thickness. Most numerical shock viscosity algorithms lump these two dissipative mechanisms together and treat the resulting viscosity as a pressure term.

Von Neumann and Richtmyer (1950) introduced a pressure viscosity term in their work with one dimensional shock propagation

$$q = -\rho(c\Delta x)^2 \frac{\partial u}{\partial x} \left| \frac{\partial u}{\partial x} \right| \quad (1)$$

where  $\rho$  is the density,  $c$  is a dimensionless constant to be selected,  $\Delta x$  is the mesh spacing and  $u$  is the velocity. This viscosity is positive for compressive strain rates, i.e.  $\partial u / \partial x < 0$ , and negative for rarefactions. Typically, numerical implementations of such shock viscosities only activate the term for compressive strain rates, LS-DYNA use this compression only implementation.

The one dimensional viscosity of Von Neumann and Richtmyer is both effective and deceptively simple. In one dimension the strain rate across the shock, and hence velocity jump, is easily determined:

$$\Delta u = \Delta x \frac{\partial u}{\partial x} \quad (2)$$

In expanding this concept to two or three dimensions, the determination of the direction for calculating the strain rate across the shock becomes more challenging. The simplest approximation is to replace

---

the element length by the square root of the element area in two dimensions, or the cube root of the volume in three dimensions. The strain rate across the shock is approximated as the trace of the strain rate tensor, i.e.

$$\frac{\partial u}{\partial x} \approx \dot{\epsilon}_{kk} \quad (3)$$

The standard form of the shock viscosity used in many explicit codes today is a combination of the quadratic term proposed by Von Neumann and Richtmyer for strong shocks and a linear term for treating small oscillations that occur after the shock, i.e. damping:

$$q = \rho l \left( Q_1 l \dot{\epsilon}_{kk}^2 - Q_2 a \dot{\epsilon}_{kk} \right) \quad (4)$$

This is the form used by LS-DYNA for compressive strain rates where  $l$  is the generalize length parameter mentioned above,  $a$  is the local sound speed, and  $Q_1$  &  $Q_2$  are dimensionless constants, by default in LS-DYNA uses to 1.5 and 0.06, respectively.

# Damping – Oscillation Elimination after Rupture

M. Dobes<sup>1</sup>, J.Navratil<sup>2</sup>

<sup>1,2</sup> Robert BOSCH spol. s.r.o., Roberta Bosche 2678, České Budějovice

**\*KEYWORDS:** damping, oscillation, rupture, Ls-Dyna

## 1 Introduction

The subject of this article is using of the Damping for Oscillation elimination after the Rupture. The problem appears in explicit simulations of the plastic parts with computational models of material damage. After the rupture or erosion of finite elements, the model of the structure oscillates. The oscillation of the structure may be significant and cause additional erosion of the structure, which is non-physical. All real structures have any damping and this damping should be considered in numerical simulation. We have a lot of possibilities of the damping options, but we need to know the correct value of the damping. So, in this contribution, very simple method for damping factor estimation for plastics is described, concretely TSCP (Typical Semi-Crystal Polymer). This method is a combination of numerical simulations and experimental estimation of the damping factor for specific eigen-frequency. Repeating this method with different boundary conditions, we can cover some frequency spectrum. The contribution shows a lot of the damping options in LS-DYNA with interesting consequences. Using different damping schemes requests dissimilar changes of the stiffness and model properties. The purpose of our work is the preservation of the same physical, material and stiffness properties of the model and the real physical structure. The physical structure of FSM (fuel supply module) is used for numerical validation of damping options, used in computational simulation.

## 2 Experiments and damping coefficient

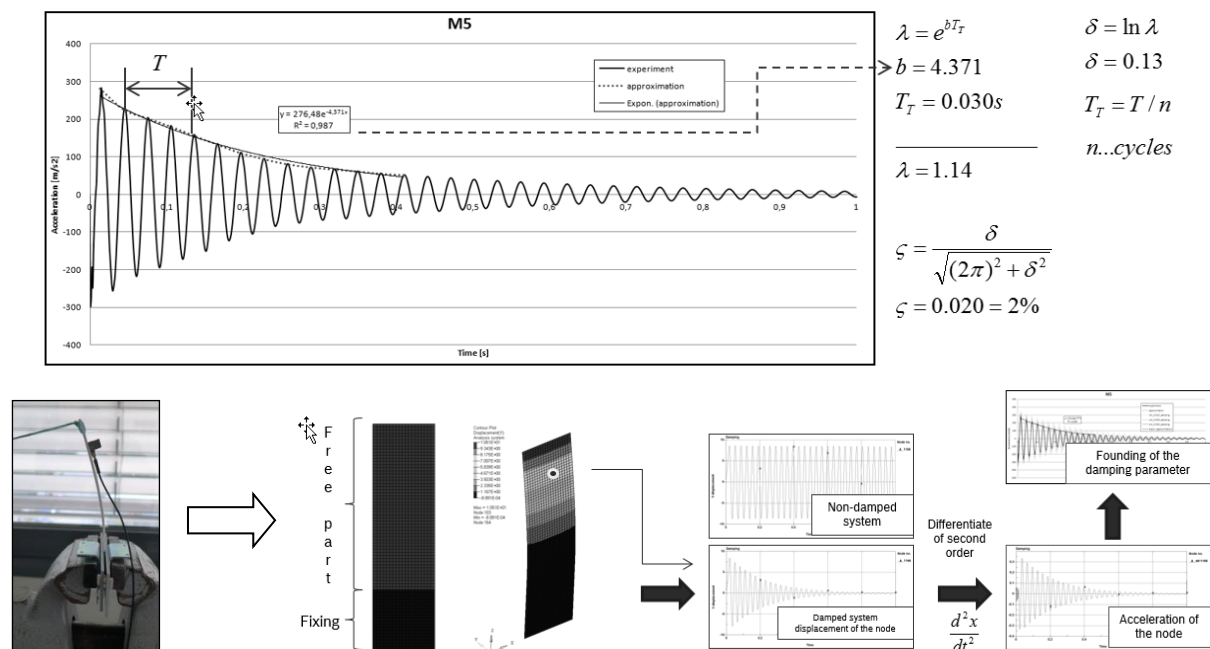


Fig.1: Analytical reverse analysis and figure of the damping coefficient verification in LS-DYNA

The damping problematic is very common in crash simulations. Generally, we can divide damping on material and structural. In this contribution material damping will be solved. The representative is TSCP without fibres. The main reason why we solve damping in crash simulation is effect on the secondary cracking after first crack propagation in numerical simulation. During this cracking process is initialized stress oscillations in the part. So, these oscillations without damping caused additional non-physical finite elements deleting-cracks. Each FE software has a lot of damping options. We are focused on the software LS-DYNA which order many keywords for damping definition ( $\alpha$ ,  $\beta$  damping, Rayleigh damping etc.) We needed some simple experiment for estimation of damping

value for TSCP material, so we used simple part geometry with damped own frequency. The experiment was very simple, but sufficient for our purposes. The test specimen from TSCP material was used for pre-stress oscillation test. Accelerometer was glued on the test specimen in prescribed point. The acceleration response was measured in this point. The test specimen was pre-stressed by initial displacement and then this pre-stressing was released. Numerical simulation was made parallelly and damping coefficient was founded from this experimental-numerical analysis. The analytical regressive-analysis was used for founding of the damping coefficient. The complete procedure is described in full paper version.

In next step we connected results of this experiment with results based on DMA analysis. The experimental results were validated on the real part with using of High-Speed camera for description of the structure moving. The sensitive analysis of the damping setup is one element of this paper.

### 3 Validation and practice using

The simulation with the material erosion was validated with a real experiment. Guiding rods of a flange, basic part of a fuel supply module, were loaded by a high speed bending test. The evocated oscillation of the guiding rod pedestal was compared. The simulation with and without the damping was performed. The most optimal damping option from previous research was used - \*DAMPING\_FREQUENCY\_RANGE. The oscillation frequency was found in the first step and obtained damping coefficient was applied in the second step.

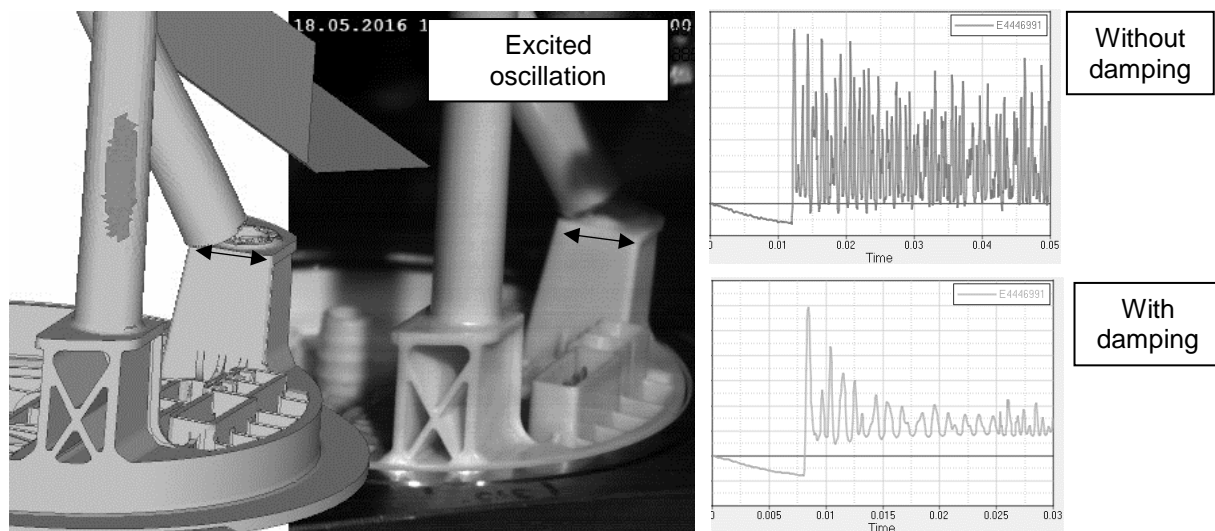


Fig.2: Experimental verification and damping using in practice task

### 4 Summary

Several stress peaks close to the ultimate stress can occur in the simulation as a secondary load after the crack propagation in the case that damping is not involved. The evaluation of these results is not possible. The damping must be used for the correct consequent behaviour description and a possible damage accumulation. The deformation behaviour of the simulation with damping and the real experiment was compared. Only a few higher amplitudes occurred in both cases. The experiment with the real part shows no additional damage. The stress oscillation in the simulation is decreased onto safe values. We can use very simple experimental method for damping ratio founding (material damping). The wide frequency spectrum (low-frequency spectrum) we can solve by using this method.

### 5 Literature

- [1] R. Brepta, M. Prokopec, Šíření napěťových vln a rázy v tělesech, Academia, Praha, t.ST05,1972
- [2] Thiruppukuzhi, Srikanth V., C.T. Sun a G.T. Gray. Models for the strain-rate- dependent behaviour of polymer composites. *Composites Science and Technology*. 2001, vol. 61, issue 1, s. 1-12. DOI: 10.1016/S0266-3538(00)00133-0.

# Abbildung von Gussgehäusen und Schrauben in der Containment Simulation

S. Edelmann<sup>1</sup>, C. Groß<sup>1</sup>, H. Chladek<sup>1</sup>, M. Marschner<sup>2</sup>

<sup>1</sup>INPROSIM GmbH, Frankfurter Str. 19, 65830 Kriftel, Germany

<sup>2</sup>KBB GmbH, Windbergstr. 45, 01728 Bannewitz, Germany

## 1 Einleitung

Im Motorenbereich können die Anforderungen an Leistungsdichte, Wirtschaftlichkeit und Umweltschutz ohne eine Aufladung kaum mehr erfüllt werden. Oft werden hierfür Abgasturbolader (ATL) eingesetzt. Neben den Ansprüchen an Festigkeit und Lebensdauer sind auch Anforderungen an die Sicherheit zu erfüllen, z.B. beim Bersten von Laufrädern. Diese Sicherheitsaspekte können heutzutage mittels der expliziten Simulation in der Entwicklung frühzeitig im Hinblick auf die Herstellerverantwortung berücksichtigt werden, sodass aufwendige Versuche und Entwicklungszeiten eingespart werden können. Je nach Größe und Anforderung sind ATL zumeist in Aluminium- oder Eisenguss beim Verdichtergehäuse und aus hochwarmfesten Sonderguss Legierungen beim Turbinengehäuse aufgebaut und über Flansche mit Spannbändern oder Schrauben verbunden. Um diese Gehäuse und Verbindungen mittels der Containment Simulation belastbar auszulegen, bedarf es gewisser CAE Techniken in der Abbildung der Bauteile und der Materialbeschreibung, die im Vortrag beschrieben werden und deren Erfolg mit dem Vergleich zu einem realen Bauteilversuch belegt wird.

## 2 Geometrie Modellierung

Ein wesentlicher Aspekt in der Containment Simulation ist eine geometrietreue und ausreichend feine Vernetzung der Gussgehäuse und deren Verbindungen. „State of the Art“ ist eine SOLID bzw. Volumen Vernetzung mit BRICK, PENTA und TETRA Elementen.

### 2.1 Gehäuse Abbildung

Bei den ATL Gehäusen mit Radialturbinen ergeben sich über die geometrische Asymmetrie der Spirale über den Umfang unterschiedliche Belastungen am Gehäuse und den Schrauben. Diese Abweichungen sind so groß, dass nur eine geometrietreue Abbildung der Gehäuse das System richtig erfassen kann. Um den Aufwand in der Vernetzung wie auch die Anzahl der Elemente gering zu halten bietet sich eine gemischte Vernetzung mit BRICK / PENTA Elementen in den rotationssymmetrischen Bereichen und Flanschen sowie mit TETRA Elementen in den übrigen, zumeist sehr komplexen Bereichen wie der Spirale an. Lediglich in der Konzeptphase sind vereinfachte rotationssymmetrische Abbildungen der Gehäuse für die Betrachtung grundsätzlicher Designaspekte sinnvoll.

### 2.2 Schrauben Abbildung

Auch bei Schraubenverbindungen sind eindimensionale Abbildungen mit Kraft-Weg-Charakteristiken oder nur numerische Kopplungen nicht mehr zeitgemäß, da lokale Interaktionen zwischen Schrauben und Flanschen für eine genaue Betrachtung berücksichtigt werden müssen. So sind z.B. geometrische Effekte wie die Schiefstellung und Verdrehung der Flansche und der daraus resultierende Kontakt der Schrauben mit den Flanschen in den Auflagen und Bohrungen zu berücksichtigen, um die lokalen Belastungen der Schrauben bis zum Versagen korrekt abzubilden. Aus diesen Überlegungen ergibt sich zwingend für hochbelasteten Verbindungen eine geometrietreue Abbildung der Schrauben mit den relevanten Querschnitten wie z.B. den Spannungs- und Dehnungsquerschnitten.

## 3 Materialbeschreibung

In LS-DYNA gibt es eine Vielzahl von Materialmodellen, um das Verformungs- und Versagensverhalten der Werkstoffe zu beschreiben. Für die hochdynamische Belastung beim Bersten von Laufrädern in wenigen Millisekunden sind für die Werkstoffe belastbare Fließkurven für die jeweiligen Bauteiltemperaturen sowie die Dehnratenabhängigkeit, die Mehrachsigkeit bzw. Triaxialität im Belastungszustand und auch die Elementgröße zu berücksichtigen. Für duktile Kugelgraphit Gusswerkstoffe wie z.B. den EN-GJS-400 bieten sich Materialbeschreibungen wie Johnson-Cook und seine Derivate, das erweiterte Gurson\_JC und das GISSMO Modell mit MAT\_ADD\_EROSION oder das MAT\_224 an. Wichtig bei der Auswahl ist der wirtschaftliche Aufwand, der bei der Gewinnung der Daten und später

in der Simulation an Rechenzeit zu tragen ist. Bei der Materialbeschreibung für Schrauben sind im Vorfeld Zugversuche und deren Abbildung in der Simulation einzuplanen, um den Belastungshorizont und die Verlängerung bis zum Bruch im Komponentenmodell korrekt zu erfassen.

#### 4 Vergleich zum Versuch

In der Entwicklung einer neuen ATL Verdichterstufe wurde die Simulation mit den aktuellen Ansätzen in den CAE Techniken genutzt, um frühzeitig ein Produkt zu entwickeln, das im Hinblick auf Belastungen und Deformationen zwischen Gehäusebauteilen und Schrauben eine gute Balance darstellt und dem Anspruch in der Containment Sicherheit genügt. Abschließend wurde zur Bestätigung der Containment Simulation ein Versuch am Prüfstand gefahren. Neben lokalen Effekten in der Deformation war global die axiale Verlängerung der Verdichterstufe eine zentrale Größe, die als Maßzahl für die Güte im Vergleich von Versuch und Simulation definiert wurde. Diese Maßzahl ist über den Umfang an acht Stellen vermessen worden und in Bild 1 dargestellt. Sowohl in der Verteilung der Asymmetrie der Belastung über den Umfang wie auch in den absoluten Werten zeigt sich in diesem Vergleich mit einer Abweichung von wenigen Prozenten eine sehr gute Übereinstimmung.

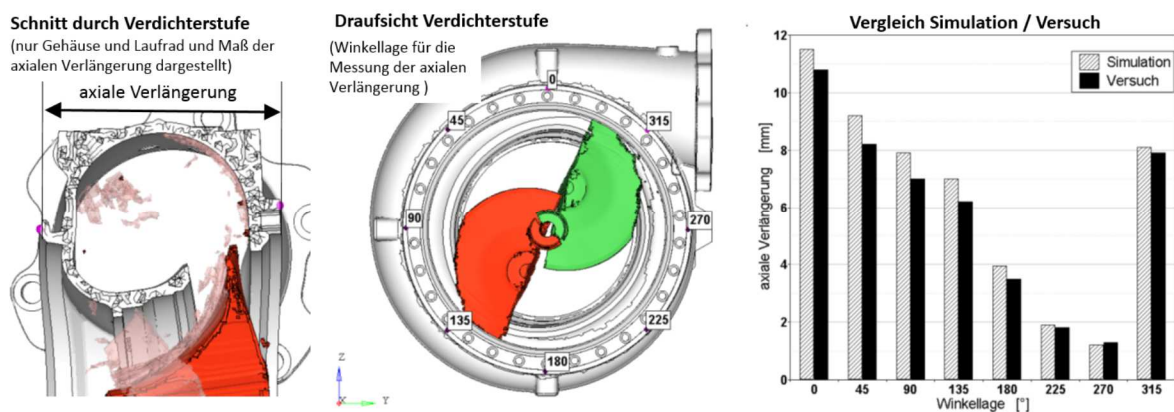


Bild 1: Axiale Verlängerung der Verdichterstufe über den Umfang

#### 5 Zusammenfassung

Die Containment Simulation hat sich unter technischen und wirtschaftlichen Aspekten als ein wichtiges numerisches Werkzeug für die kommerzielle Anwendung im Bereich von Abgasturboladern (ATL) entwickelt, bei der sich in den CAE Techniken ein gewisser Standard als „State of the Art“ für den Modellaufbau und die Materialbeschreibung etabliert hat. Anhand der Entwicklung einer neuen ATL Verdichterstufe kann die gute Übereinstimmung von Versuch und Simulation aufgezeigt werden. Neben der guten qualitativen Beschreibung der Deformation bis hin zum Bruch sind auch quantitative Maßzahlen mit wenigen Prozent Abweichung sehr gut wiedergegeben. Ferner zeigt sich in den absoluten Werten, dass die Simulation dem konservativen Anspruch gerecht wird und tendenziell etwas höhere Belastungen und Verformungen aufzeigt. Mit dem heutigen Stand der CAE Techniken ist es nunmehr möglich, die Containment Simulation als einen zentralen Baustein in der Entwicklung und Freigabe neuer ATL zu nutzen und somit aufwendige Versuche und Entwicklungszeiten einzusparen.

#### 6 Literatur

- [1] Edelmann, S., Groß, C., Chladek, H.: "Simulation of a clamping ring under high dynamic loading", 7<sup>th</sup> European DYNA Conference, 14<sup>th</sup> -15<sup>th</sup> May 2009, Salzburg, Austria
- [2] Edelmann, S., Walter, M., Chladek, H.: "Material Model for Deformation and Failure of Cast Iron for High-Speed Impacts", 3<sup>rd</sup> European Hyperworks Technology Conference, 2<sup>nd</sup> -4<sup>th</sup> November 2009, Ludwigsburg, Germany
- [3] Häcker, R., Knothe, E., Dr. Memhard, D., Dr. Andrieux, F.: "Containment Sicherheit", FVV Vorhaben Nr. 936, Abschlussbericht, Heft 928 - 2011, Forschungsvereinigung Verbrennungskraftmaschinen (FVV) e.V., 4. April 2011, Frankfurt am Main, Germany
- [4] LS-DYNA © Aerospace Working Group (AWG): "Modeling Guidelines Document", Version 15-1 dated August, 2015, <http://awg.lstc.com/tiki/tiki-index.php>, United States
- [5] LS-DYNA © Keyword User's Manual: "Volume II Material Models", LS-DYNA R7.1, May 19, 2014 (revision: 5442), Livermore Software Technology Corporation (LSTC), United States

# Simulation of Containment-Tests at a generic Model of a large-scale Turbocharger with LS-DYNA

Stefan Hennig<sup>1</sup>, Prof. Dr.-Ing. Armin Huß<sup>2</sup>, Heiko Honermeier<sup>1</sup>, Marcel Jagic<sup>1</sup>, Manuel Schönborn

<sup>1</sup> Ingenieurbüro Huß & Feickert GbR, Liederbach, Germany

<sup>2</sup> Frankfurt University of Applied Sciences, Frankfurt, Germany

## 1 Introduction

As machines that work by means of fast spinning rotors, turbochargers need to fulfill the requirement that in case of a bursting impeller no fractured parts are allowed to leave the casing. Especially for large-scale turbochargers (used on stationary or ships engines) this requirement is very important since the kinetic energy of the impeller is extremely high and poses a high potential threat to its surrounding. The objective of a containment test is to demonstrate that the housing of the turbocharger is of sound design and capable to satisfactorily contain fractured rotating parts inside the casing. Before the use of CAE such tests were carried out on a test bed during the type approval procedure of a turbocharger. On the one hand this was very expensive and time consuming and, on the other hand, the comprehension of high-speed deformation processes was restricted as well as the possibilities for measurements and improvements were limited. Due to these reasons containment tests nowadays are simulated using the explicit finite element technique before real hardware tests are performed for validation purposes. Thus the simulation technique is utilized from the early stage of the development process of a turbocharger up to its certification and also afterwards accompanying the whole machine-life.

## 2 Motivation

To accommodate the fact that turbocharger structures become more and more complex and sophisticated and to predict the bursting and damage procedure as exact as possible, the utilized simulation concepts and methodologies are developed continuously. Furthermore the increasing complexity of the structures also leads to an increasing demand in the precision of the CAE model. All cast structures are meshed with 3D elements, preferably hexahedrons which leads to a strong increase in effort for modeling and also a strong increase of computing time. To enable further economic investigations on a high level of detail, e.g. new approaches for different idealizations of certain areas, new material laws, different boundary conditions or robustness studies, a generic CAE model (Fig.1) of a large-scale turbocharger was developed at Ingenieurbüro Huß & Feickert GbR. It is the objective of this publication, to give a short overview of the state of the art of simulating containment tests and the requirements to such simulations as well as to show the level of detail of the used models. Furthermore the properties and benefits of the generic model shall be pointed out. To complete the essay, a short selection of studies which were performed with the generic model will be presented.

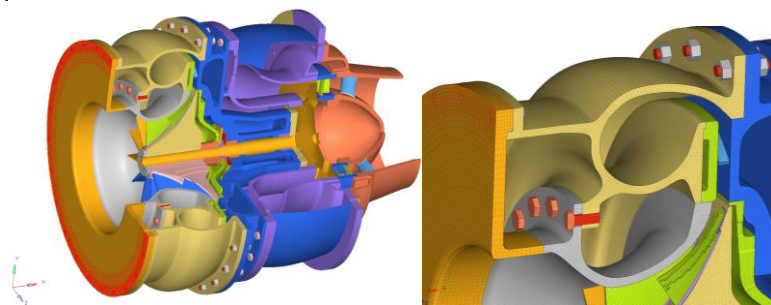


Fig.1: Turbocharger generic 3D FE-Model, Detail FE-Model [1]

## 3 Containment Simulation

Over the years a lot of different damage scenarios for compressor section and turbine section were developed and analyzed using containment simulations. There are several fracture scenarios of the compressor disk as well as blade loss scenarios at the turbine section, several rotational velocities, different impact positions and impeller sizes that lead to a high number of variations. Since the

different scenarios can lead to varying load paths, high loadings in different sections of the turbocharger are possible. Because of this, it is important for the CAE model to be able to accurately represent all areas of the model rather than having a strongly simplified FE structure. The material laws need to take strain-rate dependencies into account as well as multi-axial fracture. Furthermore several laws are necessary for one material in order to be able to represent the different temperatures in the turbocharger. Additionally boundary conditions such as pressure or screw pre-stresses have to be considered.

#### 4 Generic Model

The challenge that had to be met with the generation of a generic model was to be able to reproduce all mentioned effects while at the same time simplifying the model as much as possible in order to reduce simulation time to a minimum. This simplification was mainly reached by using a rotational symmetry for the casing. Due to this, all unsymmetrical effects were taken out of the model leading to a very efficient structure that can be modified quickly and that can even be parameterized for optimization purposes.

#### 5 Studies

The first of two studies that were performed using the generic model focused on a more realistic approach of the bursting scenario of the compressor flywheel. So far the impeller was modeled in three separate wedges to which an initial rotational velocity was applied. Since the three segments were not merged they moved apart from each other at the start of the simulation. This modeling however did neither cover the effect of the fracturing inside the impeller wheel nor the prestressing of the flywheel due to its rotation. At first a separate analysis with the complete rotor was performed to determine the influence of an implicit pre-stressing simulation on the kinematic of the segments after fracture. Furthermore the same was done with different damage scenarios (Fig.2), comparing the non-merged impeller as described above with a merged but slotted impeller. The latter being a closer reproduction of the real weakening of the impeller structure that is commonly used in containment tests. After this the global effects on the containment simulation from some combinations of the described separate analysis were reviewed using the generic model.

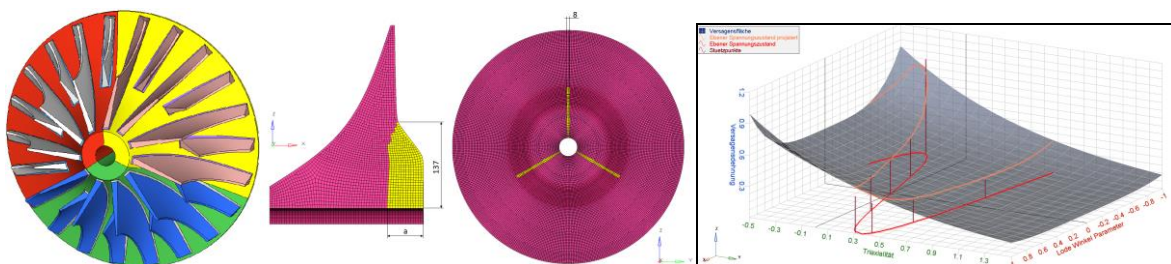


Fig.2: Damage scenarios of compressor disk: non-merged and merged+slotted impeller [1],[2]; Failure surface with plane stress curve [3]

The second study concerned the effect of including the lode-angle-parameter on the damage and failure behavior of the housing structures. So far the simulation of material failure was mainly based on stress-triaxiality alone. In order to analyze the possible effects of the lode-angle-parameter on the specific loadcase of the containment-simulation the generic model was used.

#### 6 Summary

The models for simulations of containment-tests become more and more complex. There is a high effort for meshing the complex structures. Besides a lot of boundary conditions have to be considered. For this reason studies of single or small modifications and improvements (e.g. in material laws, meshing, geometry, boundary conditions, simulation methodology) are very expensive and long-lasting. The developed generic model has proved itself a very helpful instrument. It depicts the principle behavior of real containment tests with all its complex load chains. It enables the performance of studies, sensitivity and robustness analyses in a fast and efficient way. Improvements, new features and simulation approaches can be tested and assessed comprehensively before considering them in a detailed containment simulation.



## 7 Literature

- [1] Schönborn, Manuel (Ingenieurbüro Huß & Feickert): Praxisprojekt „Erstellung eines generischen Turboladermodells für Containmentsimulationen mit der expliziten Simulationssoftware LS-DYNA“, (02/15/2016)
- [2] Schönborn, Manuel (Ingenieurbüro Huß & Feickert): BA „Weiterentwicklung eines Schadensszenarios für Containmentsimulationen mit LS-DYNA“, (05/30/2016)
- [3] Jagic, Marcel (Ingenieurbüro Huß & Feickert): Wissenschaftliches Projekt „Unterschiede des GISSMO-Versagensmodells bei der zusätzlichen Verwendung des Lode-Winkel-Parameters am Beispiel eines Großturboladers“, ( März 2016)

# NVH simulations for car seat

T.Kupczyk <sup>1</sup>, L. Guerin <sup>2</sup>

<sup>1</sup>Faurecia Grójec R&D Center, ul. Spółdzielcza 4, 05-600 Grójec, Poland

<sup>2</sup>Faurecia Automotive Seating, ZI de Brières les Scellés, 91152 Etampes, France

## 1 Introduction

Increasing requirements of the car's seat structures drive Faurecia Automotive Seating to develop robust FEA methods able to predict vibration test results. In the scope of OEM interest there is not only value of first resonance frequency but also higher frequency range or amplitude level for defined excitations.

## 2 Methodology

The article describes the methodology developed at Faurecia for NVH challenges using LS-Dyna code. Having in mind limited time during development process of new product, first and key objective was to use minimum energy to create NVH FEA model from FEA model used for crash purpose. The challenge was to validate methodology that will allow to convert highly nonlinear crash model to linear behavior in NVH domain. In the same time be able to get reliable output form Modal Analysis in order to take design decisions and solutions. Each element of the seat like: tracks, recliners or high adjuster, fasteners (screws, bolts, welds) or other kinematic connections have been "modified" to linear behavior.



Fig.1: Typical connections for car seat.

## 3 Validation

To validate NVH FEA models, several correlations with real tests have been performed following classical system engineering approach. Methodology was validated in few steps: sub-systems of backrest, cushion and tracks then whole metal frame seat and finally trimmed complete seat. Modes shapes correlations between real and virtual tests were done by calculating MAC (Modal Assurance Criterion) between modes calculated by LS-Dyna (d3eigv files) and modes extracted from Experimental Modal Analysis (Universal Files). Frequency Responses Functions (FRF) from hammer tests were also compared with Ls-dyna models using **\*FREQUENCY\_DOMAIN FRF** cards.

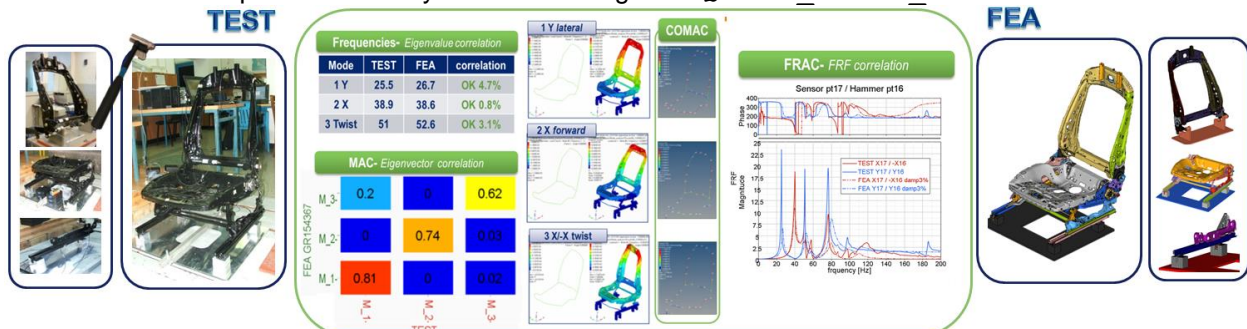


Fig.2: Validation of FEA results.

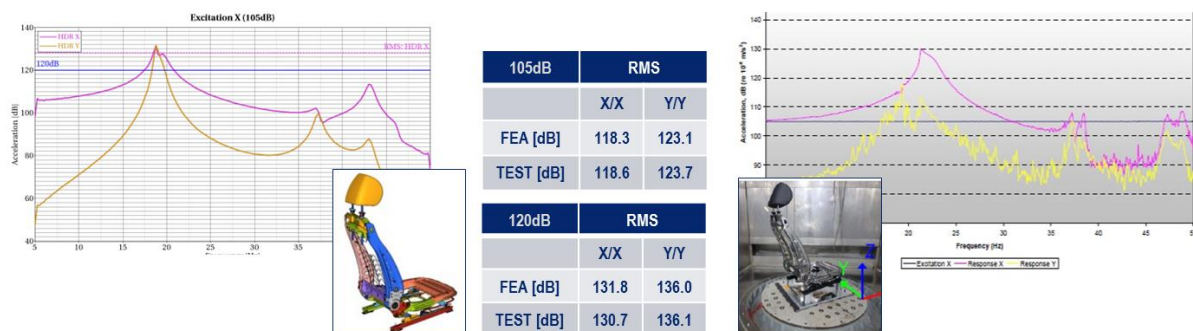
## 4 Application

Modal Analysis result is used during development process to check linear behavior of structure in frequency domain. Identification of critical areas by strain energy allow to avoid potential problems at early stage of project.

The user can generate the Super-Element by `*CONTROL_IMPLICIT_MODES` and deliver reduced model of Complete Seat in the Nastran `.DMIG` file format which can be used as input to `*ELEMENT_DIRECT_MATRIX_INPUT`.



Additionally some OEM require also to respect acceleration amplitudes level on seat frames while excited by ground signal (from theoretical acceleration spectrum to real life road signals). Using `*FREQUENCY_DOMAIN_RANDOM_VIBRATION` card, several shaker tests have been successfully correlated. The presentation will show issues encountered during correlations focusing specifically on management of damping.



## 5 SUMMARY

Despite plenty of non-linearity inside real Complete Seat, developed methodology shows good correlation level for Modal Analysis inside useful frequency range. It is successfully used during development and validation phase of project.

Additionally model is used for Frequency Response Simulations and give satisfied results.

Methodology is spread to electronics devices and mechatronics where there are trials to predict noise coming from resonance between high-adjuster actuator and frame structure.

## 6 Literature

- [1] Livermore Software Technology Corporation (LSTC): LS-DYNA Keyword User's Manual, LS-DYNA R7.1 May 26, 2014
- [2] Livermore Software Technology Corporation (LSTC): LS-DYNA Database Binary Output Files for Frequency Domain Analysis, Revised January 2015
- [3] Svend Gade, Henrik Herlufsen and Hans Konstantin-Hansen: "How to Determine the Modal Parameters of Simple Structures", Brüel&Kjær, Denmark
- [4] Randall J. Allemang: "The Modal Assurance Criterion –Twenty Years of Use and Abuse", University of Cincinnati, Sound and Vibration, August 2003

# Model Set up and Analysis tools for Squeak and Rattle in LS-DYNA

Thanassis Fokilidis<sup>1</sup>, Mehrdad Moridnejad<sup>2</sup>

<sup>1</sup> BETA CAE Systems SA, Thessaloniki Greece

<sup>2</sup> VOLVO CAR Corporation, Gothenburg Sweden

## 1 Introduction

One of the most important quality aspects during the design process of a vehicle is the provided occupant comfort. Comfort in a vehicle is achieved, among others, through a quiet and durable interior, and through the elimination of Squeak and Rattle noises. A huge amount of different tests take place in laboratories in order to produce interior and exterior components that eliminate the occurrence of such undesirable phenomena. As a result the need for the development of numerical models that explain and predict the behavior of a vehicle in Squeak and Rattle is inevitable. The implementation of automated tools benefits analysts in setting up efficient and robust processes for accurate and straightforward CAE simulations.

## 2 From reality to simulation procedure

In reality, when driving a vehicle, the road excitations cause relative displacement between different components. These relative displacements are the reason for the Squeak and Rattle noises. A simulation method used for the Squeak and Rattle numerical analysis is the E-LINE method which focuses on calculating and evaluating the relative displacement between two components in time domain.

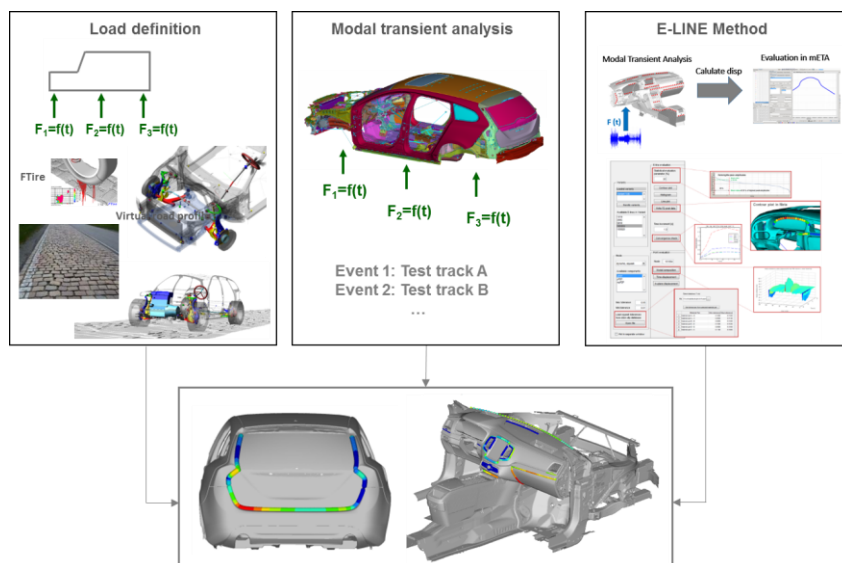


Fig. 1: Simulation procedure of Squeak and Rattle

The E-line is a part of a bigger simulation procedure which initiates by running a virtual car on the virtual road profile, and calculating the time history of all forces between the chassis and the body. Next step is to apply the forces for each test track and run a modal transient analysis. The output of this sub process is then the input for the E-LINE method which finally offers the relative displacement in different interfaces.

## 3 Pre Processing of E-LINE method in ANSA

E-LINE is a 3D curve along which the relative displacement between two components is measured. ANSA offers the ability through a dedicated tool to set up the model for Squeak and Rattle analysis (E-LINES) in LS-DYNA. The pre-processing starts with the identification of the crucial for S&R areas,

continues with the creation of the LS-DYNA keywords and it is completed with the LS-DYNA file output.

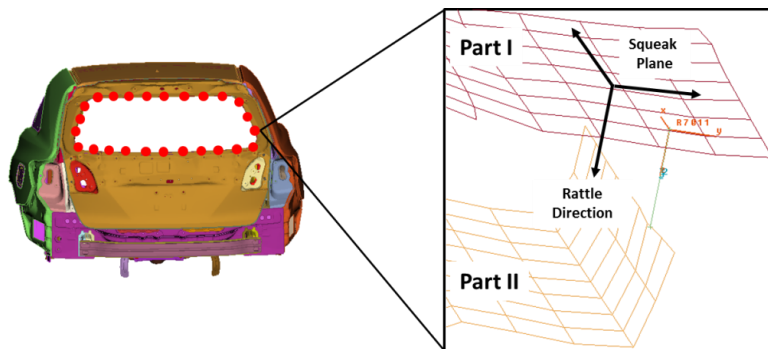


Fig.2: E-LINE in ANSA

#### 4 Post Processing of E-LINE in $\mu$ ETA

$\mu$ ETA offers to the analyst an automated tool for an easier evaluation of the Squeak and Rattle analysis results. The results of all E-LINES are read massively and one can quickly have a general view of the analysis through an automated report. Moreover, further post processing capabilities through contour and 2D plots are available for the user to evaluate the relative displacement between different combinations of components.

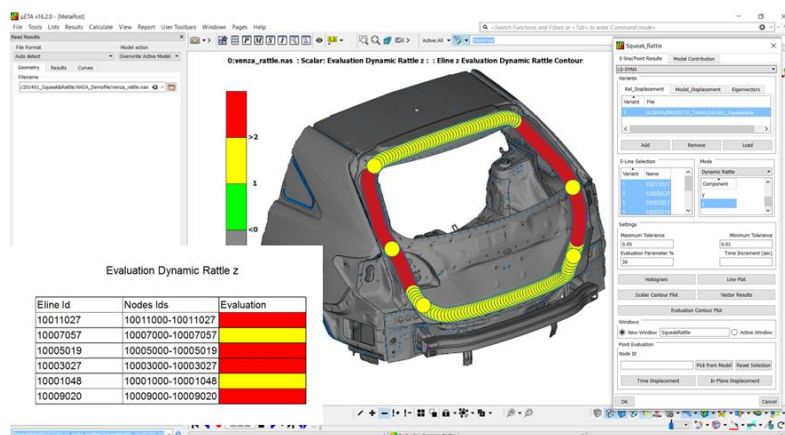


Fig.3: Results in  $\mu$ ETA

#### 5 Summary

The elimination of Squeak and Rattle noises is one of the major aspects to achieve comfort during the driving of a vehicle. The cause of those undesirable noises is the relative displacement between different components of it. E-LINE method offers the ability to simulate the relative displacement in time domain. The current paper dives deep in E-LINE method by showing both interior and exterior examples. In addition to that it presents the BETA CAE Systems automated tools that offer a complete and efficient solution in Squeak and Rattle analysis using LS-DYNA, minimizing the simulation time and human interaction

#### 6 Literature

- [1] Weber, J. : Squeak & Rattle Simulation – A Success Enabler in the Development of the New Saab 9-5 Cockpit without Prototype Hardware”, *SAE Int.J. Passeng. Cars – Mech. Syst.* 3(1):936-947, 2010
- [2] Weber, J. : “Squeak & Rattle Correlation in Time Domain using the SAR-LINE™ Method”, *SAE Int. J. Passeng. Cars – Mech. Syst.* 5(2):2012
- [3] ANSA version 16.2.x User’s Guide, BETA CAE Systems SA, June 2016
- [4]  $\mu$ ETA version 16.2.x User’s Guide , BETA CAE Systems SA, June 2016

# Evaluation of Equivalent Radiated Power with LS-DYNA®

Yun Huang, Zhe Cui

Livermore Software Technology Corporation

## 1 Introduction

In NVH analysis, computing radiated noise from vehicles is an important task. The traditional methods, like FEM and BEM, are generally slow and memory intensive. As an alternative, ERP (equivalent radiated power) method has been well established and widely used. It is a reduced calculation method to characterize the structure borne noise, especially in an early phase of the product development. With ERP, engineers can have a quick look at the possible maximum radiated power for specific excitations in the frequency domain. ERP can also provide the information about panel contribution towards radiated noise so that engineers can get some suggestions when they need to do structural optimization towards noise.

In LS-DYNA, ERP calculation has been implemented as an option for the feature Steady State Dynamic analysis (keyword **\*FREQUENCY\_DOMAIN\_SSD**). The ERP results are given in 1) binary plot database, d3erp; and 2) ASCII xyplot files, ERP\_abs and ERP\_dB. They are all accessible to LS-PrePost.

## 2 Brief theory

The ERP calculation is based on plane wave assumption for the radiated acoustic waves. First we calculate the ERP density, defined as

$$ERP_{\rho} = \frac{1}{2} \rho c \operatorname{Re}[v_n \cdot \bar{v}_n] \quad (1)$$

The ERP absolute value radiated from the vibrating panels is the integral of the ERP density over the whole surface and is given by

$$ERP_{abs} = \int_S ERP_{\rho} dS = \frac{1}{2} \rho c \int_S \operatorname{Re}[v_n \cdot \bar{v}_n] dS \quad (2)$$

## 3 Keyword

We use the keyword **\*FREQUENCY\_DOMAIN\_SSD\_ERP** to activate ERP calculation. A typical keyword input looks like this. More details can be found in LS-DYNA Keyword User's manual [1]:

```

$#   madmin   mdmax   fnmin   fnmax   restmd   restdp   lcflag   relatv
      1       100       0.       2000.
$#   dampf    lcdam    lctyp   dmpmas   dmpstf   dmpflg
      0.01
$#                               memory    nerp     strtyp   nout     notyp   nova
                                       1
$#   r0       c       erprlf   erpref
      1.21    340.0    1.       5.e-13
$#   pid     ptyp
      1
$#   nid     ntyp     dof      vad      lc1      lc2      lc3      vid
      131    0        3        0        100     200

```

## 4 Post-processing

The ERP calculation results are saved in binary plot database D3ERP, which is activated by the keyword **\*DATABASE\_FREQUENCY\_BINARY\_D3ERP**. D3ERP is accessible to LS-PrePost and the following results are included in the database for each excitation frequency:

- Normal velocity on the surface (real part, imaginary part and magnitude)
- acoustic intensity
- ERP density

The frequency variation of the ERP absolute value and ERP dB value are saved in the ASCII files: ERP\_abs and ERP\_dB. They can be plotted as xy curves with LS-PrePost.

## 5 Example

We consider a simplified engine model, which has 16041 nodes and 13484 solid elements. The whole surface of the engine is defined as sound radiating panel, by a set of segments (**\*SET\_SEGMENT**). To model the excitation from the ground, we assume that the model is fixed on a shaker table and a constant horizontal acceleration 0.02g is provided for the range of frequency 10-1000 Hz.

The ERP density results at frequency 100 Hz are shown in the following figure. It helps to visualize the contribution towards radiated noise from the whole surface, which may vary with frequencies.

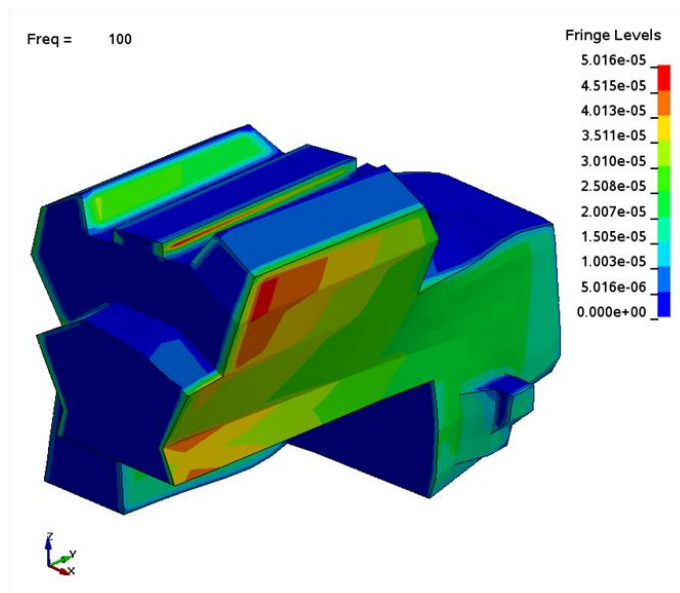


Fig.1: ERP density plot at frequency 100 Hz

## 6 References

- [1] LS-DYNA Keyword User's Manual, LSTC, 2016.

# Eigensolution Technology in LS-DYNA®

Roger Grimes

Livermore Software Technology Corporation

LSTC has been adding additional eigensolution technology to LS-DYNA.

For several years, LS-DYNA has a Block Shift and Invert Lanczos Eigensolver in both SMP and MPP implementations. But this capability did not cover the full spectrum of applications. We have supplemented the Lanczos solver with a Power Method solver for implicit mechanic problems using the Inertia Relief Feature.

As we have been adding unsymmetric modeling features through materials, elements, and contact, we have added an eigensolver based on ARPACK for such problems. Important applications for the unsymmetric eigensolver are rotational dynamics and brake squeal analysis.

We are also developing an implementation of AMLS (Automated Multilevel Substructuring Method) for applications such as NVH that want hundred, even thousands, of eigenmodes quickly which are willing to have a less accurate solution compared to the Lanczos eigensolver.

## 1 Introduction

After the finite element discretization, LS-DYNA solves the following system of ODE's.

$$\ddot{M}a + Wv + Ku = f$$

Using the characteristic equation approach for the solution of ODE's we get a quadratic eigenvalue problem (QEP)

$$-\omega^2 M\Phi + i\omega W\Phi + K\Phi = 0$$

When  $W = 0$  (no damping) this becomes the first order eigenproblem

$$K\Phi = M\Phi\Lambda$$

When  $K$  and  $M$  are symmetric this is the standard vibration analysis problem.

The rest of this paper will highlight the variations of eigenvalue problems that can now be posed and solved in LS-DYNA.

## 2 Various Eigenvalue Problems

For many years, LS-DYNA has used the Block Shift and Invert Lanczos software, both in SMP and MPP, to solve the standard vibration analysis problem. Lanczos assumes that  $K$  and  $M$  is symmetric positive semi-definite. And that some linear combination of  $K$  and  $M$  is nonsingular.

The last requirement is equivalent to requiring  $K$  and  $M$  not to have a common null space. In the engineering world this means no massless mechanisms.

LS-DYNA also uses the Block Shift and Invert Lanczos software for the buckling analysis problem where  $K$  is symmetric positive definite and  $K\delta$  (the geometric stiffness matrix) is symmetric but indefinite. Because  $K\delta$  is indefinite  $K$  must be positive definite. This requirement causes a problem with the buckling analysis of structures in flight. To perform the time simulation Implicit uses the Inertia Relief feature that uses a LaGrange formulation to constrain out the rigid body motion. Leaving out



these constraints makes K indefinite due to the rigid body motion. Removing the constraints by our usual approach turns the factorization dense. Leaving the constraints in K using the LaGrange formulation turns K symmetric indefinite and Lanczos no longer is applicable. To solve such problems we added a Power Method eigensolver. This method is chosen automatically for such problems (Buckling with Inertia Relief).

LSDYNA usually ignores the Implicit Dynamic terms for the eigenvalue analysis. But EIGMTH=6 (see \*CONTROL\_IMPLICIT\_EIGENVALUE) includes the dynamic terms to the stiffness matrix. This is particularly useful for model validation and debugging. EIGMTH=6 includes the mass matrix in the eigensolution. EIGMTH=5 analyzes only the stiffness matrix.

LSTC extended this model validation and debugging to our mechanical thermal applications using \*CONTROL\_THERMAL\_EIGENVALUE. This performs a eigenvalue computation using just the thermal conductance matrix.

Recently LSTC has been adding the ability to add certain unsymmetric terms to the stiffness matrix (see \*CONTROL\_IMPLICIT\_SOLVER). These terms can come from certain materials and certain elements and from certain contact types. These terms are required in some applications to properly model the physics. The unsymmetric stiffness matrix means that Lanczos is no longer applicable. For these problems we have added ARPACK, a public domain software from Rice University based on the Arnoldi method. A particular important application for such an unsymmetric eigenvalue analysis is brake squeal. For brake squeal capturing the unsymmetric terms from contact due to the warped rotor is critical to the modeling the physics.

At the time of the writing of this paper the use of ARPACK in LS-DYNA is only available in the SMP versions. Our long term plans do include using the Parallel version of ARPACK, PARPACK, for the MPP version.

LS-DYNA can also add damping terms to the unsymmetric analysis. This requires going back to the original quadratic eigenvalue problem. Since the eigensolution software requires a first order eigenvalue problem we make a variable substitution and double the order of the eigenvalue problem. For such problems we again are using ARPACK.

Finally the addition of Rotational Dynamics modifies the stiffness matrix with spin softening terms and adds first order terms of gyroscopic effects. Again for such problems we are using ARPACK.

### 3 Automatic Multi Level Substructuring

Automatic Multi Level Substructuring, known by its acronym AMLS, is used in the Noise, Vibration, and Harshness community to compute hundreds or thousands of eigenmodes for automotive models. These eigenmodes are used for frequency domain computations. AMLS reduces the full scale model using a recursive application of the Craig-Bampton substructuring approach to a smaller model. The eigensolution is then computed on the smaller model. The eigenvalues and eigenvectors computed by AMLS are approximations to the eigenvalues and eigenvectors for the full scale model. But AMLS requires far less computing resources than Lanczos on the full scale model.

LSTC is actively implementing AMLS. At the time of the writing of this article we have a functional implementation for small and moderate size problems. We hope to provide some full scale results with the LSTC implementation of AMLS at the time of the conference.

# Simulation with implicit time integration of high loaded areas of a forming tool for large presses using LS-DYNA

Fabian Koch<sup>1</sup>, Philipp Thumann<sup>1</sup>, Dr. Marcus Wagner<sup>1</sup>, Bertram Suck<sup>2</sup>, Dr. Josef Meinhardt<sup>2</sup>

<sup>1</sup>Ostbayerische Technische Hochschule Regensburg, Laboratory for Finite Element Analysis and Structural Dynamics, Galgenberstraße 30, 93053 Regensburg, Germany

<sup>2</sup>BMW Group, Production System, Technical Planning, Tool Shop, Plant Construction - Standards, Innovations, Knorrstr. 147, 80788 München, Germany

## 1 Abstract

The recent increase of stroke rates in sheet manufacturing for automotive industry leads to an equal increase of the structural dynamic load on the involved forming tools. This demands an evaluation of the lifetime of the tool components in order to guarantee the required life time. For a life time prediction very accurate stress values are needed, which can be achieved by using the finite element method (FEM) with implicit time integration. This project describes the workflow for creating a whole simulation of a forming tool for large presses, the investigation of a stand-alone model with explicit time integration and the use of a substructure model for life time prediction with an implicit time integration. LS-DYNA is used for the all numerical simulations.

## 2 Introduction

Nowadays, the constantly increasing higher productivity of car body sheets in automotive sheet manufacturing leads to rising the stroke rates of the forming tools and accordingly bringing higher loads to the tool components. To investigate the influence of the increased stroke rate, a complete forming tool was firstly modeled and simulated with the LS-DYNA solver including all the necessary boundary conditions [1] [2]. Subsequently, a simulation with a rate of 18 instead of 14 strokes per minute was carried out. A stand-alone model of a so-called pressure pad was then developed, where the boundary conditions were obtained from the previous forming tool simulation. Finally, a substructure model was generated to get data from the FEM simulation for a following life time fatigue analysis [3].

## 3 Working principle of a forming tool

The deep drawing tool (see Fig.1, left) is part of a press working line and it is used for sidewall framework production of a car. During the downward movement of the upper tool parts, 39 pressure pins get in contact with the pressure plate at a specific position. These pressure pins are mounted to the pressure pad. Due to a defined movement of a servo drive, the press slide, which includes six lower cylinders, moves downwards. These lower cylinders are impinged with compressed air and can perform a pressure force of 150 kN onto the pressure plate. Thereby the upper die shifts the forming slide, bringing the forming jaws to the left. The forming slide shapes the plate at the lateral area. Simultaneously, the plate is fixed by the pressure pad and is also post-shaped at few positions. An integrated trimming segment cuts the blank five times. After the forming of the sheet metal and the cutting process, the tool opens due to the movement of the upper tool parts towards to the start position. [2]



Fig. 1: Left: Principle model of a deep drawing tool according to. [2]  
Right: FEM model of the deep drawing tool with an exploded view. [3]

## 4 Simulation procedure by using LS-DYNA

In the following subchapters the single steps of developing the procedure to gain input data for a following study for life time prediction by using LS-DYNA are presented.

### 4.1 Model of complete forming tool (explicit)

The initial FEM model can be seen in Fig.1, on the right side, in which the press body, the press head and the press stand are modelled as single hexahedron solid elements. The picture on the very right side displays the most important inner parts of the deep drawing tool model, in exploded state. Among others are the upper and the lower die and also the pressure pad. Most components of the deep drawing tool model are discretized by tetrahedron elements. The complete number of elements of the model amounts to 3282593, which include tetrahedron, pentahedron and hexahedron elements. Furthermore, linear initial functions are used in the formulation of the volume elements, in order to hold the calculation time as low as possible. [3] [4]

### 4.2 Stand-alone model (explicit)

The setup of the stand-alone model of the pressure pad includes the definition of necessary boundary conditions and the transfer of parts of the complete tool model. This setup constitutes the basis for the simulation of the working stroke. In order to build the stand-alone model of the pressure pad as realistic as possible, certain boundary conditions of the complete tool model should be accessed. This relates primarily to the parts which limit and stabilize the pressure pad during the movement. Special attention is given to the parts which have a limiting function in the start position of the modelling, see Fig.2 on the left side. [2]



Fig.2: Left side: Stand-alone model of the pressure pad with slide plates and upper die surfaces. [5]  
Right side: Global stand-alone pressure pad model with integrated substructure parts. [5]

### 4.3 Substructure model (implicit)

Within the FEM-modelling, the substructure method is useful for a detailed investigation of sections of parts. After the simulation of a specific problem is completed, the most stressed sections of a part can be simulated with a refined mesh. In the case of the stand-alone model of the pressure pad, the loaded sections (Fig.2, enlargements on the right side) are investigated in detail with this method. [5]

## 5 Outlook

In the next step of this project, the results of the stand-alone pressure pad simulation and the results of the substructure model simulation will be used for a computational fatigue life prediction of the pressure pad. Additional investigations have to be still performed before a load spectrum can be defined.

## 6 Literature

- [1] LSTC Inc.: LS-DYNA® (a general-purpose finite element program). <http://lstc.com>.
- [2] Swidergal, K., et al: "Experimental and numerical investigation of blankholders vibration in a forming tool: a coupled MBS-FEM approach", Production Engineering, vol. 9, pp. 623–634, 2015.
- [3] Koch, F.: "Stress analysis of a deep drawing tool with the finite element method", Applied Research Conference ARC 2016, Augsburg
- [4] LSTC, LS-DYNA® KEYWORD USER'S MANUAL: VOLUME 1 R8.0, 2015.
- [5] Koch, F.: "Model setup and FE-simulation of a forming tool component", Project report, OTH Regensburg, FEM-Laboratory, Regensburg 2016

## **Funktionssimulation: Deckelsimulation mit LS-DYNA**

M. Geuther  
Dr. Ing. h.c. F. Porsche

H. Abboud  
GNS

## **Funktionssimulation: Spoilersimulation mit LS-DYNA**

M. Geuther  
Dr. Ing. h.c. F. Porsche

B. Gajewski  
Bertrandt

## **Funktionssimulation: Dichtungssimulation mit LS-DYNA**

M. Geuther  
Dr. Ing. h.c. F. Porsche

I. Jurrmann  
Bertrandt

# FE oriented Virtual Test of Closure Systems

Christian Gembus, Dr. Gregor Büdding, Wolfgang Rieger

Brose Schließsysteme GmbH & Co. KG, Wuppertal, Germany

## 1 Introduction

Closure systems are an important element of the automotive passenger safety concept. They include common standard functionalities such as ensuring closure, opening and locking functions. Furthermore, they are enhanced by customer specified comfort functionalities, for example central lock, double lock, open-by-wire (OBW), electrical child safety and soft close automatic (SCA). The integration and realization of all functions leads to a complex mechatronic component in the door system of a vehicle. It contains strongly coupled mechanic and mechatronic operation chains.

The continuously rising requirements regarding costs, weight and development times can't be satisfied by only analytical approaches anymore. Therefore in the field of virtual strength and structure testing at Brose, methods have been established that enable the simultaneous FE analysis of the single part strength and the overall system performance, including the main effecting boundary conditions, e.g. loads caused by springs or electrical drives. These simulations are part of a specific virtual test program that covers the various product requirements. The aim is the evaluation of a new product design in a very early design phase and therefore the reduction of expensive hardware testing loops.

## 2 General Build Up of Closure Systems

The key features of a latch are the closure parts consisting of rotor, pawl, pins and back plate, see Figure 1. They are dimensioned to withstand high static and dynamic forces (e.g. crash) but have to guarantee at the same time an easy access (in a way with low handle forces) to the door.

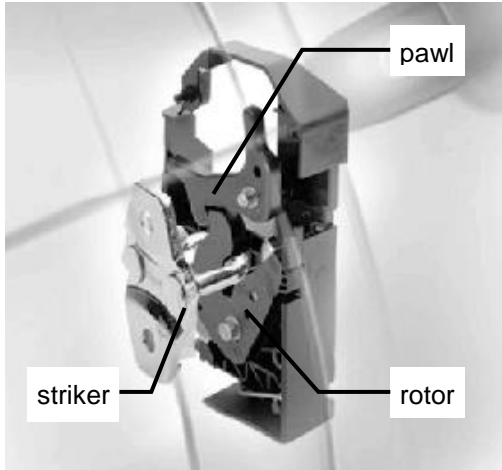


Fig.1: side door latch with striker

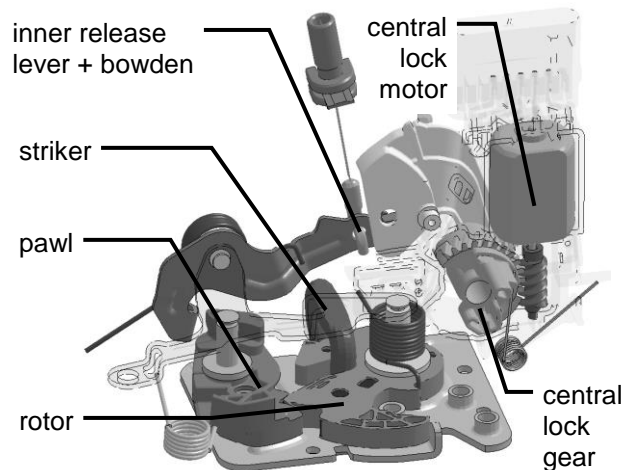


Fig.2: closure parts with mechatronic chain

Opening and locking is realized by mechanical lever chains acting onto the closure parts, e.g. outer or inner release chains, which are connected to the corresponding door handles via Bowden cables. Most of the levers are loaded by leg springs in order to rotate back and to keep its starting position, even when effected by crash accelerations. Comfort functionalities are typically implemented with motor driven gears. In Figure 2 is shown a latch with one mechatronic chain, the central locking chain.

## 3 Dynamic Overload Strength Test

The FE-based virtual test setup is divided in three main fields: (1) the quasistatic tensile test of the closure parts in all relevant directions according to FMVSS 206, (2) the quantitative and dynamic overload calculations of all existing operation chains in the latch and (3) the mechanical stop

simulations of all existing mechatronic chains. The focus of this paper is the dynamic overload test of mechanic lever chains because this load case covers most of the modeling issues.

Excluding the meshing, the main aspects regarding the model build up close to the real test set up will be discussed. Due to the high complexity, an efficient contact generation is needed. Getting the realistic nonlinear load also in the mechatronic chains a suitable model of a DC motor is created. The boundary conditions are oriented by the real test equipment.

### **3.1 Standardized automatic generation of latch specific contacts**

The basis of an efficient contact definition is the unique identification of all possibly occurring components in a latch. A part library with function oriented standardized short names and related identification numbers is created. More than 600 different parts are available in this library.

The theoretically possible number of 100'000 contact pairs had to be reduced significantly for efficient handling in simulation and post processing. An analysis of practically occurring part interactions resulted in 4'600 relevant contacts collected in a master contact template. A specific latch consists of a subset of all parts in the part library and the contacts for this subset are detected by a python script. The script derives additional contacts, where a detailed analysis requires a further subdivision of contacts. Depending on the complexity of a latch, this results in 100 to 250 actually occurring contacts.

### **3.2 Integration of electro-mechanic DC motor operation**

Due to the short operation times of locking functions a strongly nonlinear behavior of the DC motor has to be taken into account. A defined operation point cannot be detected in the characteristic curves of the motor.

The electrodynamic behavior of the DC motor can be approximated by an equivalent network. This network should be able to calculate the current in normal operation mode as well as in a short circuit constellation. The small finite elements in the latch model lead to very small integration steps. This enables the combination of the electrodynamic differential equation with a simple Euler based integration step. Thus it is possible to include the motor model together with the integrator by the usage of common LS-Dyna-Keywords.

### **3.3 Boundary conditions**

Nowadays a latch is connected to its mechanical interfaces by Bowden cables. In the corresponding test setup, the chain is activated at a constant high Bowden cable velocity that is three times the normal velocity. This reproduces the fast pulling of the door handle by the user. These cable velocities are applied by developed standard templates. Furthermore, a constant door seal load is applied onto the striker as a second force based boundary condition. Additional to the opening movement of the inner release lever chain and pawl, the status of the central lock chain including gear and motor has to be reset. It is changed from "locked" to "unlocked", the so called "override" function. The motor inertia and – when intended – the counteracting short circuit torque are passive loads.

### **3.4 Evaluable Results**

The results of this load case are the measurement of force and displacement at the Bowden cable that are necessary to open the latch. Furthermore the stresses and deformations are derived for each single part, those in the operating chain as well as for the housings. Potential for improvements regarding strength or weight is identified and verified in another simulation loop.

## **4 Summary**

This paper presents the combination of mechanic and mechatronic components into a single simulation model with the objective of reproducing the complex boundary conditions of the real test setup. This is essential in highly function oriented part designs, e.g. closure systems in order to detect the highest single part load within a wide operating range and the effect of coupled velocity dependencies. Simultaneously the total dynamic performance regarding Bowden force and travel is calculated. This virtual test allows the first verification of a concept design as well as the detailed strength evaluation.

# Simulation of Wear Processes in LS-DYNA

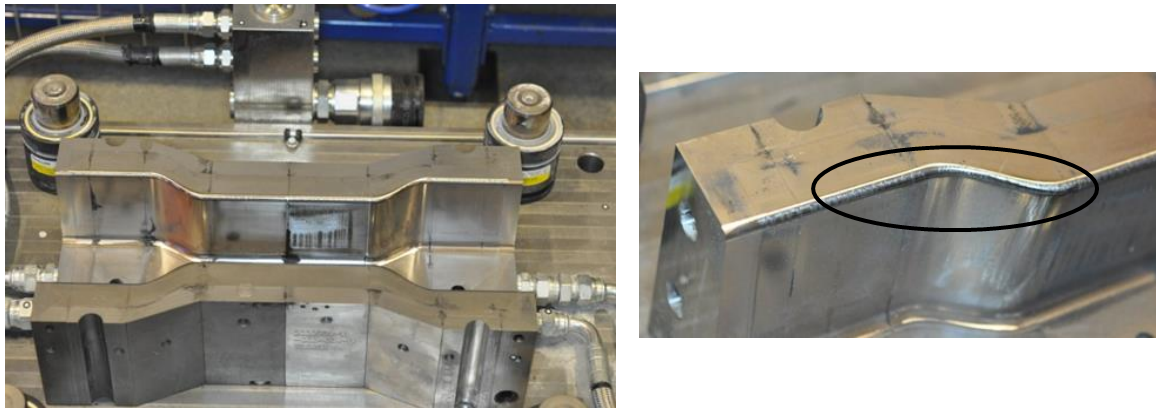
Thomas Borrvall<sup>1</sup>, Liang Deng<sup>2</sup>, Anders Jernberg<sup>1</sup>, Mikael Schill<sup>1</sup> and Mats Oldenburg<sup>2</sup>

<sup>1</sup>DYNAmore Nordic AB, Linköping, Sweden

<sup>2</sup>Luleå Technical University, Luleå, Sweden

## 1 Introduction

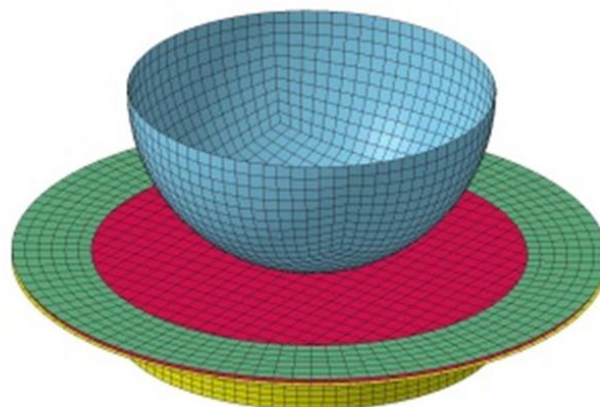
Wear is a major factor in decreasing the quality and increasing the cost of equipment maintenance of mass production. In press hardening, a heated work-piece in austenite phase is formed into a target shape and then a cooling process decreases the temperature of the work-piece below the martensite state. The harsh contact conditions, such as high pressures and cyclic temperatures, cause scratches or scars when the work-piece slides over the tools, which are so-called sliding wear, see *Fig. 1*. The present paper outlines how LS-DYNA in combination with LS-PrePost predict the tool wear of press hardening in virtual environment, which allows users to improve the tool design and deepen the understanding of the mechanism behind the wear.



*Fig. 1: Wear induced by repeated strokes in hot forming*

## 2 Keywords

By means of an example, shown in *Fig. 2*, we briefly introduce the keywords necessary for simulating wear.



*Fig. 2: Deep draw example*

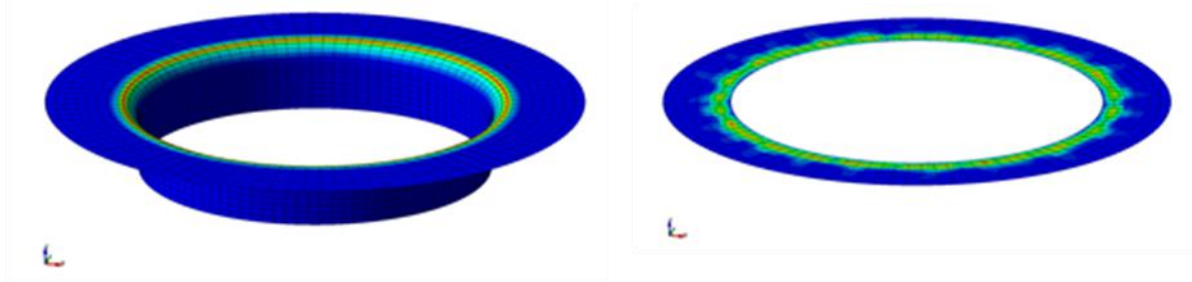


Fig. 3: Wear on tools

## 2.1 Post-Processing of Wear

The first step would be to simply add the keywords that allow for post-processing the wear depth from *one* stroke of the punch. Note that this will *not* affect the results of the simulation but is only a post-processing feature, and is available in version R9. Two cards are needed for this purpose; `*CONTACT_ADD_WEAR` and `*DATABASE_EXTENT_INTFOR`. The first will associate wear to a given contact interface and the second is used for controlling wear output to the intfor database. The wear distribution from such a simulation is shown in Fig. 3.

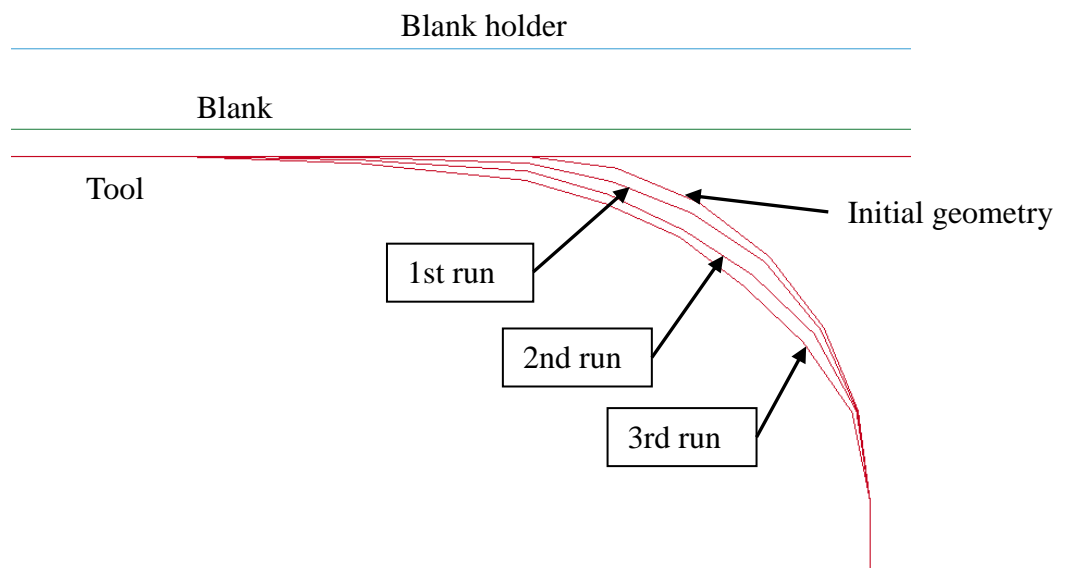


Fig. 4: Geometry change of die

## 2.2 Wear Influence on Tools

The second step would be to take it one step further, to allow wear to affect geometry, this is supported beyond R9. This requires repetitive simulations (stages) for which the *dynain* concept is used. The keyword `*INTERFACE_SPRINGBACK_LSDYNA` includes an option to write `*INITIAL_CONTACT_WEAR` keywords to *dynain*, and the *dynain* is used in subsequent simulations to modify the geometry. So in principle the procedure is fairly straightforward and simple, but it may take some efforts to make it work satisfactory. To this end, LS-PrePost has been equipped with a wear interface to facilitate the intermediate processing steps. The geometry change of the die in our example is shown in Fig. 4.

## 3 Reference

A comprehensive elaboration on the wear capabilities in LS-DYNA can be found in the proceedings of the 14<sup>th</sup> International LS-DYNA Users Conference, title "Simulation of Wear Processes in LS-DYNA", [www.dynalook.com](http://www.dynalook.com).



# Messung und Simulation von Verschleiß in einem anwendungsnahen tribologischen Prüfstand

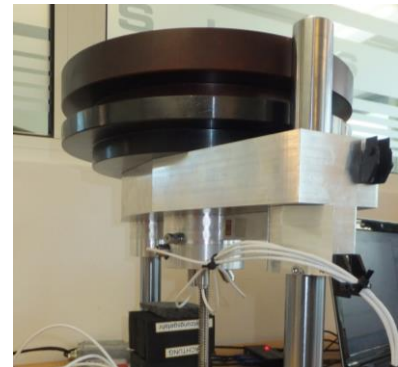
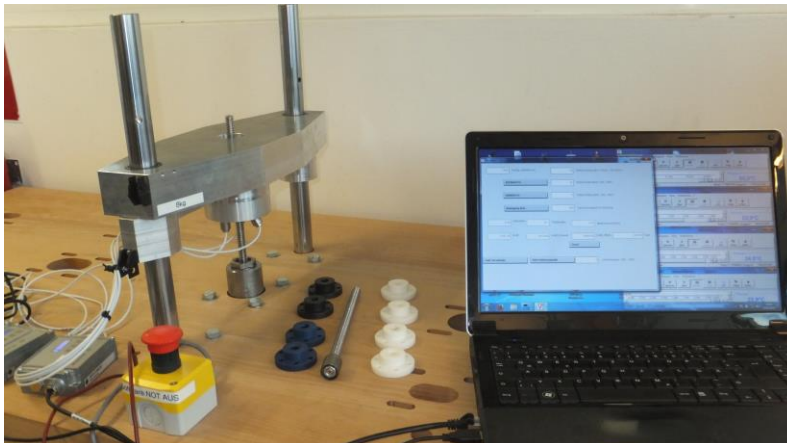
Artur Fertschej, Benjamin Hirschmann, Peter Reithofer (4a engineering GmbH)

## 1 Einleitung

Materialkombinationen Metall/Kunststoff werden heutzutage bevorzugt für tribologische Systeme eingesetzt, die einen langlebigen, wartungs- und schmierungsfreien Einsatz garantieren sollen, wie z.B. die Paarung Metallspindel/Kunststoffmutter. Spezielle dafür geeignete Kunststoffcompounds wurden an einem anwendungsnahen Tribologieprüfstand charakterisiert. Für die virtuelle Abbildung des Verschleißes wurde eine Simulationsmethodik entwickelt, anhand realer Messungen am Tribometer und dem zuvor genannten Tribologieprüfstand überprüft und verbessert. Ziel ist es, zukünftig dem Anwender durch virtuelle Vorhersage raschere und zielgerichtete Produktentwicklung und Materialauswahl zu ermöglichen.

## 2 Anwendungsnaher Tribologieprüfstand

Mit dem Tribologieprüfstand wurden anwendungsnaher Messungen an Mutter-Spindel-Systemen durchgeführt (Abb. 1). Dieser Prüfstand ist besonders geeignet, die realen Verhältnisse zwischen Mutter und Spindel (angepasste Geometrie, reale Lastverteilung und Temperaturentwicklung, diskontinuierliche Versuche etc.) bei variablen Versuchsbedingungen (Belastung, Drehzahl) wieder zu geben. Als Standard-Mutter ist eine Trapezgewindemutter TR12x3 vorgesehen.

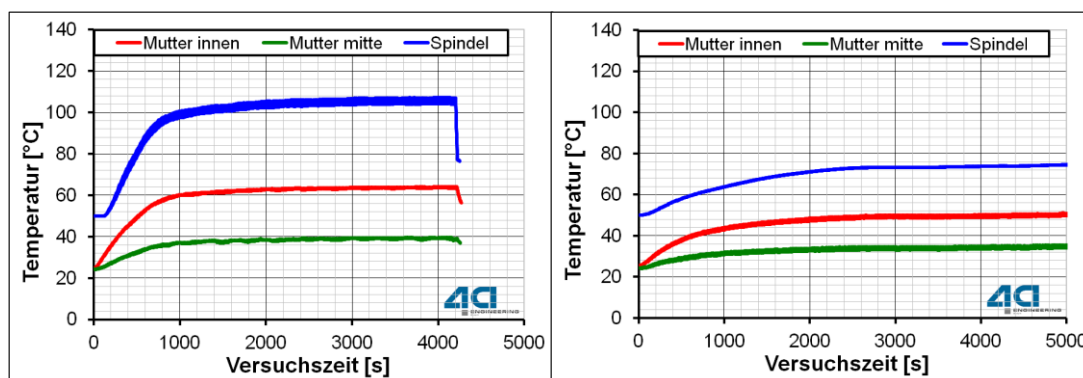


**Abb. 1:** Anwendungsnaher Tribologieprüfstand im Einsatz (links ohne und rechts mit Zusatzgewicht)

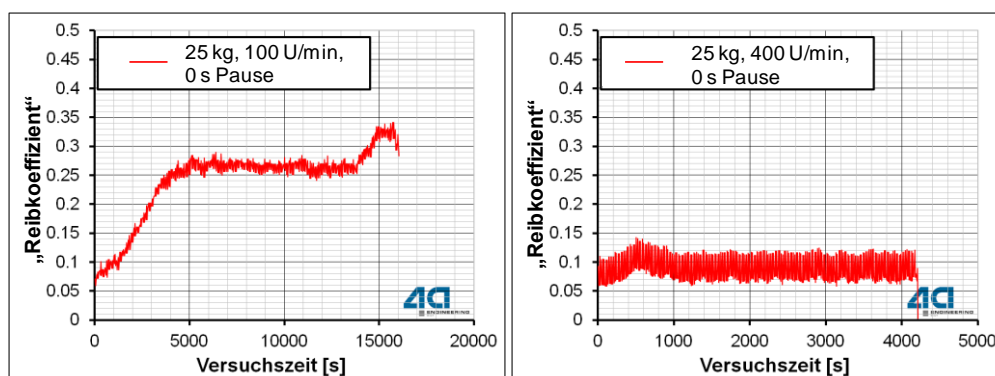
Um die örtliche und zeitliche Temperaturentwicklung von Mutter und Spindel messen zu können, wurden insgesamt 4 Infrarot-Sensoren im Messschlitten eingebaut. Ein IR-Sensor misst die Temperatur der Spindel, die anderen drei IR-Sensoren messen die Temperatur der Mutter in unterschiedlichem Abstand zur Spindel. Aus diesen drei Werten kann der Temperaturverlauf über den gesamten Bereich der Mutter für den Simulationsvergleich abgestimmt werden.

## 3 Messergebnisse

Abb. 2 (links) zeigt einen typischen gemessenen Temperaturverlauf. Die spindelnahe Muttertemperatur erreicht bis zum Ende des Versuchs ca. 65°C, die Muttertemperatur in der Mitte hingegen nur ca. 40°C. Die Spindeltemperatur kann erst ab 50°C gemessen werden und erreicht Temperaturen bis zu 115°C. Abb. 2 (rechts) zeigt vergleichsweise die Temperaturentwicklung, wenn eine Pause von 7.5 Sekunden pro Zyklus (eine Auf- und Abwärtsbewegung am Prüfstand) eingelegt wird. Die maximalen Temperaturen sind deutlich geringer. Abb. 3 zeigt am Tribologieprüfstand ausgewertete Reibkoeffizienten für zwei verschiedene Geschwindigkeiten. Für 100 U/min ergibt sich ein höherer Reibkoeffizient als für 400 U/min, der Grund könnte in der Temperaturentwicklung liegen. Bei 100 U/min ergibt sich eine geringere Spindel- und Muttertemperatur als bei 400 U/min. Möglicherweise bildet sich bei höheren Temperaturen ein Schmierfilm aus, der die Reibung senkt.



**Abb. 2:** Temperaturentwicklung der Mutter an 2 Messpunkten sowie mittlere Spindeltemperatur (400 U/min, 25kg); links: keine Pause, rechts: 7.5 s Pause



**Abb. 3:** Ausgewertete Reibkoeffizienten aus dem Versuch am Tribologieprüfstand

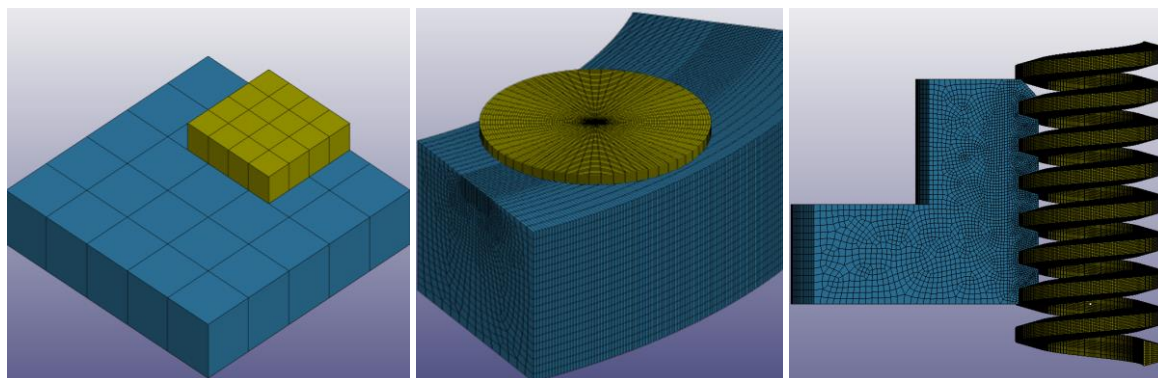
#### 4 Simulation

Zur Vorhersage des Verschleißes von Metallspindel/Kunststoffmutter Paarungen wurde eine Simulationsmethodik erarbeitet und validiert. Die virtuelle Abbildung von tribologischen Vorgängen ist komplex und somit sehr aufwändig und keineswegs mit standardmäßig verfügbaren Simulationswerkzeugen umsetzbar. Zur Methodenentwicklung wurden drei verschiedene Modelle verwendet (Abb. 4):

**einfach:** Simple-Mind Modell zum Austesten auf prinzipielle Funktionalität

**komplex:** typisch verwendetes Kugel/Scheibe-Tribometer

**realitätsnah sehr komplex:** Tribologieprüfstand



**Abb. 4:** Simple-Mind Modell (links), Kugel/Scheibe Modell (mittig) und Tribologieprüfstand (rechts)

Die Idealisierung im Kontaktbereich bzw. Verschleißzone wurde wie aus den Abbildungen hervorgeht sehr fein gewählt (Elementkantenlänge  $25\mu\text{m}$  bzw.  $100\mu\text{m}$ ). Dies stellt einen Kompromiss zwischen möglichst genauer Abbildung und Rechenzeit dar.

#### 4.1 Simple-Mind Modell

Aufgrund der einfachen Geometrie und geringen Elementanzahl können mit einem solchen Modell sehr rasch verschiedene Methoden oder Materialmodelle auf ihre prinzipielle Funktion für die Problemstellung untersucht werden.

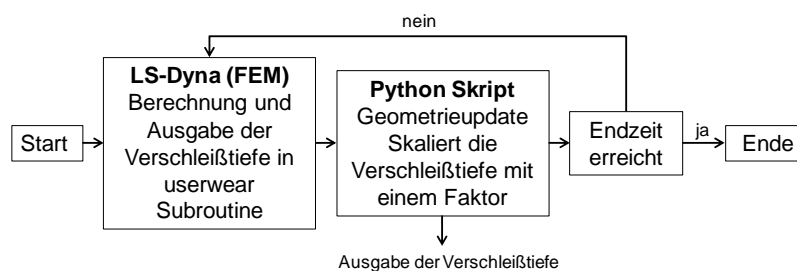
In einer Literaturrecherche wurden verschiedene Verschleißansätze gesichtet und bewertet. Berechnungen mit LS-Dyna unter Zuhilfenahme der Kontaktformulierung \*CONTACT\_ADD\_WEAR und Archard's Verschleißgesetz (direkt oder mittels USERSUBROUTINE) zeigten sich als eine geeignete Möglichkeit, Verschleiß zu prognostizieren. Derzeit ist diese Funktion nur in der LS-DYNA Development Edition 8.1 in Kombination mit LS-PrePost 4.3beta verfügbar. Als Ergebnis erhält man eine örtliche Verschleißintensität, die jedoch keinen Einfluss auf die weitere Berechnung hat (nur Ausgabewert). Für die Anpassung der Geometrie aufgrund des auftretenden Verschleißes wurde daher unterschiedliche Ansätze (LSPrePost, Skripte oder USERSUBROUTINEN) untersucht und verglichen (Kopplung zwischen Verschleiß und Geometrie, vgl. Abb. 8 mitte).

Als Materialparameter werden der Elastizitätsmodul, die Querkontraktion, der Reibkoeffizient und der Verschleißkoeffizient aus dem Gesetz nach Archard benötigt. Der Verschleißkoeffizient kann entweder der Literatur entnommen oder mit tribologischen Versuchen bestimmt werden.

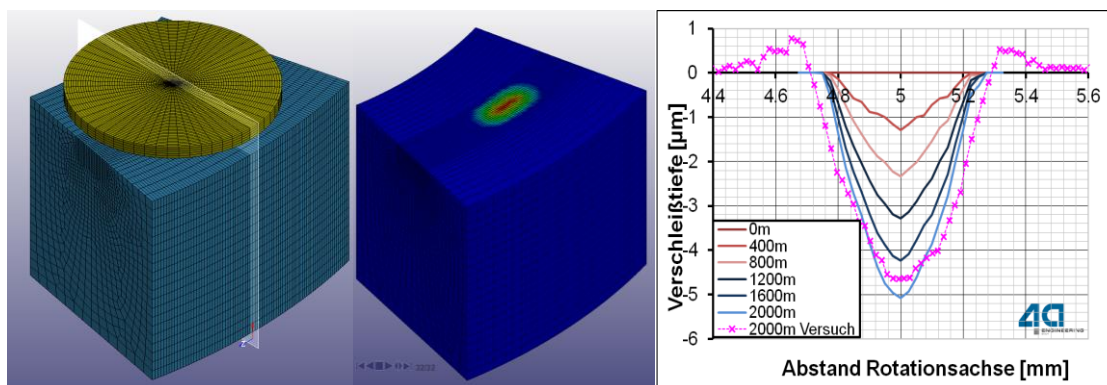
#### 4.2 Kugel/Scheibe Tribometer

Um die Verschleißtiefenprognose der entwickelten Methodik zu überprüfen und zu validieren, wurde im 2. Schritt ein Kugel/Scheibe-Tribometer herangezogen. Für diesen Fall ist ein Abgleich zwischen Versuch und Simulation möglich. Das Verschleißprofil aus dem Versuch wird mit einem Weißlichtinterferometer gemessen.

Verschleißversuche benötigen eine hohe Belastungszeit, um messbare reproduzierbare Ergebnisse zu erhalten, daher kann die Simulation des Versuches nicht direkt erfolgen. Abb. 5 zeigt die entwickelte und verwendete Berechnungsroutine, um die Geometrie aufgrund der berechneten Verschleißtiefe schrittweise zu aktualisieren. Die Routine kann prinzipiell in beliebige Zeitschritte unterteilt werden, wobei nach jedem Zeitschritt das Ergebnis mit einem dem Zeitschritt entsprechenden Skalierungsfaktor auf Basis eines Verschleißgesetzes beaufschlagt wird.



**Abb. 5:** Berechnungsroutine zur Implementierung des Verschleißes



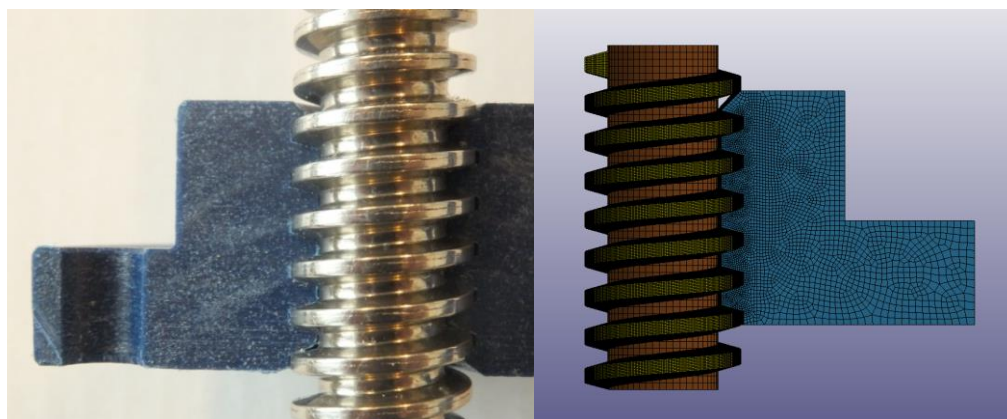
**Abb. 6:** Kugel/Scheibe Modell (links); Simulationsergebnis der Verschleißtiefe nach 1. Rechenschritt (Mitte); Vergleich Simulation (mit Zwischenergebnissen) mit Experiment nach 2000m (rechts)

In Abb. 6 Mitte ist das Verschleißergebnis des 1. Rechenschrittes dargestellt. Bei 5-fachem Durchlaufen der Schleife (Abb. 5) mit einem konstanten Verschleißkoeffizienten ergibt sich ein schmaleres Verschleißprofil im Vergleich zur gemittelten Versuchsprofilkurve (Abb. 6 rechts). Die Berücksichtigung der Viskoelastizität bzw. der Plastizität, an deren Implementierung gearbeitet wird, sollte ein breiteres Profil und somit ein bessere Übereinstimmung zwischen Versuch und Simulation ergeben.

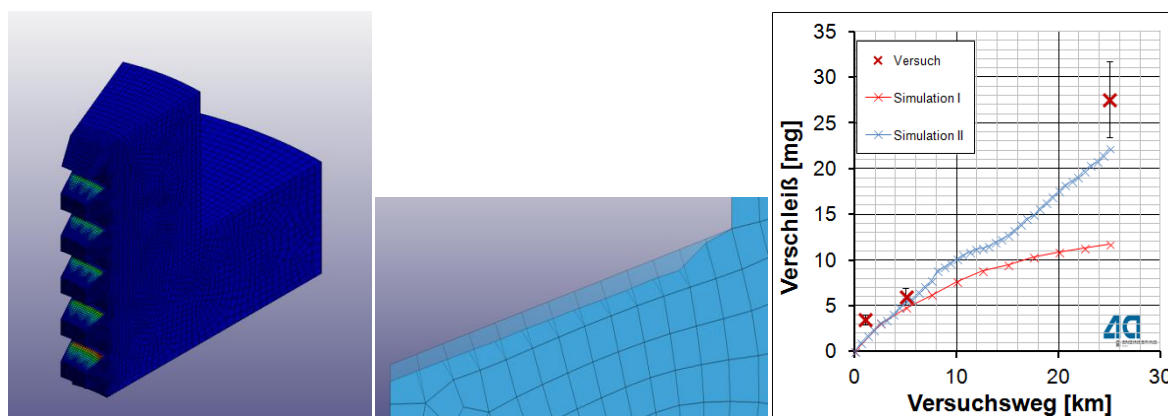
### 4.3 Tribologieprüfstand

Als anwendungsnahen Fall wurde die Simulationemethodik am Tribologieprüfstand validiert. Um die Rechenzeiten in einem sinnvollen Bereich zu halten, wurde ein Sechzehntel-Modell des Mutter-Spindel Tribometers erstellt (Abb. 7). Die Berechnungsmethode wird analog zum Kugel-Scheibe-Tribometer angewandt.

Aufgrund der Geometriediskretisierung können lokale Unstetigkeiten an der Oberfläche auftreten, welche diskontinuierliche Kontaktkraftverläufe bewirken. Diese werden mit einer weiterentwickelten Methode gefunden und geglättet, somit tritt ein gleichmäßiger Verschleiß auf. Mithilfe der Methode gelingt ein erster Kompromiss zwischen Rechenzeit und Genauigkeit, an einer Optimierung der Rechenzeitschrittweite wird derzeit noch gearbeitet. Abb. 8 zeigt erste Ergebnisse der Verschleißsimulation und den Einfluss der Rechenzeitschrittweite auf das Ergebnis.



**Abb. 7:** Querschnitt einer Mutterprobe mit Trapezspindel (links), Sechzehntel-Modell des Tribologieprüfstands (rechts)



**Abb. 8:** Verschleißsimulationsergebnis der Ausgangsgeometrie (links), Profilprognose eines Gewinde-teilstücks für 25 km (mittig) und Verschleiß über den Versuchsweg in Abhängigkeit der Rechenzeitschrittweite (rechts)

## 5 Zusammenfassung & Ausblick

Mit dem Tribologieprüfstand können Mutter/Spindel-Kombinationen anwendungsnah geprüft werden. Der Vorteil solcher Messungen gegenüber Standard-Tribometern liegt in den realitätsnahen Geometrien und Versuchsbedingungen. Erste Berechnungsergebnisse von verschiedenen tribologischen Versuchen zeigen, dass mit der entwickelten Simulationemethodik der Verschleiß und die dadurch resultierende Geometrieabnahme bereits gut berechnet werden können. Die Simulation liefert somit dem Anwender eine Unterstützung zur Verständnisgenerierung komplexer Vorgänge und somit eine deutliche Aufwandsreduktion in der Entwicklung. Als Ausblick für die Simulation kann die Verwendung komplexerer Material- (Temperatur, Plastizität, Zeitabhängigkeit) und Verschleißmodelle gegeben werden. Die Entwicklung auf Kunststoffe abgestimmter Labortests kann ebenfalls auf Basis dieser Arbeiten erfolgen. Dies würde vor allem zu einer besseren zeitlichen Abbildung des Verschleißfortschrittes und der Ausfallszeit führen.

# Control System

Isheng Yeh<sup>1</sup>, Charlotte Keisser<sup>2</sup>

<sup>1</sup>Livermore Software Technology Corporation, Detroit, MI, USA

<sup>2</sup>DYNAmore France, 78000 Versailles, France

## 1 Introduction

Cruise controls, ABS, pre-crash systems, Human Body (...) are control systems which are part of our daily life. The study and design of automatic control has become more and more popular and has been part of LS-DYNA research and development over the last 2 years.

## 2 Definition

Control is the process of making a system follows a desired behavior (example of a thermostat controlling/regulating the room temperature). The idea is to use output measurements of the system (provided by sensors) and then adjust and control the system (using actuators).

One of the most popular control tool is the so-called PID controller (`*DEFINE_CURVE_FUNCTION` with `PIDCTL` function).

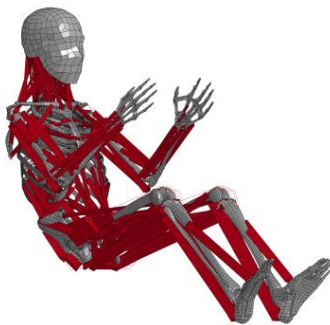


Fig.1: *PIDCTL for Active Muscle for HBM by Chalmers University, Sweden.*

## 3 LS-DYNA

Several FEM software already uses Control System capabilities, and most of them use MATLAB/Simulink Control System toolbox for that purpose.

In LS-DYNA future Control System toolbox, there will be two approaches:

- A connection between LS-DYNA results and MATLAB:
  - It will be possible to extract from LS-DYNA results a MATLAB file.
  - Then, with that file, the user could run MATLAB/Simulink toolbox for Control System purpose.
  - Finally, the user will be able to use MATLAB results to re-run LS-DYNA.
- A Control System toolbox inside LS-DYNA :
  - Directly included in LS-DYNA.
  - It will be possible to use the toolbox the same way than for MATLAB.
  - A LS-DYNA Control System GUI will be available.
  - It will be possible to do everything in only 1 run of DYNA (like for PIEZO-ELECTRIC material).

## 4 Summary

The aim of this presentation is to give you an introduction on Control System, LS-DYNA current developments and to collect any suggestions or remarks.

# Latest Developments in Automotive Aerodynamics using LS-DYNA®

Iñaki Çaldichoury<sup>1\*</sup>, Facundo Del Pin<sup>1</sup>, Rodrigo Paz<sup>1</sup>

<sup>1</sup> Livermore Software Technology Corporation, Livermore, CA, USA

\*Corresponding author. Email: inaki@lstc.com

LS-DYNA® is a general purpose explicit and implicit finite element program used to analyse the non-linear dynamic response of three-dimensional solids and fluids. It is developed by Livermore Software Technology Corporation (LSTC). A module to simulate incompressible flows has been added to LS-DYNA® for coupled fluid/mechanical/thermal simulations (ICFD solver).

It offers a response to the ever increasing need of engineers in the automotive industry sector and elsewhere to comprehend and solve complex highly nonlinear problems involving multiple domains of physics. However, if the ICFD solver is to become a viable proposition in automotive aerodynamics, it must demonstrate its ability to accurately reproduce the elementary phenomena observed on simple geometric forms in the wind tunnel.

With this objective in mind, the present paper will show for different wind speeds what results can be obtained on widely studied simplified car geometry, the Ahmed body, focusing on the complex 25° slant degree case.

## Keywords

Computational fluid dynamics (CFD), turbulent flow (RANS), Ahmed body, Multiphysics,

# Recent Updates for the Structural Conjugate Heat Transfer Solver in LS-DYNA®

Thomas Klöppel

DYNAmore GmbH, Stuttgart

## 1 Motivation

The strong multi-physics capabilities of LS-DYNA® make it a very powerful tool for the simulation of many state-of-the-art manufacturing processes. The demand for new features and code enhancements increases with increasing the complexity of the process.

This contribution presents recent developments within the heat transfer solver of LS-DYNA that have been implemented to meet this demand. Focus is put on welding and heat treatment simulations. Those are in most cases only a link in the virtual process chain and, consequently, have to be compatible with earlier and subsequent stages. Of particular importance are preceding forming steps that are usually realized using shell element discretizations for the processed part.

## 2 New Developments

### 2.1 Heat transfer along shell edges in contact

For thermal analyses of parts discretized with shell elements, LS-DYNA provides a thermal thick shell formulation with additional virtual nodes and an assumed quadratic temperature distribution along the thickness of the shell. The virtual nodes allow the reconstruction of the full three-dimensional temperature distribution.

The reconstruction is the basis of a new thermal contact algorithm designed to model heat transfer between a shell edge and a surface. The latter can either be represented by solid or by shell elements. As the results shown in Fig 1 demonstrate for a T-joint, the heat transfer from one part to the other is independent of the discretizations used for the different parts.

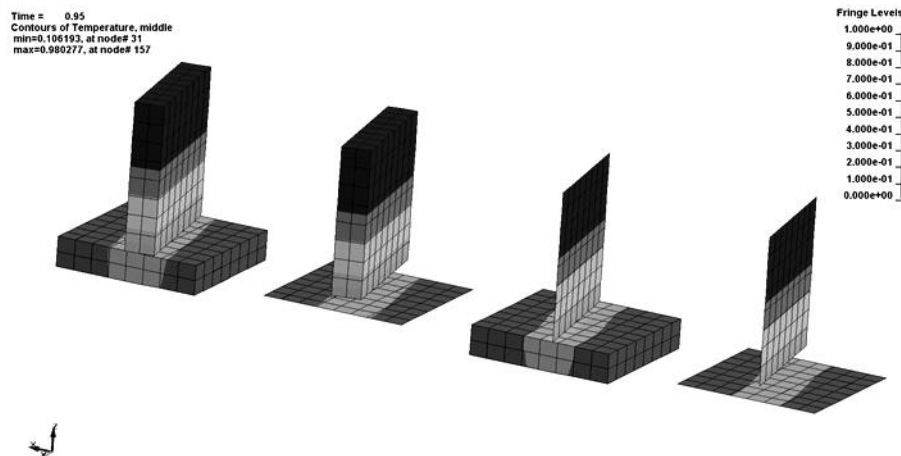


Fig.1: Resulting temperature fields in a T-joint using different discretizations. At the beginning of the simulation both parts of the T-joint have a homogeneous but different temperature distribution.

### 2.2 New heat source implementation

Welding simulations and simulations of local heat treatment require an accurate description of the heat source itself. In order to provide as much flexibility as possible in terms of the employed equivalent heat source model and of the underlying discretization of the work piece as well as to simplify the definition of the source movement, a new keyword `*BOUNDARY_THERMAL_WELD_TRAJECTORY` has been included, cf [1]. The development is based on the observation that in most line welding

processes the weld torch moves with a prescribed velocity on a pre-defined path. In the numerical representation this trajectory of the root of the weld torch is defined by a node set.

The new keyword features several methods to describe the orientation of the heat source. In many cases it is most convenient to use a segment set (usually the surface of the welded part) and to assume an aiming direction aligned with the averaged normal direction of the neighboring segments.

Although being widely used in industries, the Goldak equivalent heat source [2] might not be the best choice for all possible applications. A parameter in the keyword definition enables the user to choose between different equivalent heat source geometries, which are sketched in Fig.2.

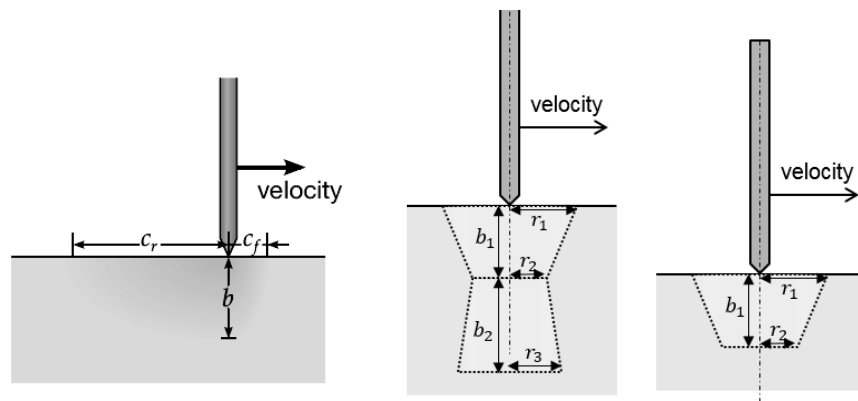


Fig.2: Sketch of different power density distributions: Ellipsoid heat source (left), double conical heat source (middle), conical heat source (right).

As already mentioned above welding and heat treatment are in most cases only links in the process chain, cf [3]. Most of the other process steps are usually simulated using shell meshes. The new keyword extends the welding functionality in LS-DYNA to the thermal thick shell elements mentioned above and, thus, enables an easy transition of data between different process stages.

### 3 Summary

This presentation puts its focus on new features implemented within the heat transfer solver of the multi-physics solver LS-DYNA. A new contact algorithm is introduced modelling the heat transfer between shell edges and surfaces by reconstructing the three-dimensional temperature distribution. Furthermore, a new boundary condition modelling the heat input by an exterior heat source moving along a prescribed and possibly complex path is presented. The keyword provides an easy and flexible input structure and can be used in combination with solid and thermal thick shell elements. The enhancements further increase the potential of LS-DYNA to be used for the complete virtual process chain..

### 4 Literature

References should be given in the last paragraph of your manuscript. Please use following scheme:

- [1] Klöppel, T., Schill, M., Loose, T., "Recent Updates for the Heat Transfer Solver in LS-DYNA with focus on computational welding mechanics," in *Proc. of 14th International LS-DYNA Conference*, Detroit, 2016
- [2] J. Goldak, A. Chakravarti and M. Bibby, "A Double Ellipsoid Finite Element Model for Welding Heat Sources," *IIW Doc.No.212-603-85*, 1985
- [3] M. Schill and E.-L. Oldenberger, "Simulation of residual deformation from a forming and welding process using LS-DYNA," in *Proc. of 13th International LS-DYNA Conference*, Detroit, 2014



---

# Saving Calculation Time for Electromagnetic/ Mechanical/Thermal Coupled Simulations by Using the New EM 2D/3D Capabilities.

Iñaki Çaldichoury<sup>1\*</sup>, Pierre L'Eplattenier<sup>1</sup>

<sup>1</sup> Livermore Software Technology Corporation, Livermore, CA, USA

\*Corresponding author. Email: inaki@lstc.com

LS-DYNA<sup>®</sup> is a general purpose explicit and implicit finite element program used to analyse the non-linear dynamic response of three-dimensional solids and fluids. It is developed by Livermore Software Technology Corporation (LSTC). An electromagnetism (EM) module has been added to LS-DYNA for coupled mechanical/thermal/electromagnetic simulations, which have been extensively performed and benchmarked against experimental results for Magnetic Metal Forming (MMF) and Welding (MMW) applications. These simulations are done using a Finite Element Method (FEM) for the conductors coupled with a Boundary Element Method (BEM) for the surrounding air, hence avoiding the need of an air mesh.

More recently, a 2D axisymmetric version of the electromagnetic solver was introduced for much faster simulations when the rotational invariance can be assumed.

In many MMF and MMW applications though, the rotational invariance exists only for part of the geometry (typically the coil), but other parts (typically the workpiece or the die) may not have this symmetry, or at least not for the whole simulation time.

In order to take advantage of the partial symmetry without limiting the geometry to fully symmetric cases, a coupling between 2D and 3D was introduced in the EM. The user can define the parts that can be solved in 2D and the ones which need to be solved in 3D and the solver will assume the rotational invariance only on the 2D parts, thus keeping the results accurate while significantly reducing the computation time.

In this paper, the coupling method will be presented along with benchmarks with fully 3D and fully 2D simulations, comparing the accuracy of the results and the simulation times.

Keywords

Simulation, Finite Element Method (FEM), Electroforming

---

# Towards a multi-physics material toolbox for LS-DYNA

Maik Schenke, Wolfgang Ehlers

Institute of Applied Mechanics, Chair for Continuum Mechanics, University of Stuttgart

## 1 Introduction

From a micro-structural point of view, many natural or engineered materials can be assigned to the class of multi-physics materials. Therein, their macroscopic observed behaviour is governed by different micro-structural physical phenomena. For instance, when electro-active polymers (EAP) are subjected to an electric field, the resulting chemical and electrical imbalances trigger micro-structural diffusion processes, which re-establish the equilibrium state, thereby causing macroscopic deformations. Further examples of these materials are partially or fully saturated porous media (e. g. foams, soils, filters, fibre-reinforced plastics), chemical- or electrical-active materials (e. g. hydrogels, lithium-ion batteries, fuel cells) or biological tissues (e. g. bone, cartilage). Addressing the simulation of multi-physics materials, which often exhibit a complex and heterogeneous micro-structure, it is convenient to proceed with a macroscopic modelling approach. In this regard, the aforementioned materials can be conveniently described exploiting the macroscopic Theory of Porous Media (TPM) as a suitable modelling framework, see, e. g., [1] for a brief insight into the underlying theory and possible application scenarios.

The present contribution illustrates the first steps in the development of a TPM-based toolbox for volume-coupled multi-physics materials for LS-DYNA. The toolbox proceeds from the stand-alone coupled finite-element solver PANDAS, which, however, is linked to LS-DYNA via the user-defined element subroutines. The coupling aims, on the one hand, at the access of the comprehensive material-model library of PANDAS and, on the other hand, allows, in comparison to the native user-element subroutines, a convenient environment for user-defined volume-coupled multi-field materials.

## 2 Co-simulation approach for multi-field materials

The co-simulation approach basically follows the procedure described in [2] and is, therefore, based on the user-defined-element subroutines `ush1_eXXX()` and `us1d_eXXX()`, respectively. In order to address the simulation of multi-physics materials through LS-DYNA, it is crucial to deal with multiple mutual interacting field variables. For instance, when addressing the simulation of porous materials, the fields of the solid displacements, which are associated with solid-skeleton deformation within the TPM framework, is extended via the pore pressure.

Within the scope of the present contribution, the additional field variables require a specific treatment, on the one hand, during the simulation run-time by incorporating the additional variables in the solution procedure and, on the other hand, to allow for a proper post-processing of the simulation results. Moreover, it is important to point out that, as PANDAS uses C and LS-DYNA uses FORTRAN programming language, special care has to be taken when mixing both languages within a single project. In particular, one needs to account for subroutine naming conventions and data-type conversion of the associated subroutine arguments. Improper treatment may lead to unpredictable results.

### 2.1 Incorporating additional field variables

In order to activate additional fields within the solution procedure, the functionality of LS-DYNA to use additional degrees of freedom (DOF), which are, in terms of the LS-DYNA terminology, denoted as extra DOF, is used. In particular, one needs to incorporate the keywords `*NODE_SCALAR_VALUE`, and `*ELEMENT_SHELL_DOF` and `*ELEMENT_SOLID_DOF`, respectively, into the LS-DYNA keyword file. Furthermore, due to the different physical natures of the governing fields, the solver of the systems of algebraic equations needs be able to handle an in general non-symmetric *Jacobian* matrix.

### 2.2 Post-processing strategy

When dealing with additional DOF within a user-defined element formulations, further efforts are necessary to allow for a proper visualisation of the extra DOF. In consequence, the subroutine `uctr11()` is additionally incorporated into the toolbox workflow. In particular, the values of the extra

DOF are initially stored in a thread-safe temporary data container during the evaluation of the element responses. Subsequently, once the time-increment is completed, the subroutine `uctrl1()` writes the nodal values of the extra DOF to a file, which can then be imported into the LS-DYNA post-processor.

### 2.3 Coupling workflow

The workflow of the co-simulation approach is summarised in Figure 1. Note that, herein, to conveniently exploit the internal data structure of PANDAS, each call to the FORTRAN-written LS-DYNA subroutines are redirected to the respective versions written in C programming language, viz. `cue1()` and `cuctrl1()`.

At first, in each increment of the iterative *Newton-Raphson* procedure, LS-DYNA gradually assembles the overall system of equations from the element-wise contributions in terms of the right-hand-side vector and the *Jacobian* matrix. Note that, at this stage, the former merely contains the internal element response with respect to the current field variables. Subsequently, LS-DYNA completes the right-hand-side vector and the *Jacobian* matrix by applying the *Dirichlet* and *Neumann* boundary conditions and, finally, solves the resulting system of algebraic equations to obtain an updated solution with respect to the iterative *Newton-Raphson* procedure. Once the solution is converged, i. e. the residual error meets a certain tolerance criterion, the time step is completed and LS-DYNA proceeds with the next time increment.

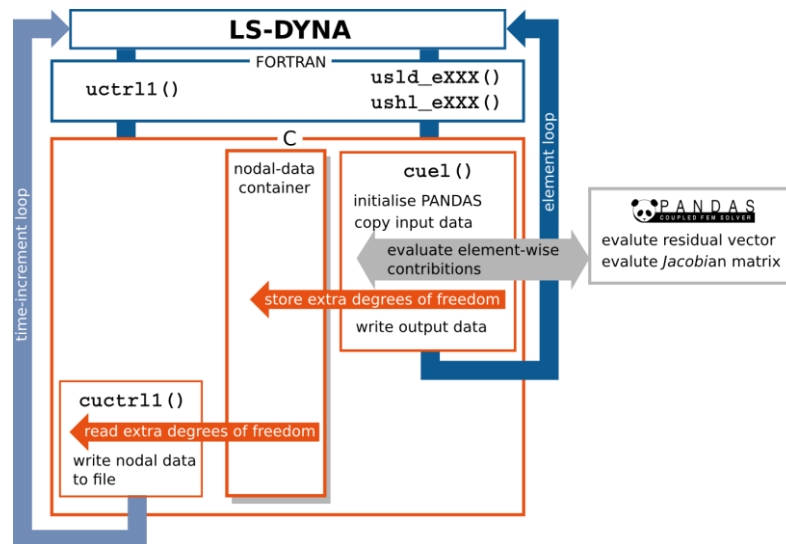


Fig.1: Schematic workflow of the co-simulation approach between LS-DYNA and PANDAS.

### 3 Summary and future aspects

The present contribution illustrated the current state of the co-simulation approach between LS-DYNA and PANDAS. In this regard, the authors need to point out that the present concept may be subjected to major changes in subsequent releases, in order to tackle diverse problems, which may arise on the way to a fully working and easy to use multi-physics toolbox.

In this regard, note that although the toolbox has so far only been tested against the background of the implicit solution procedures of LS-DYNA, the toolbox design already considers the application of explicit time-integrations schemes, which will be part of an upcoming testing procedure. Moreover, the post-processing of the dependent variables, e. g. stresses or seepage velocities, will be implemented and the coupling concept will be tested in large-scale parallel simulations in order to ensure the toolbox is applicable to practically relevant problem scenarios.

### 4 Literature

- [1] Ehlers, W.: "Challenges of porous media models in geo- and biomechanical engineering including electro-chemically active polymers and gels", International Journal of Advances in Engineering Sciences and Applied Mathematics 1, 2009, 3-86.
- [2] Schenke, M. and Ehlers, W.: Parallel solution of volume-coupled multi-field problems using an ABAQUS-PANDAS software interface. Proceedings in Applied Mathematics and Mechanics 15, 2015, 419–420.

# Tests with a Sensitive Specimen Geometry confirm solid elements when the Aspect Ratio is below four

T. Tryland

SINTEF Raufoss Manufacturing, Raufoss, Norway

## 1 Background

The 64 km/h frontal offset test is run with a deformable barrier, and the first numerical model of this barrier was made with solid elements to represent the honeycomb blocks. This required development of a special element formulation to handle the severe deformation of the solid elements together with a complex material model that could be calibrated to handle the extreme anisotropy [1]. It is herein important to notice the amount of work as well as the uncertainties with the test specimens and the test procedure to get a proper representation of the honeycomb material. It was therefore suggested to represent the barrier geometry with shell elements that were able to capture the deformation mode with local and global buckling of the honeycomb structure together with a simple model to represent the material in the 0.076 mm thick aluminium foil [2]. Effective learning based on finite element simulations requires that the numerical predictions represent the physics at a relevant level of discretisation. Here simple hand calculations following general structural rules like for example Eurocode may support the user to build a reasonable expectation of how the structure will deform. It is crucial that the numerical prediction captures the correct strain- and stress fields as input when representing the material behaviour until an eventual fracture [3]. One benefit when using a combination of element type and element mesh that predict the correct deformation mode is the simplest possible material model. The objective of this study was to present an experimental study with a sensitive specimen geometry that confirm the element/mesh rules presented two years ago [4].

## 2 Specimen geometry and test procedure

Note that the components that were tested in this study is unlike the situation for real products where the actual combination of geometry and material have to secure robust behaviour for all combinations within the tolerances. Herein the combination of profile geometry, cutting angles, wall thicknesses and material properties was chosen with propose to get an unstable folding pattern and thereby challenge the simulation tool to capture this. Focus was placed on how the geometry determine the deformation mode, and 6060 T6 was chosen with process parameters during the extrusion process that resulted in relative small geometrical imperfections and similar material properties through the wall thickness. The last statement is demonstrated in figure 1 where axial compression of the circular tubes defined by length, diameter and thickness  $L = 2D = 60T$  shows the same four concertina rings when they are deformed from initial length to half of this. Remember that aluminium extrusions often show a surface skin where somewhat different material properties gets less important when the geometry is scaled larger and 0.2 mm means about 20 %, 10 % and 5 % of the wall thicknesses in figure 1.



Fig. 1: Tests with  $L = 2D = 60T$  shows the same deformation mode independent of the scale.

The specimens were cut with angle like  $0.5^\circ$  to initiate axial folding at the upper end. It is worth to notice the same results independent of the specimen size relative to the fraction with surface layer, and it is therefore reasonable to represent this profile with the same material properties through the thickness. Here shell elements is one option when the mesh can be sufficiently coarse to fulfil aspect ratio above four while solid elements with  $ELFORM = \pm 2$  [5] is an alternative when a refined mesh seems required to describe the predicted deformation mode with a sufficiently smooth surface. However, the development of more accurate formulations for shell and solid elements requires test results with a sensitive specimen geometry as base. Here this means diameter/thickness-ratio as shown in figure 1, but the specimen length is increased to  $L = 6D = 180T$  where both local- and global instability were observed for the parallel tests presented in figure 2. It is interesting to notice the sensitive geometry that leads to global buckling in four out of five parallels, while one specimen develops seven concertina rings before it changes into 2-lobe diamond. Three different deformation modes at the same force level is a challenge for the element formulations. Even a minor change as for example specimen orientation where the cut angle and the longitudinal imperfection are working opposite is sufficient to give concertina rings instead of global buckling. The numerical model based on solid element seems to work well for this case, and the mesh can be refined to reach aspect ratio close to one to capture four concentrated concertina rings in the case from figure 1 as well. The refined mesh is also working for the longer variant in figure 2, but a practical engineer may save computational time when the deformation mode is not that localised. However, the model based on shell elements with aspect ratio about 4 struggle with global buckling, and smaller elements increases the tendency to predict a local mode. Larger shell elements with aspect ratio above 4 seems to capture global buckling in the case presented in figure 2, and the coarse mesh indicate that the numerical prediction is a rough estimate.



Fig.2: The experiments confirm a sensitive case as captured by the solid elements.

### 3 Summary

Test results with axial compression of a sensitive tube geometry defined by length, diameter and thickness  $L = 6D = 180T$  confirms shell elements with aspect ratio above four, while solid elements is recommended when the ambition is smaller elements to capture a more local deformation mode.

### 4 Literature

- [1] Kojima, S., Yasuki, T., Mikutsu, S., Takatsudo, T.: "A Study on Yielding Function of Aluminium Honeycomb", 5<sup>th</sup> European LS-DYNA Users Conference, Birmingham, UK, 2005.
- [2] Tryland, T.: "Alternative Model of the Offset Deformable Barrier", 4<sup>th</sup> LS-DYNA Forum, Bamberg, Germany, 2005.
- [3] Tryland, T., Berstad, T.: "Keep the Material Model simple with input from Elements that predict the Correct Deformation Mode", 10<sup>th</sup> European LS-DYNA Conference, Würzburg, Germany, 2015.
- [4] Tryland, T.: "Combinations of Meshes and Elements that seems able to Predict the Correct Deformation Mode", 13<sup>th</sup> LS-DYNA Forum, Bamberg, Germany, 2014.
- [5] Borrvall, T.: "A heuristic attempt to reduce transverse shear locking in fully integrated hexahedra with poor aspect ratio", 7<sup>th</sup> European LS-DYNA Conference, Salzburg, 2009.

# Predictive Fracture Modeling in Crashworthiness: A Discussion of the Limits of Shell-Discretized Structures

André Haufe<sup>1</sup>, Filipe Andrade<sup>1</sup>, Markus Feucht<sup>2</sup>,  
Daniel Riemensperger<sup>3</sup>, Karl Schweizerhof<sup>1</sup>

<sup>1</sup>DYNAmore GmbH, 70569 Stuttgart, Germany

<sup>2</sup>Daimler AG, 71059 Sindelfingen, Germany

<sup>3</sup>Adam Opel AG, 65423 Rüsselsheim, Germany

For many years shell formulations were used extensively in crashworthiness applications in order to predict deformations and even rupture of thin shell-like structures. From a general shell theory point of view there are probably no arguments to change this in the near future, unless none of the basic shell assumptions like using them for thin structures, having plane sections and only minor stresses in thickness direction, will be violated.

However, especially if damage, localization and eventually rupture is regarded, the aforementioned assumptions limit the applicability and eventually the means to calibrate such models. For instance, if the rupture strain in biaxial loading is to be calibrated from experiments one can have straight biaxial tests or penetration tests (i.e. the Nakazima tests). For both setups classical shell elements deliver the same value for triaxiality of  $2/3$ . While this is the correct solution for a biaxial test, the Nakazima test suffers from the fact that lateral stresses applied to the sheet are not being covered at all in classical shell formulations. Hence the stress triaxiality and the Lode angle are not predicted accurate enough (see Fig. 1). Another well-known issue is the inability of 5-parameter shells to correctly predict a the stress state in localization zones due to the violation of the plane section assumption.

The present contribution will describe such limitations in detail, focus on different discretization approaches with finite elements and highlight several drawbacks in the final crashworthiness application. Furthermore, available remedies – if available – will be presented and discussed.

The presentation is based on the identical but shorter contribution at the LS-DYNA World Conference 2016 in Detroit.

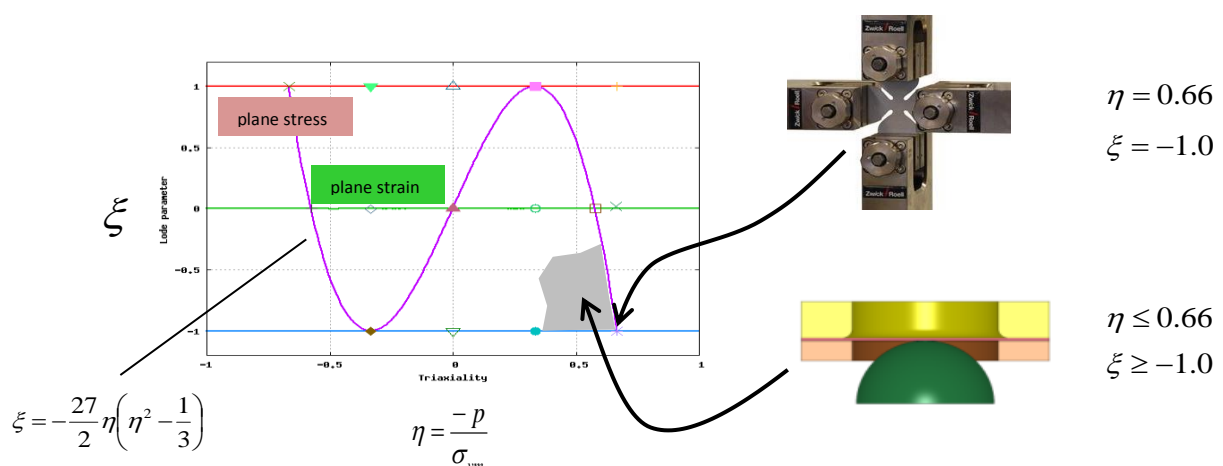


Fig. 1: States of stress in biaxial and Nakazima test setup.

# Improved Robust Low Order Solid and Solid-Shell Finite Elements with Incompatible Modes / Enhanced Assumed Strains for Explicit Time Integration

Christoph Schmied<sup>1</sup>, Steffen Mattern<sup>2</sup>, Karl Schweizerhof<sup>1,2</sup>

<sup>1</sup>Institute of Mechanics, KIT christoph.schmied@kit.edu, karl.schweizerhof@kit.edu

<sup>2</sup>DYNAMore GmbH, Stuttgart-Vaihingen, steffen.mattern@dynamore.de

## 1 Introduction

High-speed crash and impact scenarios are perfectly solved by explicit schemes, which are in addition very successfully applied for quasi-static problems where convergence with implicit schemes tends to be problematic. A high demand for robust results of the underlying already sufficiently refined finite element discretization exists in scenarios like sheet-metal forming where mixed explicit-implicit schemes are widespread. Simple to operate and suited to model sharp edges or beadings low order finite elements remain popular and improvements beyond fully and selectively underintegrated 8-node solid and solid-shell (in LS-Dyna referred to as 'thick shell') elements are highly desirable. A most popular element technology providing better accuracy for low order finite elements in general nonlinear analysis is the well known method of non-conforming or incompatible modes (IM) [1] which is closely related to so-called enhanced assumed strain (EAS) elements [2]. For both types effective 8-node solid and solid-shell elements for 3D analysis have been discussed extensively in the literature. Limits for usage in explicit time integration tend to be numerical efficiency and particularly the issue of numerical robustness - as shown in Fig. 1 - which are both discussed in this contribution.

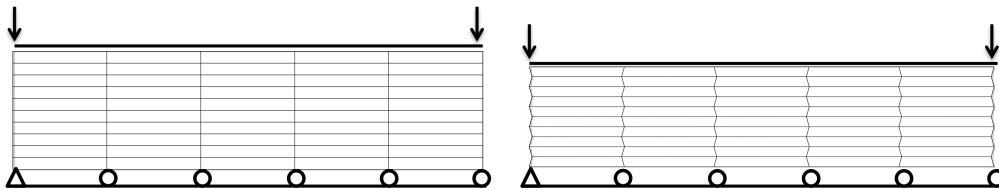


Fig. 1: Setup of an academic test case [3] in undeformed (left) and deformed (right) state showing a typical hourglassing pattern as a result of a kinematic mode caused by incompatible modes.

## 2 Numerical efficiency and robustness of incompatible mode elements

### 2.1 Circumventing static condensation

Standard treatment of incompatible modes require the condensation of extra degrees of freedom (which are incompatible modes respectively EAS terms) via the solution of an extra equation system which may considerably affect the computational efficiency in explicit schemes that are strictly related to element computations, as very small time steps are required.

A key step in an approach [4] to overcome the necessity of the numerically costly condensation procedure is the assignment of artificial mass to the incompatible parameters. In the case of incompatible mode elements the additional parameters are represented by incompatible displacements, thus the construction of a corresponding mass matrix appears to be a straightforward discretization operation analogously to the mass matrix of standard displacement degrees of freedom. Finally the incompatible mass allows integrating the incompatible displacement parameters in time allowing a fully explicit solution instead of condensation. For any type of EAS-elements a generalization technique allows to reformulate the strain parameters as displacement parameters of corresponding IM elements for which again an incompatible mass matrix can be formulated.

### 2.2 Incompatible mass scaling

Since the incompatible parameters are not condensed but integrated in time additional frequencies defined by the incompatible mass and incompatible stiffness appear which may affect the size of the critical time step. Since incompatible modes are essentially higher order modes the size of the critical time step determined by the highest frequency of the critical element may be considerably reduced,

particularly by the incompatible modes leading to enhancements of volumetric strains, compared to an element formulation without additional incompatible inertia. To recover the original time step size incompatible mass scaling or the solution of the IM displacements in subcycles are possible remedies.

### 2.3 Numerical robustness – Energy control and rate formulation

Major instability problems first reported in the nonlinear regime [5] and later also for small displacement finite elements [3] limit the application of IM/EAS elements considerably up to now. Within the suggested approach, however, it is possible to use the incompatible mass and velocity to monitor the kinetic energy related to any individual incompatible term inside of an element. Analogously to monitoring the so-called hourglass energy, which is well known from explicit analysis with one point integrated element formulations, instabilities may be detected and reduced or removed by simply scaling the mass related to the them. If the incompatible mass scaling exceeds a limit the incompatible parameter gets insignificant and the original element behaviour as if this incompatible mode was not present is restored. Interestingly incompatible mode elements formulated in the framework of rate and total formulations show significant differences in their instability behaviour which is due to the difference in the discretized element force computation. First results indicate that the mentioned instabilities are not triggered inside the rate formulation.

## 3 Implementation in LS-Dyna

A set of different IM/EAS-formulations based on 8-node solid discretizations is implemented via the LS-Dyna user element interface. The implementation is rather straightforward since the incompatibility of the extra degrees of freedom allows the solution of the latter on element level as demonstrated in Fig. 2. Further, the IM/EAS approach may be without restrictions extended by other techniques like assumed natural strains or reduced integration for further improvement of the element performance.

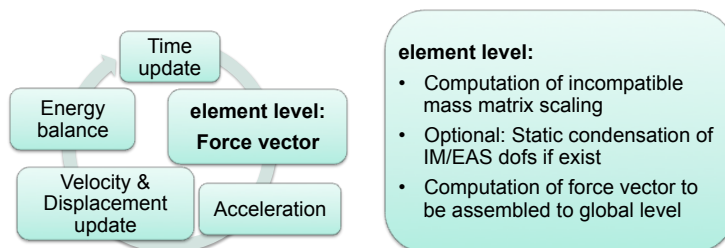


Fig.2: Typical explicit cycle with an overview of necessary computations on element level.

## 4 Summary

In this contribution we present an implementation of a modified method of incompatible modes - also applicable to enhanced assumed strains – allowing a fully explicit computation of the extra incompatible degrees of freedom. Different IM and EAS-formulations are implemented using the user element interface of LS-Dyna with the aid of AceGen [4] as an important code generation tool. Occurrence and techniques to efficiently avoid instabilities related to incompatible modes are examined on geometrically linear and nonlinear academic test cases and more demanding realistic examples. First studies on measuring the computational efficiency in terms of CPU-time are carried out. Further merits and limits of the presented scheme and its possibilities are discussed.

## 5 Literature

- [1] Wilson EL, Taylor RL, Doherty WP, and Ghaboussi J. Incompatible Displacement Models. In: Fenves SJ, Perrone N, Robinson AR, Schnobrich WC, editors. Numerical and computer models in structural mechanics. Academic Press, p. 43–57, 1973.
- [2] Simo JC, Rifai MS. A class of mixed assumed strain methods and the method of incompatible modes, Int J Numer Methods Eng, 29(8), 1595-1638, 1990.
- [3] Sussman T and Bathe K-J. Spurious modes in geometrically nonlinear small displacement finite elements with incompatible modes. Comput Struct, 140:14–22, 2014.
- [4] Mattern S, Schmied C, and Schweizerhof K. Highly efficient solid and solid-shell finite elements with mixed strain–displacement assumptions specifically set up for explicit dynamic simulations using symbolic programming. Comput Struct, 154:210–225, 2015.
- [5] Wriggers P, Reese S. A note on enhanced strain methods for large deformations. Comput Methods Appl Mech Eng, 135:201–209, 1996.



# ARENA2036 – Above and Beyond

J. Dittmann, P. Middendorf

Institute of Aircraft Design, University Stuttgart, Stuttgart, Germany

The scientific campus ARENA2036 is a long term project funded by the Federal Ministry of Education and Research Germany (Forschungscampus Arena2036). It is one of the major scientific campuses in Germany and is the only one which started directly into the main section of research. ARENA2036 is located in Baden-Württemberg (Germany) and is part of the University of Stuttgart since 2013. ARENA2036 is an acronym for Active Research Environment for the Next generation of Automobile and the amendment 2036 will be the 150th anniversary of the automobile. Until now the ARENA includes four starting projects: DigitPro (Holistic digital prototype for lightweight design in large-scale production), LeiFu (Intelligent lightweight construction with functional integration), ForschFab (Research factory: production of the future) and KHoch3 (creativity-cooperation-competence transfer). DigitPro deals with the manufacturing process chain and tries to improve the connections between the different simulation tools. At this juncture it will decrease the weight of an automotive structure by 10 % and the development time by 50 %.

Two topics of the Digital Prototype are the virtual infiltration of large structural parts and the numerical 3D permeability determination of near-net-shape preforms, which reduces time, costs and material [1]. At present permeability determination is executed in test benches and several tests are necessary to characterize just on lay-up. The experimental permeability determination for large three dimensional near-net-shape structures is only possible with enormous efforts, large molds, many sensors and a lot of time.

This publication will present the main framework of ARENA2036 and the solution for numerical 3D near-net-shape permeability prediction.

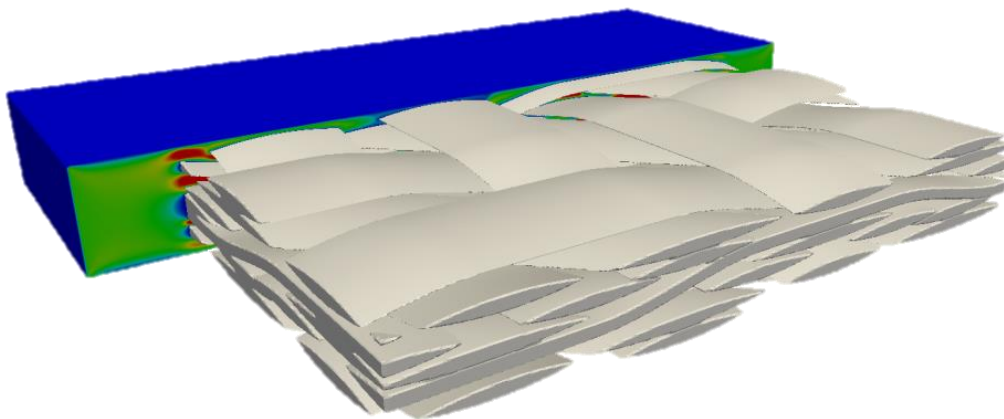


Fig.1: 3 layer of triaxial braid in OpenFOAM

- [1] J. Dittmann, S. Hügler, P. Middendorf, Numerical 3D Permeability Prediction Using Computational Fluid Dynamics, FPCM, Kyoto, 2016

# A Multiscale Approach for the Mechanical Investigation of Textile-Based Composite Structures within a Closed Process Chain

Mathieu Vinot<sup>1</sup>, Martin Holzapfel<sup>1</sup>, Christian Liebold<sup>2</sup>

<sup>1</sup> Institute of Structures and Design, German Aerospace Center, Stuttgart

<sup>2</sup> DYNAmore GmbH, Stuttgart

## 1 Motivation

In the research campus ARENA2036, the project DigitPro (**D**igital **P**rototype) aims at developing a closed numerical process chain for the investigation of textile-based composite structures, particularly braids and **O**pen-**R**eed **W**eaves (**ORW**). The present paper focuses on the ORW composites, while information about the multiscale investigation of braided structures can be found in [1]. Through the integration of additional diagonal threads during the weaving process, ORWs offer improved mechanical properties in the reinforced direction, which allows as a consequence for structure weight reduction. Simulations are performed to predict the manufacturing processes as weaving, draping or infiltrating. The mechanical properties of the composite are then numerically determined with mesoscale simulations and input in structure simulations at the macroscale. The present paper reports on the investigation of glass-fiber ORWs on a multiscale basis and the qualitative validation of the developed methodic.

## 2 Modelling approach

In this study, two periodic unit cells of a standard 4-layer 2/1 weave and a reinforced ORW are generated with the open-source software TexGen [2] coupled to Python scripts (Fig. 1). The two external layers of the ORW are reinforced with yarns in the  $\pm 41^\circ$ -direction while the other layers are kept unchanged. Due to the complexity of the ORW architecture, a cycle of thermal expansion steps and compaction steps are performed to generate a realistical textile structure and recreate the correct roving nesting. This way, the overall fibre volume content is increased to 50% by keeping the local fibre content in the rovings at a realistical level of 65%. A mesh is then generated to reproduce the matrix-rich zones in the textile. The numerical model reproduces accurately the real textile architecture, as shown in Fig. 2. In a final step, periodic boundary conditions are created automatically with the keyword `*CONSTRAINED_MULTIPLE_GLOBAL`.

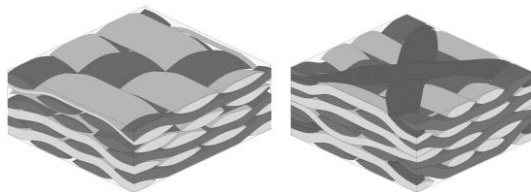


Fig. 1: Generated FE-meshes of a 2/1 weave (left) and of an ORW with rovings in the  $41^\circ$  direction (right)

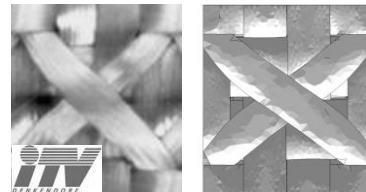


Fig. 2: Comparison between the real ORW (left) and the numerical model (right)

## 3 Virtual material testing at the mesoscale

The mechanical properties of the rovings were calculated with the rule of mixtures assuming a fiber content of 65% to reach a global fiber content of 50% and input in the material model `*MAT_LAMINATED_FRACTURE_DAIMLER_PINHO`. The epoxy matrix was modelled with `*MAT_PLASTICITY_COMPRESSION_TENSION` and `*MAT_ADD_EROSION` to take into account the dependency of the failure strain to the triaxiality and a difference of the behaviour in tension and compression. Simulations are finally performed in tension and compression in both the axial and transverse directions, and in shear. In tension, the ORW shows slightly reduced stiffness and strength compared to the standard weave. This reduction of the material properties is offset by higher properties in the reinforcement direction and in shear (Fig. 3).

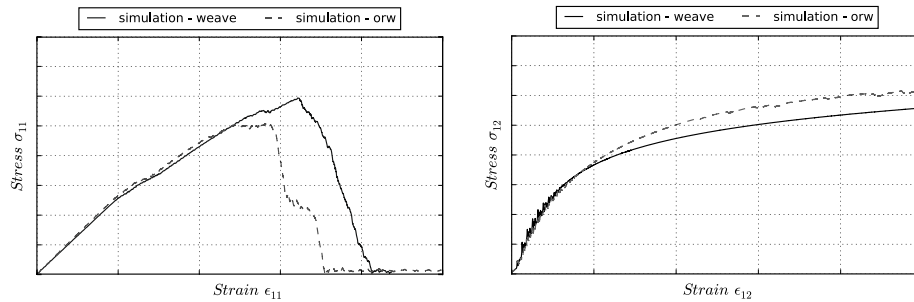


Fig.3: Comparison between the standard weave and the ORW in tension (left) and shear (right)

#### 4 Mapping and simulation at the macroscale

The benefits of the reinforcement in ORWs have been virtually investigated on the macroscale with a specimen for a hole bearing test. For this purpose, the ORW architecture has been mapped on the specimen mesh with a tool developed at DYNAmore [5]. The specimen is modelled with one single shell element in the thickness, in which each integration point represents one roving orientation. This way, the local fiber architecture and its effects are considered. The force-displacement curves for the standard weave and the ORW are represented in Fig. 4. The energy absorbed in the crushing process has been doubled through the reinforcement of the weave, with a weight increase of only 7%.

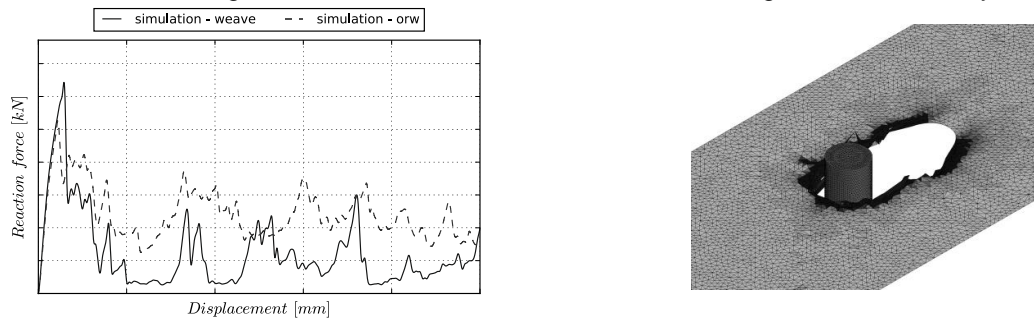


Fig.4: Reaction force (left) of the standard weave and of the ORW in the hole bearing test (right)

#### 5 Summary and outlook

In this study, unit cells of a 2/1 weave and an ORW were generated and appeared to be in good agreement with the real textile architectures. The numerical models at the mesoscale allowed for the mechanical characterization of the composites and for a reduction of the experimental effort. Finally, the composites were studied at the macroscale using a FE-mesh on which the roving orientations were mapped. The ORW reinforcement increased the energy absorption potential of the specimen. The numerical results must be validated in a further step with an experimental test campaign.

#### 6 Literature

- [1] M. Vinot, M. Holzapfel und R. Jemmali, „Numerical Investigation of Carbon Braided Composites at the Mesoscale: using Computer Tomography as a Validation Tool,“ in *10th European LS-DYNA Conference 2015*, Würzburg, 2015.
- [2] H. Lin, B. L.P. and A. C. Long, “Modelling and Simulating Textile Structures using TexGen,“ *Advances in Textile Engineering*, Vol. 331, 44-47, 2011.
- [3] C. Liebold and A. Haufe, “Closing the Simulation Process Chain using a Solver Independent Data Exchange Platform: The Digital Prototype,“ in *14. Deutsches LS-DYNA Forum*, Bamberg, 2016.

#### Acknowledgements

This research and development project is funded by the Federal Ministry of Education and Research (BMBF), Germany under the supervision of Project Management Agency (PTKA) in Karlsruhe. The author is responsible for the contents of this presentation.

# Textile Process Simulation for Composite Structures

Hermann Finckh, Florian Fritz, Prof. Dr.-Ing. Götz T. Gresser

Institute of Textile Technology and Process Engineering (ITV),  
Körschtalstraße 26, 73770 Denkendorf, Germany

## 1 ARENA2036 DigitPro: The digital Prototype

Since about three years, DigitPro, a sub-project of the government funded research project **Active Research Environment for the Next generation of Automobile (ARENA2036)** works on the development of a digital Prototype, a closed simulation process chain which covers different simulation disciplines starting with process analysis right up to crash. Along this chain various material modeling approaches on the micro-, meso-, and macro level of a carbon fiber reinforced plastic (CFRP) components are being used. The research work of ITV in DigitPro are basically process simulations using thread models are which are weaving, draping and infiltration. Braiding simulation is difficult but less complex as weaving simulation, so braiding simulation is used to test and validate new functions of LS-DYNA (explicit). Micro  $\mu$ -CT technology is used to analyze reinforcement fabrics in structure, fiber orientations permeability determination, modelling and validation propose. In the presentation, focus is laid on a new weaving process called "Open Reed Weaving" (ORW). Here an additional thread system is added to a plain  $0^\circ/90^\circ$  woven fabric which leads to an multiaxial woven textile with local reinforced areas. As part of the process chain the goal is to generate realistic models to investigate the material properties of this multiaxial fabric with by simulation.

## 2 Braiding process simulation

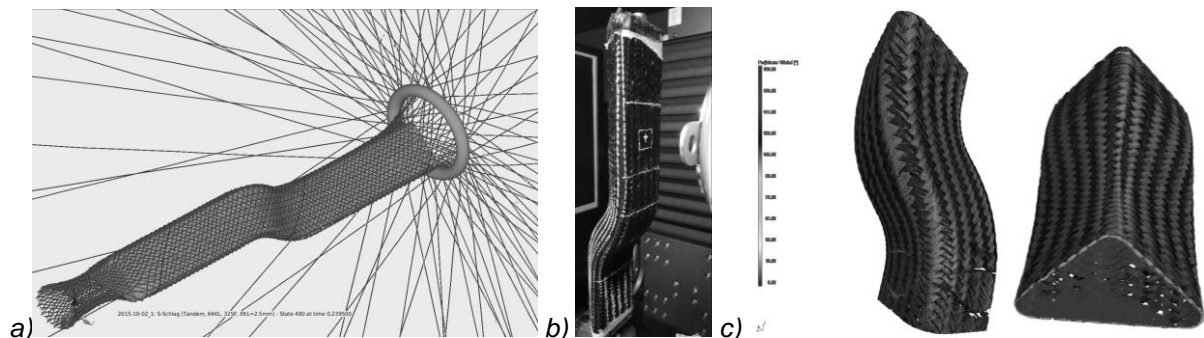


Fig.1: Triaxial braiding simulation (a),  $\mu$ -CT analysis (b), fibre orientation analysis of CT-scan (c)

The triaxial braiding simulation fig. 1a for a challenging triangle and s-curved geometry allows analyzing influence of braiding parameter as thread tensions, speed, mandrel movement and the friction dependent fiber laying to the mandrel. The model is validated by high resolution X-ray ( $\mu$ -CT, nanotom m) and fiber orientation analysis (fig. 1c). The process simulation was improved referring reduction of computation time, contact and numerical stability. To reduce the simulation time, threads should be extended during process simulation. This could be achieved by using combination of **\*ELEMENT\_SEATBELT\_RETRACTOR** and **\*ELEMENT\_SEATBELT**. This lead to good results, but now by using the new implemented functionality **\*ELEMENT\_BEAM\_SOURCE** (requested by ITV since several years) the computation time could be further reduced by approx. 20%. Therefore, this solution is the first choice for the complex and very computationally intensive weaving simulations.

## 3 Open Reed Weaving process – Multiaxial woven textiles

Here two additional thread systems are placed in the plain  $0^\circ/90^\circ$  woven fabric. The Open Reed Weaving (ORW) technology enables the addition of diagonal threads into the weaving process by using horizontally movable thread guides arranged between the reed and weaving shafts of the weaving machine. These additional warp fibers can be added partially or covering the whole width of the textile. Orientation of the 3rd or 4th thread system can varied independently between  $0^\circ$  and nearly

90° along the warp direction depending on the yarns linear density. The ITV has produced a wide range of textiles with various designs and textile constructions composed of varying materials and roving types. Fig. 2a shows the weaving machine with a multiaxial fabric composed of glass fibers with local carbon fiber reinforcement. The multiaxial yarns are supplied from the top (middle of the image) and being lead through the horizontal movable needlebars (large white blocks). Fig. 2b shows a version to reinforce areas of holes in composites.

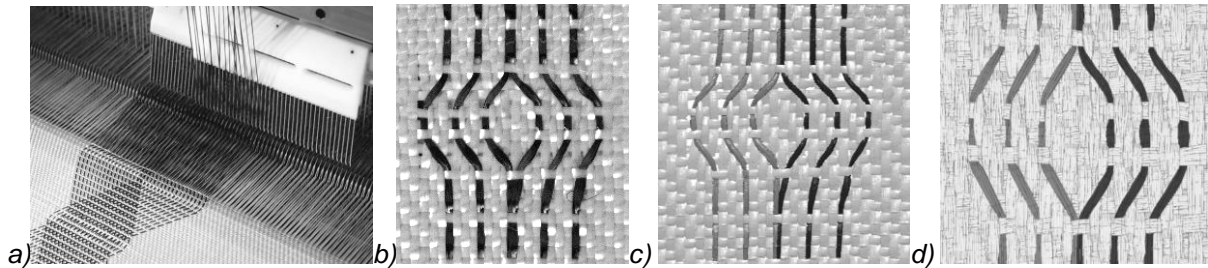


Fig.2: Open Reed Weaving Machine (a), Textile made of glass fiber twill as base fabric and local carbon fiber reinforcement threads (b), result of  $\mu$ -CT (c) and FEM simulation (d).

The pre-processing of such a complex weaving machine with many threads is a tedious and error-prone task. Therefore, a parameter driven python program has been developed to perform this repeatable task with minimal effort and minimal error. All machine parts are modeled as rigid bodies, boundary conditions are put up automatically for all parts, depending on the given weaving parameter as they are used for real weaving machine. Threads are modeled as beams using the new beam source functionality for each filament. Fig. 3b show the result of ORW fabric with hole reinforcement.

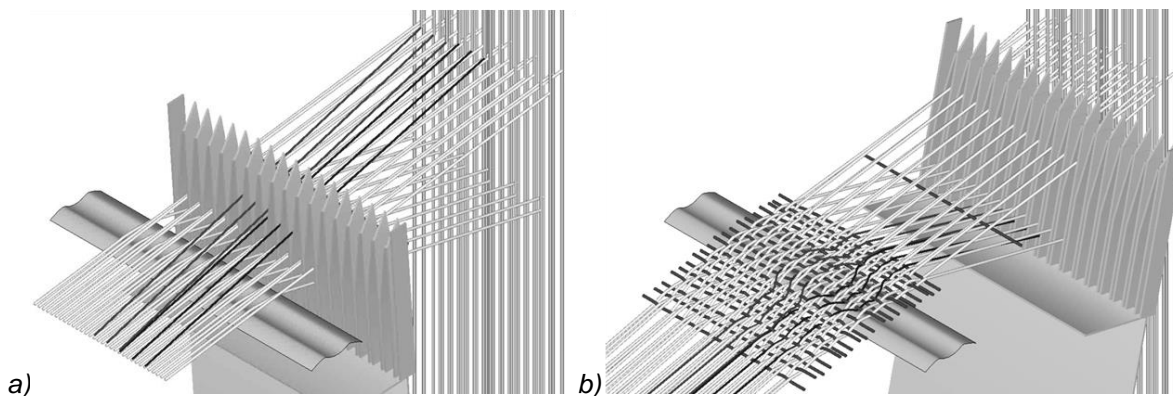


Fig.3: Initial simulation model after generation from python code (a), Result ORW-Simulation (b).

#### 4 Post-processing and verification by computer tomography

Due to computation time in process simulation monofilaments are used. To transform single filament in multifilament model the exported beam mesh is reimported into developed python code where a multifilament yarn on the centerline of beam mesh is generated. By using initial penetrations check a very realistic multifilament model of the ORW fabric (fig. 2d) could be is created. The comparison to high resolution micro-CT scan (fig. 2c) shows that the simulation of the weaving process is capable to of generating a realistic multifilament model of an ORW woven textile.

#### 5 Outlook

Described process simulations will be improved further on and will be an important tool to get realistic simulation models using input parameters from real braiding and weaving machine. This models will be used to compute mechanical properties and by homogenization methods to evaluate large composite parts before it is produced and so play an important part of the closed simulation process in to evaluate the virtual material properties and to assess the whole modeling approach.

#### 6 Summary

This presentation gives an overview on the potential of the newly developed process simulations "Braiding" and "Open Reed Weaving" and will introduce the use of virtual textile for material testing.

---

# Closing the Simulation Process Chain using a Solver Independent Data Exchange Platform: the Digital Prototype

C. Liebold, A. Haufe

DYNAmore GmbH, Industriestraße 2, 70565 – Stuttgart, Germany

**Keywords:** HDF5, Simulation Process Chain, ARENA2036, Braiding, Infiltration, Open Reed Weaving (ORW)

## 1 Abstract

Since about three years, DigitPro, a sub-project of the government funded research project **Active Research Environment for the Next generation of Automobile (ARENA2036)** works on the development of a **Digital Prototype**, a closed simulation process chain which not only covers different simulation disciplines such as crushing or process analysis, but also various material modeling approaches on the micro-, meso-, and macro level. Various software tools are being used by the project partners, namely the German Aerospace Center (DLR), the Institute of Textile Technology and Process Engineering (ITV), and the Institute of Aircraft Design (IFB) at the University of Stuttgart.

## 2 The Digital Prototype

Core of the digital prototype is a mapping tool and data exchange platform called Envyo® being developed by the DYNAmore GmbH. This tool shall bridge the gap between the different simulation disciplines and length scales as well as the different software tools being used within the research group. It offers the capability to document the steps being taken along the development of a carbon fiber reinforced plastic (CFRP) component and to link to simulation data being generated along the manufacturing process. For data storage and sharing, a HDF5 data container is used in a customized way, allowing the project partners to submit their simulation results and to access simulation data from the other disciplines being used within the project. Besides data storage, the users can perform a mapping and homogenization procedure in order to cover the needs for their further simulations, for example the direction of beam elements can be transferred as directions within an infiltration- or crushing simulation. Further homogenization procedures would consider thicknesses and width of rovings in order to estimate porosities or stiffness's at certain positions within a component. Results gained by the simulation of representative volume elements (RVEs) and stored within the database can be used to generate material models being coupled to the further analysis and to locally consider varying material properties. This mapping and homogenization procedure always has to take different discretization methods and element sizes into account, which are being used for the different simulation techniques and therefore, it is crucial to fully understand the different modeling approaches.

## 3 Mapping Capabilities

The mapping algorithm being implemented in Envyo® is by now based on a closest point scheme which considers only data from the next neighboring integration point within the source and target mesh. A simple bucket sort algorithm is implemented in order to speed up the data mapping process. For the specific needs within the ARENA2036 research environment, fiber orientations which can be derived from braiding process simulations or weaving simulations using beam or shell elements can be transferred to meshes for structural analysis with LS-DYNA® or for infiltration analysis using Pam-RTM®. In order to consider areas with pure resin, the algorithm is able to either consider the width of the shell elements representing the fiber rovings or the user can define the roving width within the mapping\_info.in – file which is used to specify the respective mapping parameters. An overview on the simulation disciplines and length scales being covered with the mapping tool are shown in figure 1.

The HDF5 data container is able to read in all different kinds of simulation data, either being already provided in an HDF5 data format (Pam-Crash®, Pam-RTM®), or in an ascii format (LS-DYNA®, FiberSim®, OptiStruct®). It is also possible to write these data again into the respective data formats in case they are needed for further analysis. In order to increase readability, some of the information

stored such as fiber orientations are written in a specific format which is defined by the project partners and therefore allows to easily monitor the steps taken along the simulation process chain.

## ARENA2036

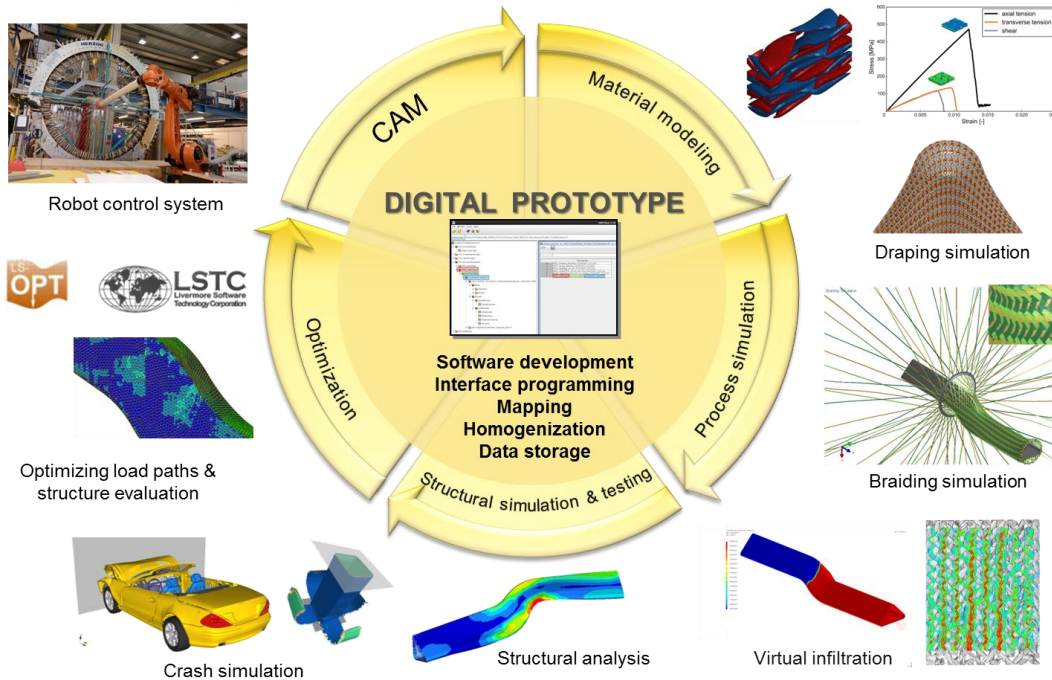


Fig. 1: The Digital Prototype combining a large variety of simulation disciplines and length scales [1].

## 4 Future Work and Summary

The next steps will include the homogenization, clustering and assignment of material data which can be derived with virtual testing methods being developed by [2]. Furthermore, one of the main goals will be the fully automatized component design including the necessary process simulations as well as the required structural analysis and additional optimization loops which will improve the stiffness and strength of the component by modifying the process parameters within a respective process window. This presentation will give an overview on the newly developed techniques for the build-up of a digital prototype and will introduce the mapping techniques being implemented within Envyo®, the developed mapping solution. An in-depth view into ongoing developments and research will be given, helping to understand the need for a closed simulation process chain for CFRP components and how this need can be targeted with the proposed solution in an active research- and industrial environment.

## 5 Literature

- [1] Dittmann, J., Böehler, P., Michaelis, D., Vinot, M., Liebold, C., Finckh, H., Middendorf, P.: "DigitPro – Digital Prototype Build-up Using the Example of a Braided Structure", IMTC, Chemnitz, GER, 2015.
- [2] Vinot, M., Holzapfel, M., Michaelis, D., Dittmann, J., Böehler, P., Middendorf, P., Liebold, C.: "Numerische Prozesskette für die Auslegung von geflochtenen Fahrzeugkomponenten – Nutzen und Herausforderungen", Symposium Hybrider Leichtbau, Wolfsburg, GER, 2016.

## Acknowledgements

This research and development project is funded by the Federal Ministry of Education and Research (BMBF), Germany under the supervision of Project Management Agency (PTKA) in Karlsruhe. The author is responsible for the contents of this presentation.



---

# Erkenntnisse aus aktuellen Performance-Messungen mit LS-DYNA

Eric Schnepf<sup>1</sup>, Dr. Eckardt Kehl<sup>1</sup>, Chih-Song Kuo<sup>2</sup>

<sup>1</sup>Fujitsu Technology Solutions GmbH, München

<sup>2</sup>ict information communication technology GmbH, Aachen

Fujitsu ist der erfahrenste und größte Hersteller von HPC-Lösungen im asiatischen Markt und einer der etablierten HPC-Anbieter in Europa. Fujitsu pflegt eine enge Zusammenarbeit mit führenden, unabhängigen Software-Herstellern (ISV) und entwickelt gemeinsam mit ihnen PRIMEFLEX für HPC Cluster-Lösungen, die für spezielle Arbeitsanforderungen optimiert sind. Zudem bietet ein globales HPC-Kompetenznetz den Anwendern qualifizierten Support und treibt die Entwicklung des gesamten Fujitsu HPC-Portfolios voran.

Fujitsu bietet eine skalierbare HPC-Architektur, die flexibel die unterschiedlichsten Anforderungen abdecken kann: von der x86 CELSIUS High-End-Workstation über leistungsfähige x86 PRIMERGY Server bis hin zur optimierten HPC Cluster-Architektur. Die Betriebssystemebene der Plattformen ist typischerweise Linux-basiert, beispielsweise Red Hat, SUSE oder CentOS. Das HPC-Portfolio von Fujitsu enthält außerdem Storage-Plattformen, HPC-Middleware, Beratung und Integrationservices.

Um unsere Kunden optimal beraten und um die HPC-Lösungen für die jeweiligen Anwendungen maßgeschneidert konfigurieren zu können, führen wir in unserem HPC Competence Center regelmäßig Performance-Messungen auf unseren Systemen durch. Hierbei werden auch unterschiedliche Settings getestet. Schwerpunkt der Performance-Messungen ist unsere aktuelle Scale-Out Server-Plattform PRIMERGY CX400 auf Basis der neusten Intel® Xeon® E5-2600 v4 Prozessorfamilie. Außerdem untersuchen wir aktuell die neue Server-Plattform PRIMERGY CX600 auf Basis der Intel® Xeon Phi™ x200 Produktfamilie (Codename „Knights Landing“) für hochgradig parallele Anwendungen.

In diesem Vortrag präsentieren wir Erkenntnisse aus aktuellen Performance-Messungen mit LS-DYNA.

Weitere Informationen zum Fujitsu HPC-Portfolio finden sich unter: [www.fujitsu.com/de/hpc](http://www.fujitsu.com/de/hpc) .



# LS-DYNA Performance auf NEC LX-Systemen

F. Unger

NEC

# How Cloud HPC enables the Digital Transformation in Product Development

T. Smith

Rescale

# Hybrid Cloud HPC Cluster Solutions – Challenges, Impact and Industrial Use Cases

J. Tamm, A. Heine

CPU 24/7

## **Title: HPC in the Cloud: Gcompute Support for LS-DYNA Simulations**

Ramon Díaz

Gcompute (Gridcore GmbH)

During the last decades, companies have been introducing CAE simulations as part of their product development with the main objective of improving reliability and reducing the costs of prototyping. It is nowadays demonstrated that introducing simulations during an early step of the product design process reduces the risk of failure as well as the associated costs, when the prototypes need to be redesigned.

Traditionally, enterprises have invested in geographical independent local workstations or clusters that nowadays resulted in non-connected computational units. Besides, CAE Software used for analysing problems like crash tests or impacts resulted in an essential tool for any Engineer, forcing the growth and development of faster and more powerful computing stations. In order to make the hardware investment more efficient, enterprises are considering new solutions like consolidation of internal resources with Private Enterprise Cloud Environments or External HPC Cloud Services. New challenges arise with this technology such large data transfers and 3D remote visualization over medium to high latency links.

Gcompute has been developing HPC solutions since 2002 to cover these needs both for enterprises and small consultants, offering a complete portfolio that allow users to fulfil all his needs from a unique HPC partner.

Keywords:

Cloud Computing, LS-Dyna on demand, HPC simulations, flexible capacity.

# LSTC and DYNAmore Cloud Services

Prof. U. Göhner

DYNAmore

---

# LoCo – Multistage Assembly with a wheel generation process example

Marko Thiele<sup>1</sup>, [Alexandru Saharnean](#)<sup>1</sup>, Daniel Rentsch<sup>1</sup>

<sup>1</sup>SCALE GmbH

## 1 Simulation Data Management Tools

The Finite Element Method (FEM) is quite spread in simulating the manufacturing and testing of different products. In the case of complex products, which are modeled as complex FEM models, for example vehicle FEM models, there are many specialists working in parallel and on different subparts of the model. In addition to this it should always be possible to provide the version of the input model which delivered some given results. Due to requirements like these, there are so called Simulation Data Management (SDM) Tools developed. These tools are used as a central storage for the model, such that all the project members can work with it and see and access the work of others. They are used for saving the configuration of the model at different time stamps, or simply for versioning the model. Other usages include automated submitting of the FEM model to a High Performance Cluster (HPC) for running the simulation, automated extraction of predefined results, storage and versioning of the results and many more.

## 2 Multi stage FEM simulations

The FEM is being used for simulating more and more stages of the production and/or the testing processes. If we take, for example, car crash FEM simulations, engineers are running several “pre” crash simulations. Some of these are sub-processes for sitting a dummy FEM model in the car seat, for inflating the wheels or for folding the airbags. Another example of extending the FEM simulation up on the production and testing chain could be the FEM modeling of the forming stage of the metal plates, later used for the vehicle body. Therefore the FEM simulation of a car crash will use results from other previous FEM simulations. These dependencies between the FEM simulations are starting to be integrated in the SDM tools such that a higher automation degree of the product development process can be achieved.

## 3 The automation of multi stage FEM simulations with LoCo – Multistage Assembly

LoCo is a SDM tool which is mainly used in the vehicle industry. It is a so called rich client application, which enables all the users to work on the same model and it also has version control features. This tool is also used for putting a FEM model together and submitting it to a HPC for computation. This operation is called simply an Assembly. The Assembly feature offers a degree of automation since it builds the FEM model from user defined components, submits the model to HPC, monitors the job on HPC and delivers the job feedback to the user.

In order to provide an even higher degree of automation for multi stage FEM simulations, the Multistage Assembly (MSA) feature was developed in LoCo. This new feature consists in defining LoCo Assemblies in a specific manner, such that the dependencies between several FEM simulations can be recognized and saved. After this LoCo is able to automatically start all the subordinate simulations, which are required for the main simulation. Since each subordinate simulation provides an output, which is imported in LoCo as input for a further simulation(s), these outputs are used by LoCo to determine the dependencies between the jobs. Therefore, the LoCo user must define only once which output in which simulation is to be used, after which, he/she must only start his/her main simulation. The subordinate jobs, necessary for the main one, will be started automatically. The main simulation or any subordinate simulation will be started only after all necessary output is available, or in other words, only after all the necessary output providing jobs were successfully ended.

## 4 A wheel generation process with LoCo – Multistage Assembly

For this example the goal is to simulate the inflation and the loading of FEM car wheel models, which are later necessary for a full car crash simulation. In this case, the inflation of one wheel is one

simulation, the loading of the wheel is the second one and it requires the already inflated wheel. These jobs have to be repeated for each wheel. At the end the loaded wheels must be used in the car crash simulation. For this, the LoCo user will import the output from the inflation simulation in LoCo and use it as input for the loading simulation. The output from the loading simulation will then be imported and used for the car crash simulation. These operations will be done for each wheel. Therefore, there are 8 subordinate simulations and one main job. After these jobs are defined in LoCo, the user must only start the car crash simulation and LoCo will automatically recognize that the car simulation requires data from 4 wheel loading simulations, that each loading simulation requires data from an inflating simulation. Therefore, it will first start the 4 inflating jobs, when these are ready it will start the 4 loading jobs and at the end it will start the car crash simulation job. From this point forward, the development of the car and wheel models can go on, but the LoCo user interested in the car crash simulations does not have to invest anymore effort in performing wheel inflation or loading simulations or in importing wheel models. In this manner a high degree of automation of the entire simulation process is achieved.

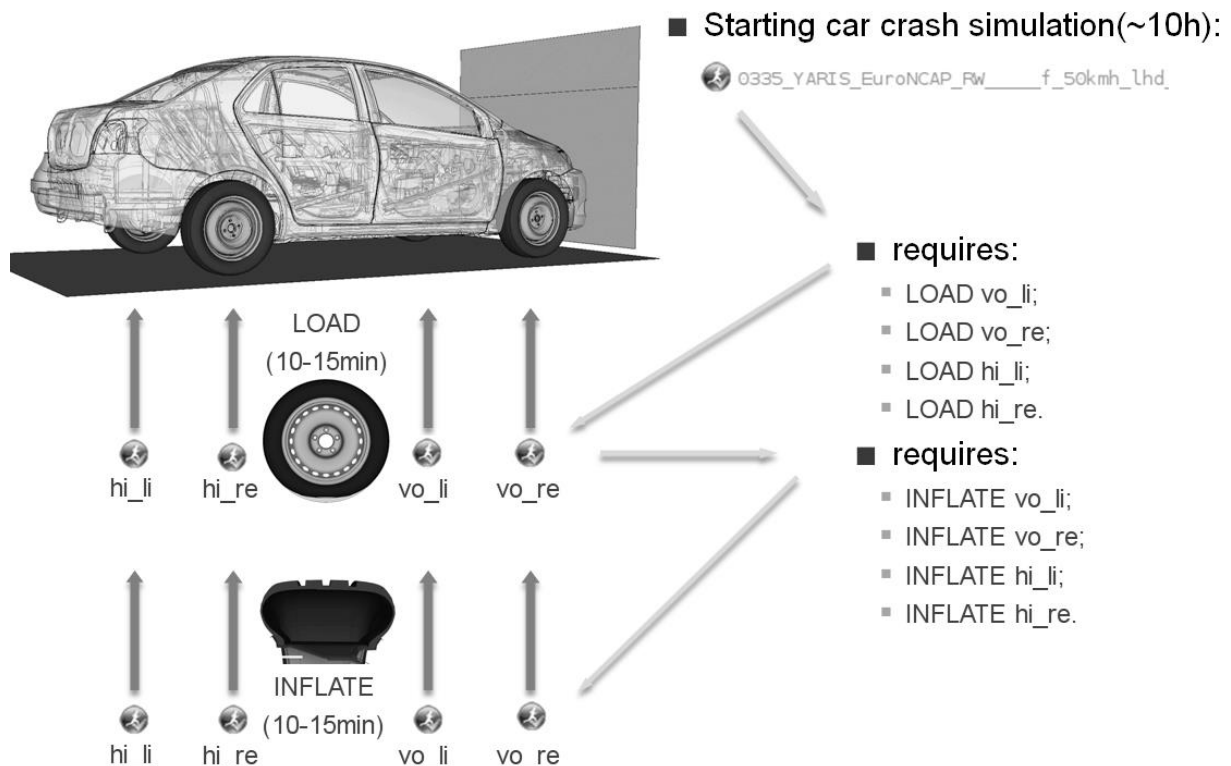


Fig.1: LoCo Assembly dependencies between the car crash simulation and the wheel simulations.

## 5 Conclusions

The high amount of time and effort necessary for performing the management of input and output between FEM simulations with several stages might be seen as a disadvantage for propagating the FEM modeling along the production and testing processes of different products. But as it was observed in the above example, this type of operations can be completely or almost completely automatized. In this manner, more effort can be invested in the development of the FEM models.

# Reducing Storage Footprint and Bandwidth Requirements to a Minimum: Compressing Sets of Simulation Results

Stefan Mertler, Stefan P. Müller

SIDACT GmbH

## 1 Introduction

Simulations are a key component of research and development in many industries. Due to the increasing number of simulations and size of their generated output, managing simulation output has become an important task [1]. Consequently, simulation data management (SDM) systems were widely deployed. Efficient storage and distribution of large numbers of simulation results is one of the major challenges many SDM-systems face nowadays. This challenge represents an opportunity to deploy advanced compression techniques and transfer protocols. SDMZIP is a new approach to compress results of LS-DYNA simulations by aggregating related simulation files into a set, thus reducing redundant information in the whole set. All information is compressed lossy in respect to user defined precisions to fit and guarantee reconstruction accuracies of all application fields.

## 2 Functionality

The basic functionality of our new approach is to store common information between simulations in a central database, which is complemented by simulation-specific detail files for each simulation result. The database can be extended incrementally to add new simulations to a set, possibly resulting in an update file for each extension. On the one hand this modular storage strategy enables decompression of each simulation file independently and on the other hand component-wise transfer and deletion protocols. Thereby the needed bandwidth and storage requirements are further reduced significantly. The common information is extracted using a technique called predictive principle component analysis (PPCA) which also calculates the remaining differences [2].

## 3 Results

A set of 30 simulations that are part of a parameter variation study was compressed applying commonly used precisions. Depending on the use case, all simulations can either be compressed all at once (AAO) or one after another (OAA), if they are not available at the same time. For both cases, a compression rate of over 120 was achieved by the new software solution, see Figure 1. Comparing this to the established standard tool FEMZIP for lossy compression [3], this correlates to an improvement of a factor of 3.5 for OAA and 4 for AAO using same precisions.

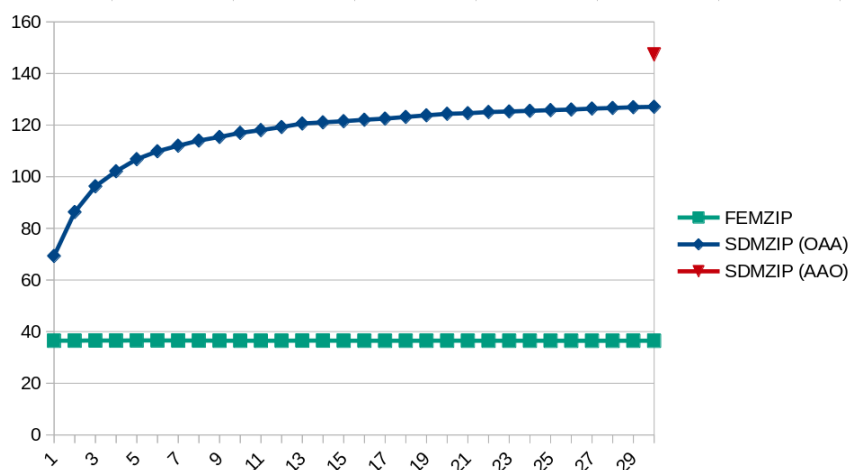


Fig. 1: Compression rates over the number of simulations.



Additional bandwidth reduction of the modular storage strategy is outlined by the factors in respect to FEMZIP displayed in Figure 2. The investigated use case of the OAA strategy applies, if the simulations are transmitted from site A to site B and the previous simulations were already transmitted. In this case, only the update for the difference must be sent to site B reducing amount of data and increasing the factor further. This is described by the delta factor.

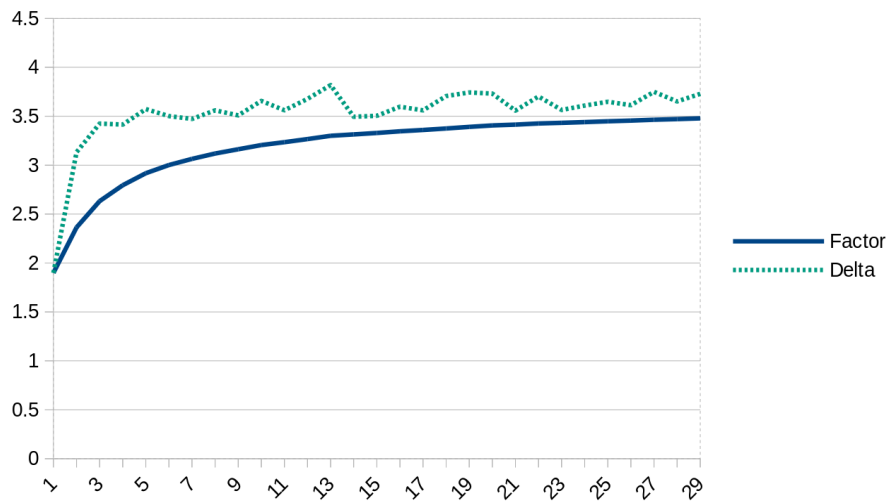


Fig.2: Improvement on FEMZIP for the OAA mode over the number of simulations

#### 4 Summary

Our new method for compression of sets of simulation results reduces the storage footprint and the bandwidth requirements through increased compression performance and modular storage strategy by a factor of 3.5 to 4 depending on the use case. Moreover, it suggests that there is a further potential for reduction in the data already available in many application areas today.

#### 5 Literature

- [1] Thiele, M.; Müllerschön, H.; Liebscher, M.; Mertler, S.; Thole, C-A.: "Reduction in Simulation Time and Storage Requirements Using LoCo for SDM.", 13. LS-DYNA Forum, 2014
- [2] Mertler, S.; Müller, S. P.; Thole, C-A.: "Predictive Principal Component Analysis as a Data Compression Core in a Simulation Data Management System.", 2015 Data Compression Conference. IEEE, 2015
- [3] Iza Teran, R.; Thole, C-A.; Lorentz, R.: "New developments in the compression of LS-DYNA simulation results using FEMZIP.", 6th European LS-DYNA Users' Conference, 2007

# Compression Methods for Simulation Models in SDM Systems

Justus Richter<sup>1</sup>, Matthias Büchse<sup>2</sup>, Wolfgang Graf<sup>1</sup>, Marko Thiele<sup>2</sup>,  
Clemens Löbner<sup>2</sup>, and Martin Liebscher<sup>2</sup>

<sup>1</sup>Institut für Statik und Dynamik der Tragwerke, TU Dresden  
<sup>2</sup>SCALE GmbH, Dresden

Models in Simulation Data Management (SDM) systems have grown tremendously in recent years. At the same time, these models typically exhibit a great deal of redundancy. This is not being fully exploited by established compression techniques, such as ZIP. In view of the size of state-of-the-art SDM systems, data storage and transfer cause large costs, which makes more advanced compression approaches necessary.

Therefore, we consider two such advanced compression approaches: *Data deduplication* on the one hand exploits the mentioned redundancy, *mesh compression* on the other hand exploits the specific mesh structure.

The first approach, data deduplication, reduces space by removing repetitive data patterns. Every pattern is saved only once, and wherever it reappears, it is replaced by a link to its first occurrence. So far, this approach has largely been applied to backup scenarios, where data is assumed to be immutable and throughput is considerably more important than latency; or it has been applied to large-scale computing with multiple nodes. In the SDM domain, however, we need random access to the data, including deletion, and we usually deal with a single machine, even for the server. Therefore, existing solutions cannot be readily applied.

We implemented a deduplicated storage system and incorporated it into SCALE's SDM solution LoCo, which runs on both Linux and Windows. In the process we solved challenges such as choice of parameters, storage, deletion, data integrity, concurrency, deduplicated transfer, and encryption. We measured runtime performance and deduplication gain (i.e., space saved compared to non-deduplicated storage) on several datasets. In summary, the runtime performance is completely adequate for an SDM client

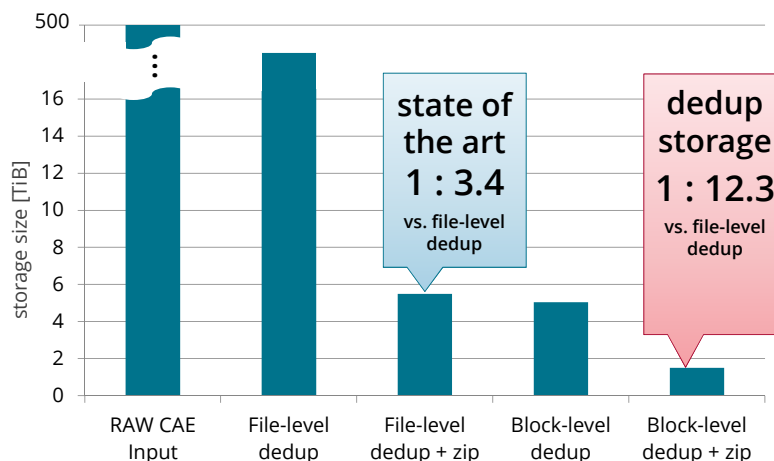


Fig. 1: Compression ratio improvements achieved using data deduplication.

(around 50 MiB/s write and 150 MiB/s read) and promising for an SDM server. Figure 1 shows the compression ratio improvements of data deduplication in comparison to the state of the art.

The second approach, mesh compression, exploits the known organisation of mesh data containing vertices and connecting elements. We use a *degree encoding* algorithm, which traverses the mesh in a determined manner and stores the element type, and the degree of vertices or edges. Provided this information, it is possible to fully reconstruct the mesh.

In the general traversal process, each step starts by choosing a focus face among a set of incomplete faces, which brings the algorithm to a new solid element to be processed. Focus expansion acknowledges the implicit known faces of the solid element. In the end only relevant data of the solid element is stored in data sequences.

This approach is combined with geometry prediction, which improves the compression by transforming the vertices in suitable coordinates. Therefore the position of each vertex is predicted, based on the already processed part of the mesh and only the offset between original and predicted coordinates is stored.

Beside the presented algorithm for solid meshes, our implementation contains also support for shell and bar elements, so that all common element types are covered. In first applications quite promising compression ratios around 10 could be observed, see Fig. 2. Although this is highly dependant on the regularity of the mesh and the chosen resolution of vertex coordinates. We chose 12 bit, so the grid resolution is a 4096-th of the model dimension.

**Acknowledgements** The work on data deduplication has been developed in the project VAVID (reference number: 01 IS 14005 C), which is partly funded by the German ministry of education and research (BMBF). SCALE would like to thank Heinrich Kießling for his support with the implementation of a few features and test cases.

The work on mesh compression was supported by the Federal Ministry for Economic Affairs and Energy (BMWi).

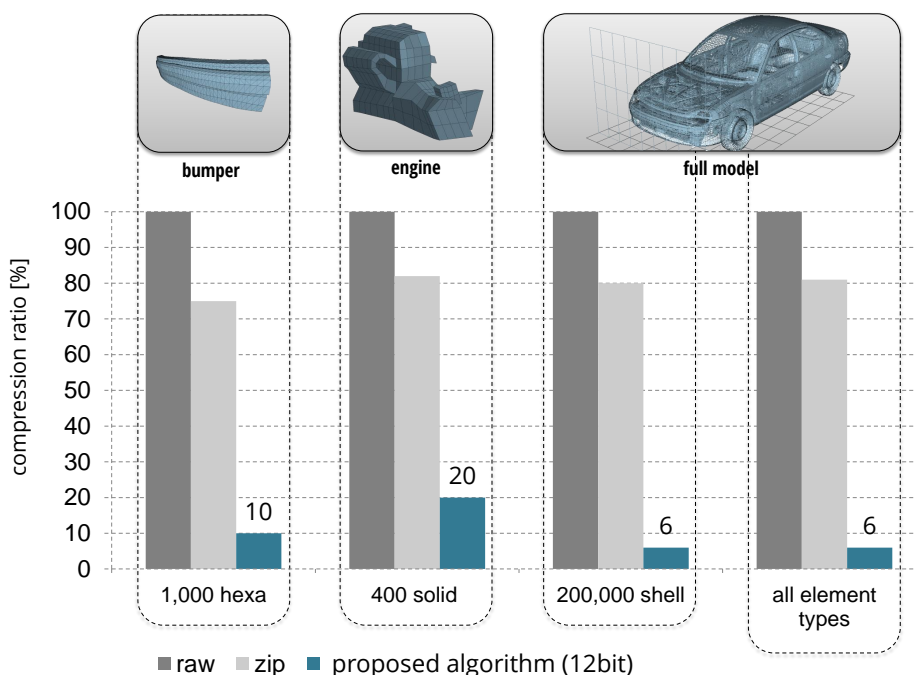


Fig. 2: Compression ratio for mesh data from a Chrysler Neon model (right) and different parts (left and center): raw data (strong gray), zipped data (light gray), and data obtained from the proposed algorithm (blue).

# Managing a Global IT Infrastructure for CAE

Christopher Woll, GNS Systems GmbH

## 1 Motivation

Global markets have led to a trend of global cooperation within companies who do product development and engineering. Computer aided engineering (CAE) is no exception to this rule since crash, CFD, NVH or thermodynamic simulations are important steps in the product development process. Leading automotive OEMs and suppliers have established CAE teams around the world, which now have to collaborate.

This business strategy has a deep impact on the underlying CAE IT infrastructure, which usually consists of high-end workstations, compute servers, and storage systems. The IT infrastructure has to be transformed from locally administered systems to globally managed systems. Changing technology or business trends like cloud computing, increased focus on data security, or communication with partners have an additional impact. GNS Systems has operated highly complex CAE IT infrastructures for its customers since 1997 and has followed these trends. Today, GNS Systems cost-efficiently manages CAE IT infrastructures, which are geographically distributed around the world.

## 2 General scenario

The presentation will show how the management of globally distributed systems can be realized, which steps have to be taken, and which organizational and technical adaptations are usually needed. The first part of the presentation will also show where global standardization is required and where local business needs should be respected. Figure 1 shows the transformation from local heterogeneous IT setups to a global harmonized setup.

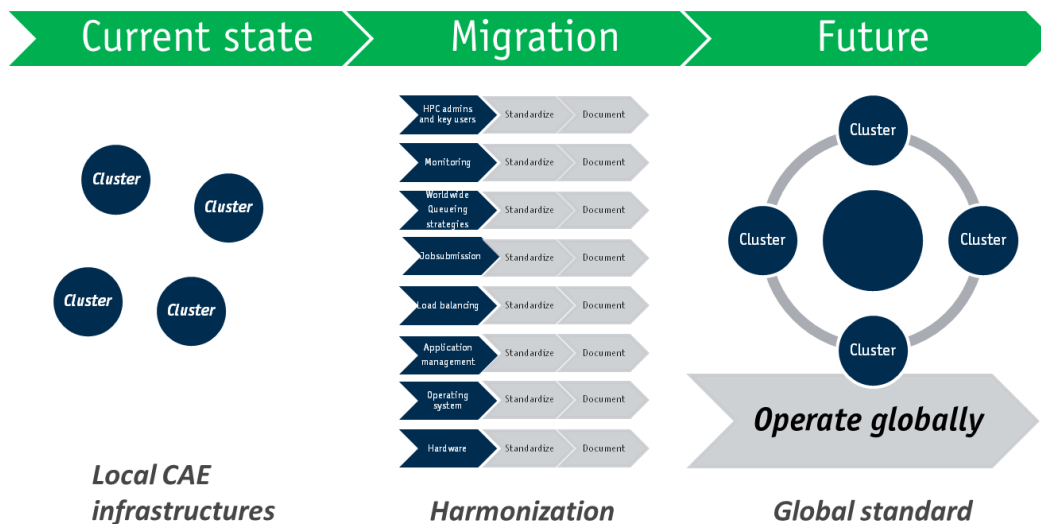


Fig.1: Steps towards a global IT infrastructure for CAE

## 3 Business example

The second part of the presentation will show an actual business example from GNS Systems customer.

The steps taken in this project were:

- Project Kick-Off and analysis of CAE business strategy and processes
- Consulting project to work out
  - o the tools, methods, and best practices for the future IT infrastructure
  - o the collaboration model between the customer IT and GNS Systems
- Documentation of strategy and budgeting plan for three to five years
- Migration project towards the new IT infrastructure in three phases:
  - o Setup of central management systems
  - o Migration of sites
  - o Transfer to ongoing operation

Figure 2 shows the actual HPC (High Performance Computing) stack of a GNS Systems customer as part of the CAE IT infrastructure.

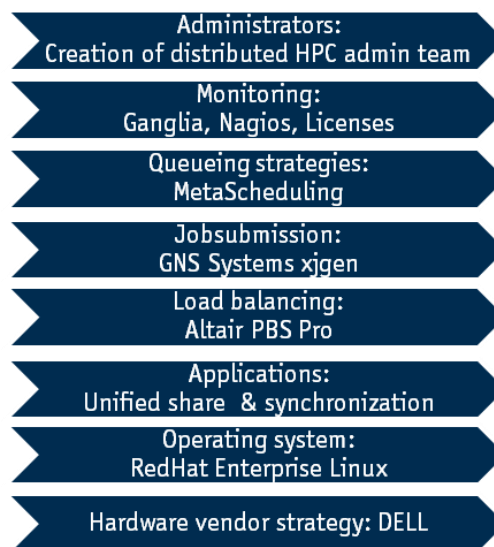


Fig.2: Actual customer HPC stack

#### 4 Summary, business benefits, and cost savings

Introducing and managing a global IT infrastructure is both an organizational and a technical challenge. Different parties such as

- CAE teams (Crash, NVH, Powertrain, CFD),
- IT departments (infrastructure, CAx technologies, application management),
- business units (e.g. license management) and
- suppliers (software vendors, hardware suppliers, consultants)

might be involved. A detailed strategy has to be developed and implemented. The result is an IT infrastructure for CAE which has the following advantages:

- Reduced administration effort:
  - o Common IT infrastructure, which can be managed by a small group of experienced administrators
- Business benefit:
  - o Efficient usage of the IT systems across teams and time zones
  - o Enhanced collaboration options for engineering teams
- Cost reduction:-
  - o Better utilization of application software licenses
  - o Better utilization of hardware resources













DYNAmore Gesellschaft für FEM Ingenieurdienstleistungen mbH

#### Deutschland

DYNAmore GmbH  
Zentrale  
Industriestr. 2  
D-70565 Stuttgart  
Tel.: +49 (0)711 - 45 96 00 - 0  
Fax: +49 (0)711 - 45 96 00 - 29  
E-Mail: info@dynamore.de  
www.dynamore.de

DYNAmore GmbH  
Niederlassung Dresden  
Pohlandstr. 19  
D-01309 Dresden  
Tel.: +49 (0)351 - 31 20 02 - 0  
Fax: +49 (0)351 - 31 20 02 - 29

DYNAmore GmbH  
Niederlassung Nord  
Im Balken 1  
D-29364 Langlingen  
Tel.: +49 (0)50 82 - 9 14 00 - 51  
Fax: +49 (0)50 82 - 9 14 00 - 49

DYNAmore GmbH  
Niederlassung Ingolstadt  
Friedrichshofener Str. 20  
D-85049 Ingolstadt  
Tel.: +49 (0)841 - 1 29 43 24  
Fax: +49 (0)841 - 12 60 48 - 38

DYNAmore GmbH  
Niederlassung Berlin  
Stralauer Platz 34  
D-10243 Berlin  
Tel.: +49 (0)30 - 20 68 79 10  
Fax: +49 (0)30 - 20 07 83 82

#### Tochterfirmen

##### Schweden

DYNAmore Nordic AB  
Zentrale  
Brigadgatan 5  
S-587 58 Linköping  
Tel.: +46 (0)13 - 23 66 80  
Fax: +46 (0)13 - 21 41 04  
E-Mail: info@dynamore.se  
www.dynamore.se

DYNAmore Nordic AB  
Niederlassung Göteborg  
Lindholmospiren 3  
S-417 56 Göteborg  
Tel.: +46 (0)31 - 3 01 23 80

##### Schweiz

DYNAmore Swiss GmbH  
Technoparkstr. 1  
CH-8005 Zürich  
Tel.: +41 (0)44 - 5 15 78 90  
Fax: +41 (0)44 - 5 15 78 99  
E-Mail: info@dynamore.ch  
www.dynamore.ch

##### Italien

DYNAmore Italia S.r.l.  
Piazza Castello, 139  
I-10122 Turin  
Tel.: +39 335 157 05 24  
E-Mail: info@dynamore.it  
www.dynamore.it

##### Frankreich

DYNAmore France SAS  
2 Place de Touraine  
F-78000 Versailles  
Tel.: +33 (0)1 70 29 08 18  
E-Mail: info@dynamore.eu